Vascular endothelial release of xanthine oxidoreductase

Hewinson, James

Award date:
2005

Awarding institution:
University of Bath

Vascular Endothelial Release of Xanthine Oxidoreductase

James Hewinson

A thesis submitted for the degree of Doctor of Philosophy

University of Bath

School for Health

July 2005

ProQuest LLC
789 East Eisenhower Parkway
P.O. Box 1346
Ann Arbor, MI 48106-1346

Dedication

To my Wife Meera

Acknowledgements

I would like to thank:

Dr Tim Millar for guidance throughout my PhD, and for useful discussion and proof reading that helped this document come together.

Dr Cliff Stevens and Prof Michael Horrocks for supervision within the laboratory.

The patients attending the RUH who kindly donated umbilical cords for these studies.

The Arthritis Research Campaign funding this research.

Abstract

Many vascular processes, including the control of vascular tone, coagulation, and inflammation are regulated by reactive oxygen and nitrogen species (RONS). Although RONS play key roles in vascular physiology they also function in vascular-associated pathological processes. The enzyme xanthine oxidoreductase (XOR) generates RONS, and its circulatory form has been linked to several pathologies. However, the source and mechanism of release of circulating XOR is not known. The vascular endothelium was hypothesized to be a source of circulating XOR and using human umbilical vein endothelial cells (HUVECs) the release of XOR was studied.

Initial experiments demonstrated that the cell type being isolated was of endothelial origin. The expression of active XOR in HUVECs was demonstrated. XOR protein was found diffusely in the cytoplasm and also in punctate structures. To measure XOR release from HUVECs a sensitive fluorescence-based assay was chosen and modified. Endothelial cell activation was verified by von Willebrand factor secretion, and release of XOR could be stimulated using known endothelial cell protein secretagogues. XOR release was independent of vWf secretion and cell death, could be stimulated by an increase in intracellular calcium, and required microtubule function.

The activity of xanthine oxidase (XO) from several sources was shown to increase in the presence of thrombin. In the presence of thrombin the protective antibacterial functions of XO were significantly enhanced. The mechanism of thrombin-enhanced XO activity is unknown. In support of proteolytic "activation" of XO, thrombin recognition and cleavage sites were discovered in the XO amino-acid sequence. However, inhibition of thrombin did not convincingly inhibit the enhancement of XO activity. Thrombin does not increase XO activity through an antioxidant mechanism.

A model was proposed suggesting a protective function for circulating XO, incorporating its release and antibacterial function that may be relevant in a wound environment. However, as with many inflammatory mediators, XOR has a role in pathology, therefore the release mechanism described may function in XOR-related disease states.

Table of Contents

Table of Figures

List of Tables

Table of Equations

Abbreviations

°C	Degrees Celsius
A.D.U	Arbitrary Density Units
ADP	Adenosine Diphosphate
ADRP	Adipocyte Differentiation-Related Protein
ANOVA	Analysis of Variance
AP	Alkaline Phosphatase
APM	Apical Plasma Membrane
ARDS	Acute Respiratory Distress Syndrome
ATP	Adenosine Triphosphate
BH_4	Tetrahydrobiopterin
BSA	Bovine Serum Albumin
Ca_2^+	Calcium
cAMP	Cyclic Adenosine Monophosphate
cDNA	Complementary Deoxyribonucleic Acid
CDS	Cell Dissociation Solution
cGMP	Cyclic Guanosine Monophosphate
CHD	Coronary Heart disease
CHF	Chronic Heart Failure
CHF	Chronic Heart Failure
CuZnSOD	Copper/Zinc-Superoxide Dismutase
DAPI	4',6-Diamidino-2-Phenylindole
DMEM	Dulbecco's Modified Eagles Medium
DMSO	Dimethyl Sulphoxide
DNA	Deoxyribonucleic Acid
DPI	Diphenyleneiodonium
ECGM	Endothelial Cell Growth Medium
ecSOD	Extracellular Compartment Superoxide Dismutase
EDRF	Endothelium-Derived Relaxation Factor

EDTA	Ethylenediaminetetraacetic Acid
ELISA	Enzyme-Linked Immunosorbent Assay
Em	Emission Wavelength
eNOS	Endothelial Nitric Oxide Synthase
ESL	E-Selectin Ligand
ETC	Electron Transport Chain
Ex	Excitation Wavelength
FAD	Flavin Adenine Dinucleotide
FBF	Forearm Blood Flow
FCS	Foetal Calf Serum
FDD	Flow-Dependent Dilation
Fe-S	Iron-Sulphur Clusters
FITC	Fluorescein Isothiocyanate
GAG	Glycosaminoglycan
GAPDH	Glyceraldehydes-3-Phosphate Dehydrogenase
GlyCAM-1	Gycosylation-Dependent Cell Adhesion Molecule-1
GPIb	Glycoprotein Ib
GPIIb/IIIa	Glycoprotein IIb/IIIa
GSH	Glutathione
GSSG	Oxidised Glutathione
H_2O_2	Hydrogen Peroxide
HBSS	HANKS Balanced Salt Solution
HEV	High Endothelial Venules
hr	Hour
HRP	Horse Radish Peroxidase
HUVEC	Human Umbilical Vein Endothelial Cell
ICAM-1	Intracellular Adhesion Molecule-1
IFN-γ	Interferon Gamma
IL	Interleukin

iNOS	Inducible Nitric Oxide Synthase
IXP	Isoxanthopterin
KDa	Kilodaltons
LB	Luria Broth
LDH	Lactate Dehydrogenase
Luc^{++}	Lucigenin
M	Molar
MAdCAM-1	Mucosal Vascular Addressin Cell Adhesion Molecule-1
MB	Methylene Blue
min	Minute
ml	Millilitre
MLD	Milk Lipid Droplet
MLG	Milk Lipid Globules
mM	Millimolar
mm	Millimetre
Mo	Molybdenum
MoCo	Molybdenum Cofactor
MP	Microparticles
MVEC	Microvascular Endothelial Cells
NAD^+	Nicotinamide Adenine Dinucleotide
NADH	Nicotinamide Adenine Dinucleotide (Reduced)
NaOH	Sodium Hydroxide
NBT	Nitroblue Tetrazolium
nNOS	Neuronal Nitric Oxide Synthase
$NO^{\cdot}$	Nitric Oxide
NOS	Nitric Oxide Synthase
O_2	Oxygen
$O_2^{\cdot -}$	Superoxide
$^{\cdot}OH$	Hydroxyl Radical

$ONOO^-$	Peroxynitrite
P	Passage
PAF	Platelet Activating Factor
PAR	Protease-Activated Receptors
PARS	Poly (ADP-Ribose) Synthatase
PBS	Phosphate Buffered Saline
PECAM-1	Platelet Endothelial Cell Adhesion Molecule-1
PCR	Polymerase Chain Reaction
PG	Prostaglandin
PI	Propidium Iodide
PL	Phospholipid
Pt	Pterin
RNA	Ribonucleic Acid
RNS	Reactive Nitrogen Species
ROS	Reactive Oxygen Species
rpm	Revolutions Per Minute
SD	Standard Deviation
SDS-PAGE	Sodium Dodecylsulphate Polyacrylamide Gel Electrophoresis
sec	Second
SEM	Standard Error of the Mean
SOD	Superoxide Dismutase
TAFI	Thrombin-Activatable Fibrinolysis Inhibitor
TNF-α	Tumor Necrosis Factor Alpha
tPA	Tissue-type Plasminogen Activator
TRIR	Total RNA Isolation Reagent
TXA_2	Thromboxane A_2
U	Unit
VCAM-1	Vascular Cell Adhesion Molecule-1
vWf	von Willebrand Factor

WPBs	Weibel-Palade Bodies
XDH	Xanthine Dehydrogenase
XO	Xanthine Oxidase
XOR	Xanthine Oxidoreductase
µl	Microlitre
µm	Micrometre
µM	Micromolar

Chapter 1. Introduction: Vascular Biology

1 Introduction: Vascular Biology

1.1 The Circulatory System

In unicellular and simple organisms expulsion of waste products and the acquisition of nutrients to or from the external environment can occur by simple diffusion across cell membranes. Exchange time, to or from the external environment, is proportional to diffusion distance. Consequently cells in complex multicellular organisms, located at a distance from the external environment, can not rely on diffusion alone to support their life. Therefore complex organisms have evolved a circulatory system that delivers and removes products from cells not able to rely on diffusion-exchange from the external environment directly.

The circulatory system not only plays a role in nutrient and waste distribution but also has a key role in many processes including: i) Cellular communication, for example, the distribution of hormones and cytokines to target cells, tissues, or organs, ii) the distribution of body-defence agents, such as, leukocytes, immunoglobulins, and complement components, and iii) the regulation of body temperature.

1.2 Vascular Structure

The circulatory system is composed of the heart, a series of distributing and collecting vessels, and an extensive system of thin-walled vessels. The general structure of a blood vessel, shown in Figure 1, consists of three layers: i) the *tunica adventitia*, a layer of connective tissue that anchors the vessel in place, ii) the *tunica media*, which is composed of a circular layer of smooth muscle, elastin, and collagen sandwiched between two layers of elastic tissue, and iii) the *tunica intima,* which consists of a thin layer of connective tissue and a layer of endothelial cells that make direct contact with the blood. However, this describes general vessel structure and is applicable to arteries for example, but differences are seen in vessels such as capillaries which are composed solely of a simple layer of endothelial cells and are the principal diffusion-exchange vessels.

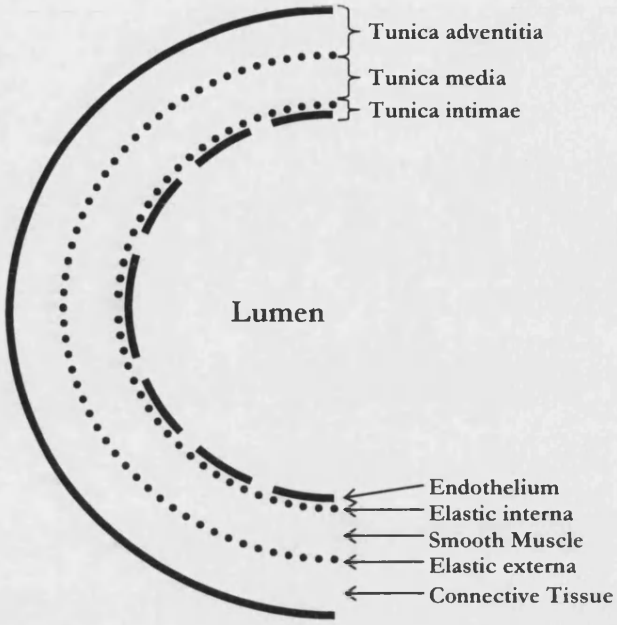

Figure 1. The Generalised Structure of a Blood Vessel.

See text for description (adapted from Pocock and Richards, 1999).

The inner most layer of the blood vessel, the vascular endothelium, was once thought to play only a simple role in the blood vessel as a semi-selective barrier to the diffusion of macromolecules. However, the endothelium is now known to participate in many important physiological and pathological processes, for example the modulation of inflammation and coagulation, and regulation of vascular tone, processes which will be reviewed subsequently.

1.3 Vascular Tone

Vascular tone refers to the degree of constriction experienced by a blood vessel relative to its maximal dilation. The tone of a blood vessel is important in the regulation of blood pressure and blood flow within an organ, and is determined by the balance of vasoconstrictor and vasodilator substances acting ultimately on vascular smooth muscle. Loss of control over vascular tone is associated with several disease states including hypertension, atherosclerosis, and chronic heart failure. Previously it was believed that the control over blood vessel constriction and dilation was via the action of neurochemical substances on the vascular smooth muscle.

However, the importance of the vascular endothelium in the control over vascular tone was discovered (Furchgott and Zawadzki, 1980) and it is now known that the majority of vasoactive substances act via the vascular endothelium, which in turn releases vasoactive factors that dictate vascular tone (Rang *et al.*, 2003) (reviewed in Figure 2). Many vasodilatory substances stimulate the production of nitric oxide ($NO^{\cdot}$) by the vascular endothelium which in turn acts on the smooth muscle causing relaxation, the action of $NO^{\cdot}$ is given in more detail in section 2.1.2.

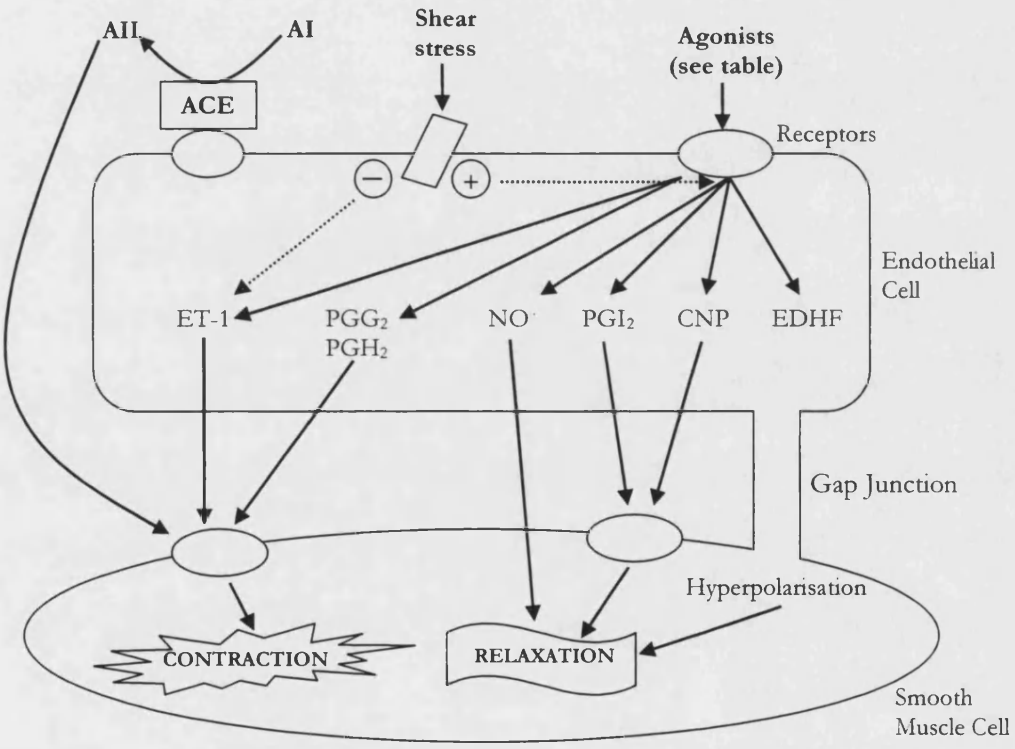

Vasodilators	Vasoconstrictors
Thrombin	Angiotensin II
Histamine	Epinephrine
Acetylcholine	Vasopressin
Bradykinin	

Examples of vasoactive agonists that act via the endothelium.

Figure 2. Vasoactive Substances in Control of Vascular Tone.

Many vasoactive substances control vascular tone via the stimulation of endothelial cells, and the subsequent generation of mediators dictate the degree of smooth mucle contraction v's dilation.

Abbreviations: A, Angiotensin; ACE, Angiotensin-converting enzyme; CNP, C-natriuretic peptide; EDHF, Endothelium-derived hyperpolarising factor; ET-1, Endothelin-1; PG, Prostagalndin (adapted from Rang *et al.*, 2003).

1.4 Haemostatsis

Haemostasis, the arrest of bleeding from a site of vascular damage, is a major host defence mechanism that occurs in two stages known as primary and secondary haemostasis. In primary haemostasis, vasoconstriction reduces blood flow from the damaged vessel, and damage to the endothelial cell layer exposes subendothelial tissues which results in platelet adhesion, accumulation, activation, and aggregation, forming a structure termed the primary haemostatic plug. The primary haemostatic plug is fragile and the consolidation of the platelet aggregate is essential or bleeding will recommence. In secondary haemostasis consolidation of the primary haemostatic plug is brought about by the enzymic conversion of fibrinogen to fibrin, the result of the blood coagulation cascade, which forms a tough mesh around the initial plug (Pallister, 1994).

1.4.1 Primary Haemostasis – Haemostatic Plug Formation

Platelets, the smallest blood cells in the body, are anucleated cells formed in the cytoplasm of megakaryocytes. Platelets contain two major types of intracellular granule, termed dense- and α-granules. Dense-granules contain ADP, ATP, and serotonin, whereas the α-granules contain a variety of substances involved in primary and secondary haemostasis, including platelet factor 4, thrombospondin, fibrinogen, von Willebrand Factor (vWf), P-selectin, and coagulation factors V and VIII (Pallister, 1994).

Platelets display four distinct properties during the formation of the haemostatic plug, i) surface adhesion, ii) shape change, iii) granule release, and iv) aggregation. Platelets may be activated by a variety of physiological and non-physiological substances. *In vivo* damage to the vessel wall exposes sub-endothelial fibers, for example collagen, which promotes platelet adherence. The protein vWf is particularly important for strong

platelet adhesion to the blood vessel. Platelets contain two vWF receptors, glycoprotein Ib (GPIb) and glycoprotein IIb/IIIa (GPIIb/IIIa), occupation of GPIb induces a conformational change and therefore activation of GPIIb/IIIa which forms the second vWf binding site. Platelet adhesion is usually accompanied by a transformation in platelet structure which is associated with the centralization of cytoplasmic granules and their subsequent release. The contents of platelet granules promote further platelet adhesion and aggregation. Initial platelet aggregation is mediated via fibrinogen, a molecule that contains two domains that binds GPIIb/IIIa receptors therefore forming a platelet-platelet bridge. Further aggregation is promoted by release of ADP and the metabolism of arachidonic acid in activated platelets which results in the synthesis of thromboxane A_2 (TXA_2), a powerful inducer of platelet aggregation (Pallister, 1994).

1.4.2 Secondary Haemostasis – The Coagulation Cascade

The blood coagulation cascade is composed of a series of protein coagulation factors that exist, under normal physiological conditions, in an inactive form. Upon stimulation the coagulation factors interact in an ordered sequence that culminates in the production of fibrin. The cascade model was originally conceived from *in vitro* data (Davie and Ratnoff, 1964; MacFarlane, 1964) and *in vivo* data have subsequently been reviewed (Furie and Furie, 1992) (see Figure 3).

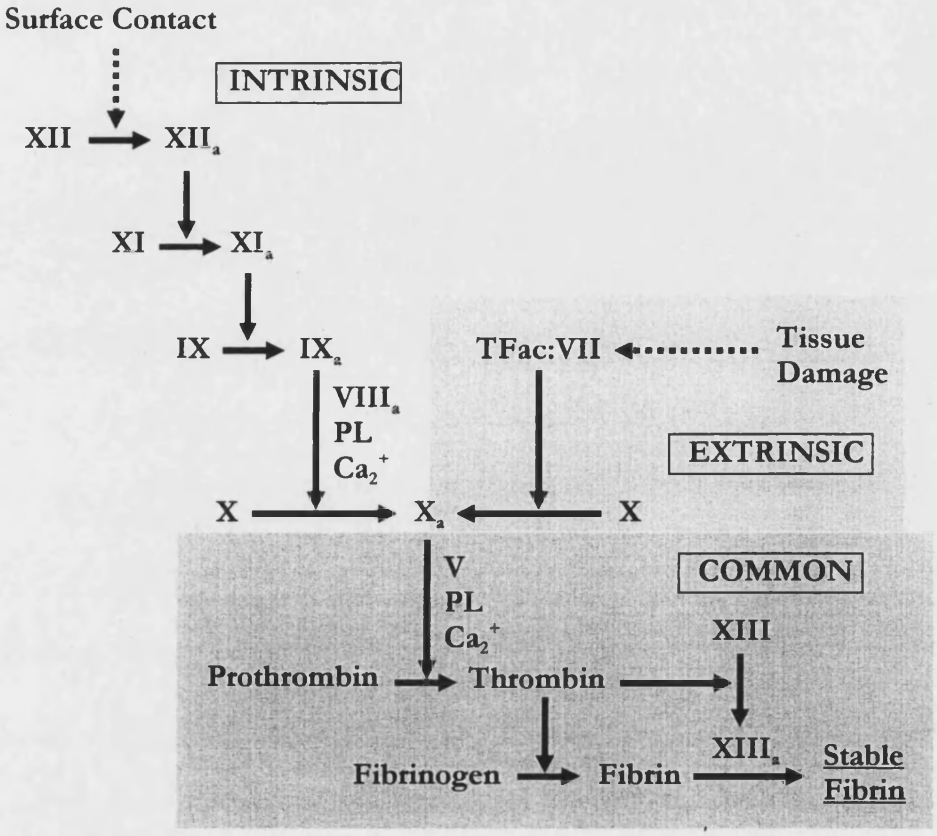

Figure 3. The Coagulation Cascade.

The blood coagulation cascade can be divided into two pathways, the intrinsic and extrinsic pathways, which both share a common end-phase that results in the formation of a stable fibrin network. The intrinsic pathway can be initiated by contact of blood with a "foreign" surface, for example collagen, basement membrane, lipopolysaccharide, or non-physiological surfaces such as glass. The extrinsic pathway, on the other hand, is initiated by the exposure of tissue factor (TFac) to blood following tissue damage. The coagulation factors, that are referred to by Roman numerals, occur as two main types: i) Zymogens, which exist has inactive plasma proenzymes but are activated by enzymatic cleavage (the active state is denoted by the suffix "a"), are a group that include factors II (prothrombin), X, XI, XII, and XIII, and ii) Accelerators, which act as catalysts for other enzymatic reactions are a group that include fators V and VIII. It must be noted that the two pathways are not exclusive, this is a simplified diagram and some crossovers do exist other than the common end-phase. Abbreviations: Ca_2^+ : Calcium, PL : Phospholipid. (Adapted from Pallister, 1994).

1.4.3 The Role of von Willebrand Factor in Haemostasis

Many of the factors required for the coagulation cascade are synthesised by the liver and platelets. However, the vascular endothelium contributes to the regulation of the coagulation cascade through the synthesis and release of thrombomodulin, tissue factor pathway inhibitor, and tissue plasminogen activator (tPA) (inhibitors of

coagulation), and von Willebrand factor (vWf), a promoter of coagulation. Endothelial and platelet vWf is an extensively glycosylated 250kDa protein that can form disulphide-linked multimers that maybe >20,000kDa. vWf is constitutively secreted by endothelial cells from unique cytoplasmic storage granules called Weibel-Palade Bodies (WPBs), the formation of which appears to require synthesis of vWf (reviewed in Michaux and Cutler, 2004). Vascular endothelial cells secrete vWf from WPBs in response to a variety of agents which can be classified on the intracellular-signalling mechanism induced prior to release. Secretagogues such as histamine and thrombin induce release by a mechanism dependent on a rise in intracellular free-calcium ($[Ca^{2+}]_i$) (Birch *et al.*, 1994), whereas epinephrine, forskolin, and vasopressin stimulate release by a cyclic adenosine monophosphate (cAMP)-dependent mechanism (Visher and Wollheim, 1997).

vWf regulates haemostasis in two ways: i) vWf contributes to primary haemostasis via the binding to the sub-endothelium of damaged vascular tissue and to platelet receptors GPIb and GPIIb/IIIa (reviewed in Sadler, 1998). Thus vWf forms a bridge between platelets and subendothelial connective tissue that contributes to platelet aggregation, ii) vWf contributes to secondary haemostasis as it binds to and acts as a carrier protein for factor VIII, thus protecting the factor from enzymatic degradation (reviewed in Sadler, 1998). In the absence of vWf, factor VIII is rapidly removed from the circulation significantly reducing blood coagulation. The role of vWf in coagulation is highlighted in patients with von Willebrand's disease, caused by a defect in vWf. von Willebrand's disease is likely to be the most common inherited haemorrhagic disorder (Pallister, 1994).

1.4.4 The Roles of Histamine and Thrombin in Haemostasis

The $[Ca^{2+}]_i$ raising agents thrombin and histamine are used in experimental chapters of the thesis, therefore it is important to highlight their roles in vascular processes. Thrombin has a major role in the coagulation cascade (see Figure 3) in the enzymatic-cleavage of fibrinogen to form fibrin, the component responsible for the

consolidation of the haemostatic plug. However, thrombin also plays other significant roles in haemostasis, which are reviewed in the next section.

1.4.4.1 Thrombin Effects on the Endothelium and Platelets

As mentioned previously, both thrombin and histamine stimulate the release of vWf from the endothelium. Thrombin is formed in the coagulation cascade by the cleavage of prothrombin, whereas the major source of histamine is the mast cell which secretes factors during inflammatory stimulus (see later section), thus providing a cross over between coagulation and inflammation. The intracellular signalling cascade for histamine and thrombin-induced vWf release is shown in Figure 4. Additionally, thrombin has a multi-functional role in the regulation of platelets, it triggers shape change and the release of contents from dense- and α-granules (Pallister, 1994).

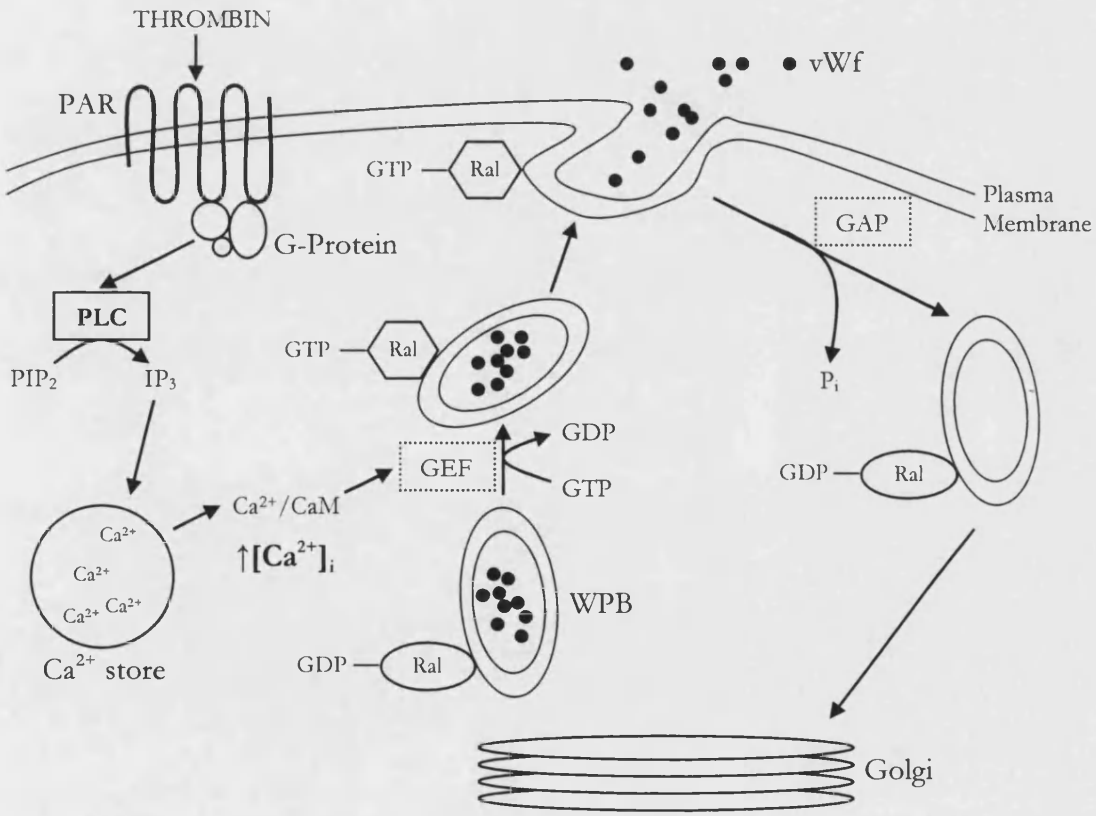

Figure 4. Signal Cascades in histamine and Thrombin-Stimulated vWf Release.

The activation of endothelial G-protein-linked protease-activated receptors (PARS) by thrombin stimulates the activity of the enzyme phospholipase C (PLC). PLC-catalysed generation of inositol 1,

4, 5-triphospahte (IP_3) signals the release of calcium (Ca^{2+}) from intracellular stores. The resulting increase in $[Ca^{2+}]_i$ leads to calcium-calmodulin association (Ca^{2+}/CaM) which activates Ral guanine nucleotide exchange factor (GEF). GEF activity switches Ral to its active form, via a conformational change induced by guanosine triphospahte-guanosine diphosphate (GTP-GDP) exchange. Activation of Ral promotes the binding of other proteins that are responsible for cytoskeletal rearrangement, and ultimately the exocytosis of WPBs (adapted from van Mourik and Voorberg, 2002). Histamine stimulates a similar signalling cascade resulting in an increase in $[Ca^{2+}]_i$ but acts via the G-protein linked histamine receptor (Lo *et al.*, 1987; Tilly *et al.*, 1990; Hough, 2001).

Thrombin's stimulatory action on endothelial cells and platelets occurs via protease-activated receptors (PARs). There are four members to the PAR family, PAR_{1-4}, but thrombin only cleaves $PAR_{1,3,4}$. All PARs belong to a family of seven-transmembrane spanning G-protein-linked receptors, which are activated by a novel mechanism, as shown in Figure 5. Human platelets are regulated by PAR_1 and PAR_4 (Kahn *et al.*, 1998), whereas only PAR_1 and PAR_2 play a functional role in the vascular endothelium (Hirano and Kanaide, 2003).

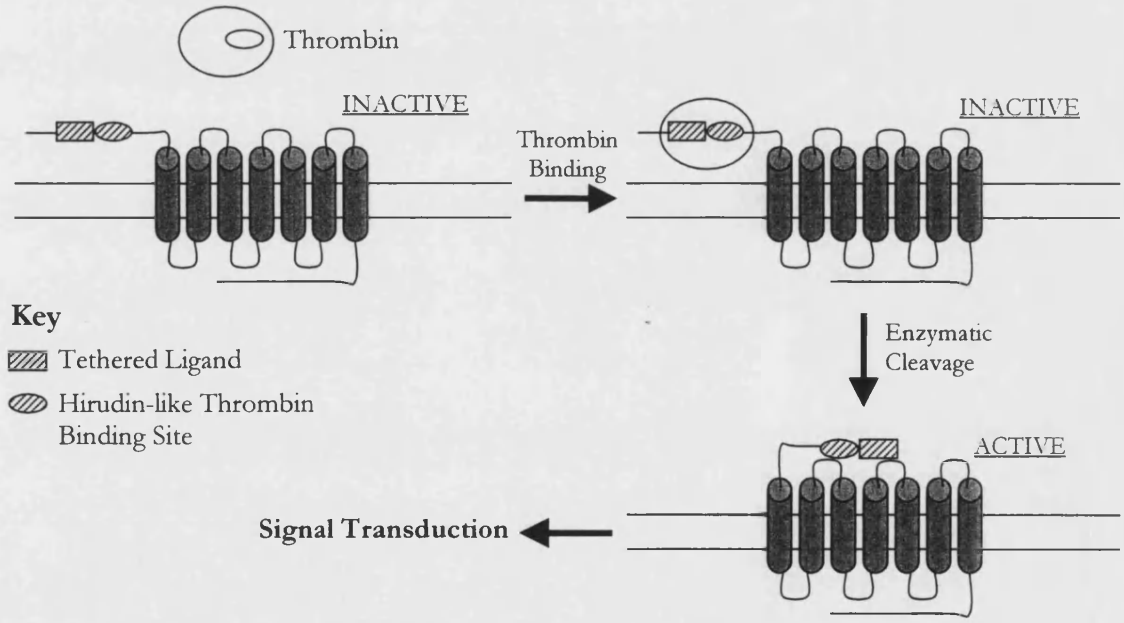

Figure 5. Thrombin Activation of Protease-Activated Receptors.

In inactive PARs the extracellular tethered ligand is masked by an amino-acid sequence. Thrombin activation of PAR_1 and PAR_3 occurs in a two step process. Firstly, thrombin binds to a hirudin-like domain, and secondly, thrombin cleaves to expose the PAR-tethered ligand which subsequently interacts with extracellular domains and activates the receptor (adapted from Ossovskaya and Bunnett, 2003).

1.5 Inflammation

Inflammation is an important physiological response to a variety of stimuli including bacterial infection, tissue injury, and chemical exposure. Clinically, the inflammatory response may be characterized by the following symptoms:

• *oedema* (swelling) caused by the accumulation of inflammatory exudate (a fluid that contains proteins and cells from local blood vessels and affected tissue).

• *rubor* (redness) due to dilation of local blood vessels and a consequential increase in blood flow.

• *calor* (heat) caused by increased blood flow and/or systemic fever.

• *dalor* (pain) as a result of pressure build up at site of oedema and release of certain inflammatory mediators.

• *loss of function* due to pain and swelling of affected area.

Although the clinical appearance of inflammation may seem deleterious, the increase in blood flow and accumulation of fluid at affected tissues has beneficial effects including, delivery of immune cells and proteins, nutrients and oxygen, and the dilution of toxins.

1.5.1 Mediators of Inflammation

During the inflammatory response a variety of mediators are either released from cells or activated in response to certain stimuli and serve to enhance specific aspects of the inflammation.

1.5.1.1 Cytokines

Cytokines form a large group of secreted-proteins that regulate the intensity and duration of an immune response by mediating the actions of leukoctyes and other inflammatory cells. Cytokines important to the inflammatory process include interleukin-1, and -6 (IL-1 and IL-6), tumor necrosis factor alpha (TNF-α), interferon gamma (IFN-γ), and chemokines (see below). Collectively cytokines influence the inflammatory process in many ways, for example, inducing fever and the synthesis of acute-phase response proteins, increase adhesion molecule expression on the endothelium, and activate immune cells (Kuby, 1997).

1.5.1.2 Chemokines

Chemokines are a group of small polypeptides that are responsible for the chemotactic attraction of leukocytes and the regulation of integrin expression on the surface of leukocytes. Chemokines act by inducing the adherence of leukocytes to the vascular endothelium (an essential step for the migration of inflammatory cells into an affected area) and attract leukocytes to affected areas following migration from the circulation. The chemokine family includes macrophage chemotactic and activating factor, macrophage inflammatory protein-1a and b, RANTES, platelet factor 4, and interleukin 8 (IL-8). Probably the best characterized chemokine is IL-8, which is generated by a variety of cells including monocytes/macrophages, neutrophils, and endothelial cells. IL-8 is retained on the inflamed endothelium where it acts to activate integrin expression in neutrophils, allowing firm adhesion (see section 1.5.2) (Kuby, 1997).

1.5.1.3 Plasma Enzyme Mediators

The plasma contains four enzyme-mediated systems that are involved in the inflammatory response (Kuby, 1997). i) The kinin system is activated following tissue damage and results in the formation of bradykinin. Bradykinin is a vasoactive protein that induces vasodilation, increases vascular permeability, induces pain, and activates the complement system. ii) The complement system may be activated by several pathways but results in a common end point, the formation of the membrane attack complex that serves to punch holes in invading pathogens. During the complement cascade, enzymatic cleavage of complement components generates both opsonins and anaphylatoxins. Anaphylatoxins bind to receptors on tissue mast cells inducing degranulation, which results in the release of histamine and other mediators. iii) The coagulation system, which may be activated by damage to blood vessel walls, has an important role in inflammation. The generation of the fibrin clot at sites of vessel damage serves as a barrier to stop the spread of invading pathogens and fibrinopeptides formed during thrombin cleavage of fibrinogen to fibrin act by increasing vascular permeability and as neutrophil chemotactants. iv) The fibrinolytic

system opposes the coagulation system by the break down of the fibrin clot. The end product of the fibrinolytic system is the enzyme plasmin, which activates the complement pathway and is responsible for fibrin destruction, which forms chemotactic peptides for neutrophils, as mentioned above.

1.5.2 Molecular Biology of Transendothelial Migration

An important step in the inflammatory process is the migration of inflammatory cells from the circulation into the affected tissue. However this is not a simple process as the leukocyte must first bind to, remain bound and then traverse the endothelium against the shear-forces of the circulating blood. To achieve this feat the endothelium and leukocyte co-ordinate a sophisticated interplay of signalling and adhesion molecules, as reviewed in Figure 6. The principal signalling and adhesion molecules will now be discussed in more detail.

1.5.2.1 Selectins and Ligands

Three selectins have been identified and are classified by their site of expression, i.e. platelets, endothelium, and leukocytes and are consequently named P-, E- and L-selectin, respectively. Selectins have similar structures, each have a lectin-like domain (the principal region for ligand binding), an endothelial growth factor motif, a number of consensus repeats (nine, six, and two in P-, E-, and L-selectin respectively), and an anchoring transmembrane domain with cytoplasmic tail. Selectins appear to have a role in the initial binding and rolling of leukocytes on the vascular endothelium (Kuby, 1997).

P-selectin, also called GMP-140, is expressed in preformed secretory granules; α-granules in platelets and WPBs in endothelial cells (Hsu-Lin *et al.*, 1984; McEver *et al.*, 1989). In endothelial cells, surface-expression of P-selectin occurs when WPBs fuse with the plasma membrane on stimulation by histamine or thrombin for example (Hattori *et al.*, 1989). Human P-selectin may also be transcriptionally regulated; the synthesis of P-selectin mRNA in endothelial cells is upregulated in response to IL-4

and IL-13 stimulation (Yao *et al.*, 1996; Woltmann *et al.*, 2000). Stimulation of transcriptional activity accounts for the bimodal distribution of P-selectin expression, an early peak appears within minutes, i.e. release from preformed granules, and later a peak after approximately four hours i.e. expression of newly synthesised P-selectin. P-selectin is a receptor for neutrophils and monocytes, and therefore regulates binding of these cell types to the endothelium and platelets (Larsen *et al.*, 1989; Geng *et al.*, 1990). The P-selectin glycoprotein ligand (PSGL-1) is expressed on leukocytes and platelets, and is responsible for interactions between these two cell types and the endothelium (Frenette *et al.*, 2000).

Similar to P-selectin, E-selectin is expressed in vascular endothelial cells, however unlike P-selectin its expression is not constitutive. E-selectin synthesis and cell-surface upregulation requires stimulation of endothelial cells by inflammatory agonists such as TNF-α and IL-1, and maximal expression occurs approximately four hours after stimuli and declines after approximately 24 hours (Belvilacqua *et al.*, 1987). Two glycoprotein ligands have been identified for E-selectin, the leukocyte-expressed E-selectin Ligand (ESL-1) which binds only to E- and not P-selectin (Ehrhardt *et al.*, 2004), and the above mentioned PSGL-1.

The leukocyte-expressed receptor L-selectin is required for the binding of leukocytes to the endothelium (von Andrian *et al.*, 1992). Four L-selectin ligands have been identified in high endothelial venules (HEV), Sgp50 (glycosylation-dependent cell adhesion molecule-1, GlyCAM-1), Spg90 (CD34), Spg200, and mucosal vascular addressin cell adhesion molecule-1 (MAdCAM-1). Spg90 is identical to CD34 and is expressed on endothelial cells.

1.5.2.2 Immunoglobulin Superfamily Receptors and Integrins

Initial tethering of leukocytes to the endothelium via selectins and their ligands is a comparatively weak and reversible process. For leukocytes to migrate through the endothelium they must arrest on the vessel wall, a process that is exclusively mediated

by integrin-receptors on leukocytes and immunoglobulin superfamily members expressed on the endothelium (see Figure 6).

Similarly to E-selectin, the expression of intracellular adhesion molecule-1 (ICAM-1) and vascular cell adhesion molecule-1 (VCAM-1) occurs after stimulation of the endothelium. The platelet endothelial cell adhesion molecule-1 (PECAM-1) on the other hand is constitutively expressed. VCAM-1 is an important ligand for the integrin VLA-4, whereas ICAM-1 binds to LFA-1 and Mac-1 on the leukocyte (Hou and Ley, 2001).

Through their interaction with the above mentioned receptors, leukocyte arrest is mediated primarily by the VLA-4 ($\alpha 4\beta 1$), LAF-1 ($\alpha L\beta 2$) and Mac-1 ($\alpha M\beta 2$) integrins (Springer, 1994). A unique feature of the integrin family is that their activity is regulated independently of their surface expression, i.e. circulating leukocytes express integrins but in non-adhesive states (Hynes, 1992). Conformational changes within the integrin are required for adhesion, and stimuli for this change are thought to come from chemokines and occurs in a matter of seconds (Grabovsky *et al.*, 2000). Chemokines, such as IL-8, are displayed on the endothelial surface at sites of inflammation (Weber *et al.*, 1999), therefore it has been proposed that initial tethering and rolling events increase the chances of chemokine-stimulation of leukocytes that leads to integrin-conformational change, firm adhesion, and migration.

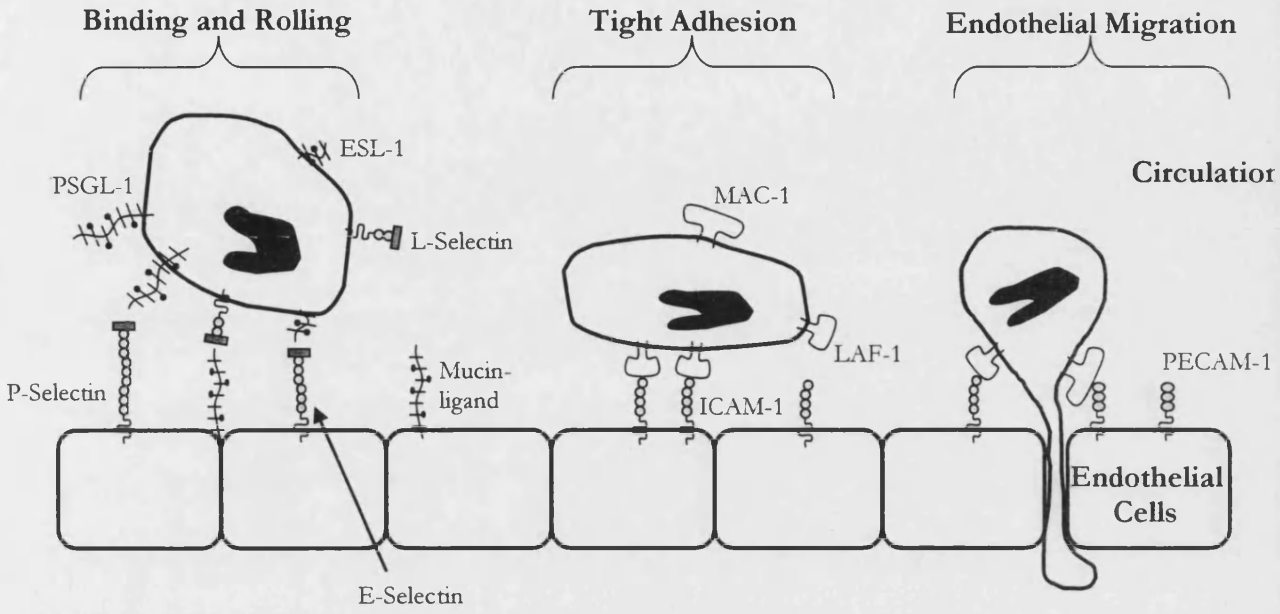

Figure 6. Leukocyte-Endothelial Cell Interactions in Inflammation.

The processes involved in leukocyte-transendothelial migration can be split into three stages: i) initial binding and rolling, ii) tight adhesion, and iii) trans-endothelial migration. Initial binding of circulating leukocytes is established by interactions between endothelial-expressed P- and E-selectin, leukocyte L-selectin, and their cognate mucin-ligands. Tight adhesion occurs between activated endothelial cells expressing CAM's and activated leukocytes expressing functional integrin. Leukocytes may then migrate across the endothelium (adapted from Ehrhardt *et al.*, 2004).

1.5.3 The Roles of Thrombin and Histamine in Inflammation

As previously stated, the formation of a fibrin-clot following the disruption of the endothelium is an important measure to stop the spread of invading microorganisms. The processes by which thrombin and histamine modulate haemostasis are reviewed in the coagulation section. As thrombin and histamine function to induce the release of vWf from endothelial cells, they also stimulate the concomitant release of pre-synthesised P-selectin, therefore thrombin and histamine contribute to leukocyte adhesion events in inflammation. Indeed, the induction of leukocyte adhesion and rolling can be mediated by histamine stimulation of the endothelium (Jones *et al.*, 1993) or by thrombin-activation of endothelial cells mediated via PAR_4 (Vergnolle *et al.*, 2002). Also, thrombin and histamine function as mediators of another important step in inflammation, the increase in vascular permeability. Thrombin and histamine induce shape-change in the endothelial resulting in gap formation that accounts for

increased permeability. Thrombin and histamine mediate this effect via the PAR_1 and H1 receptors, respectively (Laposata *et al.*, 1983; Vergnolle *et al.*, 1999; Rotrosen and Gallin, 1986).

Chapter 2. Introduction: Reactive Oxygen and Nitrogen Species in the Vasculature

2 Introduction: Reactive Oxygen and Nitrogen Species in the Vasculature

Reactive oxygen and nitrogen species (RONS) are a class of highly reactive molecules that have a broad function ranging from host defence to the maintenance of vascular processes. Although RONS play important physiological roles their excessive generation, with respect to endogenous defence molecules against these highly active molecules, can lead to pathological conditions (as discussed in a later section).

Superoxide ($O_2^{\cdot -}$), hydrogen peroxide (H_2O_2), and the hydroxyl radical ($^{\cdot}OH$), form a group of molecules known as reactive oxygen species (ROS). The superoxide anion is formed by the single electron reduction of molecular oxygen (O_2) by enzymic processes or non-enzymic redox-reactive compounds. $O_2^{\cdot -}$ is poorly membrane-permeable due to its charge and therefore usually remains in the cell compartment where it is produced. $O_2^{\cdot -}$ has a short half-life and is rapidly converted to the more membrane-permeable ROS H_2O_2, which is commonly generated by the dismutation of two $O_2^{\cdot -}$ molecules by a process catalysed by superoxide dismutase (SOD) (McCord and Fridovich, 1968; Fridovich, 1978). In the presence of transition metal ions, such as iron and copper, $O_2^{\cdot -}$ and H_2O_2 maybe converted to the damaging radical species, $^{\cdot}OH$, by the Fenton or by the Haber-Weiss reaction (Hancock, 1999).

The reactive nitrogen species (RNS) nitric oxide ($NO^{\cdot}$) is generated by enzymatic processes and depending on the microenvironment $NO^{\cdot}$ can be converted to other RNS including nitrosonium cation, nitroxyl anion, and peroxynitrite ($ONOO^-$) (Stamler *et al.*, 1992). $NO^{\cdot}$ has a half-life of about 5-10 seconds, is lipid soluble, and readily diffuses across cell membranes. Although $NO^{\cdot}$ has a short half-life, studies have suggested that other RNS, especially peroxynitrite, can react with thiols to form *S*-nitrosothiols that serve as stable reservoirs of $NO^{\cdot}$ (Reviewed in Kelm, 1999).

2.1 Reactive Oxygen and Nitrogen Species in Vascular Function

2.1.1 Antioxidant Systems

The effect of RONS generated within the vascular system are not only dependent on the site and quantities generated but also on the processes that scavenge or degrade RONS, processes also termed the antioxidant systems. Antioxidant systems comprise a group of enzymatic and non-enzymatic molecules. Enzymatic antioxidants include superoxide dismutase (SOD), catalase, and glutathione peroxidase (GSH peroxidase), however other systems exist including thioredoxin reductase and heme oxygenase (Yamawaki *et al.*, 2003; Parrella and Yet, 2003). If the generation of RONS is far in excess of the antioxidant systems then a state of oxidative stress arises which can be responsible for many pathological conditions in the vasculature (see Xanthine Oxidase and Vascular Pathology section for examples).

2.1.1.1 Superoxide Dismutase

SOD was first discovered in 1969 (McCord and Fridovich, 1969) and catalyses the following antioxidant reaction:

$$2O_2^{\cdot -} + 2H \rightarrow H_2O_2 + O_2$$

Three isoforms of SOD exist in humans, the mitochondrial manganese-containing SOD and two copper/zinc-containing isoforms that exist either in the cytoplasmic (CuZnSOD) or extracellular compartment (ecSOD). The secreted SOD, ecSOD, is the most abundant in the endothelium and is primarily associated with the vascular endothelial surface (Stralin *et al.*, 1995), where it binds to sulphated polysaccharides, such as heparin and heparin sulphate (Fridovich, 1997). ecSOD may function as an interceptor of ROS released from activated phagocytes and/or regulate extracellular $NO^{\cdot}$ availability (Oury *et al.*, 1996), whereas the CuZnSOD will predominantly control intracellular ROS availability.

2.1.1.2 Catalase

Superoxide dismutase functions to remove the potentially damaging $O_2^{\cdot -}$ radical, however in that process the ROS H_2O_2 is generated, a more stable and more membrane soluble compared to $O_2^{\cdot -}$. The enzyme catalase hfunctions in the disposal of H_2O_2 by the following process (Hancock, 1999):

$$2H_2O_2 \rightarrow 2H_2O + O_2$$

2.1.1.3 Glutathione

Another mechanism for the breakdown of H_2O_2 into harmless by-products involves glutathione (GSH). GSH serves as a substrate for the selenium-containing enzyme glutathione peroxidase in the elimination of lipid peroxides and H_2O_2 (Dickinson and Forman, 2002). In this reaction GSH becomes converted to oxidised GSH (GSSG), however the enzyme glutathione reductase rapidly converts GSSG back to GSH. The GSH/GSSG ratio is usually kept at a high level to maintain this antioxidant buffering system.

2.1.1.4 Non-Enzymatic Antioxidants

A number of non-enzymatic antioxidants exist within the vasculature including ascorbic acid (vitamin C), α-tocopherol (vitamin E), β-carotene, and uric acid, which act as radical scavengers (i.e. they donate an electron to free-radicals which leads to the inactivation of the initial radical species) (reviewed in Schultz *et al.*, 2004). Also metal chelators, for example transferrin and ferritin, reduce the formation of antioxidants by reducing the availability of transition metals. This process limits the production of $^{\cdot}OH$ by the reaction of $O_2^{\cdot -}$ or H_2O_2 with free iron.

2.1.2 Reactive Oxygen and Nitrogen Species in Vascular Tone

As mentioned in Chapter 1 the control of vascular tone is important in the regulation of blood pressure. The loss of control over vascular tone has implications in several vascular diseases including hypertension, atherosclerosis, and chronic heart failure (CHF) (see Xanthine Oxidase and Vascular Pathology section). The discovery that an endothelium-derived relaxation factor (EDRF) was responsible for relaxation of smooth muscle in the blood vessel (Furchgott and Zawadzki, 1980) led many researchers to attempt to characterise the substance. In 1987 two research groups discovered that EDRF is in fact $NO^{\cdot}$ (Palmer *et al.*, 1987; Ignarro *et al.*, 1987), one of the most influential RONS in the control of vascular tone. Many of the biological effects of $NO^{\cdot}$ are mediated through the regulation of guanylate cyclase and the subsequent generation of cyclic guanosine monophosphate (cGMP), which is involved in a broad range of physiological responses (Münzel *et al.*, 2003). In the control of vascular tone, $NO^{\cdot}$ is synthesised and released by the vascular endothelium in response to shear stress or chemical stimulation (e.g. acetylcholine), but acts on smooth muscle cells to cause dilation (see Figure 7). However, the presence of superoxide may attenuate this signal (Gryglewski *et al.*, 1986) through the diffusion limited reaction between $O_2^{\cdot -}$ and $NO^{\cdot}$ forming $ONOO^-$ (Huie and Padmaja, 1993), which occurs approximately three times faster than the reaction of $O_2^{\cdot -}$ with SOD.

Although the role of $NO^{\cdot}$ in vasodilation has been well characterised, it appears that other RONS may function to induce smooth muscle relaxation. A recent paper has suggested that H_2O_2 is responsible for shear stress-induced dilation in human blood vessels, probably acting as an endothelium-derived hyperpolarising factor (Miura *et al.*, 2003).

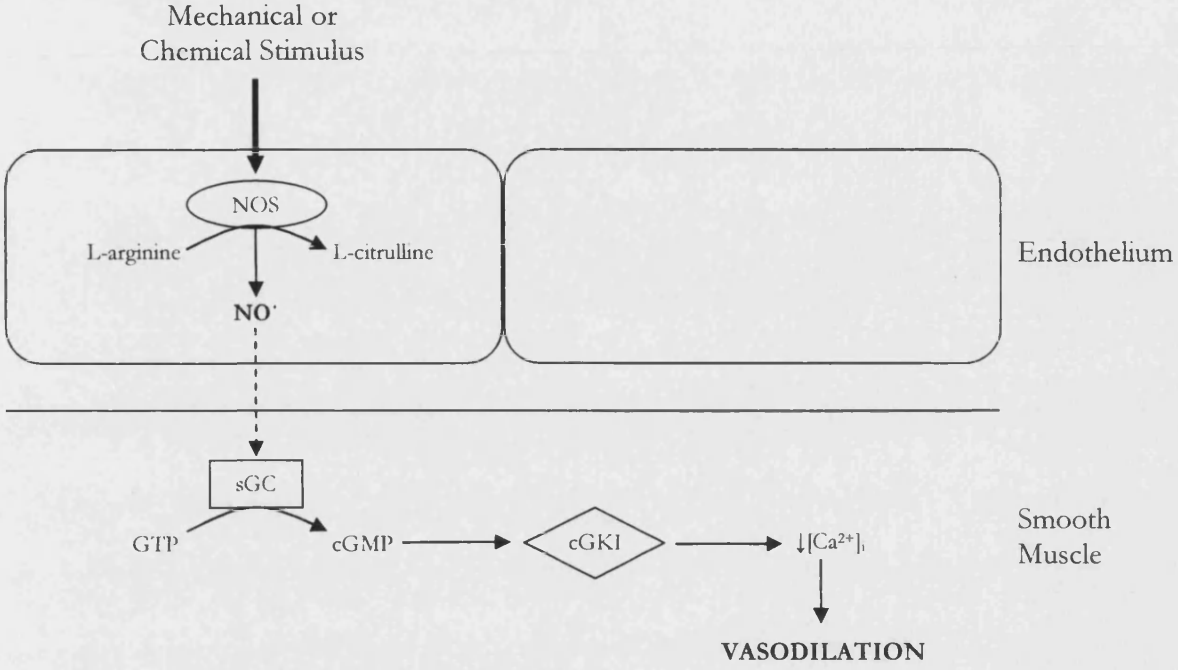

Figure 7. Maintenance of Vascular Tone – Vasodilation.

In response to an appropriate chemical stimulus or shear stress $NO^{\cdot}$ generation by nitric oxide synthase (NOS) in endothelial cells is triggered. $NO^{\cdot}$ diffuses into nearby smooth muscle cells where it is responsible for the activation of soluble guanylate cyclase (cGC). Subsequent generation of cGMP activates cGMP-dependent protein kinase I (cGKI). cGKI is responsible for decreasing intracellular Ca^{2+} concentration $[Ca^{2+}]_i$, which in turn decreases the activation of calcium-calmodulin myosin light chain kinase. Decreased phosphorylation of myosin light chains induces smooth muscle relaxation and therefore vasodilation (adapted from Ignarro and Kadowitz, 1985; Archer *et al.*, 1994; Münzel *et al.*, 2003).

2.1.3 Reactive Oxygen and Nitrogen Species in Coagulation

With respect to the coagulation cascade (as discussed in chapter 1) very little information regarding the effects of RONS is known. In Bayele *et al* 2002, it was suggested that the extrinsic and intrinsic coagulation cascades are modulated by shifts in redox balance, but their work was based on in vitro experiments that may not apply in vivo. Conversely, the influence of RONS on platelet aggregation has been well studied.

In haemostasis, platelets function to form the primary haemostatic plug that is consolidated by fibrin. It is essential that under physiological conditions circulating platelets do not aggregate as this leads to thrombosis. $NO^{\cdot}$ is an important molecule

in the inhibition of platelet aggregation, and akin to its vasodilatory actions it can signal via guanylate cyclase activation, as reviewed in Figure 8. An important source of $NO^{\cdot}$ in the inhibition of platelet aggregation is the vascular endothelium (Azuma *et al.*, 1986; Radomski *et al.*, 1987), and is likely to be generated by endothelial nitric oxide synthase. However, xanthine oxidoreductase (found in the vascular endothelium) also generates $NO^{\cdot}$ in the presence of glyceryl trinitrite, which inhibits platelet aggregation (O'Byrne *et al.*, 2000). Also, a constitutive $NO^{\cdot}$ synthase has been found in human platelets (Sase and Michel, 1995; Zhou *et al.*, 1995) which modestly modulates platelet function (Freedman *et al.*, 1997).

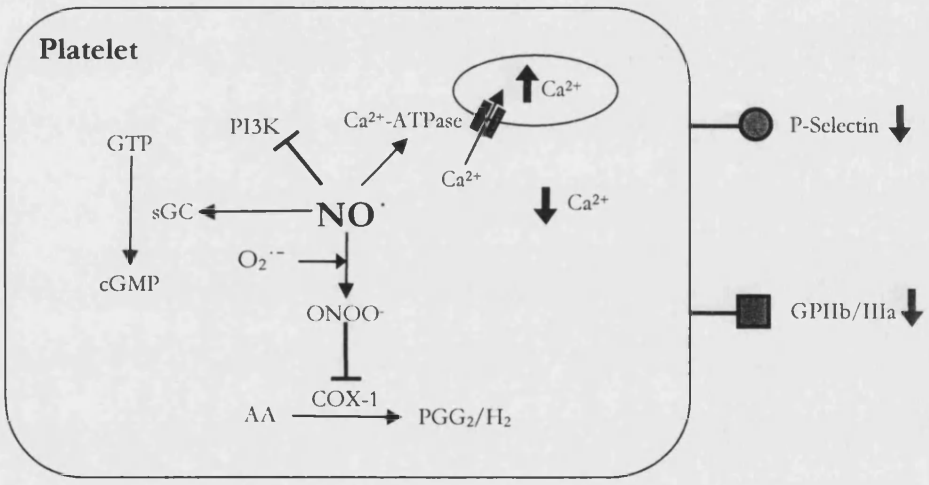

Figure 8. The Effects of Nitric Oxide on Platelet Function.

$NO^{\cdot}$ from endothelial cells or platelets inhibits aggregation via several signalling pathways. $NO^{\cdot}$ is responsible for the generation of cGMP by activating soluble guanylate cyclase and reduces cytoplasmic $[Ca^{2+}]$ by activation of calcium-ATPases. As a result of these mechanisms cytoplasmic $[Ca^{2+}]$ is reduced which suppresses the expression of P-selectin and the active conformation of glycoprotein IIb/IIIa (GPIIb/IIIa). $NO^{\cdot}$ inhibition of phosphoinositide 3-kinase (PI3K) inhibits the activation of platelet NADPH oxidase and therefore significant generation of $O_2^{\cdot -}$. $NO^{\cdot}$ may react with $O_2^{\cdot -}$ forming $ONOO^{-}$ which inhibits the enzyme cyclooxygenase (COX-1) and the generation of prostaglandin G_2 and H_2 (PGG_2/H_2) from arachidonic acid (AA). PGG_2 and PGH_2 are precursors of thromboxane A_2 synthesis, a potent inducer of platelet aggregation and vasoconstriction. (adapted from Loscalzo, 2001).

In vitro experiments have shown that thrombin activated platelets exposed to $O_2^{\cdot -}$ present increased aggregation and adhesion properties compared to controls (Salvemini *et al.*, 1989). Enhanced aggregation and adhesion occurred with $O_2^{\cdot -}$ but

not H_2O_2. Stimulated platelets are a rich source of $O_2^{\cdot -}$ themselves, and exhibit the above mentioned characteristics (Jahn and Hansch, 1990). The role $O_2^{\cdot -}$ has over the regulation of platelet function is probably conducted through its reaction with $NO^{\cdot}$ and the subsequent reduction in $NO^{\cdot}$-inhibition of aggregation (Clutton *et al.*, 2004).

2.1.4 Reactive Oxygen and Nitrogen Species in Inflammation

Controlled changes in cell adhesive properties play a key role in the early stages of an inflammatory response. As mentioned in Chapter 1, the adhesion of leukocytes to endothelial cells in post-capillary venules prior to transendothelial migration is an early and critical step in inflammation. The expression of a range of cell-surface adhesion molecules is required for firm adhesion between leukocytes and endothelial cells and RONS are important regulators of adhesion molecule expression.

One of the first cell-surface molecules to be expressed in response to an inflammatory signal is the Weibel-Palade body-associated protein P-selectin, an endothelial cell protein that binds to counter receptors on circulating leukocytes. It has been know for several years that the cell-surface expression of P-selectin can be induced by ROS (Patel *et al.*, 1991). Further studies have confirmed this finding and have attempted to decipher the ROS signalling mechanism. In Terada *et al.*, 1997 and Folch *et al.*, 2000 the role of H_2O_2 in P-selectin up-regulation was demonstrated. In the latter publication it was discovered that H_2O_2 activation of the enzyme Poly (ADP-ribose) synthatase (PARS) mediates the expression of P-selectin in pulmonary endothelial cells (Folch *et al.*, 2000). To contradict these findings other publications have suggested a role for $O_2^{\cdot -}$ in the upregulation of P-selectin expression (Suzuki *et al.*, 1989; Gaboury *et al.*, 1994). Also, studies have revealed that $O_2^{\cdot -}$ upregulates the expression of endothelial platelet activating factor (PAF) (Gaboury *et al.*, 1994; Folch *et al.*, 2000), a protein that acts cooperatively with P-selectin in the binding of leukocytes, for example neutrophils (Zimmerman *et al.*, 1990) (see Figure 18).

Further analysis into ROS control over P-selectin expression has shown that thrombin-induced P-selectin expression is ROS-dependent. Takano *et al.*, 2002 have demonstrated that thrombin-induced early expression of P-selectin was reduced when inhibiting endogenous cellular ROS generators, thus suggesting that ROS may serve as signalling intermediates in this process.

Although the expression of the adhesion molecule P-selectin may be rapidly upregulated by release from preformed stores, other adhesion molecules such as ICAM-1, VCAM-1, and E-selectin require synthesis before being expressed significantly. The role of ROS in the regulation of ICAM-1 expression has been investigated, and the treatment of endothelial cells with ROS upregulates ICAM-1 expression (Bradley *et al.*, 1993; Lo *et al.*, 1993). Similar to the thrombin-induced P-selectin release, TNF-α-stimulated endothelial cells regulate ICAM-1, VCAM-1, and E-selectin expression via ROS signalling intermediates, a process that may be inhibited by antioxidants (Chen *et al.*, 2003). In this process ROS are believed to increase adhesion protein expression through the regulation of the redox sensitive transcription factor NF-κB. A summary of ROS induced transcription is shown in Figure 9.

Nitric oxide appears to have an opposing role in the regulation of inflammation compared to ROS. Two lines of evidence have suggested that $NO^{\cdot}$ has a role in modulating leukocyte-endothelial cell interactions: 1) the inhibition of $NO^{\cdot}$ generation by endothelial cells elicits the recruitment and adhesion of leukocytes to endothelial cells (Kubes *et al.*, 1991) and 2) the exposure of $NO^{\cdot}$-generating substances attenuates adhesion (Gaboury *et al.*, 1993). The mechanism by which $NO^{\cdot}$ modulates these processes is thought to be through its reaction with $O_2^{\cdot -}$ (thus forming $ONOO^-$), leading to a reduction in the bioavailability of ROS and therefore down-regulation of the ROS-mediated processes mentioned above. However, to complicate this theory the formation of $ONOO^-$ elicits leukocyte adhesion molecule

expression via the Raf/MEK/Erk pathways (see Figure 9) which leads to leukocyte-endothelial association (Zouki *et al.*, 2000), and has been shown to cause inflammation (Hayashi *et al.*, 2004).

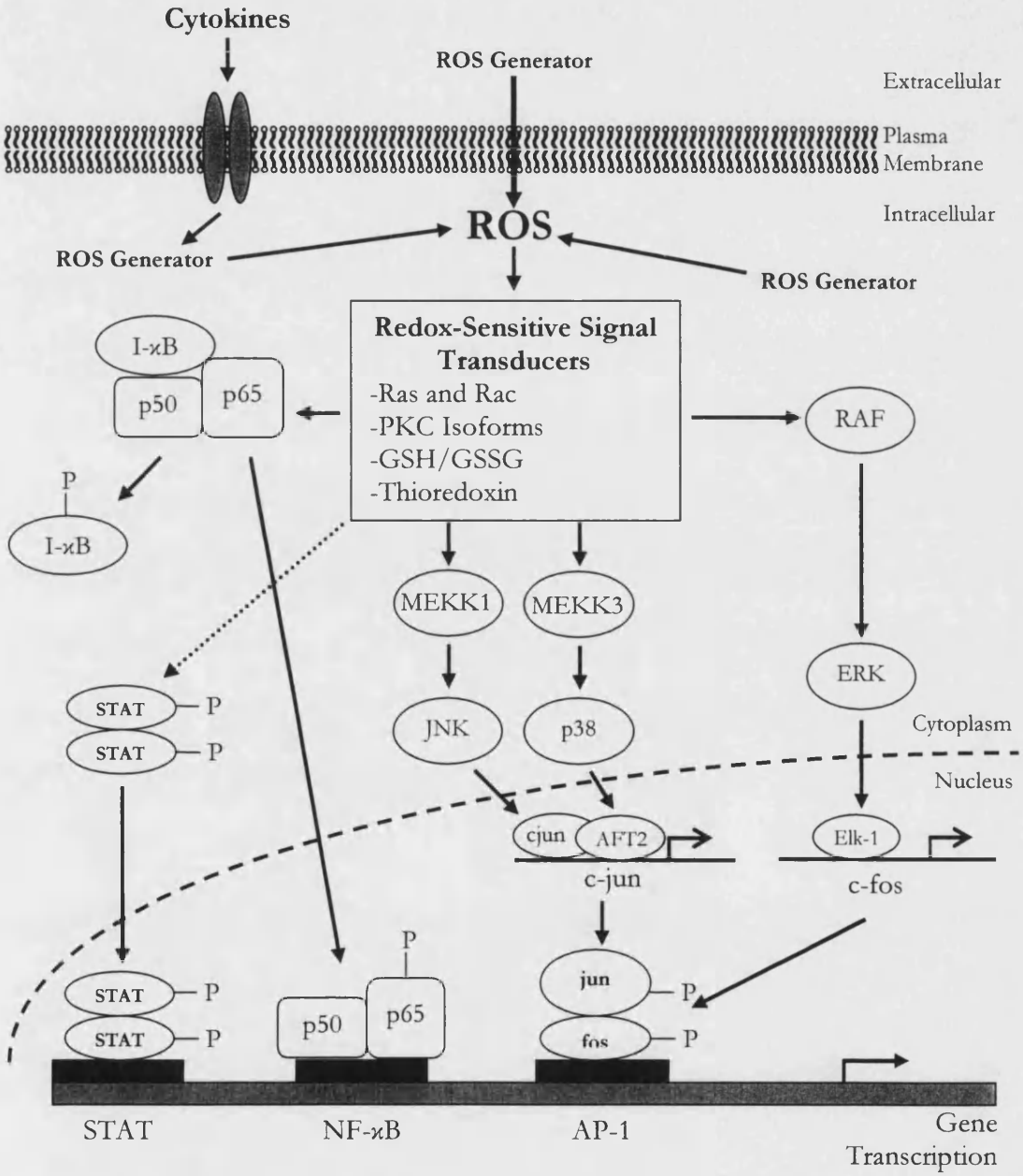

Figure 9. Reactive Oxygen Species Control over Gene Expression.

Intracellular ROS signal changes in gene expression via redox-sensitive signal transducers, a group made up of monomeric G-proteins (Ras and Rac), protein kinase C (PKC), the ratio of GSH and GSSG, and thioredoxin. ROS species promote nuclear translocation and binding of STAT (Signal Transducers and Activators of Transcription) to promoter elements. NF-κB is usually maintained in the cytoplasm in an inactive form by the

association of the inhibitory factor I-κB. Upon stimulation I-κB dissociates and active NF-κB translocates to the nucleus. NF-κB activation is modulated by glutathione, thiredoxin and PKC. The AP-1 transcription factor is composed of a Jun and Fos heterodomer. AP-1 is activated by three MAP Kinase pathways that regulate the transcription of *jun* and *fos*, and phosphorylate these proteins. The three transcription factors STAT, NF-κB, and AP-1 may act independently or cooperatively to activation transcription of genes such as ICAM-1. (Adapted from Lum and Roebuck, 2001)

2.2 Endothelial Reactive Oxygen and Nitrogen Species Generators

Potential sources of RONS within the vascular endothelium include nitric oxide synthase, NAPDH oxidase, the mitochondrial electron transport chain, and xanthine oxidoreductase. Each generator has implications in pathological processes and therefore it is important to highlight the function of each generator in turn. Other endothelial sources of RONS include cytochrome *P*-450 (Fleming, 2001).

2.2.1 Nitric Oxide Synthase

The Nitric Oxide Synthase (NOS) family of enzymes, consisting of neuronal NOS (nNOS), inducible NOS (iNOS), and endothelial NOS (eNOS), (reviewed in Porasuphatana *et al.*, 2003), are well documented for the generation of $NO^{\cdot}$ from the oxidation of L-arginine to L-citruline in an oxygen dependent process. However it has been demonstrated that each isoform is also capable of generating $O_2^{\cdot -}$ (reviewed in Porasuphatana *et al.*, 2003). The constitutively expressed isoform eNOS is a functionally active as a homodimer. Each monomer is composed of a flavin-containing C-terminal domain with binding sites for flavin adenine dinucleotide, flavin mononucleatide, and NADPH, and a catalytic N-terminal oxygenase domain with binding sites for L-arginine and tetrahydrobiopterin (BH_4). Calcium/calmodulin-activated eNOS generates $NO^{\cdot}$ in the presence of the ubiquitous pterin cofactor BH_4. However the absence of functional BH_4 switches activated eNOS to generate $O_2^{\cdot -}$ (Vásquez-Vivar *et al.*, 1998; Vásquez-Vivar *et al.*, 2003), which is often referred to as "uncoupling". Interestingly BH_4 is susceptible to oxidative degradation. It has been shown that the oxidative loss of functional BH_4 by increased ROS generation, by NADPH oxidase for example (Landmesser *et al.*, 2003),

amplifies oxidative stress through the resultant loss in $NO^{\cdot}$ generation and increased NOS-dependent $O_2^{\cdot -}$ production.

2.2.2 NADPH Oxidase

The $O_2^{\cdot -}$-generating enzyme NADPH oxidase has been well characterised in the phagocyte (Hancock, 1999). NADPH oxidase is located in the plasma membrane and within the membrane of specific granules of neutrophils. The enzyme consists of four components required for activity: a heterodimeric membrane-associated flavocytochrome b_{588}, composed of gp91-*phox* and p22-*phox*, and cytoplasmic components p47-*phox*, p67-*phox*, and GTPase Rac1 or Rac2. Upon neutrophil stimulation the cytoplasmic components associate with the membrane-bound cytochrome to form an active enzyme complex that catalyses the production of $O_2^{\cdot -}$ essential for host defence (see

Figure 10). In recent years it has become clear that endothelial cells express an $O_2^{\cdot -}$-generating enzyme analogous to phagocyte NADPH oxidase (Bayraktutan *et al.*, 2000; Görlach *et al.*, 2000; Li and Shah, 2002). The endothelial-NADPH oxidase differs from that of the neutrophil as it continuously generates a low level of $O_2^{\cdot -}$ in unstimulated cells and $O_2^{\cdot -}$ generation occurs mainly intracellularly (Li and Shah, 2002).

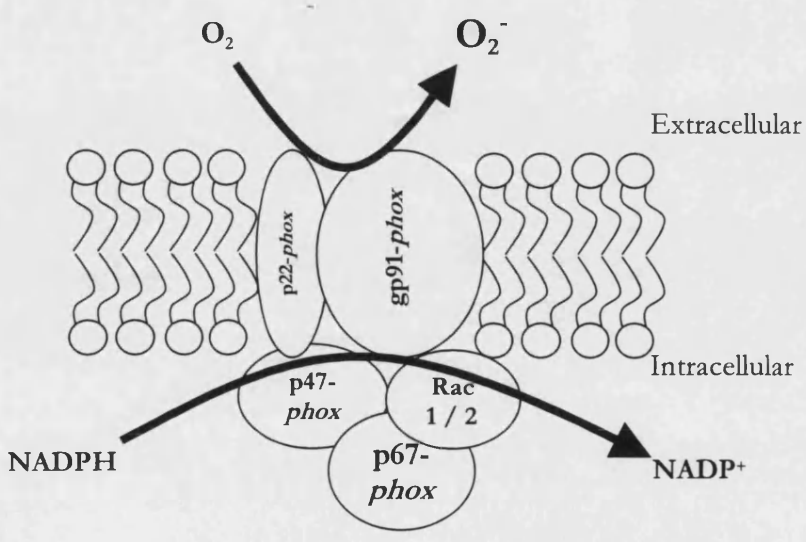

Figure 10. Superoxide Generation by NADPH Oxidase.

The membrane-bound, functional, NADPH complex of the neutrophil catalyses the production of $O_2^{\cdot -}$ from the substrates O_2 and NADPH, note $O_2^{\cdot -}$ generation occurs mainly in the extracellular compartment.

2.2.3 Mitochondrial Electron Transport Chain

The electron transport chain (ETC) of mitochondria has been recognised as one of the major cellular generators of ROS, known to generate $O_2^{\cdot -}$, and H_2O_2, (Loschen *et al.*, 1971; Loschen *et al.*, 1974). Electrons donated to the chain by NADH or succinate are passed along a series of electron carrier molecules (complexes I-IV, ubiquinone [Q], and cytochrome c [C]) embedded in the inner mitochondrial membrane. At each transfer electrons fall to a lower energy state and released energy is used to maintain an electrochemical proton gradient across the inner mitochondrial membrane. The gradient drives a flux of electrons through an enzyme, ATP synthase, thus generating ATP, "cellular energy". Electrons are believed to leak from the ETC, from complexes I and III (Turrens and Boveris, 1980; Turrens *et al.*, 1985; St-Pierre *et al.*, 2002), and reduce O_2 forming $O_2^{\cdot -}$ (see Figure 11) that can be dismutated by mitochondrial SOD thus forming H_2O_2 (Loschen *et al.*, 1974). It has been stated that 2% of electron flow during mitochondrial respiration gives rise to H_2O_2 (Chance *et al.*, 1979), which would indicate significant ROS species generation. However, experimental evidence which proves that mitochondria are a source of ROS under physiological conditions is lacking (Forman and Azzi, 1997; Staniek and Nohl, 2000; St-Pierre *et al.*, 2002) as procedures used to demonstrate $O_2^{\cdot -}$ and H_2O_2 generation by the ETC disrupt normal antioxidant function and/or the ETC. In Staniek and Nohl, 2000, it was discovered that intact mitochondria could not be made to release H_2O_2. However it has been concluded that mitochondria could be a significant source of ROS under certain conditions, for example insufficient ROS scavenging by SOD or catalase or the presence of free transition metals that could initiate Habor-Weiss or Fenton chemistry.

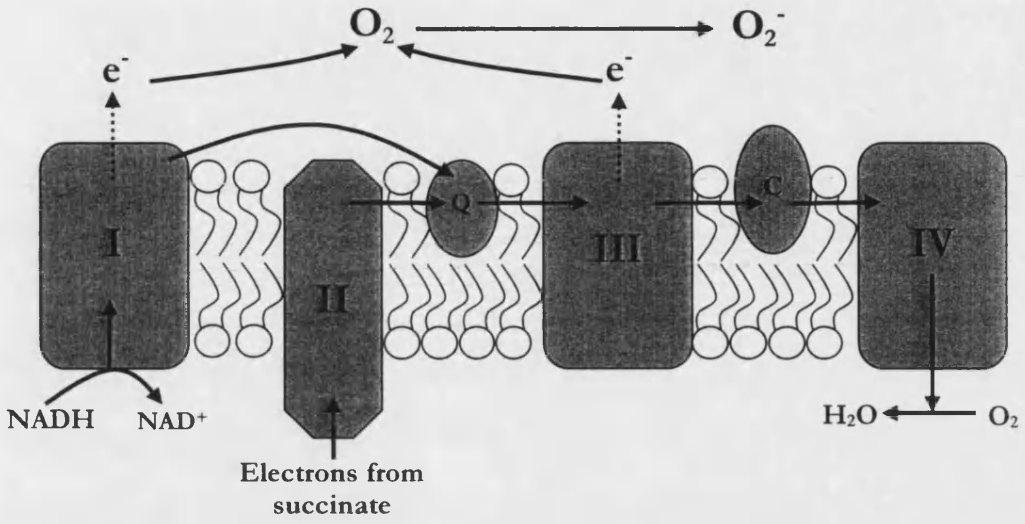

Figure 11. Superoxide Formation by the Mitochondrial Electron Transport Chain.

Leakage of electrons (e^-) from the mitochondrial ETC complexes I and III are believed to be responsible for the reduction of O_2 thus forming O_2^- (arrows indicate electron movement through the electron carrier molecules of the ETC)

2.2.4 Xanthine Oxidoreductase

The enzyme Xanthine Oxidoreductase (XOR), first identified over 100 years ago (Schardinger, 1902), belongs to a family of molybdenum cofactor-containing enzymes which also includes Sulphite oxidase, Aldehyde oxidase, and DMSO reductase (Kisker *et al.*, 1997; Garattini *et al.*, 2003). XOR exists as one of two interconvertible forms, xanthine oxidase (XO) and xanthine dehydrogenase (XDH), which historically have been differentiated by their oxidizing substrate, i.e. XO reduces oxygen, whereas XDH preferentially reduces nicotinamide adenine dinucleaotide (oxidized) (NAD^+) (Waud and Rajagopalan, 1976). XOR may oxidise a variety of compounds including purines, pteridines, and aldehydes. However hypoxanthine and xanthine appear to be physiological substrates for XOR, and therefore XOR has been assigned the physiological role of catalysing the terminal two steps in purine degradation; the conversion of hypoxanthine to xanthine to uric acid (Berg *et al.*, 2001). All mammalian XOR's are inhibited by allopurinol, one of the oldest and most selective inhibitors of XOR (Massey *et al.*, 1970).

As XOR is the principal enzyme reported on in this thesis, the enzyme will be reviewed in sufficient detail for understanding of experimental chapters.

2.2.4.1 Gene and Protein

2.2.4.1.1 The gene

The evolutionary conserved gene *xanthine oxidoreductase* (*xor*) has been sequenced in many organisms from bacteria to man (Ichida *et al.*, 1993; Xu *et al.*, 1994; Cazzaniga *et al.*, 1994; Kunst *et al.*, 1997; Schultz *et al.*, 2001). Human *xor* has been mapped to a single locus on the p22 band of chromosome two (Xu *et al.*, 1994) and is composed of 36 exons and 35 introns that span at least 60 000 nucleotide bases (Xu *et al.*, 1996). The mouse *xor* gene, for example, has a similar composition but is about 10kb longer (Cazzaniga *et al.*, 1994), however the organisation of the *xor* gene in insects is significantly different. The *Drosphila melangaster xor* gene is composed of just four exons (Keith *et al.*, 1987). Interestingly, the four exon/intron junctions of the *D. melangaster xor* gene are retained at exactly the same positions of corresponding junctions in the human gene, thus suggesting that the division of the *xor* gene into more exons has occurred during evolution (Xu *et al.*, 1996).

2.2.4.1.2 Transcriptional Control

In general, XOR activity in humans is low compared to other mammalian species (see XOR tissue distribution section), thus indicating a potential difference in control over human XOR expression and/or posttranslational activity. Investigations by Xu *et al.*, 2000 have produced a model whereby the human *xor* gene is repressed. They discovered that the human *xor* gene is suppressed by factors bound to upstream E-box and TATA-like elements. The TATA-like element is not found in other mammalian species such as the mouse (Cazzaniga *et al.*, 1994) and may account for differences in XOR activity between species. However human XOR gene expression, as in other mammals, is know to be activated in response to various stimuli.

In 1996 the 5′-flanking region of the human *xor* gene consisting of approximately 2000 nucleaotide base pairs was analysed for consensus sequences of potential promoter elements (Xu *et al.*, 1996). Potential binding sites for factors involved in inflammation and the acute phase response (a response characterised by a coordinated change in the production of plasma proteins acting to protect the host) were discovered. These sites included, four CCAAT/enhancer binding protein binding sites, three IL-6 responsive elements, a NF-κB site and potential tumour necrosis factor-, interferon-γ-, and interleukin-1-responsive elements. Indeed, the treatment of cell cultures with tumour necrosis factor-α (TNF-α), interleukin-1β (IL-1β), interleukin-6 (IL-6), and interferon-γ (INF- γ) have lead to the increase in *xdh* gene expression (Pfeffer *et* al., 1994; Page *et al.*, 1998). Therefore suggesting expression of *xdh* during an inflammatory episode and potentially a role for XOR in inflammation.

Further regulatory factors include the ubiquitous transcription factor, Nuclear Factor-Y (NF-Y), its binding to the human *xor* gene promoter sequence, CCAAT motif (Mantovani, 1998), has been demonstrated to enhance promoter activity (Martelin *et al.*, 2000). NF-Y functions through the interaction with TATA-binding proteins (Bellorini *et al.*, 1997), and promotes the binding of other TFs to nearby sequences (Mantovani, 1999). Also *xor* expression is under hormonal control. Treatment of cultured mouse mammary epithelial cells with prolactin and cortisol led to elevated levels of XOR mRNA (McManaman *et al.*, 2000).

2.2.4.1.3 Amino-Acid sequence

The amino acid sequence of human XOR protein contains 1333 residues that have been calculated to form a protein with a molecular weight of 146.6 kilodaltons (kDa) (Ichida *et al.*, 1993). The sequence length in other species is homologous, for example compared to the cow, mouse, rat, and insect, residue number only differs +/- two amino acids (Keith *et al.*, 1987; Amaya *et al.*, 1990; Terao *et al.*, 1992; Berglund *et al.*,

1996). Avian XDH on the other hand contains 1358 residues due to additional amino acids at the NH_2-terminal portion (Sato *et al.*, 1995).

Human XOR protein expression is highest in the liver, small intestine, and the lactating mammary gland (Linder *et al.*, 1999; Harrison, 2002). The presence of XOR in other tissues has been investigated, but results from separate studies are contradictory. However, using sensitive detection methods XOR has been found in other tissues including the heart, lung, kidney (Jarasch *et al.*, 1986). Significantly, XOR protein has been located in the human vascular endothelium (Jarasch *et al.*, 1981) and in the serum (Battelli *et al.*, 1999), therefore XOR is distributed throughout the body.

In the past the subcellular localisation of XOR was thought to be solely cytoplasmic (Ichikawa *et al.*, 1992). However, more recent studies have shown that intracellular XOR has a punctuate stain, suggesting vasicularisation, and may also have a perinuclear location (Rouquette *et al.*, 1998). Also, XOR is found in peroxisomes of rat heptaocytes (Frederiks and Vreeling-Sindelarova, 2002) and on the endothelial and epithelial cell surface of human cells (Rouquette *et al.*, 1998), probably by association with cell surface glycosaminoglycans (GAGs) (Adachi *et al.*, 1993).

The XOR enzyme, a non-glycosylated protein, exists as a homodimer forming a 290kDa protein (Enroth *et al.*, 2000). The two subunits are traditionally thought to be catalytically independent, however a recent study has shown that catalysis is "cooperative" in the homodimer subunits (Tai and Hwang, 2004). That is, in the presence of substrate at one active site affects the affinity of substrate binding at the other, and if both active sites where filled, conversion rate is increased by 2.95 fold compared to only one being filled.

2.2.4.2 Cofactor Synthesis and Insertion

A substantial part of all biological reactions rely on the action of cofactor-dependent enzymes. The final two steps of purine metabolism are no exception, as they require the catalytic activity of the cofactor-dependent enzyme XOR. For a full spectrum of catalytic activity, the XOR apoenzyme monomer requires the posttranslational insertion of four cofactors into four distinct redox centres; one molybdenum cofactor (MoCo), two non-identical iron-sulphur clusters (of the 2Fe-2S type) and one flavin adenine dinucleotide (FAD) moiety, forming the MoCo-, two Fe-S- and FAD-containing redox centres respectively (Massey *et al.*, 1969). In addition to cofactor insertion, the XOR enzyme can undergo another important posttranslational modification, the conversion of XDH to XO which can have significant bearing on catalytic activity. These processes are discussed below.

2.2.4.2.1 Molybdenum Cofactor Synthesis and Insertion

Molybdenum cofactor biosynthesis is an evolutionary conserved pathway essential for cofactor production for a diverse group of redox enzymes including, XOR, aldehyde oxidase, and sulphite oxidase (Kisker *et al.*, 1997). In humans, mutations in MoCo biosynthetic genes leads to MoCo deficiency (Reiss and Johnson, 2003), a disease that is manifested as severe neurological abnormalities, including seizures and attenuated brain growth that are mainly associated with lack of sulphite oxidase activity. Many of the details regarding the MoCo biosynthetic pathway have arisen from mutation studies in *Escherichia Coli* (Rajagopalan, 1997), however the enzymes involved in the human pathway have recently been described (Reiss and Johnson, 2003) and are summarised in Figure 12.

The amino acid sequences of the MoCo contact and insertion in human XOR have been indicated in Ichida *et al.*, 1993 but are described in more detail for Cape buffalo and cattle XOR (Wang *et al.*, 2002). The sequences given in Wang *et al.*, 2002 are highly conserved in human XOR (Ichida *et al.*, 1993) and it is likely that they correspond.

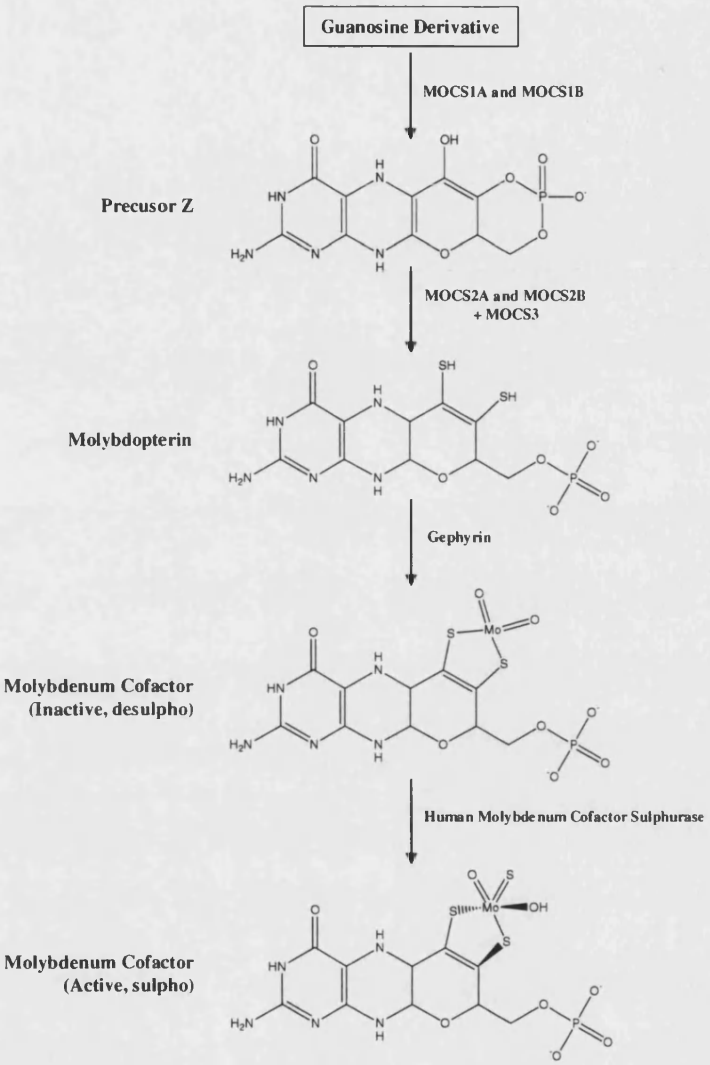

Figure 12. The Human Molybdenum Cofactor Biosynthesis Pathway.
The steps involved in MoCo biosynthesis can be split into three stages: i) Conversion of guanosine derivative into Precursor Z, ii) Transformation of Precursor Z into molybdopterin (MPT), and iii) Metal incorporation. The mechanism of Precursor Z formation (i) has not yet been determined, however it is known to be formed from a guanosine derivative and requires the MOCS1A and MOCS1B proteins for conversion. The transformation of Precursor Z into molybdopterin (MPT) (ii) is catalysed by MPT synthase (MOCS2A and MOCS2B), requires MPT synthase sulphurylase (MOCS3) for activity, and is responsible for the generation of a dithiolene group that is required for Molybdenum (Mo) insertion. The final step in MoCo biosynthesis is the incorporation of Mo into MPT (iii) and is catalysed by Gephyrin. In XOR the inactive "desulpho" MoCo is converted to its active "sulpho" form by human molybdenum cofactor sulphurase (Ichida *et al.*, 2001). This final conversion step is also required for active aldehyde oxidase, however active sulphite oxidase utilizes the desulpho MoCo form.

2.2.4.2.2 Iron-Sulphur Cluster Synthesis and Insertion

The formation of the Fe-S cluster is not spontaneous but requires a consortium of highly conserved proteins for their synthesis (Frazzon *et al.*, 2002). The proteins

required for the synthesis of Fe-S clusters for the metallocentres of the nitrogenase enzyme in *Azotobacter vinelandii* have been characterised and will be described here, as the process is applicable to Fe-S cluster synthesis in humans. Three key proteins are required for the synthesis process, NifS, NifU, and CysE1, but others form a greater repertoire (Frazzon *et al.*, 2002). The NifS protein uses L-cysteine as a substrate to form a NifS-cysteine persulphide complex that is thought to contain the source of sulphur for the Fe-S cluster. NifU, which is believed to provide a molecular scaffold for Fe-S synthesis may complex with NifS-cysteine persulphide which donates sulphur, thus forming the NifS-NifU-sulphur complex and following the acquisition of iron, Fe-S cluster synthesis occurs on the NifU scaffold. Finally, the CysE1 protein, a homologue of serine acetyltransferase (a rate limiting enzyme in cysteine biosynthesis), probably serves to boost the generation of L-cysteine (the substrate of NifS).

The insertion of the Fe-S cluster occurs by a mechanism that is currently not understood (Frazzon *et al.*, 2002). However, the amino acid sequence for the insertion of the two 2Fe-2S clusters has been described for XOR (Ichida *et al.*, 1993; Nishino and Okamoto., 2000).

Interestingly, cellular iron levels have been shown to be critical for XO activity. In cell culture and animal studies it has been demonstrated that iron depletion results in markedly reduced XO activity, which may be associated with an increase in the proportion of iron-lacking apoenzyme, and an increase in XO activity is measured when intracellular iron concentration is increased (Martelin *et al.*, 2002; Ghio *et al.*, 2002). These findings are of clinical importance as the release of cellular-stored iron following ischaemia (Huang *et al.*, 2001) could contribute to increased XO activity as part of XO mediated ischemia-reperfusion injury (McCord , 1985).

2.2.4.2.3 Flavin Adenine Dinucleotide Synthesis and Insertion

Flavin adenine dinucleotide is synthesised from riboflavin (Vitamine B_2) and two molecules of adenosine triphosphate (ATP) by a series of reactions catalysed by riboflavin kinase (EC 2.7.1.26) and FAD synthase (EC 2.7.7.2) (Berg *et al.*, 2001), see Figure 13. The Synthesis of Flavin Adenine Dinucleotide.

Details of the flavinylation process (FAD-cofactor insertion) of the XDH apoenzyme have not been published. However flavinylation of other enzymes, for example monoamine oxidase and vanillyl-alcohol oxidase, have been investigated and is believed to occur by an autocatalytic process (Edmondson and Newton-Vinson, 2001; Fraaije *et al.*, 2000). Although there is evidence for autocatalytic flavinylation of several enzymes, flavinylation of the mitochondrial matrix enzyme dimethylglycine dehydrogenase (Me_2GlyDH) precursor is strictly dependent on the presence of mitochondrial proteins. It is believed that a mitochondrial flavinylation stimulating factor is required to promote holo-Me_2GlyDH formation (Brizio *et al.*, 2002). As the XDH apoenzyme is expressed in the cytoplasm it is unlikely that a mitochondrial flavinylation stimulating factor is responsible for the flavinylation process. Therefore flavinylation of XDH apoenzyme is more likely to be via an autocatalytic process, although further more specific work is required in this area.

The amino acid residues that are believed to be required for FAD cofactor binding into the XDH apoenzyme have been predicted and are conserved between many species (Wang *et al.*, 2002). In comparison to the MoCo and Fe-S redox centres, naturally occuring FAD-lacking XOR (deflavo) has not so far been described.

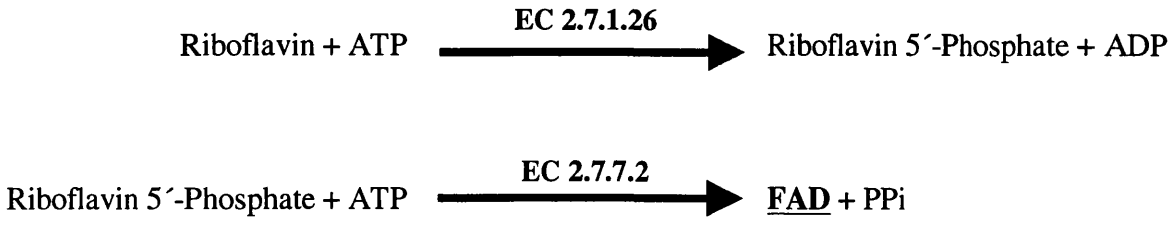

Figure 13. The Synthesis of Flavin Adenine Dinucleotide.

The synthesis of FAD from riboflavin is catalysed by riboflavin kinase and FAD synthase, respectively, and requires two molecules of ATP per FAD molecule formed.

2.2.4.3 Xanthine Dehydrogenase – Oxidase Conversion

Historically the XOR enzyme form, either XDH or XO, has been differentiated by the preference of oxidising substrate, either NAD^+ or O_2, respectively. As will be discussed in a later section (see Xanthine Oxidase and Vascular Pathology), the form of the XOR enzyme has a bearing on catalytic activity, physiological processes and the aetiology of several pathological conditions. The XOR protein is apparently expressed as XDH in tissues but can be converted, either reversibly or irreversibly, to XO by posttranslational modification (Stirpe and Della Corte, 1969; Della Corte & Stirpe, 1972).

XDH can be reversibly converted to XO via heating or oxidation of cysteine thiols of XDH to form intra-subunit disulphide bonds (Stripe and Corte, 1969; Corte and Stirpe, 1972), a process that is reversible by treatment with agents such as dithiothreitol (Corte and Stirpe, 1972). Structural and conformational analyses of the reversible conversion process have been investigated (McManaman and Bain, 2002). These studies have shown that significant disulphide bonding occurs in the N-terminal region, but not between the N- and C-terminal regions and it seems likely that the conversion process requires a structural change within the Phe 560-containing region. Residues Cys 535 and Cys 992 have been shown to be critical in the disulphide bond formation process but probably form bonds with so far unidentified cysteine residues.

XDH may also be irreversibly converted to XO via limited proteolytic cleavage (Stirpe and Della Corte, 1969) that can occur in the presence of proteases, low oxygen tension, and in response to inflammatory cytokines (Friedl, *et al.*, 1989; Meneshian and Bulkley, 2002). The determination of the crystal structure of both XDH and XO has allowed detailed studies into a structural-based mechanism of the irreversible conversion process (Enroth *et al.*, 2000). It was discovered that in XDH, two closely associated side chains, one around Phe 549 and the other from Arg 427, may be cut causing a structural rearrangement in another highly charged loop, Gln 423-Lys 433,

close to the FAD cofactor. The rearrangement of loop Gln 423-Lys 433 is thought to block the access of the NAD^+ acceptor substrate and alter the local electrostatic environment of the FAD cofactor, therefore reflecting the shift in preferred oxidising substrate from NAD^+ in XDH to O_2 in XO.

A study published in 2003 (Kuwabara *et al.*, 2003) confirmed that both reversible and irreversible XDH-XO conversion processes result in a conformational change in the active loop (Gln 423-Lys 433). It was also noted that the conformational change in the active loop opens a solvent channel leading to the FAD-moiety, allowing easier access for molecular oxygen.

2.2.4.4 Reactive Oxygen and Nitrogen Species Generation

The ability of XOR to generate a diverse range of RONS has been the driving force for the intense study of the XOR enzyme. The XOR-generation of the reactive oxygen species $O_2^{\cdot -}$, H_2O_2 (see Figure 14), and $^{\cdot}OH$, and the reactive nitrogen species $NO^{\cdot}$ and $ONOO^-$ have been demonstrated (Kuppusamy and Zweier, 1989; Millar *et al.*, 1998; Godber *et al.*, 2000) and are dependent on substrate availability in the microenvironment in which XOR is situated. The hypothesised scheme for $O_2^{\cdot -}$ and H_2O_2 generation during the re-oxidation of reduced XO with O_2 was confirmed in 1981 (Porras *et al.*, 1981) and is summarised in Figure 15. It was concluded that a fully reduced (six electron reduced) XO monomer could generate two H_2O_2 and two $O_2^{\cdot -}$ molecules.

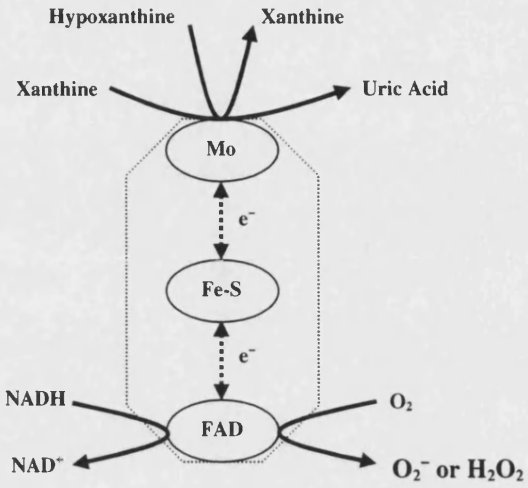

Figure 14. Generation of Reactive Oxygen Species by Xanthine Oxidase.

Highlighted are the redox centres (Mo = Molybdenum Cofactor; Fe-S = Iron-Sulphur Clusters; FAD = Flavin Adenine Dinucleotide Moiety) and substrates required for $O_2^{\cdot -}$ and H_2O_2 generation by XOR (Electron movements between the centres are represented by dashed-line arrows). Electrons involved in the reduction of XO are derived from the oxidation of hypoxanthine or xanthine, for example, and $O_2^{\cdot -}$ and H_2O_2 are generated via the oxidation of reduced XO by O_2. However, XOR also possesses NADH oxidase activity. Electrons donated to XOR during NADH oxidation may be used in the reduction of O_2 thus forming $O_2^{\cdot -}$ and H_2O_2 (Sanders *et al.*, 1997). Catalysis of this process is much quicker by dehydrogenase than the oxidase enzyme form. Also, XDH has been shown to generate $O_2^{\cdot -}$ and H_2O_2 in the presence of xanthine as a reducing substrate (Harris and Massey, 1997), although the generation of ROS occurs at about 16 % of the rate of XO catalysis.

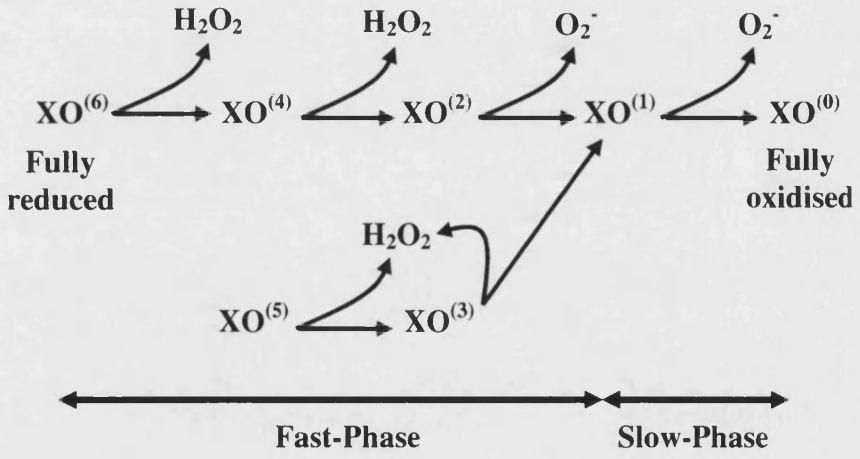

Figure 15. The Proposed Scheme of XO Oxidisation with Oxygen.

In each of the oxidation steps with O_2 (except the last), O_2 can bind to the fully reduced FAD-moiety and an electron is transferred, thus forming the flavin semiquinone-superoxide complex. When the enzyme contains more than two electrons, fully reduced FAD is regenerated so rapidly that a second electron can be passed to flavin semiquinone-superoxide complex, and form H_2O_2 before $O_2^{\cdot -}$ can diffuse out of the FAD-active site. The two electron oxidation process, forming H_2O_2, continues until $XO^{(2)}$ is formed. Following the subsequent binding of O_2 to $XO^{(2)}$ one electron is transferred to

form $O_2^{\cdot-}$, however fully reduced FAD cannot be regenerated, therefore $O_2^{\cdot-}$ is released. The $XO^{(1)}$ enzyme only has the potential to form the flavin semiquinone-active site that may generate $O_2^{\cdot-}$ but at a much slower rate than the previous oxidations. The release of H_2O_2 is confined to the fast-phase of enzyme-oxidation and the release of $O_2^{\cdot-}$ occurs at the close of the fast-phase and in the slow phase of oxidation (adapted from Porras *et al.*, 1981). The generation of ROS by NADH-reduced XOR follows the same scheme, but only from $XO^{(4)}$, as NADH will not reduce XOR beyond this point (Hunt and Massey, 1994). $^{(n)}$ represents the electron number contained within the enzyme.

The discovery of XOR-nitric oxide synthase and -peroxynitrite synthase activity has added further interest to the XOR enzyme. The initial discovery that XOR is capable of reducing organic and inorganic nitrate to nitrite, and nitrite to $NO^{\cdot}$, under hypoxic conditions, was made in 1998 (Millar *et al.*, 1998) (see Figure 16A). XOR as a peroxynitrite synthase has been the subject of a recent review (Millar *et al.*, 2002) and the process is reviewed in Figure 16B.

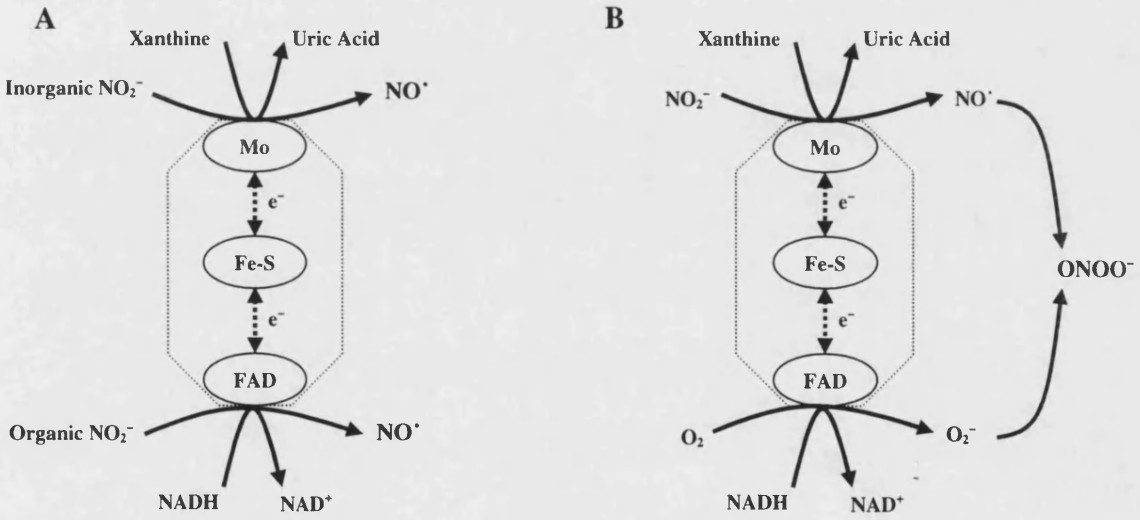

Figure 16. Reactive Nitrogen Species Generation by Xanthine Oxidoreductase.

A) The generation of $NO^{\cdot}$. Under hypoxic conditions, electrons required for the reduction of nitrate to nitrite and nitrite to $NO^{\cdot}$ are derived from either hypoxanthine, xanthine, or NADH oxidation. The reduction of inorganic nitrates and nitrites is thought to occur at the MoCo whereas organic nitrates and nitrites are likely to be reduced at the FAD cofactor (Millar *et* al., 1998; Doel *et* al., 2001). **B) The generation of $ONOO^-$.** Under hypoxic conditions XOR can generate $NO^{\cdot}$, however if O_2 concentrations rise to around 70 μM (Millar, 2004), pairs of electrons derived from either hypoxanthine, xanthine, or NADH, can be used to reduce nitrite or O_2 (the preferred substrate), therefore generating $NO^{\cdot}$ and $O_2^{\cdot-}$, respectively. $NO^{\cdot}$ and $O_2^{\cdot-}$ can react together forming $ONOO^-$ (Huie and Padmaja, 1993).

2.2.4.5 Xanthine Oxidase and Vascular-Associated Pathology

Chronic endothelial dysfunction is associated with several cardiovascular disorders including atherosclerosis, heart failure, and hypertension (reviewed in Li and Shah, 2004). The term vascular dysfunction covers a range of abnormalities but the most widely studied is the loss of $NO^{\cdot}$ bioavailability which can promote pro-inflammatory and pro-thrombotic environments, and reduces control over vascular tone (see Figure 17).

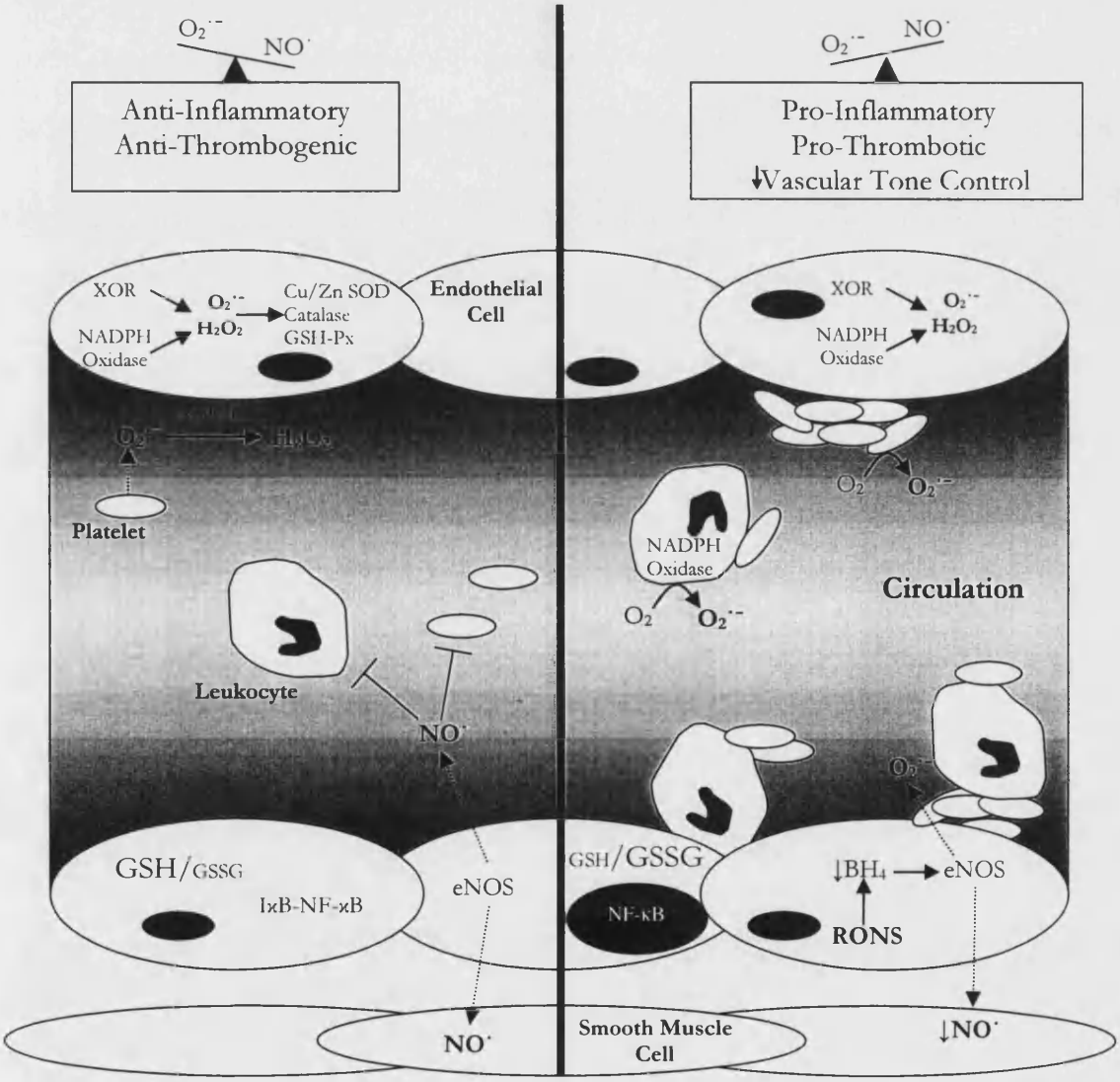

Figure 17. The Regulation of Vascular Tone, Inflammatory, and Thrombotic Environments by Reactive Oxygen and Nitrogen Species.

Under physiological conditions (left hand side of diagram) levels of $NO^{\cdot}$ greatly exceed those of $O_2^{\cdot-}$ and antioxidant systems are sufficiently expressed to detoxify comparatively low levels of ROS. Under these conditions the action of $NO^{\cdot}$ gives good control over vascular tone, and an anti-

inflammatory and anti-thrombotic environment. However, under periods of oxidative stress, i.e. when antioxidant systems are overrun by levels of ROS, the bioavailability of $NO^{\cdot}$ is reduced and results in loss of control over vascular tone and a pro-inflammatory and pro-thrombotic environment arises. $NO^{\cdot}$ bioavailability may be reduced by several ways: reduced expression of NOS, deficiency of NOS substrate or cofactors (especially BH_4), and by the fundamentally important mechanism, increased inactivation of $NO^{\cdot}$ by $O_2^{\cdot -}$ (adapted from Cooper *et al.*, 2002).

Although this section focuses on the role of XOR-generated ROS in vascular pathology, other ROS generators, for example NADPH oxidase and un-coupled NOS, are likely to contribute to the aetiology of the disease states mentioned.

2.2.4.5.1 Xanthine Oxidase and Heart Failure

Chronic Heart Failure (CHF) is a complex clinical syndrome characterised by reduced cardiac contractile function, increased vasoconstriction, decreased vasodilator response during exercise, and reduced peripheral perfusion (Linke *et al.*, 2003). These symptoms have previously been attributed to reduced cardiac myocyte function. However it is now believed that a vascular component contributes to heart failure, and the endothelium forms a potential therapeutic target for the condition (Linke *et al.*, 2003). The contributing vascular component is likely to be $NO^{\cdot}$, or lack of, as a reduction in the production of $NO^{\cdot}$ by eNOS (Smith *et al.*, 1996) or the depletion $NO^{\cdot}$ bioavailability by increased $O_2^{\cdot -}$ (Münzel and Harrison, 1999) are know to be involved in heart failure.

As the generation of $O_2^{\cdot -}$ has a significant function in the aetiology of CHF researchers have investigated the role of ROS-generating enzymes in this disease. The contribution of XO to CHF in human subjects has been investigated. In studies by Landmesser *et al.*, 2002 endothelial-bound XO and ecSOD levels were measured (via a bolus dose of heparin and subsequent release of the two enzymes into the plasma) in patients with CHF and controls. Compared to controls it was discovered that ecSOD activity was reduced in CHF patients and correlated with flow-dependent, endothelium-mediated vasodilation (FDD) (i.e. with reduced ecSOD a reduced vasodilatory response was observed), whereas XO activity was significantly increased

and was inversely related to FDD. Also, in CHF patients FDD response was improved by vitamin C administration, whereas no such improvement was seen in controls. These results suggest that increased XO-ROS generation and reduced ecSOD activity are responsible for increased oxidative stress and therefore endothelial dysfunction in CHF.

The beneficial effect of vitamin C in improving endothelial function in CHF patients has also been shown in Hornig *et al.*, 1998. However, evidence for a role of XO-generated ROS in CHF is better provided in experiments where the XOR-inhibitor allopurinol is given to patients (reviewed in Landmesser and Drexler, 2002). In Farquharson *et al.*, 2002, CHF patients were administered allopurinol or placebo and endothelial function was measured by a change in forearm blood flow (FBF) in response to acetylcholine stimulation (which should stimulate vasodilation and therefore increased blood flow). Allopurinol treatment significantly improved FBF and reduced oxidative stress in the vasculature, and therefore improves endothelial dysfunction in CHF patients. These findings are supported by other studies suggesting improved peripheral vasodilator capacity with allopurinol treatment (Doehner *et al.*, 2002).

2.2.4.5.2 Xanthine Oxidase and Coronary Heart Disease

Coronary heart disease (CHD) is a condition where the vascular supply to the heart is impeded. This may impair the supply of oxygenated blood to cardiac tissue sufficiently to cause myocardial ischemia, which if prolonged may present with death of cardiac tissue or with pain (angina) if reversible. A reduction in blood supply may be caused by thrombosis, spasm of coronary arteries, or widespread atherosclerosis. Of these causes, the vast majority of CHD occurs in patients with atherosclerosis of the coronary arteries.

The formation of an atherosclerotic plaque is responsible for the narrowing of the blood vessel and reduction in blood flow that can be responsible for myocardial

ischemia. Plaque formation is initiated by the transendothelial migration of monocytes and the accumulation of "fatty streaks" which contain lipid rich macrophages and T lymphocytes. Following the formation of "fatty streaks" smooth muscle cells may migrate into the tunica intimae and proliferate. The smooth muscle cells together with fibroblasts can secrete collagen, proteoglycans, elastin, and glycoproteins that form a fibrous cap termed a plaque (Walker and Edwards, 2003).

Traditional causes of atherosclerosis include hypercholesterolemia and heavy smoking that both affect the endothelium by increasing the generation of ROS. Increased ROS production decreases $NO^{\cdot}$ bioavailability, which leads to vascular dysfunction and to a proinflammatory state, as summarised in Figure 17. The contribution of NADPH oxidase to the formation of the atherosclerotic plaque is reviewed in Li and Shah, 2004, however XO has also been implicated in this pathology. Spiekermann *et al.*, 2002 compared XO activities in CHD patients v's controls. Subcellular fractionation of vessel homogenates, and heparin injection into subjects, revealed that endothelial-bound XO activity was significantly increased in CHD patients compared to controls, (a study comparable to that performed by Landmesser *et al.*, 2002 in the above section). Also, treatment of patients with vitamin C significantly improved FDD whereas as no change was seen in controls, which was also discovered in Landmesser *et al.*, 2002. Therefore, these findings underline the suggestion that endothelial dysfunction due to reduced $NO^{\cdot}$ bioavailability is common in the aetiology of various vascular pathologies.

In support of a role for XO in CHD, other publications suggest XO provides a link between the traditional causes of atherosclerosis (i.e. heavy smoking and hypercholesterolemia) and endothelial dysfunction that can lead to the disease itself. In heavy smokers, inhibition of XO by the administration of allopurinol improved endothelial dysfunction, whereas no such effect was seen in controls (Guthikonda *et al.*, 2002). Also, the level of circulating XO in hypercholesterolemic rabbits is

increased two-fold and is associated with reduced endothelial-dependent vasorelaxation. Due to improved vasorelaxation in the isolated aorta following heparin, allopurinol, or SOD treatment, it was suggested that increased circulating XO results in an increase in endothelial-bound enzyme that interferes with NO·-dependent relaxation via $O_2^{\cdot -}$ generation (White *et al.*, 1996).

2.2.4.5.3 Xanthine Oxidase and Acute Respiratory Distress Syndrome

Inflammation of the pancreas, pancreatitis, can be classified as acute or chronic. Acute pancreatitis is usually caused by excess alcohol consumption or by gallstones and is sudden, lasts for a short period of time, and resolves itself. Whereas chronic pancreatitis does not resolve itself and results in the slow destruction of the pancreas. Acute pancreatitis is often associated with systemic complications including pulmonary dysfunction, observed in about 50% of human patients (Folch *et al.*, 2000). Respiratory dysfunction is often mild and reversible but in one third of cases can lead to Acute Respiratory Distress Syndrome (ARDS), the most important factor contributing to death in these patients (Willemer *et al.*, 1991).

The development of the inflammatory response in the lung is reliant on interactions of circulating leukocytes with the pulmonary vascular endothelium, and the subsequent activation and migration of leukocytes into the lung parenchyma. As mentioned in section 1.5.2., this process is controlled by interactions between leukocyte and endothelial cell receptors and ligands. P-selectin, found integrated into the surface of WPBs, is one of the first cell surface receptors to be expressed on the endothelial cell surface in response to inflammatory stimuli, and is responsible for the initial leukocytes binding events.

Until recently the mechanism by which inflammation in the pancreas leads to secondary inflammation in the lung was unknown, however it was thought to be a neutrophil and $O_2^{\cdot -}$-mediated event (Guice *et al.*, 1989; Inoue *et al.*, 1995). Studies have suggested that XO-generated ROS can induce lung damage *in vivo* and

neutrophil adhesion to cultured endothelial cells (Johnson *et al.*, 1981; Ichikawa *et al.*, 1997), and a potential mechanism that describes circulating XO as a link between the two pathologies has been suggested in a series of papers (Folch *et al.*, 1998; 1999; 2000). In the Folch *et al.* investigations, pancreatitis was induced in rats by an injection of sodium taurocholate into the biliopancreatic duct. Following pancreatitis induction, P-selectin expression on the endothelium of various organs was measured and was shown to be significantly upregulated in the lung and pancreas only, whereas ICAM-1 expression was unaffected (Folch *et al.*, 1999). As predicted, the upregulation of P-selectin appears to be responsible for neutrophil accumulation seen at the lung, as this was attenuated by the administration of anti-P-selectin during pancreatitis induction (Folch *et al.*, 1999). The upregulation of P-selectin expression was shown to be by an oxidant-mediated process in experiments where the administration of antioxidants (SOD and catalase) reduced P-selectin expression to control levels (Folch *et al.*, 2000). Results indicate that three hours after pancreatitis induction (the time it takes for inflammation to be seen at the lung) there is a significant rise in circulating XO activity (Folch *et al.*, 1998). The induction of P-selectin expression and neutrophil infiltration in the lung was attributed to the rise in circulating XO as this process was inhibited with the administration of the specific XO-inhibitor oxypurinol (Folch *et al.*, 1998; Folch *et al.*, 1999). Further analysis into the mechanism of XO-upregulated P-selectin expression and neutrophil binding was carried out in Folch *et al.*, 2000 and is reviewed in Figure 18.

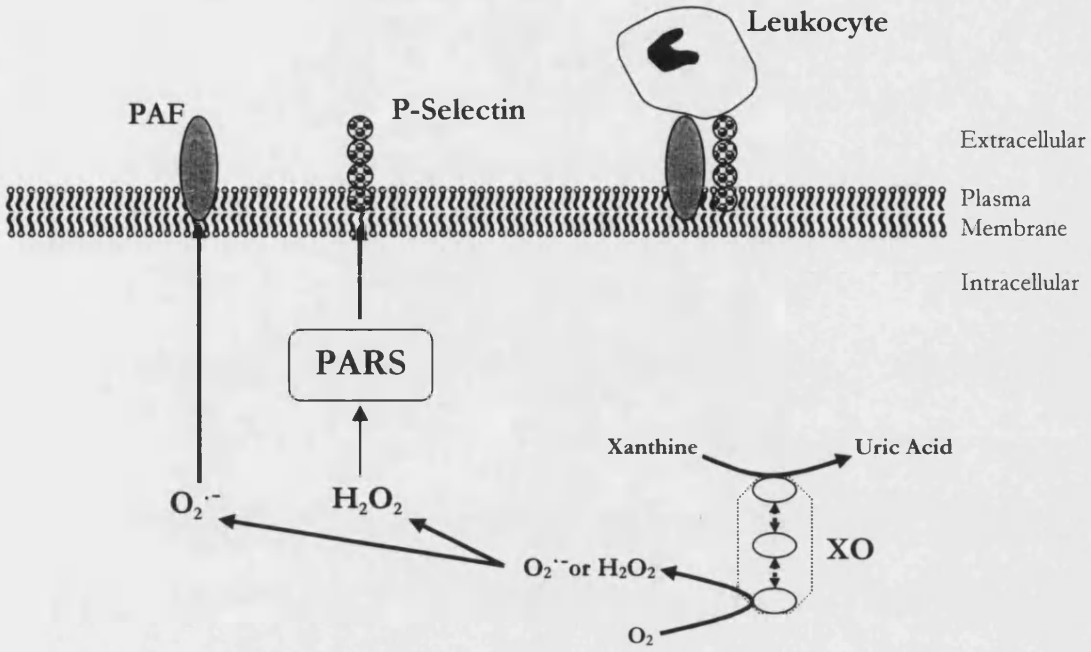

Figure 18. Xanthine Oxidase Regulated Expression of Endothelial Adhesion Molecules.

The suggested mechanism whereby XO-generated ROS upregulate the expression of endothelial-leukocyte receptors. XO catalysed ROS induce the cell-surface expression of platelet activating factor (PAF) and P-selectin, which subsequently bind circulating leukocytes. PAF expression is likely to be regulated by $O_2^{\cdot -}$, whereas H_2O_2 can upregulate P-selectin expression via a mechanism involving poly (ADP-ribose) synthetase. Extracellular expression of ROS species, especially the membrane-permeable ROS H_2O_2, could also contribute to this process. (Adapted from Folch *et al.*, 2000)

But why is the lung affected by the rise in circulating XO more so than other organs of the body? It has been hypothesised that as XO requires molecular oxygen to generate ROS, the concentration of free oxygen in the lung capillaries is sufficient for XO-ROS-mediated P-selectin expression. In the blood and in other organs the concentration of free oxygen is less and is not sufficient for such a response. In a recent paper with Folch, E. (Granell *et al.*, 2004) this hypothesis was investigated. Pancreatits was induced as in previous experiments, however rat lungs were cannulated and one was ventilated with air and the other with nitrogen. P-selectin expression and inflammation were compared between the lungs. Results demonstrated that in the absence of oxygen, XO-mediated P-selectin expression did not occur and inflammation was significantly reduced, indicating that only free-oxygen concentrations in the lung are sufficient to cause this response.

Acute pancreatitis is not the only pathological example where an increase in circulating XO-activity occurs, circulating levels of XO also increase in liver disease (Battelli *et al.*, 2001), thermal injury (Friedl *et al.*, 1989), hemorrhagic shock (Tan *et al.*, 1993), and ischemia-reperfusion injury (Terada *et al.*, 1992; Koike *et al.*, 1993) which can lead to secondary pathologies, especially in the lung.

2.3 Hypothesis

As mentioned in the introductory chapters XO exists in a circulatory form. The quantity of circulating XO in a healthy human has been measured in several publications but results vary substantially (reviewed in Harrison *et al.*, 2002). However there is agreement that levels of circulating XO increase in several disease states (as mentioned in section 2.2.4.5), for example, in liver disease such as chronic hepatitis, levels rise to an average of 7.6μg/ml compared to a normal of <1 μg/ml, as assessed by enzyme-linked immunosorbent assay (ELISA) (Battelli *et al.*, 2001). But the question that has not been answered in studies that provide evidence for increased circulating XO is: how does XO enter the circulation? Researchers have speculated that XO maybe released from ailing cells rich in cytosolic enzyme (Meneshian and Bulkley, 2002; Wang *et al.*, 2002), similar to enzymes such as alkaline phosphatase (AP) (Kristensen, 1994). However levels of AP, transaminases, or necrosis in histological sections do not correlate with circulating XO in the liver diseases cirrhosis and chronic hepatitis for example (Battelli *et al.*, 2001). But, another hypothesis for the source of circulating XO exists.

The endothelium is a rich source of XO (Jarasch *et al.*, 1981; Jarasch *et al.*, 1986), and studies by Partridge *et al.*, 1992 have demonstrated the release of XO from microvascular endothelial cells (MVEC). This paper shows the constitutive release of XO from MVEC independent of cell death, which is reduced under hypoxic conditions, therefore they suggest that XO is released by an active process. However

comparisons between controls and test sample in this paper should be taken with caution as the data presented only show standard error from the mean values, and do not show *n* numbers or statistics. This was a limited study where no attempt was made to look further at the release mechanism, but nonetheless it serves as a good indication of a constitutive XOR-release process. Other proteins in the endothelium are released by constitutive processes, for example vWf (see section 1.4.3) but release may also be stimulated, could this be the same for XO? Inflammatory agents can induce XOR expression (see section 2.2.4.1.2) and elevation in circulating XO occurs in several disease states, particularly in inflammatory pathology. Can inflammatory agents induce the release of XO from the endothelium?

Hypothesis: The vascular endothelium can release xanthine oxidoreductase by constitutive and controlled mechanisms.

Chapter 3. Results: Characterisation of Xanthine Oxidoreductase Expression in a Vascular Model

3 Results: Characterisation of Xanthine Oxidoreductase Expression in a Vascular Model

3.1 Introduction

Once thought to be an inert lining of the blood vessel, the vascular endothelium is now know to contribute a vast number of vascular processes, a selection of which are reviewed in the introductory chapters. The emergence of the human umbilical vein endothelial cell (HUVEC) as an endothelial model has allowed scientists to rapidly study endothelial processes and has certainly contributed to the vast number of publications with reference to the endothelium (Nachman and Jaffe, 2004). The isolation and culture of endothelial cells was probably achieved in 1958 (Ingenito, 1958), however at that time there was no way of verifying an endothelial cell culture, except by morphological assessment. Five years later the culture of HUVECs may have been accomplished (Maruyama, 1963), but the means to positively identify cells from endothelial origin were still not available. However this would soon change, an antihaemophilic factor (now know as von Willebrand factor) was discovered in endothelial cells that was not expressed in smooth muscle cells or fibroblasts (Hoyer *et al.*, 1973). This discovery quickly led to the verified isolation of endothelial cells from the human umbilical vein (Jaffe *et al.*, 1973; Jaffe *et al.*, 1973a), the HUVEC.

As mentioned in the hypothesis section microvascular endothelial cells express active XOR. However, the HUVEC (a macrovascular cell) was chosen as a vascular model for the analysis of XOR release, and this choice was selective. Firstly, cells are isolated from human tissue, therefore results using this model would be more applicable to human physiology/pathology compared to the bovine cells used in previous studies (Partridge *et al.*, 1992). Secondly, the source of cells is easily accessible (once Ethical Approval is aquired) as the umbilical cord is essentially a waste product. Finally, the HUVEC model maintains many important properties of the microvascular endothelium and therefore should behave in a similar fashion compared to previous investigations (Partridge *et al.*, 1992). For example, with respect to inflammation,

HUVECs contain WPBs and P-selectin and their expression, along with other adhesion molecules, can be upregulated by inflammatory stimuli (Kagawa and Fujimoto, 1987; Sugama *et al.*, 1992; Jones *et al.*, 1993).

3.2 Chapter Aim

To investigate the hypothesis set, the use of a vascular endothelial model was essential. The aim of this chapter is to characterise the vascular endothelial model chosen for investigations, the HUVEC, with emphasis on xanthine oxidoreductase expression. As in Jaffe *et al.*, 1973, isolation of cells from endothelial origin will be confirmed using vWf as a positive marker. Expression of the XOR gene and protein will be assessed by the polymerase chain reaction and antibody-based techniques, respectively.

3.3 Principles, Materials, and Methods

Frequently used protocol are described below, however less frequently used methods, as indicated below, can be found in the appendix.

3.3.1 Tissue Preparation and Haematoxylin and Eosin Stain

3.3.1.1 Materials

DePeX Mounting Medium, Iso-pentane; Superfrost Plus Microscope Slides (VWR International Ltd, Dorset, UK); Tissue-Tek (Sakura. Berkshire, UK); Harris Haematoxlin, Eosin (Sigma Aldrich Company Ltd. Dorest, UK).

3.3.1.2 Protocol

A beaker of iso-pentane was chilled in liquid nitrogen. Tissue-Tek was spotted onto a cork disk and was submerged in the iso-pentane for approximately 5 minutes after which time the Tissue Tek was sufficiently hardened. The cork disk was removed and a tissue sample, approximately 0.5cm^2, was pressed into the set Tissue-Tek. The sample was then covered in Tissue-Tek and was incubated in the chilled iso-pentane for about 5mins, or until all Tissue-Tek was solidified. Following this preparation, the sample mounted onto the cork-disk was stored at -70°C for several hours to ensure the sample was completely frozen.

Using a Cryostat (Bright Instruments Company Ltd, Huntingdon, UK) the frozen sample was sectioned into 5μm slices which were immediately placed onto microscope slides. Sections were then stained with Haematoxylin and Eosin using the protocol given in Appendix I Section 8.1. Samples were viewed under a Zeiss Axioscope microscope and images were captured using the Zeiss KS300 program (Carl Zeiss Ltd. Hertfordshire, UK). Following the above mentioned staining protocol cell nuclei appear blue and cytoplasmic structures pink-red.

3.3.2 Cell Isolation and Culture

The human umbilical cord contains two arteries and one vein, the vein being the largest of the three blood vessels. Isolated HUVECs were used as a model for the vascular endothelium.

3.3.2.1 HUVEC Isolation and Culture Materials List

Cell Disociation Solution, Collagenase (Type II from *Clostridium histolyticum*) (Sigma Aldrich Company Ltd. Dorest, UK). 95% CO_2 in air (BOC Gases. Guildford, UK). Endothalial Cell Growth Medium, Proliferating HUVECs (PromoCell. Heidelberg, Geramny). Glass cover slips (VWR International Ltd. Dorset, UK). HANKS balanced salt solution (HBSS; Invitrogen. Paisley, UK). Syringe filters (0.22μm) (Fisher Scientific UK Ltd. Leicestershire, UK). Tissue culture plastics: T25 filter-cap flasks, 12-well plates, 15 and 50ml centrifuge tubes (Triple Red Ltd. Oxfordshire, UK).

3.3.2.2 HUVEC Isolation Protocol – Collagenase Digestion

The isolation of HUVECs by collagenase digestion is a commonly used technique (Jaffe *et al.*, 1973; Visher *et al.*, 2000; Kuhlmann *et al.*, 2005). Umbilical cords were kindly donated by mothers attending the local maternity ward (with full ethical and R&D approval; Bath Local Research Ethics Committee reference number BA635). Cords were stored at 4°C for no longer than three days before HUVEC isolation under sterile conditions. Before the introduction of cannula into one end of the umbilical vein, any punctured or clamped regions of the cord were removed. Cannulated umbilical veins were washed using HBSS until the expelled medium ran true to its starting colour (i.e. the majority of cord blood was removed). HUVECs were dissociated from the vessel wall by collagenase digestion. The cord was blocked at the non-cannula-inserted end and 37°C filter-sterilised 1mg/ml collagenase in HBSS was used to fill the umbilical vein (as shown in Figure 19). The collagenase filled cord was incubated at room temperature for 30-45mins. Following this incubation the collagenase solution was collected, and the vein was washed once with HBSS to ensure a full harvest of endothelial cells. HUVECs were brought out of

suspension by centrifugation at 1600rpm for 5mins at room temperature. Following centrifugation the supernatant was removed and the cell pellet was resuspended in Endothelial Cell Growth Medium (ECGM).

Figure 19. The Cannulated Human Umbilical Cord.

Cannulae were inserted into the human umbilical cord vein. Following initial washing steps the non-cannula end was blocked off and the human umbilical cord vein was filled with a collagenase solution.

3.3.2.3 HUVEC Culture Protocol

Following isolation the HUVEC culture was routinely grown in T25-flasks (one flask per cord) with 5mls ECGM, incubated at 37°C and 5%CO_2 in air, in a Jencons Millenium CO_2 incubator (Jencons Ltd. Bedfordshire, UK). The initial culture was termed the primary culture. Alternatively HUVECs were aquired from PromoCell, but were incubated and treated under the same conditions as isolated HUVECs (Note: HUVECs purchased from Promocell were passage 1, not primary cultures). When the HUVECs reached confluence (100% monolayer covering of the flask base) they were split 1-to-5 into T25-flasks by the following process. Confluent HUVECs were dissociated from each T25-flask using 3mls non-enzymic Cell Dissociation Solution (CDS), incubated at 37°C for about 20mins (tapping the flask occasionally helped the dissociation process), and cells were pelleted by centrifugation as previously decribed. This culture, Passage One (P1), was grown under the same conditions as the primary isolation. Upon reaching confluence, P1 cells were split, as above, into 12-well plates (with, flame-sterilised 13mm diameter glass coverslips number 1 thickness for cell staining experiments, or without coverslips, for HUVEC protein secretion experiments), one flask per plate, and were incubated with 1ml

ECGM per well in the same conditions as above. These cells, Passage Two (P2), were used in all HUVEC experiments. At all stages, medium was changed three times a week.

3.3.2.4 Mean Generation Time

In HUVEC experiments (and bacterial experiments in a later results chapter), the mean generation time for the cell population was calculated. The mean generation time may be calculated from the following equation (Equation 1) using data from the exponential growth phase of cell division.

$$k = n/t$$
$$= (\log N_t - \log N_0) / 0.301t$$

If the population doubles $t = g$, therefore $Nt = 2N_0$, which can be substituted into the above equation:

$$k = (\log(2N_0) - \log N_0) / 0.301g$$
$$= (\log 2 + \log N_0 - \log N_0) / 0.301g$$
$$k = 1/g$$

Therefore the mean generation time is the reciprocal of the mean growth rate constant (k):

$$g = 1/k$$

Equation 1. Calulation of the Mean Generation Time of a Cell Culture.

Where g = mean generation time; k = mean growth rate constant; n = number of generations in time t; N_0 = the initial population number; N_t = the population at time t; t = time (Prescott *et al.*, 1996).

3.3.3 MDA-MB-231 Culture

The immortalised human mammary epithelial cell line MDA-MB-231 served as a positive control for the expression of XOR.

3.3.3.1 Materials List

Cryo 1°C Freezing Container and 1ml NUNC Cryo-tubes (Fisher Scientific UK Ltd. Leicestershire, UK), Dimethyl Sulphoxide (DMSO; Sigma Aldrich Company Ltd. Dorest, UK), Dulbecco's Modified Eagle's Medium (DMEM) (Invitrogen. Paisley, UK), Foetal calf serum (FCS) (GlobePharm Ltd. UK), MDA-MB-231 (LGC Promochem. Middlesex, UK), Pencillin/Streptomycin (Invitrogen. Paisley, UK), Normal human dermal neonatal fibroblasts (American Type Culture Collection, UA, USA).

3.3.3.2 Culture Protocol

MDA-MB-231 and fibroblasts were routinely grown in T25 flasks in 5mls DMEM + 10% FCS + Penicillin and Streptomycin 20U/ml and 20μg/ml, respectively, and were incubated at 37°C and 5%CO_2. Medium was changed two times a week until cells reached desired confluence and as the MDA-MB-231 cell line is immortalised passage number was not recorded. For cell staining, cells were passaged onto 13mm diameter cover slips in 12-well plates, as previously described, and were incubated in 1ml of the DMEM-based medium.

3.3.3.3 MDA-MB-231 Cell Storage

MDA-MB-231 cell stocks were routinely stored in liquid nitrogen. Confluent T25-flasks were harvested by non enzymatic cell dissociation solution treatment. The cell pellet was then resuspended in a freeze-down medium, consisting of 50% FCS, 40% growth medium and 10% DMSO. 1ml volumes of freeze-down medium were used to resuspend the pellet from each T25 flask of cells. Cell suspensions were stored in NUNC Cryo-tubes and were frozen to -70°C, -1°C per min, in the Cryo 1°C Freezing Container, and were then placed in liquid nitrogen storage. Cells were resurrected rapidly by placing NUNC Cryo-tubes under warm running water. Cells were washed once by centrifugation of the cell suspension at 1600rpm for 5mins and the subsequent pellet resuspended in normal DMEM-based medium.

3.3.4 Trypan Blue-Exclusion Cell Viability Counts

Trypan blue does not permeate viable cells which appear clear under the light microscope, whereas dead/compromised cells allow entry of trypan blue and appear blue in colour.

3.3.4.1 Materials List

Accutase (TCS Cellworks LTD. Buckinghamshire, UK), Trypan Blue (Sigma Aldrich Company Ltd. Dorest, UK).

3.3.4.2 Trypan Blue Exclusion Cell Count Protocol

HUVECs grown in 12-well plates or T25-flasks were dissociated by incubation with 500µl or 2000µl Accutase, respectively, per well/flask at 37°C, 5%CO_2 for about 5mins. The resulting cell suspension was mixed 1:1 with trypan blue and cells were counted using a Neubauer double rhodium coated counting chamber (Fisher Scientific UK Ltd. Leicestershire, UK). Approximately 15µl of the cell/trypan blue mixture was applied to fill the counting chamber and, blue (dead) and clear (viable) cells were counted from five of the nine 1mm^2 squares on the counting chamber (as indicated in Figure 20). The average number of cells per square was used in the calculation of the number of cells per ml of the starting cell suspension, as shown in Equation 2.

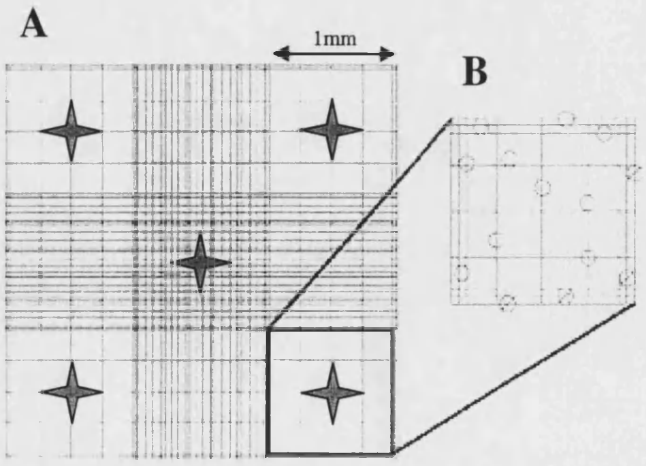

Figure 20. Cell Counts Using the Haemacytometer.

The typical grid layout of the haemocytometer, divided into nine 1mm squares. Cell counts were taken from the five highlighted squares (as indicated by a red stars in A). Only cells in contact with

two of the four boundaries of each square were counted (as indicated in B, crossed cells were not counted)

Viable cells/ml = Mean cells per square x 2 x 10 000

Equation 2. Cell Viability Count.

Following trypan blue-exclusion protocol cells viable cell counts could be calculated using this equation The percentage of viable cells could be calculated after repeating the above calculation for trypan blue stained cells only. (x2: dilution factor, trypan blue dilution, x10 000: volume correction from volume of 1mm square under cover slip, 10^{-4}ml, to 1ml).

3.3.5 SDS-PAGE, Western and Dot Blot

The immunodetection of proteins were assessed using the sensitive Western Blot and Dot Blot techniques.

3.3.5.1 Materials List

ECL™ Western Blot Detection Reagents, Hybond™-C extra nitrocellulose (Amersham Biosciences UK Ltd. Buckinghamshire, UK). Kodak BioMax XAR Film (VWR International Ltd. Dorset, UK). Polyoxyethylene sorbitan monolaurate (Tween 20) (Sigma Aldrich Company Ltd. Dorest, UK). Xanthine Oxidase (Biozyme, UK).

3.3.5.2 Western Blot Protocol

All materials and recipes for sample buffer, running buffer, blotting buffer, washing buffer, blocking buffer, the stacking gel, and the resolving gel are shown in Appendix I 8.2. All antibodies are shown in Appendix I 8.3.

Protein samples and the molecular weight marker were mixed one-to-one with reducing sample buffer and were heated to 100°C for 5mins. Sample proteins were separated by sodium dodecylsulphate polyacrylamide gel electrophoresis (SDS-PAGE) at 100V for about 2hrs or until the gel-front neared the end of the resolving gel. Following SDS-PAGE, proteins were transferred onto nitrocellulose under reducing conditions at 150mA for 2hrs.

The nitrocellulose-bound proteins were prepared for immunodetection by a 1hr incubation in blocking buffer at room temperature with continuous agitation (this

step could also be performed overnight at 4°C; all further steps were performed at room temperature with continuous agitation). Blocking buffer was discarded and replaced with the 1° antibody of choice, diluted in fresh blocking buffer (for vWF and XOR analysis a 1 in 5000 and a 1 in 1000 dilution of the 1° antibody was used, respectively). The nitrocellulose was incubated with the 1° antibody for 1-1.5hrs (in some control experiments partially saturated 1° antibody was used, this was achieved by incubating the antibody with an equal amount of antigen (w/w) for 5min at room temperature before applying to nitrocellulose). Unbound 1° antibody was removed by 6 x 5mins wash steps in excess washing buffer. To enable visualisation of the antigen-bound 1° antibody, the nitrocellulose was incubated with a 1 in 200 dilution 2°-horse radish peroxidase (HRP)-conjugated antibody, prepared in blocking buffer, for 1hr. Excess 2° antibody was removed by 6 x 5mins wash steps in excess washing buffer. Following the wash steps, the nitrocellulose membrane was bathed in ECL detection reagents (prepared using manufacturers instructions) and luminescence was detected on Kodak film (the principle behind the use of the ECL reagents in visualising antigen is shown in Section 3.3.5.4)

3.3.5.3 Dot Blot Protocol

The main difference between the Dot and Western Blot protocols is the method of protein transfer onto the nitrocellulose. In the Dot Blot, SDS-PAGE is not necessary, instead proteins are transferred onto nitrocellulose by applying samples to a Dot Blot apparatus (Jencons Ltd. Bedfordshire, UK) attached to a vacuum. The Dot Blot has advantages compared to the Western blot as it takes a shorter time to run, and proteins can be concentrated to one small space, but has the disadvantage that the molecular weight of the protein detected cannot be calculated.

Blotting paper and nitrocellulose where soaked in transfer buffer before assembling the Dot Blotter (see Figure 21). See Western Blot protocol for the visualisation of bound protein.

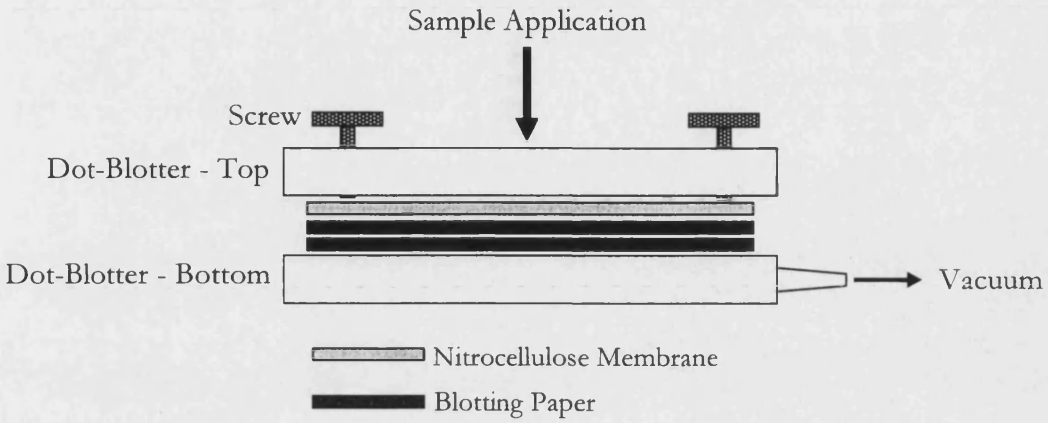

Figure 21. The Assembled Dot-Blotter.

Blotting paper and nitrocellulose were soaked in transfer buffer before assembly as shown in this figure. The screws were tightened and the vacuum was applied for approximately one minute before sample application. The top part of the dot-blotter is arranged in a 96-well format, samples were applied to wells with the vacuum running.

3.3.5.4 The ECL-Reagent Principle

In combination with a relevant HRP-conjugated antibody, the ECL reagent detection system provides a non-radioactive detection method for immobilised antigen. The ECL system is based on luminol-chemiluminescence for antigen detection, the process is summarised in Figure 22.

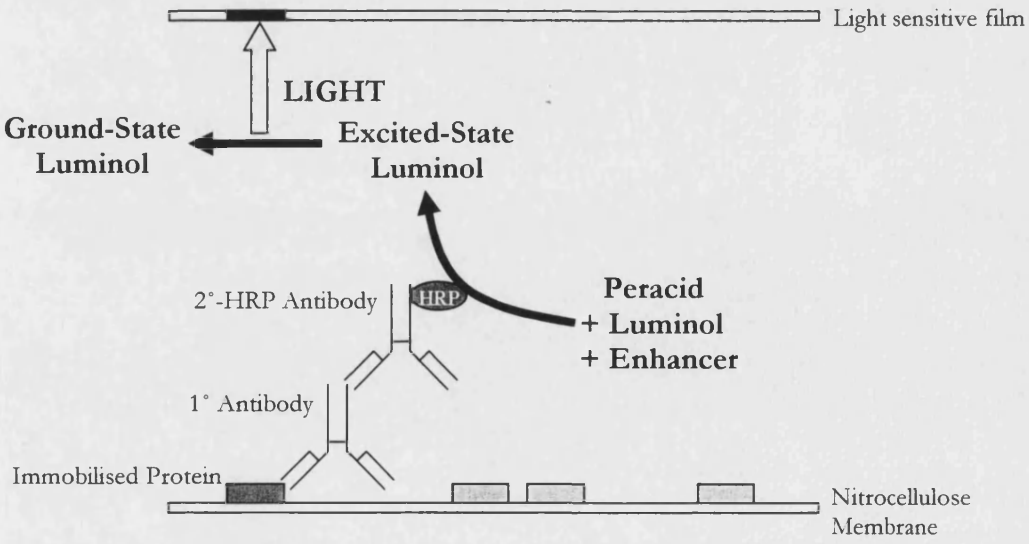

Figure 22. The ECL Reagent System in the Detection of Immobilised Antigen.

Following the incubation of nitrocellulose-immobilise antigen with the relevant 1° and 2° HRP-conjugated antibody the ECL reagents are employed. In the presence of the peracid substrate luminol is oxidised by HRP. Oxidised luminol is in an "excited-state" which decays to "ground-state" via a light emitting/luminescent pathway, which may be detected using light-sensitive film. In the presence of chemical enhancers such as phenols, the intensity and duration of luminescence is increased greatly. The generation of luminescence in the ECL system peaks at around 5-20mins and the half life of decay is about 60mins (Adapted from manufacturers information).

3.3.6 Immunofluorescent and Fluorescent Labelling of Cells

3.3.6.1 Fluorescence – The Principles

Fluorescent molecules or fluorophores are widely used in research, especially in imaging and quantification studies. When sufficiently excited by a certain wavelength of light, fluorophores emit fluorescent light at an intensity proportional to the amount of fluorophore present, a property that is exploited for research applications. As fluorescence-based techniques are widely used in this thesis, some background information on this subject will be mentioned here.

3.3.6.1.1 Atomic Structure - Orbitals

A volume of space around an atom's nucleus where an electron is likely to be found is termed an orbital. Several different types of orbitals exist including *s*, *p*, and *d* (see Figure Figure 23). Orbitals are organized into different layers, or shells, that increase successively in both size and energy. Shells contain different numbers and types of orbital, as summarised in Figure 24.

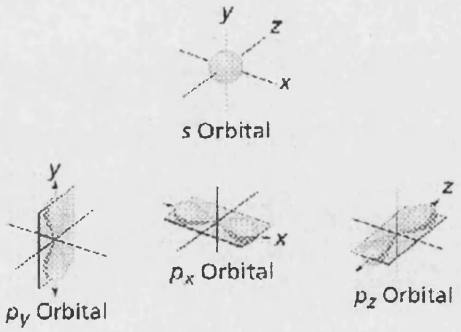

Figure 23. The Orbitals of an Atom.

The *s* orbitals are spherical with the nucleus at the centre; *p* orbitals are dumbbell-shaped, whereas the *d* orbitals (not shown) are usually cloverleaf in shape.

Shell	Orditals
3rd Shell (18 electron capacity)	3*d*, 3*p*, 3*s*
2nd Shell (8 electron capacity)	2*p*, 2*s*
1st Shell (2 electron capacity)	1*s*

Figure 24. The Electron Energy Levels within an Atom.

Each consecutive shell increases in both energy and electron capacity. Not shown in this diagram is the 4*s* energy level that lies between 3*p* and 3*d*.

3.3.6.1.2 Fluorescence - Excitation

During excitation a fluorophore absorbs a photon of light. If the energy from the absorbed photon is sufficient an electron will "jump" from a lower energy orbital to a higher one, the fluorophore is said to have been excited from ground-state energy level (S_0) to an excited-state energy level (S_n) (see Figure 25). The probability that a fluorophore will be excited is dependent on the wavelength of light that is absorbed, i.e. certain wavelengths will more efficiently excite certain fluorophores. This information may be presented on an Excitation and Emission Spectra, an example is shown in Figure 26.

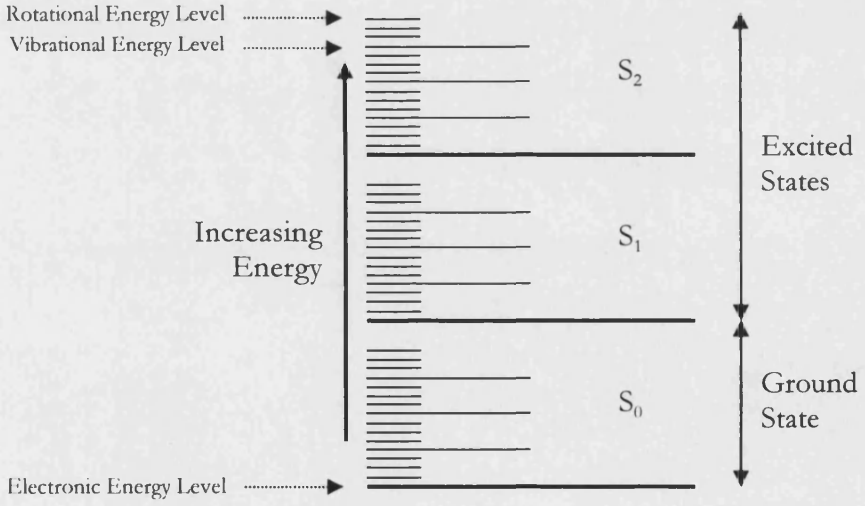

Figure 25. Electron Energy Levels.

The energy levels within a fluorescent molecule, including vibrational and rotational energy levels.

3.3.6.1.3 Fluorescence Emission

Following excitation, fluorescence emission begins instantaneously, the half-life of the emission stage for many fluorophores is usually a few nanoseconds. During emission the electron initially decays towards the lowest vibrational energy level within the electronic excited state, during this decay energy is lost in the form of heat, this process is termed internal conversion. However during the decay from the excited electronic level to ground state, energy is dissipated as a photon of light – fluorescence. The energy of an emitted photon equals the energy from the excited level minus the energy of the ground state to which it falls, this energy difference determines the wavelength of emitted light and consequently the colour of the admission (Figure 27 illustrates the colour associated with different wavelengths of light). Due to the loss of energy as heat during internal conversion, the emission spectrum is always shifted toward a longer wavelength of light (lower energy) relative to the excitation spectrum (see Figure 26), this phenomenon is referred to as the Stokes Shift. From a practical point of view the Stokes Shift is very important as it allows the emitted fluorescent photons to be distinguished from the excitation photons.

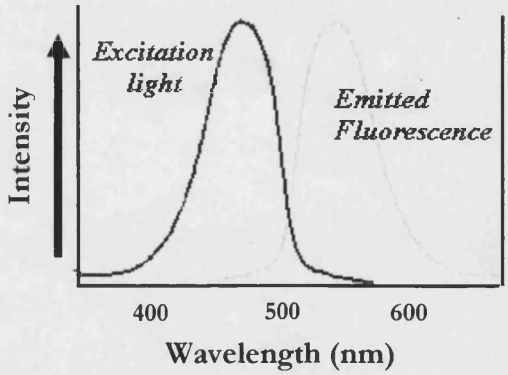

Figure 26. Excitation and Emission Spectra for Fluorescein Isothiocyanate (FITC).

The green-fluorescent fluorophore FITC is typically analysed using the maximal excitation and emission wavelength of approximately 495nm and 525nm, respectively (Homer and Beighton, 1990).

Figure 27. The Wavelength of Light and its Associated Colour.

From an emission wavelength of a fluorophore it is possible to predict its fluorescent colour.

3.3.6.1.4 The Photobleaching Effect

The photodestruction or photobleaching of a fluorophore usually occurs when a fluorophore is in its excited state. The excited state of a fluorophore is generally more chemically reactive compared to its ground state and may undergo chemical reactions that alter the fluorophore's structure generating a molecule with reduced fluorescence.

There are many applications of fluorescence for research purposes. Of particular interest to my research are the applications for studying enzyme activity, for example in the detection of xanthine oxidase activity in the isoxanthopterin assay, and also for immunofluorescent detection of cellular antigens. A list of commonly used fluorophores and their spectral characteristics is given in Table 1.

Table 1. Spectral Characteristics of Popular Fluorophores.

Fluorophore	Excitation Wavelength (nm)	Emission Wavelength (nm)
Cy3	550	570
4',6-Diamidino-2-Phenylindole (DAPI)*	358	461
Fluorescein-5-isothiocyanate (FITC)	494	518
Propidium Iodide (P.I)*	536	617
Texas Red	595	615
1-(4-trimethylammoniumphenyl)-6-phenyl-1,3,5-hexatriene *p*-toluenesulfonate (TMA-DPH)	355	430
Isoxanthopterin (IXP)**	345	390

Maximum excitation and emission wavelengths for popular fluorophores. (Haugland 2002a; Beckman *et al.*, 1989). *Excitation and Emission peaks for the fluorophore-DNA complex. **Values are not maximum wavelengths but the wavelengths used in IXP analysis.

3.3.6.2 Fluorescent Staining of Cultured Cells

3.3.6.2.1 Materials

4'-6-diamidino-2-phenylindole, dilactate (DAPI), Prolong Anti-Fade, Propidium Iodide (PI) (Molecular Probes Europe BV. Leiden, Netherlands). Nuclear Yellow, Paraformaldehyde, RNase, Saponin, Triton X-100 (Sigma Aldrich Company Ltd. Dorest, UK). Phosphate Buffered Saline (PBS) Tablets (Oxoid Ltd. Hampshire, UK). A list of antibodies used in staining procedures is given in Appendix I 8.3.

3.3.6.2.2 Fixation of Cells

Adherent cells were grown on 13mm diameter coverslips in 12-well plates. Conditioned medium was aspirated and cells were washed with 1ml 37°C HBSS which was subsequently removed. Cells were fixed using either 1ml 4% Paraformaldehyde at 37°C or Ice-cold acetone/methanol (50:50) at 4°C, and were permeabilised with 0.2% Triton X-100 in PBS at 37°C, 0.08% Saponin in PBS at 37°C, where appropriate. At the required incubation time point the fixative was aspirated and cells were kept in 1ml PBS per well before staining.

3.3.6.2.3 Fluorescent Staining

PBS was aspirated and cells were blocked in 500µl blocking buffer/well (5% Marvel in PBS) for 20mins at room temperature. The blocking buffer was removed and cells were incubated with the primary (1°) antibody (optimal concentrations are determined in results section) in 500µl blocking buffer/well for 1hr at room temperature. Excess 1° Antibody was removed by washing cells in 1ml PBS/well with continuous agitation, three times for 5mins. If required, 500µl of 2° antibody in blocking buffer was added to the cells for 30mins at room temperature. Excess 2° antibody was removed by a repeat of the wash steps used for the 1° antibody. Cellular DNA was stained using DAPI, PI, or Nuclear Yellow (optimal concentrations were determined in results section) in distilled water (dH_20) per well, incubated for 5mins at room

temperature. When using PI, cells were treated with 500µl 100µg/ml RNase per well before the application of the nuclear stain. Excess stain was removed by three 5min wash steps using dH_20 (PBS was not used as crystals on drying that interfere with visualisation). Note: All staining with fluorophores was performed in limited light conditions to reduce photobleaching.

Coverslips holding the fluorescently stained cells were turned out of the 12-well plate and mounted cell-side-down onto microscope slides using a couple of drops of ProLong Antifade (Antifade reduces the photobleaching process of certain fluorophores), and were viewed under a Zeiss Axioskop 2 microscope (Carl Zeiss Ltd. Hertfordshire, UK) equipped with a mercury arc lamp and Zeiss filter sets 01 (for DAPI), 10 (FITC), and 15 (for Cy3). Separate fluorescent images were captured using a Nikon Coolpix digital camera and were overlaid using Adobe Photoshop 5.0 LE (Adobe Systems Inc).

3.3.7 Preparation of HUVECs for Electron Microscopy

HUVECs were prepared for electron microscopy using a new procedure developed by QuantomiX™ (Nes-Ziona, Israel). In this protocol, sample preparation is comparable to that used for light microscopy however the visualisation of samples is achieved using a scanning electron microscope, therefore resulting in far better magnification and resolution compared to light microscopy techniques. The technology is based on a capsule that contains a thin, electron-transparent membrane on which samples can be attached or grown. The capsule seals the sample from the vacuum generated within the electron microscope sample-chamber, and thus enables imaging of fully hydrated samples.

3.3.7.1 Materials

Antibodies: See Appendix I 8.3. Glycine, Saponin, Triton X-100, Uranyl Acetate (Sigma Aldrich Company Ltd. Dorest, UK). Goat Serum (DAKO. Chambridgeshire, UK). LI silver enhancement kit (Nanoprobes. NY, USA). Calibration capsule, MA-4

Multi-well aspirator, MP-10 Multi-well plates, QX-102 Imaging buffer, QX-102 Capsules (QuantomiX™. Nes-Ziona, Israel).

3.3.7.2 Protocol

This protocol can be found in Appendix I 8.4.

3.3.8 Reverse Transcriptase-Polymerase Chain Reaction (RT-PCR)

3.3.8.1 Materials

Agarose, blue/orange loading dye 6x, boric acid, EDTA (Promega. WI, USA). Ethidium bromide, Mineral oil, Tris-Base (Sigma Aldrich Company Ltd. Dorest, UK). Molecular Weigh Marker (MWM XIV) (Roche Diagnostics GmbH. Mannheim, Germany). ReddyMix 2x, Reverse-iT™ 1st Strand Synthesis Kit, Total RNA Isolation Reagent (TRIR) (Abgene. Surry, UK). Mouse Liver RNA (Chemicon, UK). RNA-Stat 60 (AMS Biotechnology Ltd. Oxford, UK). UltraPure water, DNAse and RNase-free (Invitrogen. Paisley, UK). Sequences of designed primers are shown in Appendix I 8.5.

3.3.8.2 RNA Isolation

Following manufacturer's protocol, RNA was isolated from cultured cells using either RNA-Stat 60 or TRIR, however the method will be briefly described here. Cells were lysed by the addition of 1ml RNA isolation solution per confluent T25 flask of cultured cells, the lysate was passed through a pipette several times. Following lysis the homogenate was transferred to a 1.5ml centrifuge tube and incubated at room temperature for 5mins to allow dissociation of nucleo-protein complexes. After this time 0.2mls chloroform was added to the lysate, was mixed vigorously for 15secs, and allowed to stand at room temperature for 2-3mins. The lysate was then centrifuged at 12 000g for 15min at 4°C. During this step the lysate well form two phases, the lower organic phase and interface containing DNA and protein, and an upper aqueous phase containing RNA. The aqueous phase was carefully transferred to a fresh 1.5ml centrifuge tube and 0.5mls isopropanol. After incubation at room temperature for 5-

10mins the RNA was centrifuged at 12 000g for 10min at 4°C, forming a RNA pellet in the bottom of the tube. Supernatant was removed and the pellet was washed in 1ml 75% ethanol (diluted in UltraPure water) and centrifuged at 7 500g for 5min at 4°C. Supernatant was removed and the pellet was air-dried, then resuspended in approximately 30µl UltraPure water. An aliqote of RNA solution was diluted and absorbaces at 260 and 280nm were recorded. The RNA concentration was calculated using the equation below (Equation 3) and purity was calculated using the A260/A280 ration. A ratio >1.8 signifies a clean preparation free of significant protein contamination.

$$[RNA](\mu g/\mu l) = (A_{260} * 40 * \text{dilution factor}) / 1000$$

Equation 3. RNA Concentration.

3.3.8.3 Reverse Transcriptase Reaction

The reverse transcriptase reaction was carried out using the Reverse-iT™ 1st strand synthesis kit, following manufacturer's instructions. Briefly, 1µl anchored oligos were added to 2µg RNA solution in 12µl UltraPure water and was heated to 70°C for 5mins using Touchgene Gradient Thermocycler (Techne, Cambrigde, UK). Then 4µl 1st strand synthesis buffer, 2µl dNTP mix, and 1µl reverse transcriptase blend were added to the tube. The contents were vortexed and briefly centrifuged to ensure mixing, then heated to 42°C for 1hour then 75°C for 10min. Following this procedure cDNA concentration was determined by measuring A_{260} as previously described.

3.3.8.4 PCR

Specific gene products were amplified by the PCR. 1µl of forward and reverse primers (see Appendix I 8.5) were added to 1µg cDNA and 15µl ReddyMix. Following vortex and brief centrifugation, samples were overlaid with 30µl mineral oil, and a specific PCR program was run depending on primer set used (see Appendix I 8.5). PCR products were analysed using agarose gel electrophoresis. PCR reaction

products were applied directly to a 1.2% agarose gel (see Appendix I 8.5) (10µl per well), which was run at 50V until gel front ran approximately ¾ of the gel length. To calculate PCR product size a standard was also applied, prepared as follows: 4µl MWM, 2µl loading dye, 6µl UltraPure water. PCR products were visualised under UV light.

3.4 Results

3.4.1 The HUVEC: Morphological Analysis

The aim of this section is to assess the predominant cell type isolated from the human umbilical cord vein by appearance, i.e. to show that the cell type isolated is the HUVEC as expected.

The human umbilical cord contains three large blood vessels, two arteries and one vein. The vein is easily distinguished due to its larger diameter compared to the arteries (see Figure 28). HUVECs were isolated using the collagenase digestion method, a method that gently removes cells lining the human umbilical cord vein (see Figure 29), without significant removal of other cell types.

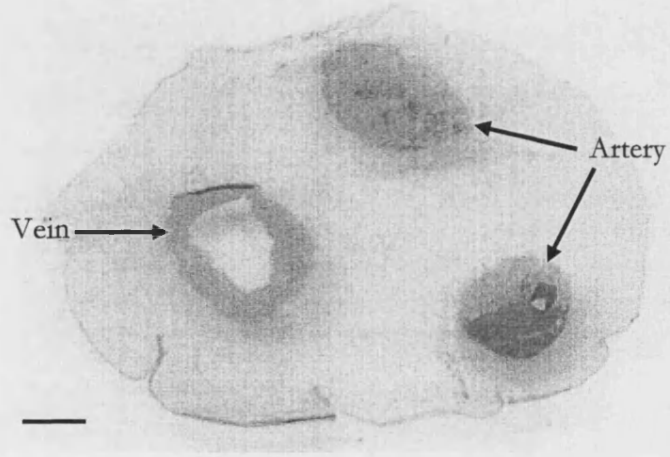

Figure 28. The Human Umbilical Cord Cross Section.

A specimen of human umbilical cord was fixed using the Tissue-Tek/liquid nitrogen method as described in section 3.3.1. 5μm sections of umbilical cord were stained using haematoxylin and eosin-stain protocol. The morphological differences between the umbilical cord vein and arteries are clear, especially vessel diameter, and are important to note when selecting a vessel for endothelial cell isolation protocol. Bar = 1mm.

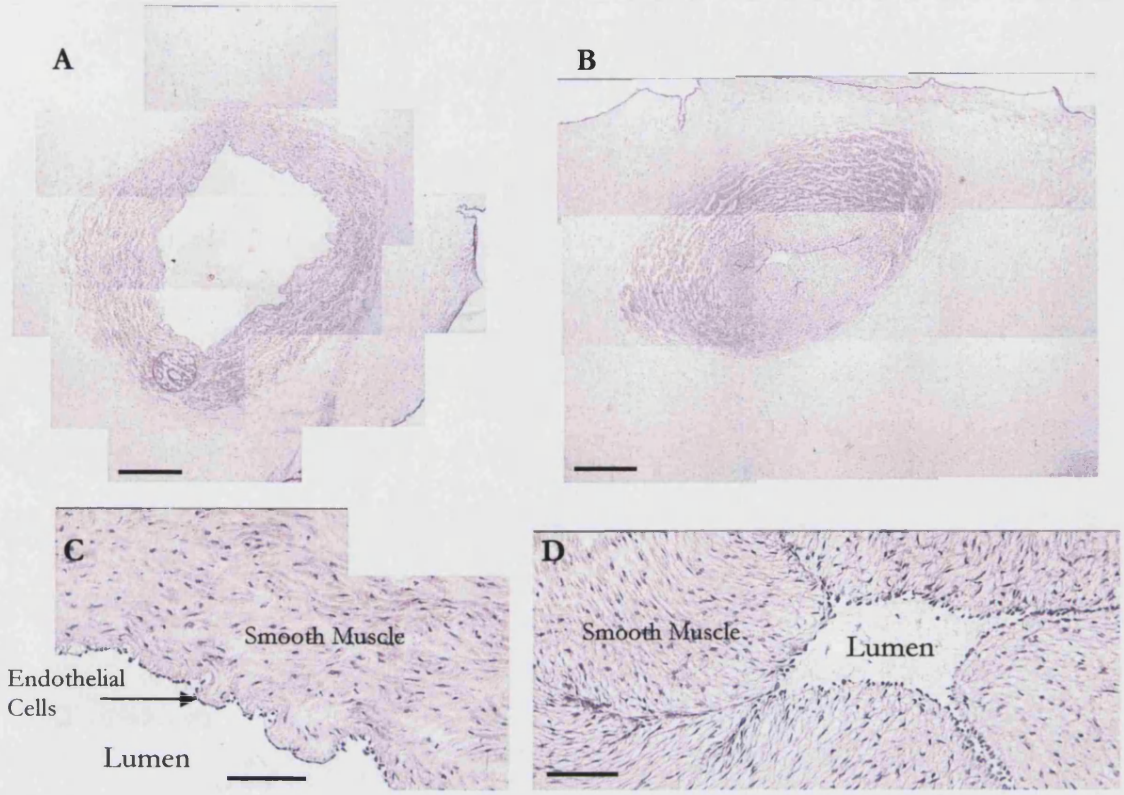

Figure 29. The Human Umbilical Vein and Artery.

The umbilical cord was prepared as described in Figure 28. The umbilical vein and artery are shown in A, and C, and B, and D, respectively. With the haematoxylin-eosin stain cell nuclei appear blue/purple, whereas cytoplasmic structures are pink/red. Higher magnification clearly demonstrates the differences between the vein and artery, considerably more smooth muscle is present in the artery wall. In C, the HUVEC layer is clearly visible. Bar = 500μm in A and B, and 100μm in C and D.

For investigations into the hypothesis, HUVECs were used at passage two (P2). Living, cultured HUVECs at this stage are shown Figure 30. Confluent HUVECs form sheet-like, polygonal monolayers, and have morphology distinct from that of smooth muscle and fibroblasts which confirms early investigations (Jaffe *et al.*, 1973).

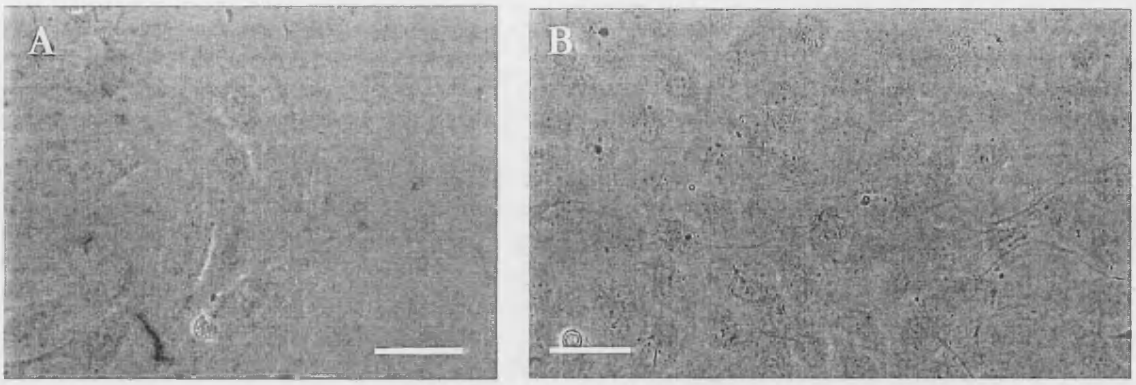

Figure 30. Living HUVECs in Cell Culture.

Living P2 HUVECs were viewed under phase contrast microscopy and images were captured using a Nikon Coolpix digital camera (Nikon UK Ltd. Surrey, UK). A and B show sub-confluent and confluent human umbilical vein isolations, respectively (Bar = 50μm).

To further characterise the morphology of isolated cells and to help confirm the cells were from endothelial origin, cultures were initially compared to purchased HUVECs (see Figure 31). HUVECs purchased from PromoCell undergo several tests to ensure the population is from endothelial origin. The morphology of isolated cells was identical to the cells purchased from PromoCell.

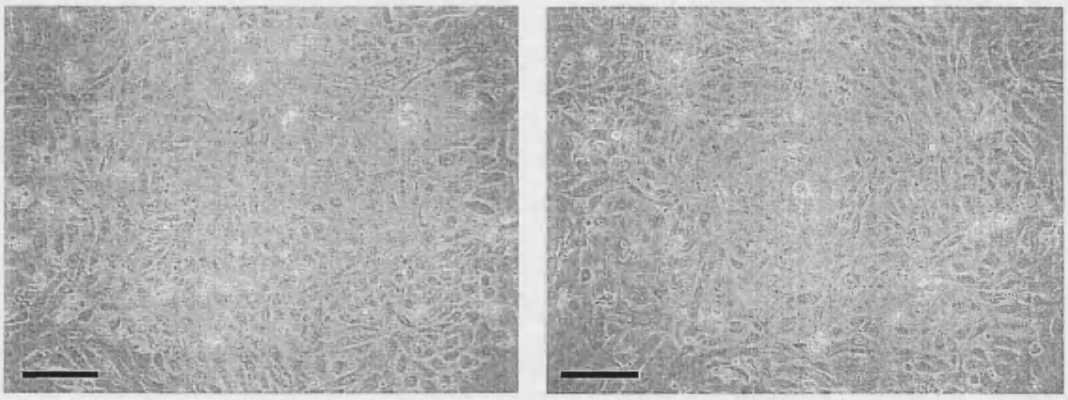

Figure 31. PromoCell HUVECs in Cell Culture.

Living P2 HUVECs purchased from PromoCell were viewed under phase contrast microscopy. (Bar = 100μm).

The formation of tubular structures by cultured HUVECs has been described (Maciag *et al.*, 1982). To further characterise the isolated cells as HUVECs cultures were assessed for tube formation. In these experiments P1 cell-isolates were cultured to

confluence, however instead of passage the isolated cells were incubated and fed as normal. After a period of approximately 7-14days it was apparent that in some areas groups of cells changed to a more elongated morphology, and ran parallel with one another. Within a week of this time tube-like structures were observed. With continued culture, cells growing close to the tube became more sparse leaving a free-standing tubular structure (see Figure 32).

To assess the isolated cell type further, the generation time of the cultures was measured. To achieve this 20 000 P1 cells/well were seeded into 12-well plates (therefore P2 cells) and were cultured under normal conditions. At selected time points viable cell counts were taken using the trypan blue-exclusion protocol, two wells of cells were counted for each time point. A growth curve was plotted (see Figure 33) and generation time was calculated using Equation 1. The generation time of this culture was 32hr, compared to a 49hr generation time calculated by PromoCell for their HUVECs (PromoCell GmbH. Heidelberg, Germany).

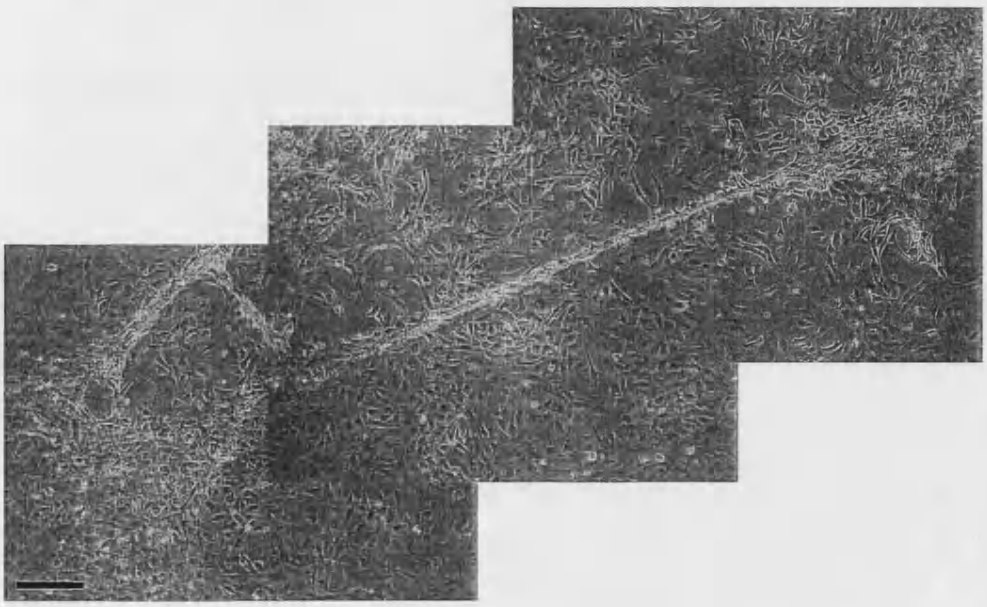

Figure 32. HUVEC Tube Structure Formation.

Cell isolates (P1) were cultured in T25 flasks for approximately 21days beyond confluence under normal culture conditions. During this time tube-like structures were observed as shown under phase

contrast microscopy. Note that although cells are confluent near the ends of tubes areas running alongside tubes have lost confluence (Bar = 100μm).

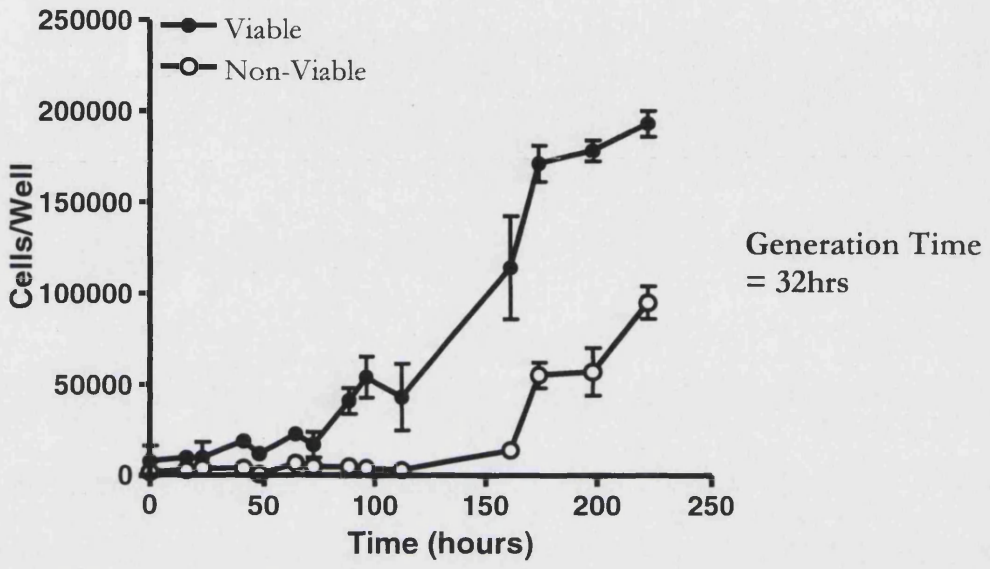

Figure 33. HUVEC Growth Curve.

Over selected time points the cell number of cultured umbilical vein-cell isolates was calculated. Time zero was the first cell count (the morning after the cells were seeded). Generation time was calculated from the linear portion of the growth curve (Error bar = SD).

3.4.2 The HUVEC: Protein Expression Analysis

The aim of this section is to assess the predominant cell type isolated from the human umbilical cord vein by protein expression, i.e. to show that the cell type isolated is the HUVEC as expected. A technique frequently employed for this purpose is the staining of isolated cells for the endothelial cell marker von Willebrand factor. This technique was used in the first confirmed isolation of HUVECs (Jaffe *et al.*, 1973) and has been widely used ever since.

3.4.2.1 Optimisation of Fluorescent Staining

To visualise protein expression in HUVECs it is important to label cells for DNA to confirm cellular location. Several DNA-binding fluorophores can be employed for this purpose, and fluorophore selection was based on the fluorescent emission wavelength of the immuno-labelled protein of interest, i.e. nuclear and protein fluorophores of different colours were used. DNA staining with three chemical

nuclear-labels, DAPI, PI, and Nuclear Yellow, was optimised. The optimal concentrations for the protocol were found to be 10nM DAPI, 0.1μg/ml PI, and 50μM Nuclear Yellow. DAPI and Nuclear Yellow stains were specific to DNA, however PI stained the cell nucleus and cytoplasm, i.e. DNA and RNA were both detected (see
Figure 34). Therefore an additional step was added to the PI stain protocol, the incubation of fixed cells with 100μg/ml RNase for 0.5hours prior to PI staining (see Figure 34).

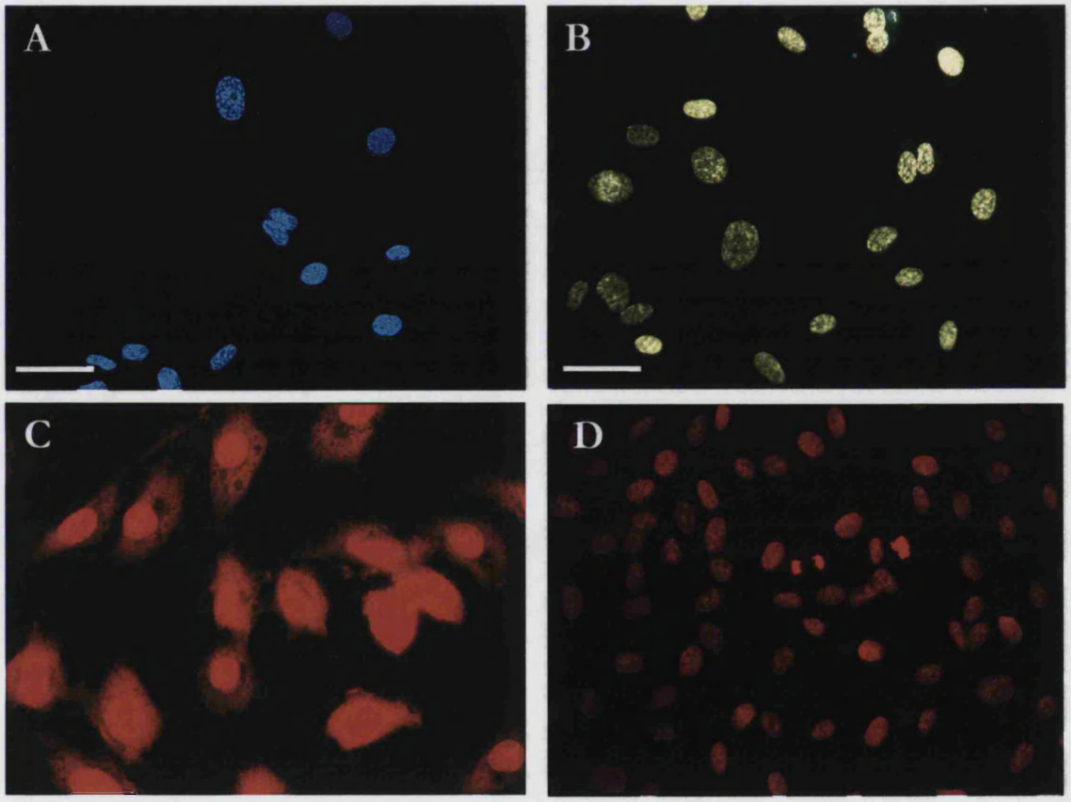

Figure 34. Optimisation of Fluorescent Nuclear Stains.

Different nuclear labels were assessed in HUVECs. The concentrations of the A) DAPI, B) Nuclear Yellow, and PI were optimised. The cellular stain with PI with and without RNase treatment is shown in D and C, respectively. Optimum concentrations of stain are described in text. (Bar = 50μm).

The nuclear stain aids in locating cells during the staining procedure, however to see cellular boundaries staining of cytoskeletal elements can be used. Microtubules are a major cytoskeletal component and are predominantly composed of molecules of α-

and β-tubulin (Alberts *et al.*, 1994). Optimal staining of microtubules was achieved using a 250x dilution of a β-tubulin antibody (see Figure 35). Using the microtubule staining protocol the different fixation methods were assessed. A more intense microtubule stain was seen in permeabilised cells, especially those fixed with acetone/methanol combinations (see Figure 36).

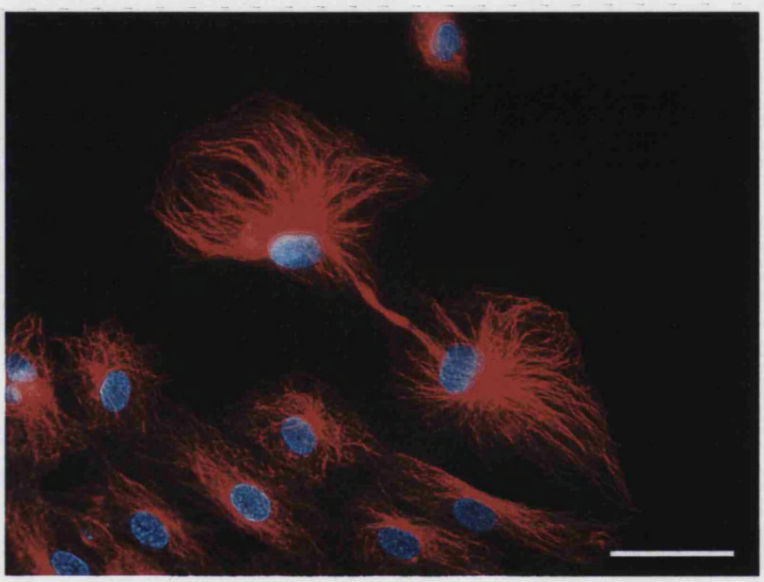

Figure 35. Microtubule Stain in HUVECs.

P2 HUVECs grown on coverslips were fixed with acetone/methanol for 5mins and were stained for β-tubulin (red) and DAPI (blue) using optimal conditions (see text) (Bar = 50μm).

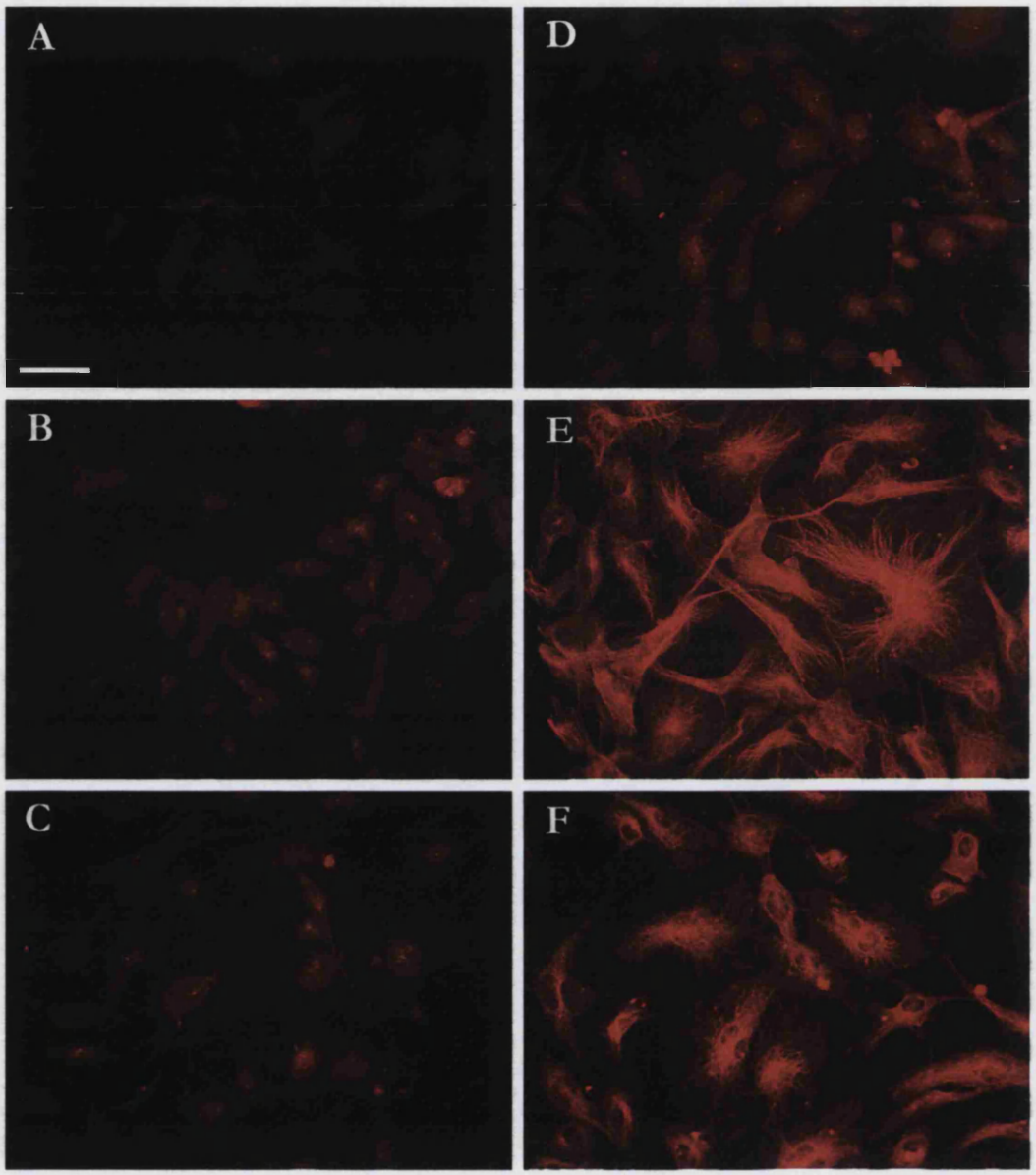

Figure 36. The Effect of Fixation Techniques on Membrane Permeability.

HUVECs were fixed with: A) Paraformaldehyde for 10mins, B) Paraformaldehyde for 10mins followed by Saponin for 1min, C) Paraformaldehyde for 10mins followed by Triton X-100 for 1min, D) Paraformaldehyde for 10mins followed by Acetone/Methanol for 1min, or E) Acetone/Methanol for 5mins or F) 10mins, and stained for β-tubulin with a Cy3-conjugated antibody (red fluorescence). Mercury arc lamp intensity and camera exposure times were constant for all images Bar = 50μm).

3.4.2.2 von Willebrand Expression in HUVECs

Staining for the endothelial cell marker, vWf, was optimised. A 150x dilution of the polyclonal and 300x dilution of the monoclonal anti-human vWf antibodies was optimal. vWf staining of human umbilical vein cell isolates (see Figure 37) revealed

staining of compartmentalised, punctate, or "rod"-shaped structures, and a more diffuse stain around the nucleus (probably staining the endoplasmic reticulum).

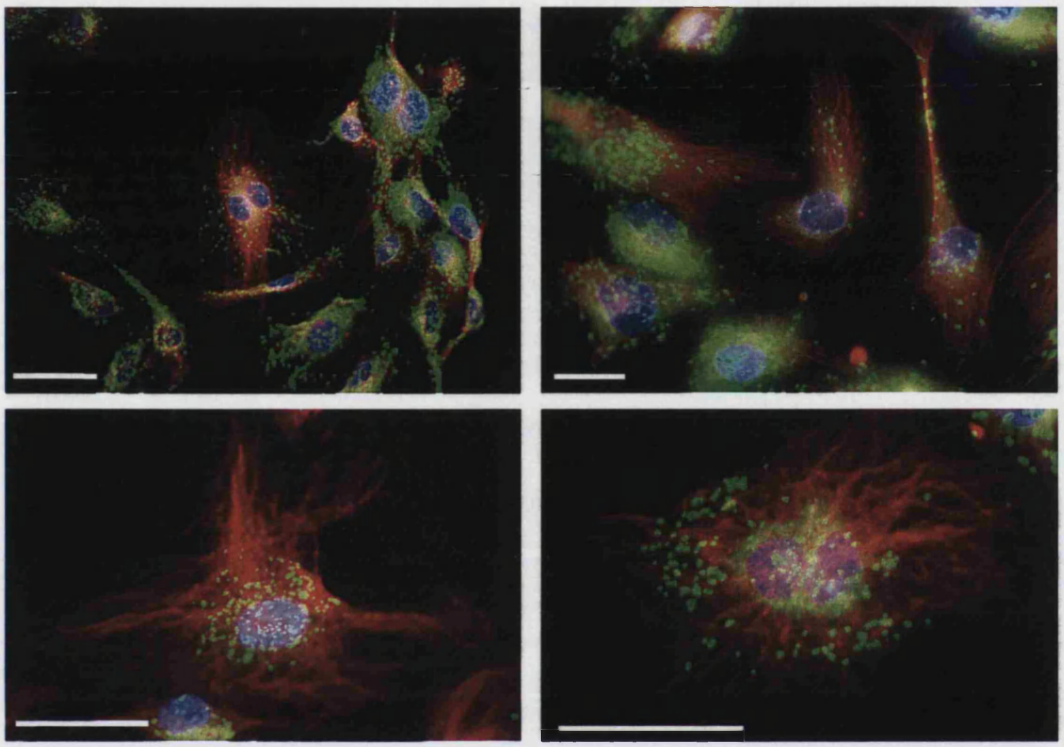

Figure 37. von Willebrand Factor Immunofluorescent Stain in HUVECs.

P2 umbilical cord vein cell isolates were grown on coverslips were fixed with acetone/methanol for 5mins. Immunofluorescent stains for vWf (green) and β-tubulin (red) were carried out. vWf was stained using a polyclonal antibody and FITC-conjugated secondary. Cellular nuclei were stained with DAPI (Blue) (Bar = 50μm).

To assess the number of endothelial cells in a typical umbilical cord vein isolation, the percentage of vWf positive cells was measured by fluorescent staining. Fields of view were chosen randomly by observing the nuclear stain under the fluorescence microscope. An image was captured and filters were changed to view the vWf stain, and a second image was captured. Images of the same field of view were overlaid and the number of vWf positive cells was counted and total number of cells was calculated by nuclear stain (see Table 2).

Table 2. Calculation of vWf Positive Cells from the Umbilical Cord Isolate.

vWf positive	vWf negative	Total cells	Percentage vWf positive
274	6	279	98.2%

P2 cell isolates were fixed with paraformaldehyde and permeabilised with triton X-100. Cells were stained for vWf using DAKO polyclonal and nuclei were stained with DAPI. Pictures were taken randomly and vWf-positive and total cells were counted.

3.4.3 Xanthine Oxidoreductase Expression in HUVECs

The aim of this section is to assess the expression of XOR within the chosen vascular endothelial model, the HUVEC. Microvascular endothelial cells have been shown to express and release XOR (Jarasch *et al.*, 1981; Jarasch *et al.*, 1986; Partridge *et al.*, 1992). However, for HUVECs to be used in investigations into the hypothesised endothelial release of XOR, it is essential to demonstrate XOR expression within this cell type.

3.4.3.1 XOR Protein Expression

A range of XO antibodies were commonly used within the laboratory. The effectiveness of the antibodies was compared on Western Blots of purified XO and milk samples which contain XO (see Figure 38). No staining was observed using the monoclonal antibody and the most intense staining was seen using the polyclonal Polysciences antibody with a specific secondary antibody.

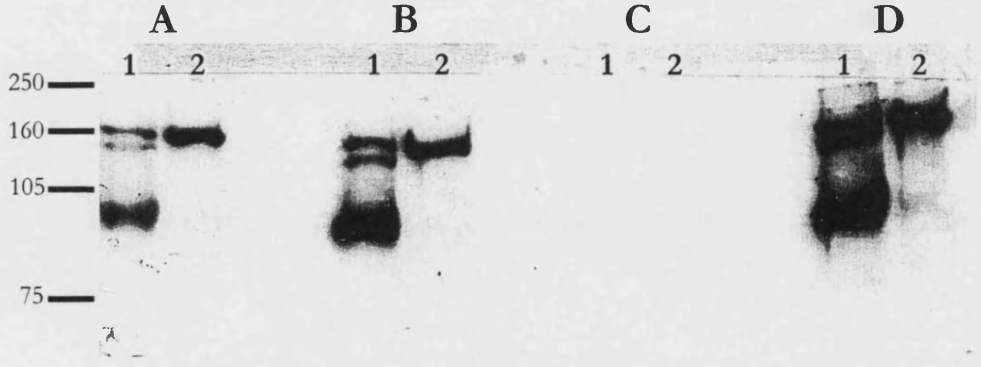

Figure 38. Comparison of Xanthine Oxidase Antibodies in Western Blot.

Pure XO (25ng; Lane 1) and milk (10μg protein; Lane 2) were run on SDS-PAGE and following Western Transfer nitrocellulose membranes were probed with four commercially available XO-antibodies: A: Chemicon 5000x dilution; B: BioDesign 1000x dilution; c: NeoMarkers 1000x dilution;

D: Polysciences 5000x dilution. The secondary antibody was used as appropriate: 200x dilution of swine anti-rabbit IgG or 1000x dilution of rabbit anti-mouse IgG.

To demonstrate the presence or absence of XOR in the HUVEC vascular endothelial model, a T25 flask of confluent P2 HUVEC was lysed directly in 150µl sample buffer. 20µl of the lysate was loaded directly onto SDS-PAGE, and following Western-transfer XOR was probed using the optimal antibody conditions (i.e. using the Polysciences XO antibody; see Figure 39). XOR is detected in HUVECs, strong staining of ~150, ~90, ~60, and ~38KDa bands are seen.

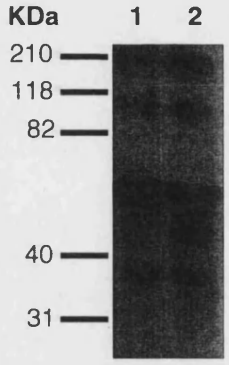

Figure 39. The Detection of Xanthine Oxidoreductase in the HUVEC – Western Blot.

Two T25 flasks of HUVECs (Lanes 1 and 2) were lysed in sample buffer and lysates were loaded directly onto SDS-PAGE. Following Western-transfer nitrocellulose membranes were probed with Polysciences Anti-XO.

With Western-Blot confirmation that HUVECs contain XOR, the cellular expression of the enzyme was investigated using fluorescence microscopy. P2 HUVECs were grown on glass coverslips and using two fixation methods staining for XOR was compared (see Figure 40). Irrespective of fixation method, XOR expression in HUVECs has a granular, cytoplasmic appearance in all cells, however in some cells a more punctuate stain is seen. As a control, XOR staining in the mammary epithelial cell line MDA-MB-231 was performed using two XOR antibodies (see Figure 41). Compared to the HUVEC a similar staining profile was seen, i.e. all cells express a granular cytoplasmic stain but some cells exhibit a more punctate appearance (see Figure 42). As in the Western blot (Figure 38) the Polysciences antibody stain was more intense compared to the Chemicon equivalent. Saturatation of the 1° antibodies

before application reduced staining and no detection of XOR was seen using the 1° or 2° antibodies alone.

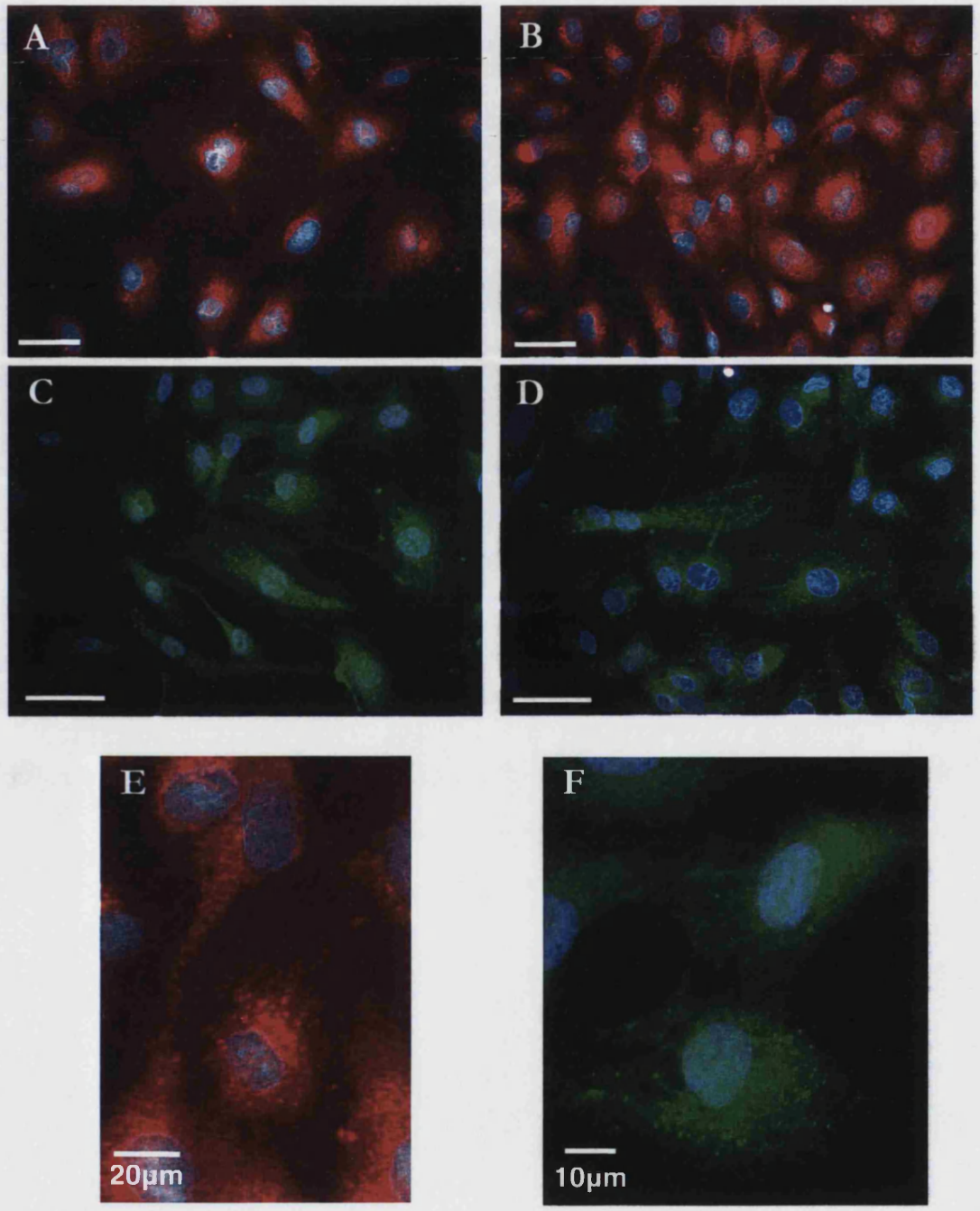

Figure 40. HUVEC XOR Expression – Immunofluorescence Study.

P2 HUVECs were grown on coverslips and were fixed with acetone/methanol for 5mins at 4°C (A-C, E, F) or 4%Paraformaldehyde for 10mins at 37°C and with 0.2% Triton X-100 for 1min at 37°C (D). Cells were stained using the Polyscience XO-antibody and either a FITC (green) or Rhodamine

(red)-conjugated 2°antibody. Cell nuclei were stained using DAPI. Results are from two experiments. A-D bar = 50μm).

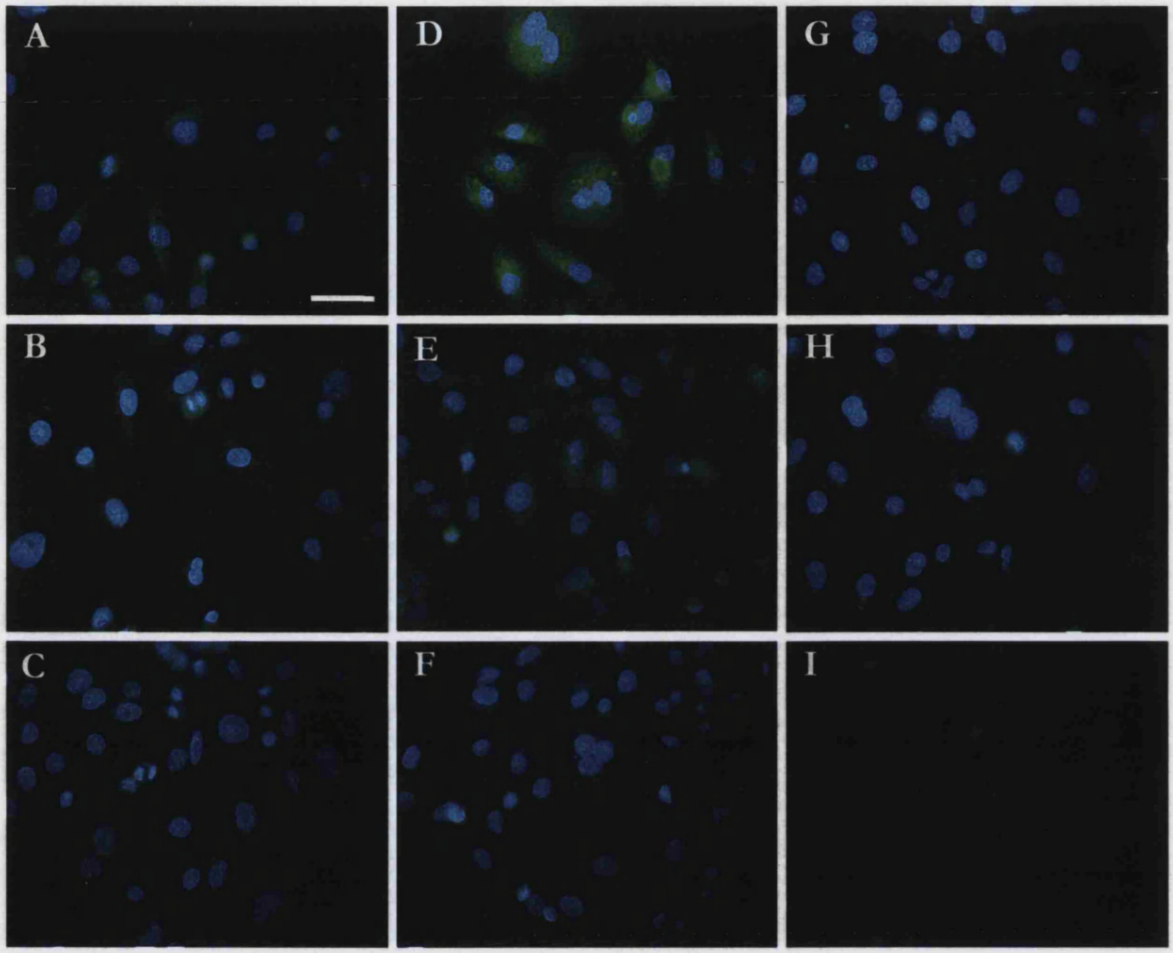

Figure 41. MDA-MB-231 XOR Expression – Immunofluorescent Control.

Subconfluent MDA-MB-231 cells grown on coverslips were fixed with acetone/methanol for 5mins at 4°C. Fixed cells were stained with: A) Chemicon XO antibody, B) Saturated Chemicon XO antibody C) Chemicon XO antibody only, D) Polysciences XO antibody, E) Saturated Polysciences XO antibody, F) Polysciences XO antibody only, G) 2° antibody only, H) No antibody stain, I) No staining. All cells, apart from condition I, were DNA-stained with DAPI (blue). A FITC conjugated 2°antibody was applied to A-G (Bar = 50μm).

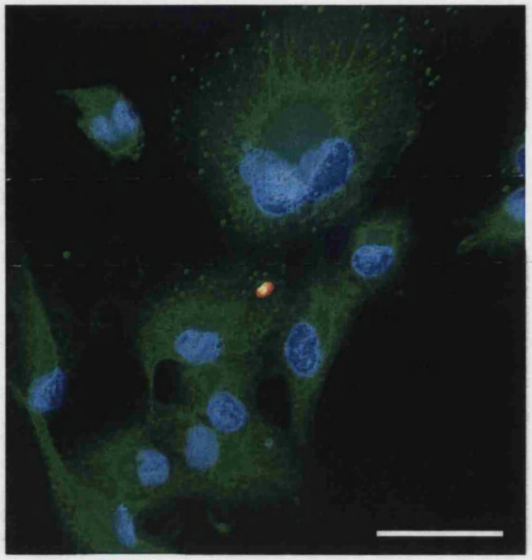

Figure 42. MDA-MB-231 XOR Expression Profile – Immunofluorescence.

Subconfluent MDA-MB-231 cells grown on coverslips were fixed with acetone/methanol for 5mins at 4°C. Fixed cells were stained with the Polysciences XO antibody and a FITC-conjugated 2°antibody (green) and nuclei were stained with DAPI (blue) (Bar = 50μm).

To confirm the staining profiles seen with the immunofluorescent technique, HUVECs were prepared and labelled for electron microscopy using the Quantomix kit (as described in section 3.3.7). The resultant labelling of vWf and XOR was consistent with findings using immunofluorescent techniques (see Figure 43).

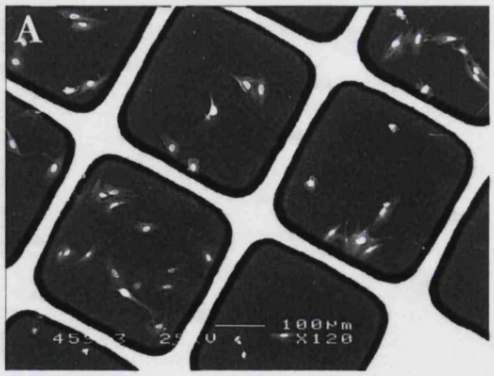

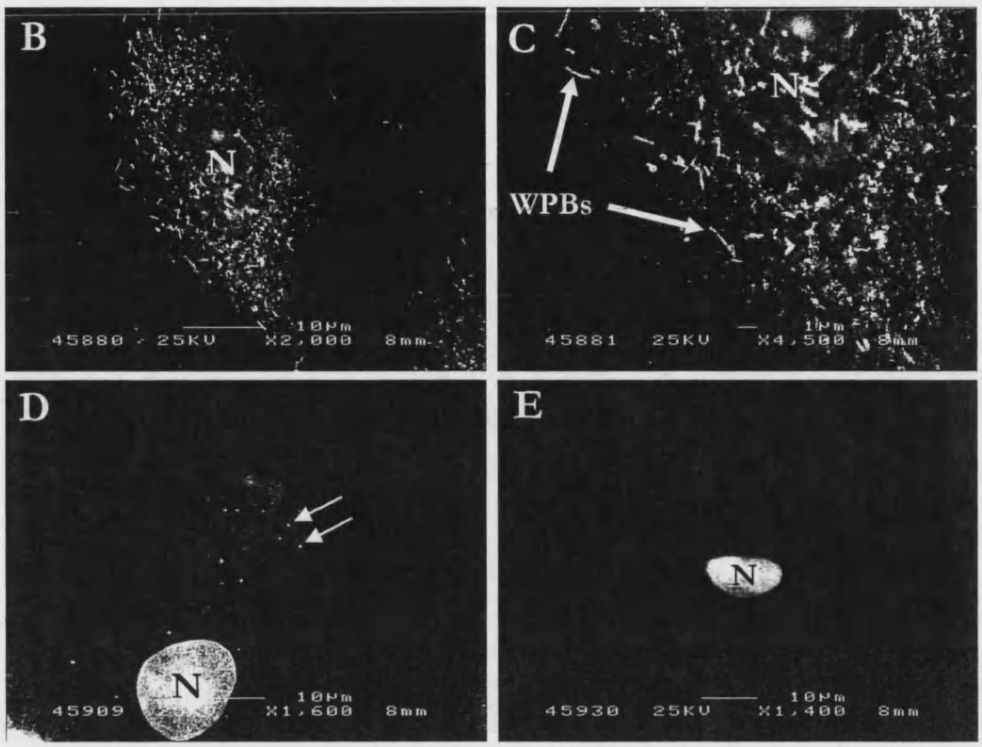

Figure 43. HUVEC Expression of vWf and Xanthine Oxidoreductase – Electron Microscopy Study.

P2 HUVECs were grown on Quantomix capsules and were fixed with 4% Paraformaldehyde and permeabilised with 0.2% Triton X-100. vWf (B and C) and XOR (D) were labelled with DAKO and Polysciences 1°-antibodies, respectively. A gold-conjugated 2°-antibody was applied and labelling was silver-enhanced. Uranyl acetate was used to faintly stain general cell structure. Incubation with the 2°-antibody alone (E) and HUVECs growing on the capsule membrane (A) are shown. N= Nucleus, WPBs = Weibel-Palade Bodies. Unless indicated arrows show punctate XOR staining.

Xanthine oxidoreductase appears to be expressed in a cytoplasmic form but also in a packaged form in HUVECs. To attempt to characterise the storage granule of XOR, co-localisation studies with the WPB-protein vWf were performed, a positive co-localisation would suggest WPB storage of XOR. In this study HUVECs were stained using a dual immunofluorescent technique, whereby XOR and vWf were labelled with 1° antibodies (raised in different species) and cognate 2° antibodies. XOR and vWf were probed with rhodamine-, and FITC-conjugated 2° antibodies, respectively. Images were taken and overlaid as previously described. In overlaid pictures, any co-localisation is indicated by a yellow colour (see Figure 44). The majority of XOR staining was independent of vWf staining.

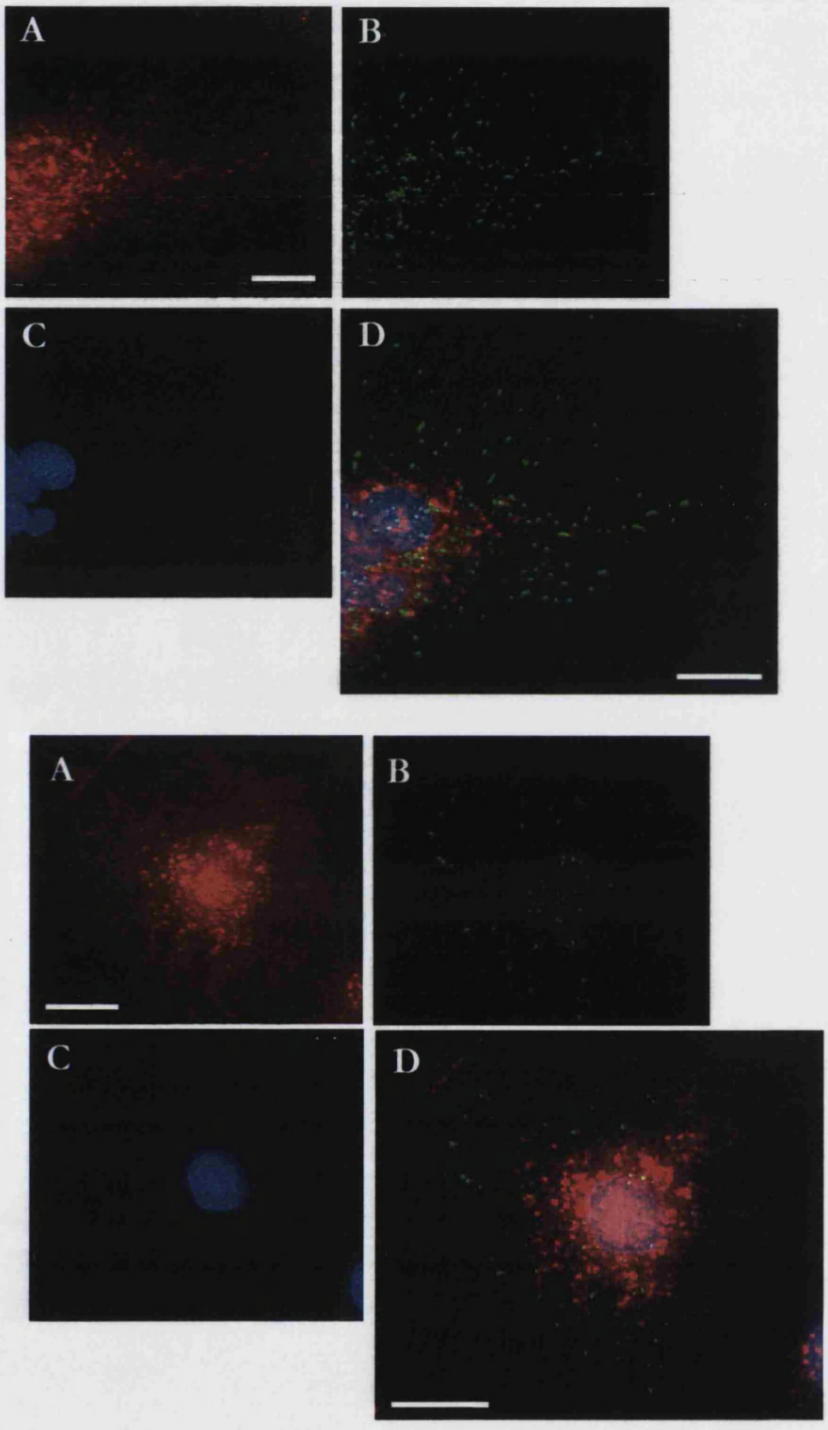

Figure 44. Co-localisation of Xanthine Oxidoreductase Storage with vWf?

P2 HUVECs were grown on glass coverslips and were fixed with acetone/methanol for 5mins at 4°C. XOR (A, red) and vWf (B, green) were detected using 1°antibodies raised in different species in combination with relevant 2° antibodies. Nuclei were stained the DAPI (C, blue). Yellow areas indicate co-localisation of vWf and XOR (D) (Bar = 20μm).

3.4.3.2 XOR Gene Expression

Vascular-associated XOR could originate from two sources: i) endogenous expression, or ii) by endocytic retrieval of the protein from the circulation following its release from XOR-rich organs (a process that has not yet been verified). Therefore RT-PCR for the detection of HUVEC mRNA expression was performed to help answer this question. In this experiment conditioned ECGM from confluent T25 flasks of P2 HUVECs was replaced with fresh ECGM, and at relevant time points medium was removed and cells were lysed in RNA STAT-60. RNA was isolated and integrity was checked by agarose gel electrophoresis (see Figure 45). It is expected that intact RNA separated by agarose gel electrophoresis should from two bands, the 18S and 28S rRNA (Skrypina *et al.*, 2003), therefore the RNA in the sample shown is intact.

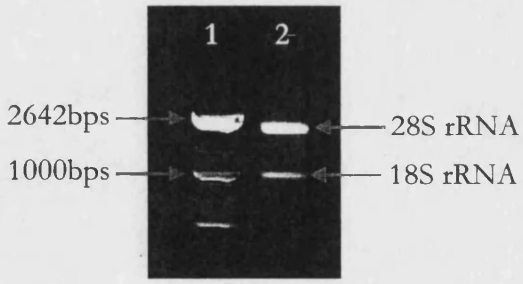

Figure 45. HUVEC RNA Integrity Checks.

1μg HUVEC RNA was separated by agarose gel electrophoresis: Lane 1) Base pair (bp) ladder, which runs in 100bp increments except where indicated, Lane 2) 1μg HUVEC RNA.

cDNA was prepared using the 1st-Strand Synthesis Kit as described in the methodology section and 1μg cDNA was used in PCR reactions with Rat XOR and human GAPDH primers. The XOR primers were originally designed to anneal to the rat XO sequence, however these primers are complementary to the human XO sequence (see Figure 46). PCR results are shown in Figure 47. XOR was constitutively expressed in HUVECs and no change in expression occurs following the medium change. 1μg Mouse liver cDNA was used as a positive control for the PCR reaction and a lane with no cDNA served as a negative control. Using the same samples PCR for the constitutively expressed gene glyceraldehyde-3-phosphate dehydrogenase

(GAPDH) was used as a loading control. Therefore demonstrating that equal quantities of cDNA from each HUVEC sample were used in the PCR reactions and therefore no change in XOR expression occurred. GAPDH expression is commonly used as a constitutive control for PCR in HUVECs (Tabengwa *et al.*, 2000; Sasaki *et al.*, 2004) (as well as other cell types).

```
                                          Sense (forward) 5'-3'
Rat Primer      ---------------------------------CTGTCCATCGAGATCCCCTA------- 20
Human XO        AGAAAGACCCTGCTGAGCCCGGAGGAGATACTGCTCTCCATAGAGATCCCCTACAGCAGG 1320
                                           ** ***** ***********

                                        Non-sense (reverse) 3'-5'
Rat Primer      ---------------------------------TCTCAGCCCTCAAGACCACT--------- 20
Human XO        CTTTGCTATGGTGGAATGGCCAACAGAACCATCTCAGCCCTCAAGACCACTCAGAGGCAG 1500
                                           ********************
```

Figure 46. Binding of the Rat XO Primer Pair to the Human XO Sequence

The annealing positions of the rat XO primer set to the human nucleotide sequence are given. The non-coding human XO sequence is shown, numbers at the right hand side of the sequence indicate the position of the last nucleotide.

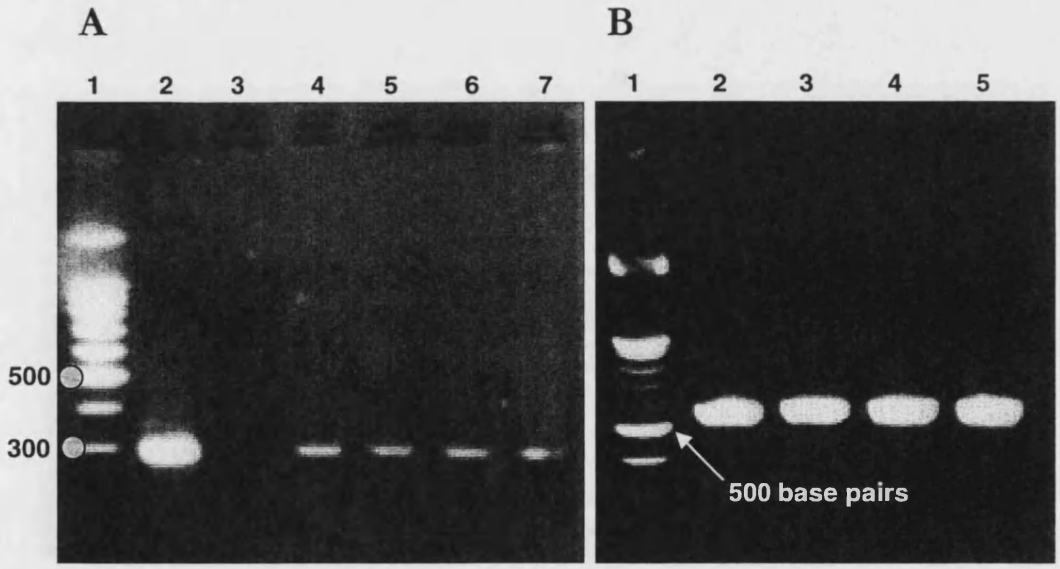

Figure 47. HUVEC *xor* Gene Expression.

Fresh ECGM was added to HUVECs and cells were lysed in RNA STAT-60 at 0, 1, 2, and 4 hours following medium change. RNA was isolated and cDNA was prepared. PCR reactions were performed using rat XOR and human GAPDH primer sets, expected product sizes are 288 and 576 base pairs, respectively. A) XOR PCR, lane 1: base pair ladder, lane 2: mouse liver cDNA, lane 3: no cDNA, lane 4: HUVEC cDNA 0hr, lane 5: HUVEC cDNA 1hr, lane 6, HUVEC cDNA 2hr, and lane 7: HUVEC cDNA 4hr. B) GAPDH PCR, lane 1: base pair ladder, lane 2: HUVEC cDNA 0hr, lane 3: HUVEC cDNA 1hr, lane 4, HUVEC cDNA 2hr, and lane 5: HUVEC cDNA 4hr.

3.5 Discussion

3.5.1 Umbilical Cord Cell Isolates – Morphological and Behavioral Analyses

Cells that form the endothelial cell model, the HUVEC were isolated from umbilical cords kindly donated by mothers attending the maternity ward at Bath Royal United Hospital (with Bath Local Research Ethics Committee approval: Ref: BA635). As indicated in stained transverse sections of the human umbilical cord (Figure 28 and Figure 29) there are three blood vessels; two arteries and one vein. These vessels are easily distinguished from one another by eye, by differences in vessel diameter, and by microscopy, by differences in vessel morphology. The arteries and vein have morphologies that match text-book descriptions of these vessels, i.e. the arteries contain significantly more smooth muscle compared to the vein (Figure 29; Pocock and Richards, 1999).

For planned endothelial XOR-release experiments, it was important to demonstrate that the cells being isolated from the umbilical cord are in fact from endothelial origin. Therefore following collagenase digestion, a range of morphological and protein expression analyses were performed to assess the cell type being isolated. Initial studies observing isolated cells under phase contrast microscopy showed a culture with uniform structure (Figure 30). Cultures grown to confluence formed a monolayer of polygonal cells, and look identical to cultures of cells confirmed to be HUVECs (Jaffe *et* al., 1973; Nachman and Jaffe, 2004). Components of the human umbilical vein that could potentially contaminate HUVEC cultures include fibroblasts and smooth muscle cells. However, the morphology of the isolated cells is distinct from that of smooth muscle and fibroblasts which grow as overlapping layers of parallel arrays of spindle-shaped cells (Jaffe et al., 1973). The morphology of the cultured umbilical cord vein cell-isolate was compared to that of commercially available HUVECs (Figure 31). Cultures appeared identical, therefore suggesting that, by appearance, the isolated cells were indeed HUVECs.

An interesting feature of HUVECs is their ability to form tube-structures. In conditions that do not favour proliferation, the HUVEC may non-terminally differentiate, as seen by an organisational change in their structure that ultimately leads to tube-structure formation (Maciag *et al.*, 1982). Endothelial cell growth can be regulated by contact inhibition (Buonassisi and Venter, 1976), therefore when confluent, HUVECs would be growing under conditions that do not favour proliferation. Cultures that were grown to confluence and were incubated without passage formed tube-like structures within 21days (Figure 32), therefore demonstrating that the cells isolated from the umbilical cord vein have endothelial cell properties.

3.5.2 Umbilical Cord Cell Isolates – Protein Expression Analyses

3.5.2.1 Protein Staining in Cultured Cells - Fixation

For the protocols used within this thesis, a fixative step is required for the detection of cellular proteins in cultured cells. Several fixation techniques available were compared for their effect on plasma membrane integrity by the subsequent staining of the intracellular antigen β-tubulin (Alberts *et al.*, 1994) (Figure 36). The action of the fixation agents used has been described (Bacallao *et al.,* 1995). Paraformaldehyde, a protein-cross linking fixative, fixes cells by forming covalent crosslinks between proteins, whereas acetone/methanol, a protein-coagulation fixative, fixes cells by rapidly changing the hydration state of the cell and proteins are either extracted or coagulate during this process. Triton X-100 and Saponin, at the concentrations used, are mild detergents that gently permeabilise the fixed cells by removing some lipid from membranes. In Figure 36, significant β-tubulin staining was only seen in acetone/methanol fixed cells, which would suggest that much of the plasma membrane is removed during the fixation process, thus allowing excellent cellular-entry of the β-tubulin antibody. Whereas paraformaldehyde-fixed cells showed little/no β-tubulin staining, suggesting that the plasma membrane remains intact, therefore not allowing the antibody to enter. The detection of β-tubulin increases in

paraformaldehyde-fixed cells following the addition of the permeabilising detergents Triton X-100 or saponin, therefore reinforcing the view that paraformaldehyde fixation leaves the plasma membrane intact. The opposing effects of the different fixation techniques on plasma membrane structure can be exploited. Using either paraformaldehyde or acetone/methanol fixation the location of an antigen could be discovered. For example, an intracellular antigen will only be significantly stained if the cell was fixed with acetone/methanol or permeabilised with a mild detergent following paraformaldehyde fixation. Whereas a cell surface-located antigen, which is likely to be removed using acetone/methanol fixation, is more likely to be detected if paraformaldehyde fixation was used. Using these fixation techniques would be particularly useful when investigating the secretion of a protein, for example, using different fixation techniques at different time periods one could track the release of a protein from an intracellular store to the plasma membrane (i.e. its cell-surface expression or disappearance). This reasoning has been exploited in experiments by Takano *et al.*, 2002, whereby the cell surface expression of P-selectin was measured by a cell-based ELISA on paraformaldehyde fixed HUVECs, thus avoiding the detection of intracellular stores of this protein.

3.5.2.2 Protein Staining in Cultured Cells – von Willebrand Factor

To discover the localisation of individual cells and cellular boundary definition in immunofluorescence, nuclear stains and cytoskeletal stains were optimised (Figure 34 and Figure 35). Depending on the fluorophore being used to probe cellular proteins, different nuclear stains could be used to enable a contrast in fluorescence between stained structures. For the analysis of vWf protein expression in HUVECs, nuclei were stained with DAPI as FITC and rhodamine were used in immunofluorescent detection of vWf and β-tubulin, respectively (Figure 37). Within the HUVEC, vWf was seen in classic punctate, often rod-shaped storage granules and more diffusely near to the cell nucleus (Figure 37 and Figure 43). The punctate staining described is vWf packaged into WPBs (Kagawa and Fujimoto, 1987), whereas the more diffuse staining is likely to be newly formed vWf found in the rough endoplasmic reticulum

and Golgi apparatus where the protein is synthesised and modified (reviewed in van Mourik *et al.*, 2002). The vWf staining profile seen in HUVECs in this study is identical to other studies where vWf protein has been labelled in endothelial cells (Jaffe *et al.*, 1973; Knop *et al.*, 2002).

Weibel Palade Bodies are only found in endothelial cells (Weibel and Palade, 1964). Therefore, the WPB acts as a unique marker for endothelial cells, and was used to determine the cell type being isolated during collagenase treatment of the umbilical cord vein. Together with morphological and behavioural characteristics of the isolated cell type, one could be confident that the cell type isolated is predominantly endothelial in origin and is therefore the HUVEC.

3.5.2.3 Xanthine Oxidoreductase Expression in HUVECs

3.5.2.3.1 Protein Expression Profile

To detect XOR protein expression in cultures of HUVECs an immunofluorescent technique, similar to that used for vWf detection, was planned. However, before HUVEC expression could be assessed, certain control experiments were required to ensure the XOR antibodies available bind to XOR protein. Several XOR antibodies are available and therefore their binding to purified and milk-XOR was compared by western blot (Figure 38). No detection was seen using the NeoMarkers antibody, possibly because the stock was old and the antibody may have come out of solution. Comparing the other three antibodies, the Polysciences antibody appears to bind better to XOR, as indicated by a stronger signal-to-noise ratio. The HRP-conjugated BioDesign XOR-antibody predictably resulted in less exposure as no 2° antibody is used to amplify the HRP-signal, however equal quantities of Chemicon and Polysciences antibody were used, therefore the Polysciences antibody was chosen to be used in subsequent XOR protein-detection experiments. Prior to cellular staining with the XOR antibody, a HUVEC lysate was probed for XOR content using the western blot technique (Figure 39). The lysates tested showed the XOR protein is found in HUVECs and the banding pattern seen was very similar to that seen with

liver XOR (Waud and Rajagopalan, 1976). These results suggest HUVECs contain the XOR enzyme, which confirms results with other vascular endothelial cell types (Jarasch *et al.*, 1981; Jarasch *et al.*, 1986; Partridge *et al.*, 1992).

3.5.2.3.2 The Endothelial XOR Storage Granule?

The HUVEC endothelial cell model was probed for XOR using an immunofluorescent technique, the results from two separate experiments are shown in Figure 40. The results from these experiments were interesting, XOR appeared as a diffuse cytoplasmic stain in all cells, however in some cells, a punctate stain could be seen, which would suggest packaging of this protein. The appearance of this punctate stain is unlikely to be an artefact from the fixation process for two reasons: i) the punctate stain is not seen in all cells but a diffuse stain is always present. Therefore if fixation caused the coagulation of XOR resulting in a punctate stain, then it should appear in all cells, however it does not, and ii) Acetone/methanol fixation does result in punctate staining (Figure 40 A-B, E and F), however this staining is not an artefact of this technique because it is also seen with paraformaldehyde fixation plus triton X-100 permeabilisation (Figure 40 D). To confirm the staining seen using immunofluorescence a different technique was used, scanning electron microscopy with gold-conjugated 2° antibodies (Figure 43). Again, cytoplasmic and punctate staining of XOR could be seen.

The appearance of XOR-"packages" was not expected, because the XOR protein does not contain any known signal sequences for cellular compartmentalisation (Ichida *et al.*, 1993). Despite this fact, several research groups believe they discovered XOR in peroxisomes of rat hepatocytes (Angermuller *et al.*, 1987; Dikov *et al.*, 1988; Frederiks and Vreeling-Sindelarova, 2002). This finding would suggest that XOR must contain a sequence for direction to the peroxisome. However a separate study has questioned these findings (Ichikawa *et al.*, 1992), in their experience XOR was present in the cytosol of these cells only.

Interestingly, the mammary epithelial cell line, MDA-MB-231, also contained punctate staining of XOR (Figure 42). A control for the XOR-stain was performed with the 1° or 2° antibody alone, or with a saturated 1° in combination with the 2° antibody, which resulted in fluorescent staining being absent or greatly reduced (Figure 41), suggesting that the antibody binding is specific. In the mammary epithelial cell, however, the punctate appearance can be explained. Milk lipid occurs in two forms, as membrane fragments in the skim phase and as milk lipid droplets (MLDs) that provide essential nutrition to the suckling neonate. MLDs are released from mammary epithelial cells by a novel mechanism. Lipid droplets form at the endoplasmic reticulum (Deeney *et al.*, 1985) and are transported to the apical plasma membrane before being secreted. The process of secretion involves the enveloping of the MLD in plasma membrane, which pinches-off to release the MLD into the mammary alveolar lumen. The mechanism of MLD release from mammary epithelial cells has been proposed by Mather and Keenan, 1998 (see Figure 48).

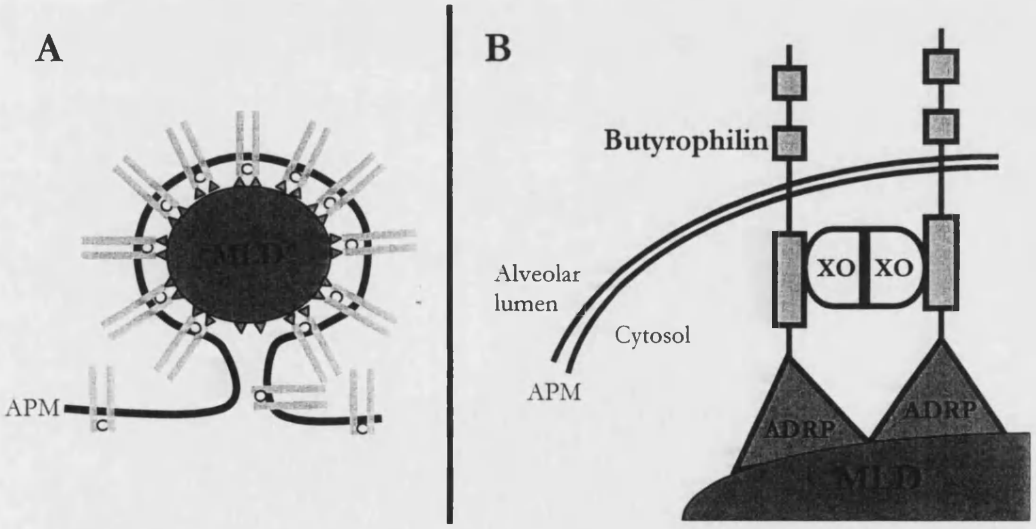

Figure 48. The Proposed Protein Interactions Involved in MLD Secretion from Mammary Epithelial Cells.

A) The enveloping of the MLD, which occurs prior to its release, is thought to be driven by the interactions between the apical plasma membrane (APM)-protein butyrophilin, the cytoplasmic protein XO, and the MLD-associated protein adipocyte differentiation-related protein (ADRP). These inactions are summarised in B). XO is thought to be responsible for the dimerisation of butyrophilin, therefore increasing the affinity of butyrophilin for ADRP. These interactions maybe sufficient to "pinch-off" the enveloped MLD (adapted from Mather and Keenan, 1998).

Considering the proposed process, the concentrated areas of XOR seen in MDA-MB-231 cells could be regions where milk lipid droplet-release is in process. However the process of lipid-droplet secretion does not occur in the vascular endothelium, and previous studies have demonstrated that butyrophilin is only present in mammary epithelial cells (Jack and Mather, 1990). Therefore the endothelial XOR-"package" must have a different function.

In an attempt to characterise the endothelial XOR-"package", colocalisation studies with vWf and therefore WPBs was performed (Figure 44). However co-localisation was not significantly observed and therefore XOR is "packaging" independently of the WPB (the few areas of co-localisation seen are only by virtue of the microscopy technique being used, i.e. visualising the entire depth of the cell. Images taken using confocal microscopy on the other hand, looking at a single plain through the cell, are likely to show no colocalisation). To discover whether the punctate XOR stain is in fact an XOR-storage granule, then co-localisation with other endothelial-packaged proteins should be performed, for example with tissue-type plasminogen activator (tPA) (an anti-coagulant, fibrolytic protein), which is stored in small punctate structures independent of WPBs (Emeis *et al.*, 1997; Knop *et al.*, 2002; Zupanic *et al.*, 2002) [However it must be noted that other research groups have found tPA to colocalise with vWf (Rosnoblet *et al.*, 1999)]. If the XOR-package does not colocalise with another endothelial-stored protein, either a new storage granule has been discovered or packaged XOR is formed by another process, e.g. by endocytosis. As mentioned in the introductory chapters, XOR is known to bind to the surface of the vascular endothelium by association with GAGs (Adachi *et al.*, 1993). Endothelial-bound XOR may be internalised by endocytic events (Houston *et al.*, 1999) that would result in compartmentalisation of XOR protein. These events could explain the structures seen in HUVECs, however the process is reliant on an extracellular source of the enzyme. To assess whether the punctate staining of XOR observed is derived from endocytic processes, colocalisation with endocytic markers should be attempted,

for example with EEA-1 for early endosomes or Lamp-1 for late endosomes and lysosomes (reviewed in Watson *et al.*, 2005).

3.5.2.3.3 HUVEC XOR-Gene Expression?

To detect whether HUVECs express the XOR gene an RT-PCR technique was used. RNA was purified from HUVEC lysates and was shown to be intact (Figure 45). The Rat XOR primers used in the PCR protocol were shown to be complimentary to the human XO sequence (Figure 46), and therefore were used in these studies. PCR applification of cDNA preparations showed that XOR mRNA was present in HUVEC lysates. Furthermore, the expression of XOR appears to be constitutive and, as indicated by the expression of GAPDH, does not vary over the time course tested (i.e. 4 hours; Figure 47). Therefore the XOR enzyme within HUVECs is likely to be of endogenous origin.

As a note of caution. GAPDH is a catalytic enzyme involved in glycolysis. The enzyme is constitutively expressed and therefore is often used as a positive control for PCR and/or as an indication of equal loading of RNA or cDNA in the PCR process (Tabengwa *et al.*, 2000; Sasaki *et al.*, 2004). However, care should be taken when using the expression of GAPDH as a control, as under certain conditions the expression of GAPDH can be effected, for example under hypoxia or in diabetes (Graven *et al.*, 1994; Wentzel *et al.*, 2003).

3.6 Summary

Through morphological, behavioural, and protein marker analysis, cells isolated from the human umbilical vein have been shown to be predominantly of endothelial origin and are therefore the HUVEC. Using immunofluorescent and immuno-gold labelling, XOR protein expression in the HUVEC has been demonstrated. In the HUVEC, XOR is distributed diffusely throughout the cytoplasm but may also be found in possible storage granules. As XOR is not believed to contain any signal sequences for compartmentalisation the mechanism of granule formation is unknown. However

XOR has been localised to peroxisomes in other studies, therefore a mechanism for XOR compartmentalisation must exist. The expression of the XOR gene was shown in HUVECs by RT-PCR.

Chapter 4. Assessment of Methods for the Measurement of Xanthine Oxidoreductase

4 Results: Assessment of Methods for the Measurement of Xanthine Oxidoreductase

4.1 Introduction

As demonstrated in Chapter 3 the chosen vascular model (the HUVEC) has XOR distributed throughout the cytoplasm and is also found packaged into granules. If the hypothesised release of XOR by the endothelium is to have any impact on human physiology or pathology, then enzyme released would have to be active. In this chapter, various XOR activity assays will be assessed and in some cases optimised, ultimately for the purpose of measuring XOR activity in HUVEC vascular endothelial model.

Many XOR activity assays have been produced and measure XOR activity through the formation of reaction products, either by analysing oxidised electron-donating substrates or the generation of reduced electron-acceptors, typically ROS. Techniques available for the measurement of reduced electron-acceptors include the ROS-detecting methods: lucigenin-based chemiluminescent assays (Storch and Ferber, 1988), the cytochrome C assay (Murrell *et al.*, 1990), nitroblue tetrozolium precipitation assays (Özer *et* al., 1998), and electron spin resonance spectroscopy (Speikermann *et al.*, 2003). Techniques that measure oxidised electron-donating substrates include: the uric acid assay (as used in Saunders *et al.*, 1997) and the fluorescence-based isoxanthopterin assay (Beckman *et al.*, 1989).

4.2 Chapter Aim

The aim of this chapter is to compare the XOR-activity assays available to the lab for specificity, sensitivity, and through-put. The XOR assays to be compared include, ROS-detecting assays based on lucigenin and nitroblue tetrazolium reduction, the assay of uric acid generation in the presence of the xanthine substrate, and the fluorescence based assay based on XOR-catalysed generation of isoxanthopterin from the xanthine analogue pterin. The effectiveness of each assay will be discussed and

the most specific and sensitive assay will be used in later results chapters for analysis endothelial derived XOR activity.

4.3 Principals, Materials, and Methods

4.3.1 Bio-Rad Protein Assay

The Bio-Rad assay was used to determine unknown solubilised protein concentrations in samples. The assay is based on the method of Bradford (Bradford, 1976), which analyses a dye-colour change, and therefore absorbance change in the presence of protein. The reagent used in this procedure is an acid solution of Coomassie® Brilliant Blue G-250 dye. Free of protein the reagent's maximal absorbance is 465nm, however in the presence of soluble protein the dye binds and absorbance shifts to 595nm. Absorbance at 595nm is proportional to soluble protein.

4.3.1.1 Materials

Bovine serum albumin (BSA) standard (1.35mg/ml), Protein assay dye reagent concentrate (Bio-Rad Laboratories Ltd. Hertfordshire, UK). 20ml syringe without needle, 0.22μm syringe filter (Fisher Scientific UK Ltd. Leicestershire, UK).

4.3.1.2 Method

The method used is based on manufacturer's instructions, which will briefly be described here. Depending on the expected protein concentration in a sample, two methods for detection are available, the Standard and Microassay procedures, each run in the 96-well plate format. In the standard procedure the dye reagent concentrate was diluted one part to four parts Milli-Q water, and was filtered to remove particulate matter. The BSA standard was serial diluted in Milli-Q water, and in a 96-well plate, 10μl diluted standard and of unknown-protein sample were applied in triplicate. 200μl of the diluted dye reagent was added to each well and samples were mixed by gentle pipeting ensuring no bubbles were formed. Following a five minute incubation at room temperature the absorbance at 595nm was measured using a plate reader (Dynex Technologies Ltd. West Sussex, UK). Using the absorbance values from the BSA standard, a standard curve was created enabling the calculation of

unknown protein concentrations in samples. The Microassay procedure followed the same protocol as above, however, 160µl serial-diluted sample and unknown-protein samples were mixed with 40µl dye reagent concentrate.

4.3.2 Lucigenin-Enhanced Chemiluminescence

Lucigenin-enhanced chemiluminescence has been widely used as a method for detecting $O_2^{\cdot -}$ generation by $O_2^{\cdot -}$-generating systems (Corbisier *et al.*, 1987; Storch and Ferber, 1988) and been used to determine $O_2^{\cdot -}$ generation by cultured cells, tissue homogenates, and even whole vascular tissue (Gyllenhammer, 1987; Pagano *et al.*, 1993). The mechanism of $O_2^{\cdot -}$-induced luminescence is believed to require the univalent reduction of lucigenin (Luc^{++}), forming $Luc^{+\cdot}$, followed by a secondary reaction with $O_2^{\cdot -}$ that results in the formation of light (Faulkner and Fridovich, 1993).

4.3.2.1 Materials

Lucigenin, NADH (Sigma Aldrich Company Ltd. Dorest, UK).

4.3.2.2 Luminescence Measurement Protocol

2mM solutions of lucigenin and NADH were prepared in PBS. Using a 96-well plate, wells were filled with 100µl sample diluted in PBS. The plate was placed into the luminescence-reader (Anthos Lucy 1.0 Microplate Luminometer. Anthos. Wals, Austria). Following the programmed injection of 50µl 2mM solutions of lucigenin and NADH, luminesecence readings were recorded at set time intervals, and luminescence generation over time was calculated.

4.3.3 In-Gel Xanthine Oxidase Assay

Like lucigenin, the compound nitroblue tetrazolium (NBT) may also be used to detect $O_2^{\cdot -}$-generation. When in solution, NBT can react with $O_2^{\cdot -}$ and forms a blue/purple formazan precipitate. NBT has frequently been used to detect $O_2^{\cdot -}$ generation in cultured cells (Czerniecki, *et al.*, 1986; DiGregorio *et al.*, 1987; Joneson and Bar-Sagi, 1998). However, taking advantage of precipitate formation, Özer *et al.*, 1998

developed an in-gel assay that enables the detection of $O_2^{\cdot -}$-generating systems and was used for the detection of XO activity.

4.3.3.1 Materials

For polyacrylamide gel see Section 3.3.5. Nitroblue tetrazolium, Tris-HCl, Hypoxanthine (Sigma Aldrich Company Ltd. Dorest, UK).

4.3.3.2 Protocol

Adapted from Özer *et* al., 1998. Samples were run on polyacryamide gels as described in Section 3.3.5, however in the in-gel assay procedure non-denaturing and non-reducing conditioned were used, i.e. SDS and β-mercaptoethanol were omitted from all buffers and the gel. Following electrophoresis, the gel was bathed in a solution that enabled the detection of XOR activity (see Appendix I 8.6). Gels were incubated at room temperature for sufficient time for blue/purple formazan-precipitate bands to develop (see individual results). Following this period gels were rinsed several times in distilled water to remove non-reduced NBT, and could be stored in water at 4°C in the dark before analysis.

4.3.4 Uric Acid Assay

As described in the introductory Chapter 2 Section 2.2.4.4, XOR generates uric acid during the oxidation of xanthine. This fact forms the basis of a simple assay measuring XOR activity through the formation of uric acid, as used in Sanders *et al.*, 1997.

4.3.4.1 Materials

Xanthine (Sigma Aldrich Company Ltd. Dorest, UK). Xanthine Oxidase (10.61U/ml; 10.5mg/ml) (Biozyme Laboratories. Gwent, UK).

4.3.4.2 Protocol

Xanthine oxidoreductase activity in selected samples was measured spectrophotometrically (Hitachi U-2010 spectrophotometer. Hitachi. Berkshire, UK). In the presence of 100μM xanthine at 25°C, the formation of uric acid at absorbance 295nm (A_{295}) was recorded. Using an extinction coefficient of 9.6mM^{-1} cm^{-1} (Avis *et*

al., 1956), data were anaylsed to calculate XOR activity as a function of uric acid generation per unit time.

4.3.5 Isoxanthopterin Assay

A sensitive, fluorometric assay for XO and XDH has been developed over several decades (Lowry *et al.*, 1949; Haining and Legan, 1967; Markley *et al.*, 1973; Beckman *et al.*, 1989.). The fluorometric assay is based on the use of pterin (2-amino-4-hydroxypteridine) as a substrate for XOR, which is oxidised to the fluorescent compound isoxanthopterin (2-amino-4,7-dihydroxypteridine, IXP). The protocol from the Beckman *et al.*, 1989 assay will now be described and, where indicated, is used as the XOR assay in the results chapters. XO activity is assayed in the presence of the pterin substrate alone, using oxygen as an electron acceptor for the reduced enzyme. With the addition of methylene blue, an electron acceptor from the Fe-S clusters of XO and XDH, the combined activity of XO and XDH are assayed (methylene blue is used instead of NAD^+ as an XDH electron acceptor, as NADH fluorescence overlaps with that of IXP). Allopurinol is added to the sample to inhibit XOR activity, thus allowing the calculation of XO- and XDH-specific generation of IXP [both lactoperoxidase in the presence of H_2O_2 and aldehyde oxidase were shown to catalyse pterin-IXP conversion but were not allopurinol inhibitable (Beckman *et al.*, 1989)]. Finally the addition of an IXP internal standard, of a known concentration, allows for the correction of any fluorescence quenching and the quantification of IXP production. The XOR catalysed conversion of Pterin to IXP and the role of methylene blue and allopurinol are shown in Figure 49.

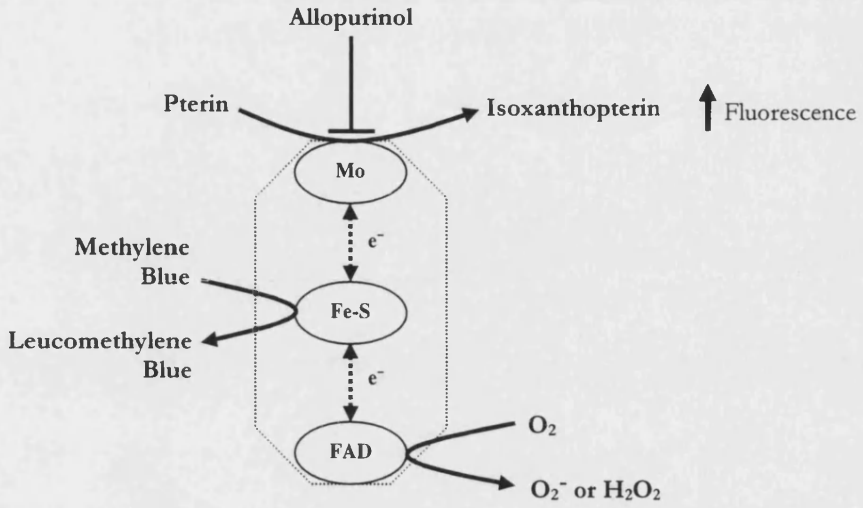

Figure 49. XOR Catalysed Generation of IXP from the Pterin Substrate.

Electrons donated to XOR during the oxidation of pterin to IXP (leading to increased fluorescence) are accepted by O_2 at the FAD-containing moiety in XO, however in the presence of methylene blue electrons are accepted at the Fe-S cluster-containing moiety of XO and XDH. Allopurinol inhibits the oxidation of pterin at the Mo-containing moiety.

4.3.5.1 Materials

Allopurinol, Isoxanthopterin (IXP), Methylene Blue (MB), and Pterin (Pt) (Sigma Aldrich Company Ltd. Dorest, UK). Quartz crystal cuvettes (Fisher Scientific UK Ltd. Leicestershire, UK). Xanthine Oxidase (Biozyme Laboratories. Gwent, UK).

4.3.5.2 Protocol

To analyse XOR-activity the protocol described in Beckman *et al.*, 1989 was followed, except for minor adjustments. Briefly, samples to be assayed were made up to 960µl in PBS in quartz-crystal cuvettes with magnetic stirrers. As a control 100ng/ml XO (final concentration) was typically used. Using a Hitachi F-4500 Fluorescence Spectrophotometer (set at: excitation wavelength (Ex) 345nm, emission wavelength (Em) 390nm, monochromator Ex slit width 5nm, Em slit width 5nm, and the photomultiplier voltage set at 700V) fluorescence measurements were initiated. After a baseline reading of about 30secs 10µM pterin was added and measurements continued for sufficient time to enable rate calculations, following this period 10µM methylene blue was added. Again after sufficient time, 10µM allopurinol was applied to inhibit the reaction and after fluorescence measurements had stabilised a solution

of approximately 100nm isoxanthopterin was added (the exact concentration of IXP added was calculated from the IXP stock absorbance at 336nm using ϵ_{336} = 13mM^{-1}cm^{-1} and Beer's Law). All incubations were at room temperature. A typical plot for the measurement of XOR activity is shown diagrammatically in Figure 50.

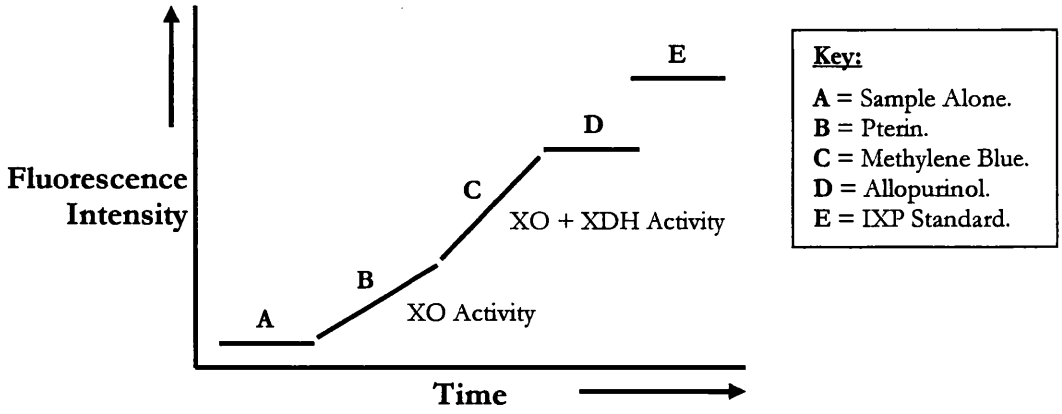

Figure 50. A Typical Spectum from the Time-Scan XOR Assay.

XO is assayed in the presence of pterin alone (with oxygen as the acceptor substrate), whereas the combined activities of XO and XDH are measured in the presence of methylene blue, which replaces the need of NAD^+ as an electron acceptor for XDH. Following the inhibition of XOR activity using allopurinol, the measurement of the fluorescence change following the addition of a known concentration of IXP (which acts as an internal standard) allows the quantification of IXP generation by XO and XDH.

From the data recorded the change in fluorescence per unit time was calculated, and using the change in fluorescence readings following the addition of the IXP standard it was possible to calculate [IXP] generated, as shown in Equation 4.

$$[\text{IXP}] = \Delta F * (IXP_C / F_{IXP})$$

Equation 4. Calculation of Isoxanthopterin Generation in XOR Activity Time-Course Assay.

Where ΔF = Change in fluorescence units per unit time, IXP_C = concentration of IXP standard added, and F_{IXP} = the change in fluorescence units immediately following the addition of the IXP standard.

4.4 Results

4.4.1 Lucigenin-Based Chemiluminescence Xanthine Oxidase-Assay

The lucigenin-based chemiluminescence XOR assay was routinely performed in the laboratory. To assess this assay, XOR activity in human milk samples was measured. Milk samples were kindly donated by lacating mothers post partum, and were stored at -20°C before the XOR-assay was performed. An example of a raw data read-out is given in Figure 51A which includes a negative control of PBS without milk. XOR activity in a series of milk samples was compared over a period of 18 days post-partum (see Figure 51B). During the first week post-partum XOR activity is comparatively high, however after this time milk-XOR activity decreases and remains at a lower level for the remaining 11 days assessed.

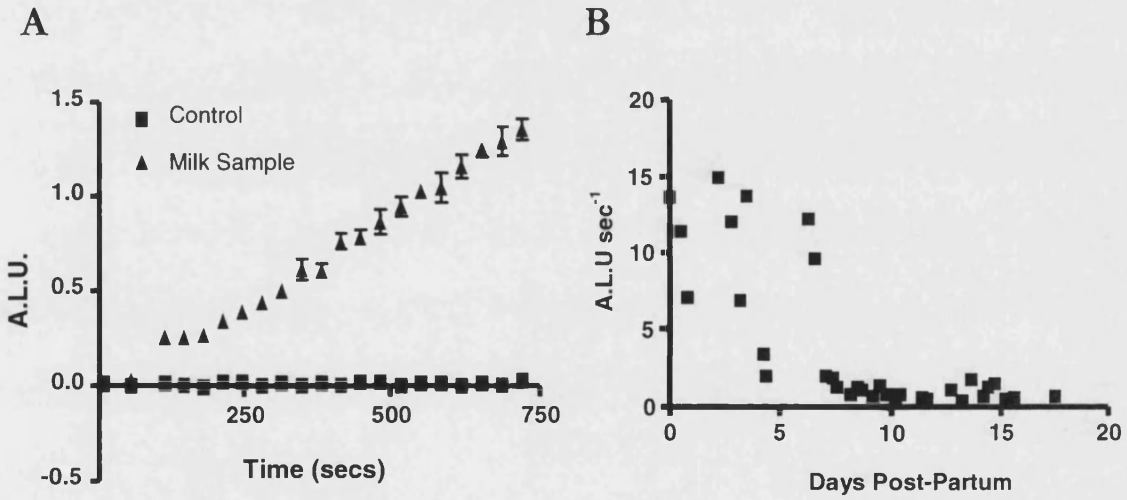

Figure 51. Lucigenin-Based Chemiluminescence XOR-Assay on Human Milk Samples.

Human milk samples were assayed in triplicate for XOR-activity by recording luminescence generated as a result of XOR-$O_2^{\cdot -}$ generation (B). An example of a raw data progress curve with a PBS negative control is shown (A).XOR activity was recorded in arbitrary luminescence units (A.L.U.). Error Bars = SD.

4.4.2 In-Gel Xanthine Oxidase Assay.

The in-gel XO-assay was developed in Özer *et al.*, 1998 and is based on the reduction of a yellow nitroblue tetrazolium solution by superoxide forming a dark blue precipitate. The assay was developed using partially-purified XO from bovine milk

(Özer *et al.*, 1998), a sample with high activity compared to other XO-containing substances or tissues. Therefore before this assay could potentially be applied to detect XO release from HUVECs, its sensitivity was tested on various XO-containing samples.

Using XO purified from bovine milk as a positive control, an initial study compared the activity of different plasma, liver, and milk samples. Rat liver and plasma, and human plasma samples were kindly donated by Dr D. Speden and Dr T. M. Millar, respectively. In plasma and liver preparations from tungsten or allopurinol-fed rats, XOR activity was shown to be effectively inhibited (Speden, 2003), therefore these preparations were used as negative controls for XOR activity. The preparation of these samples is described in Appendix I 8.7. Total protein in each sample preparation was measured using the Bio-Rad protein assay. The linear region of a bovine serum albumin (BSA) standard curve was used to calculate unknown sample-protein concentrations, a typical example is given in Figure 52.

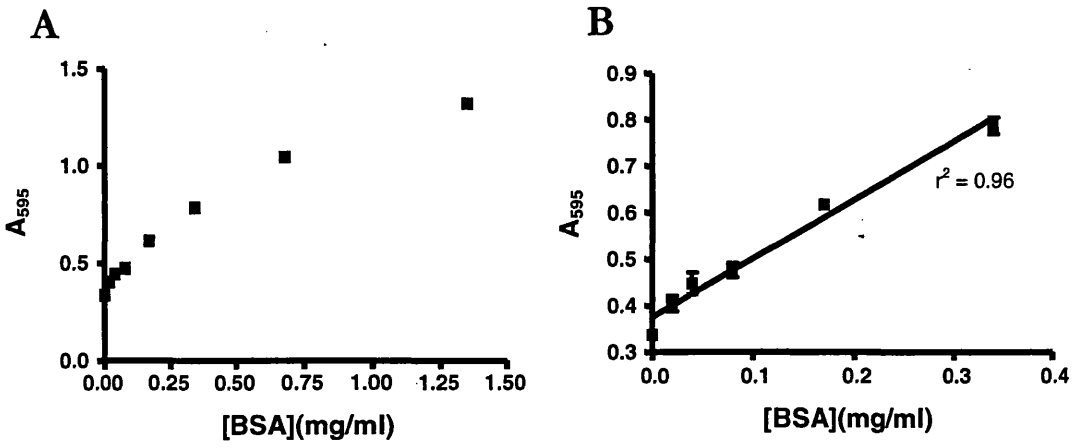

Figure 52. An Example of the Bio-Rad Protein Assay Standard Curve.

The Bio-Rad protein assay standard curve was generated using a doubling-dilution of a BSA stock of known concentration. At higher protein-standard concentrations absorbance readings are no longer linear (A). Therefore, for the generation of the standard curve, linear regression was only performed using the absorbance values of the lower concentrations of BSA (B). Unknown protein concentrations could be calculated from the curve following linear regression.

In all in-gel assays, except where indicated, 30μg of each sample was run on a non-reducing and non-denaturing gel. In this initial study, XO activity was assessed using

concentrations of hypoxanthine and NBT as described in Özer *et al.*, 1998. For activity analysis, gels were incubated at 37°C and following 30mins incubation a strong band could be seen in the lane containing the purified XO sample. After 2hrs incubation additional bands could be seen in the lanes containing rat plasma, rat liver, and human milk. However, with an overnight incubation no additional bands formed (see Figure 53), therefore activity in human plasma and in tungsten-fed rat liver could not be detected by this assay.

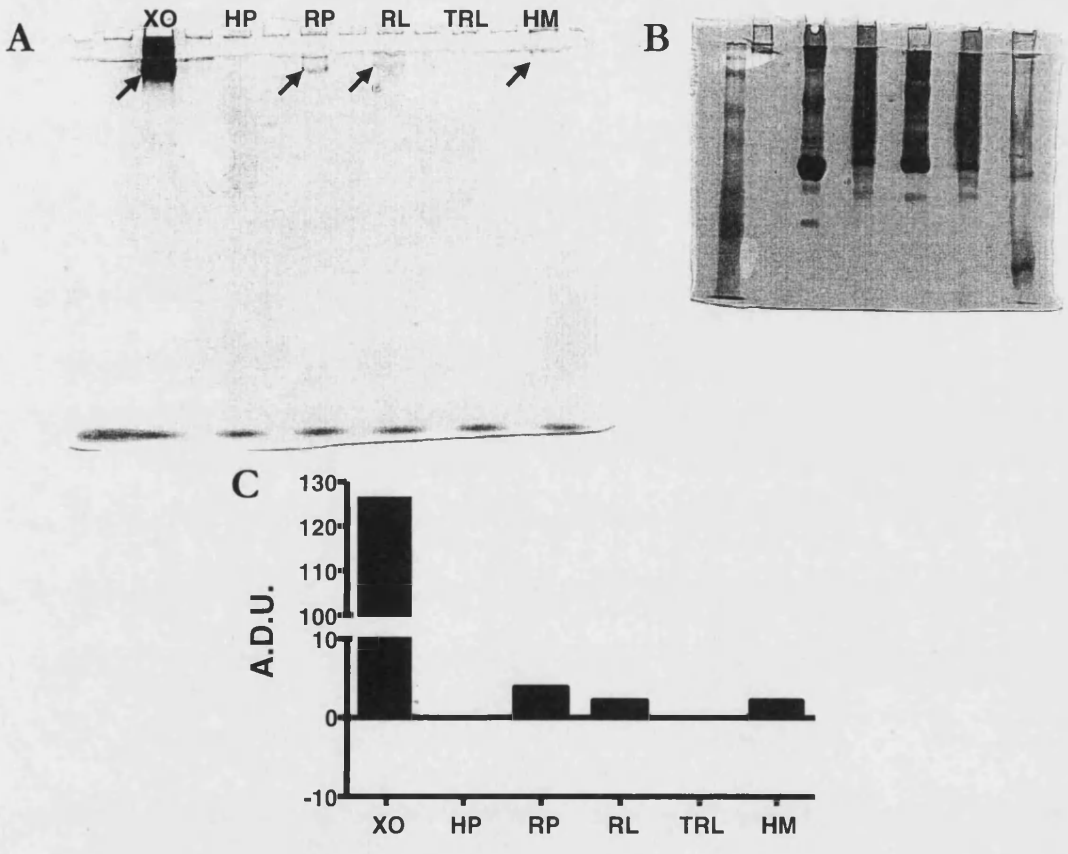

Figure 53. Initial Test of In-Gel Assay Sensitivity.

A) XO-activity in 2μg purified XO (XO), and 30μg protein from human plasma, rat plasma, rat liver, tungsten-fed rat liver, and human milk (HP, RP, RL, TRL, and HM, respectively) was assessed using the in-gel assay method as described in Özer *et al.*, 1998. The activity gel shown results from an overnight incubation at 37°C. Arrows indicate bands of XO-activity. B) The gel was replicated and stained with coomassie blue. C) Activity gels were scanned and density analysis was performed (Arbitrary Density Units, A.D.U).

With a view to improve the sensitivity of the in-gel assay described by Özer *et al.*, 1998, reaction conditions, i.e. concentrations of assay substrates and incubation

temperature, were optimised. Firstly, concentrations of hypoxanthine equal to and greater than those used in Özer *et al.*, 1998 were tested in the analysis of XO-activity in purified XO and rat plasma (see Figure 54A). Increasing concentrations of hypoxanthine were not proportional to an increase in the detection of XO-activity in rat plasma samples. However, it was found that by increasing the concentration of NBT stronger activity-bands were detected in purified XO and rat plasma (see Figure 54B).

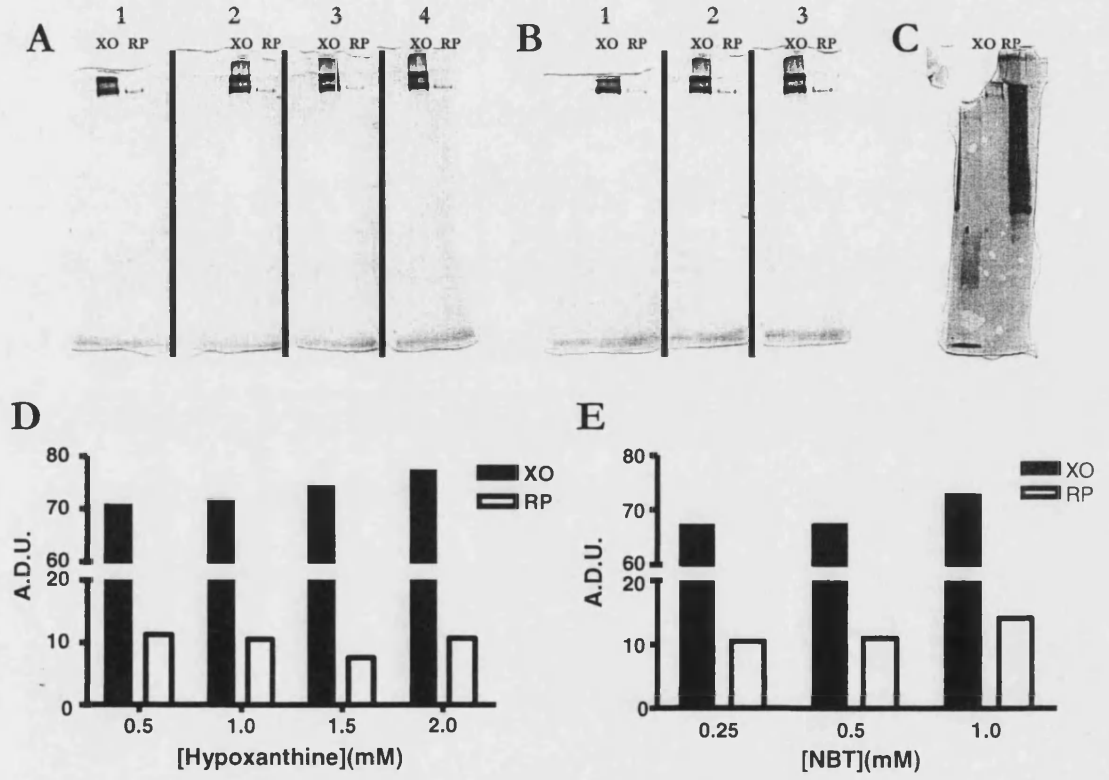

Figure 54. In-gel Assay Optimisation of Hypoxanthine and NBT Concentrations.

A) XO activity in 1μg purified XO (XO) and 30μg protein from rat plasma (RP) was assessed using the in-gel assay solution containing 0.5mM NBT and 0.5, 1.0, 1.5, or 2.0mM hypoxanthine, see gels 1, 2, 3, and 4, respectively. B) For the same samples, in-gel assays solutions containing 0.5mM hypoxanthine 0.25, 0.5, 1.0mM NBT were assessed, see gels 1, 2, and 3, respectively. C) The gel was replicated and stained for protein using coomassie blue. D and E) Density analysis was performed on the resulting gels (Arbitrary Density Units, A.D.U).

From other experiments performed in the laboratory it was discovered that the activity of purified XO was stable when incubated at temperatures up to ~60°C (Dr Millar, unpublished results). Therefore a range of incubation temperatures, up to

50°C, were compared in the in-gel assay. After approximately 30mins incubation strong activity-bands were observed in both XO and rat plasma lanes in the 50°C incubation, activity-bands were present in the 25 and 37°C incubations but appeared much fainter in comparison. Following 1hr of incubation strong activity-bands were seen in gels incubated at all temperatures, however intensity increased as incubation temperature increased (see Figure 55), i.e. temperature was proportional to activity-band intensity in purified XO and rat plasma preparations. Therefore, the optimal conditions for the in-gel assay were found to be incubation at 50°C in an activity-assay solution containing 0.5mM hypoxanthine and 1mM NBT.

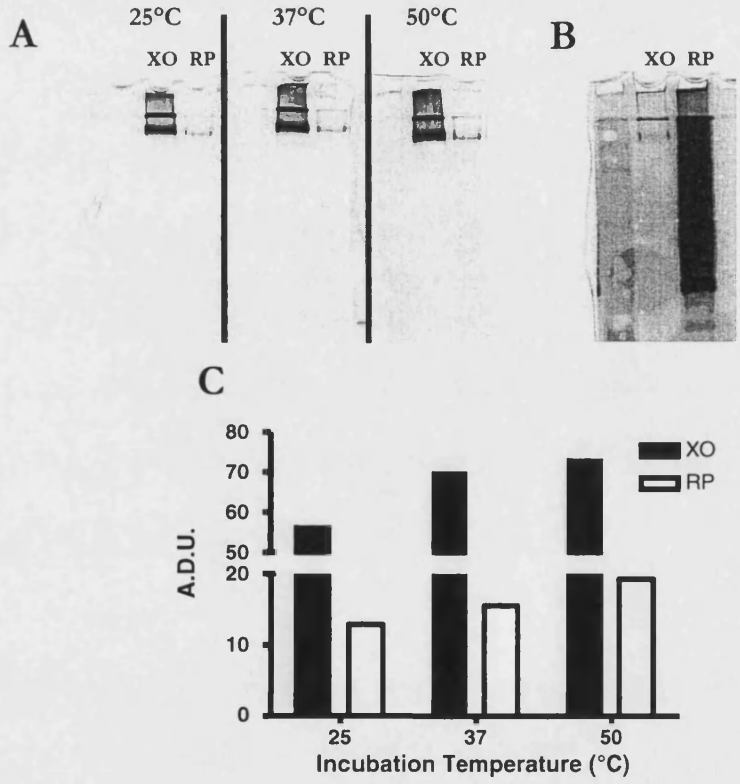

Figure 55. In-gel Assay Optimisation of Incubation Temperature.

A) XO activity in 1μg purified XO (XO) and 30μg protein from rat plasma (RP) was assessed using the in-gel assay solution containing 1.0mM hypoxanthine and 1mM NBT, incubated at 25, 37, and 50°C for equal periods of time. B) The gel was replicated and stained for protein using coomassie blue. C) Density analysis was performed on the resulting gels (Arbitrary Density Units, A.D.U).

As a control for the optimal conditions, purified XO and rat plasma samples were incubated in a XO-activity assay solution without hypoxanthine (therefore just NBT)

or with the XO-inhibitor allopurinol (see Figure 56). Compared to the positive control, the presence of allopurinol greatly reduced XO activity and therefore the formation of the formazan precipitate, and in the absence of the XO-substrate hypoxanthine no XO activity was detected.

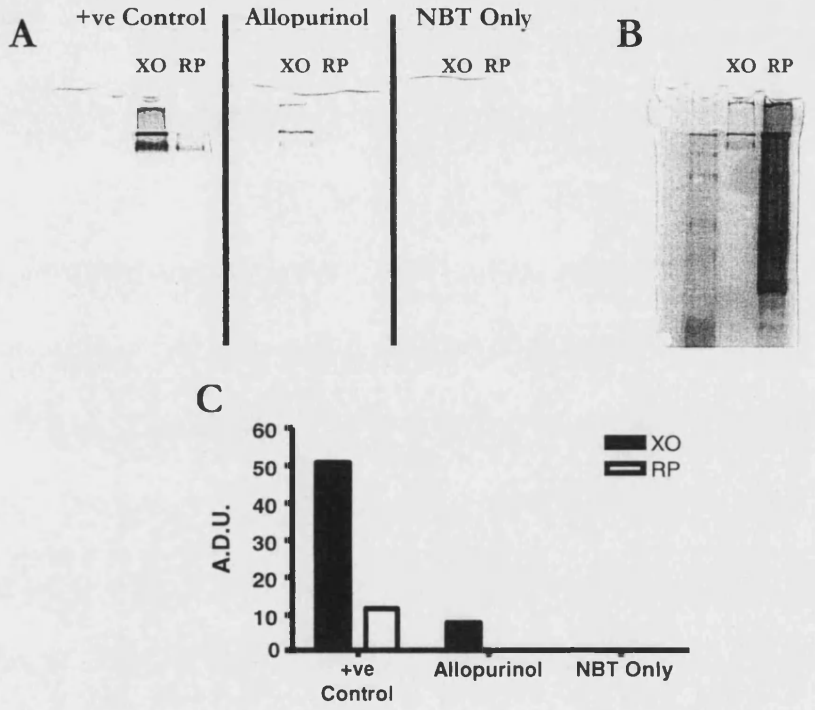

Figure 56. Control for Optimal In-gel Assay Conditions.

A) XO-activity in 2μg purified XO (XO), and 30μg protein from rat plasma, was assessed using the optimal in-gel assay method (+ve control), in the presence of 0.5mM allopurinol (allopurinol), or in the absence of hypoxanthine (NBT only). B) The gel was replicated and stained with coomassie blue. C) Activity gels were scanned and density analysis was performed (Arbitrary Density Units, A.D.U).

The optimal in-gel assay conditions were used to assess XO-activity in the original samples tested (see Figure 57, compare with Figure 53), therefore allowing a comparison of the published assay conditions against the new protocol. Using optimal conditions, activity-bands developed in purified XO, rat plasma, and rat liver after just 30mins incubation. After 1.5hrs incubation faint bands could also be seen in human milk and tungsten-fed rat liver samples. However no change was observed following an overnight incubation (as shown in Figure 57).

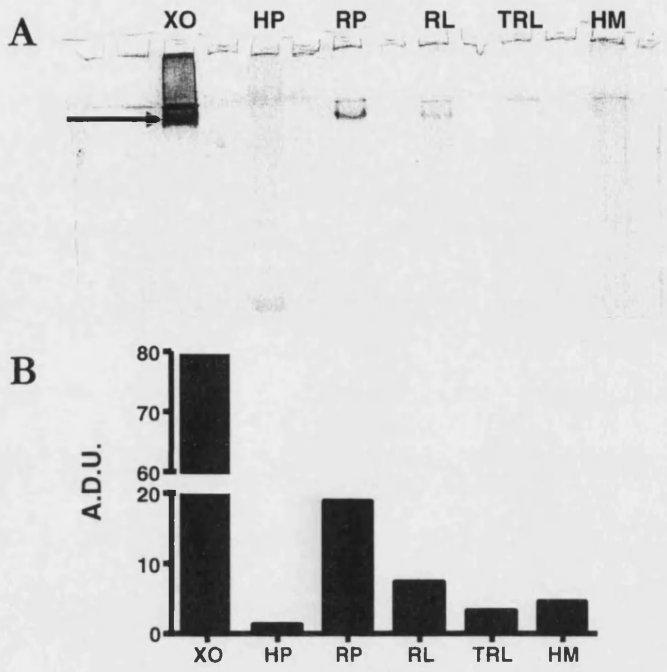

Figure 57. Assessment of In-Gel Assay Sensitivity Using Optimal Conditions.

A) XO-activity in 2μg purified XO (XO), and 30μg protein from human plasma, rat plasma, rat liver, tungsten-fed rat liver, and human milk (HP, RP, RL, TRL, and HM, respectively) was assessed using the optimised in-gel assay method. Arrow indicates bands of XO-activity B) Activity gels were scanned and density analysis was performed (Arbitrary Density Units, A.D.U).

4.4.3 Isoxanthopterin-Based Xanthine Oxidase Assay

To assess the sensitivity of the fluorescence-based isoxanthopterin (IXP) assay, the assay was compared to the in-gel assay with optimal incubation conditions. For the in-gel assay 1μg purified XO and 30μg plasma, liver, and milk samples were loaded. For the IXP-assay comparison, the same quantities were assessed using the method described by Beckman *et al.*, 1989, except for purified-XO where only 0.1μg was used (see Figure 58). An example of the raw data output in the IXP-assay is shown in section 4.4.4. The results from the in-gel assay presented are following 2hrs incubation, whereas in the IXP-assay an activity rate for each sample was calculated from just 1min assays at 37°C. Comparing the samples used, a similar XO-activity profile was seen from both XO-assays (Figure 58B and C). Interestingly, in a protein-

to-protein comparison more activity is seen in cow milk compared to human, and the XO-inhibitory effects are greater using tungsten feeding compared to allopurinol in rats.

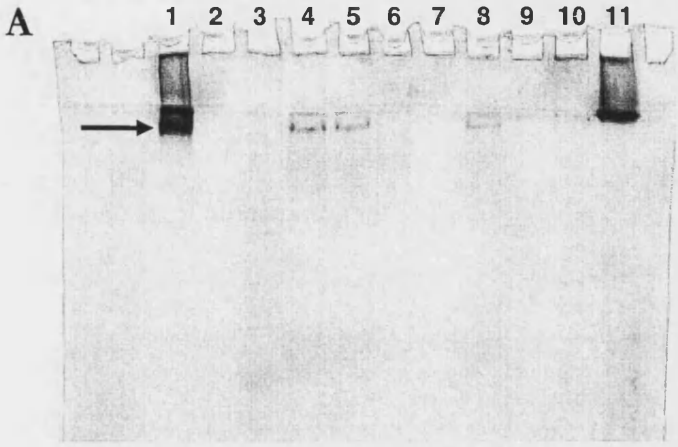

Lane	Sample
1	XO
2	...
3	HP
4	RP
5	ARP
6	TRP
7	...
8	RL
9	TRL
10	HM
11	CM

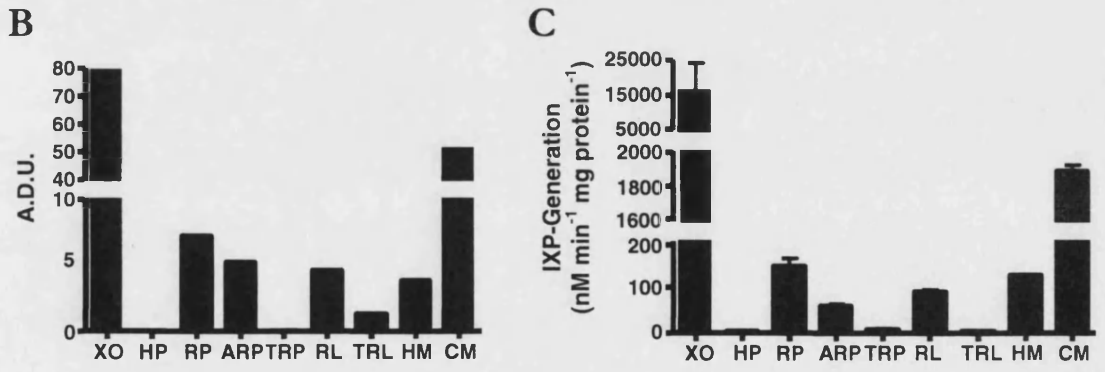

Figure 58. Isoxanthopterin Sensitivity Test – Comparison with In-gel Assay.

A) XO-activity in 2μg purified XO (XO), and 30μg protein from human plasma, rat plasma, allopurinol-fed-rat plasma, tungsten-fed-rat plasma, rat liver, tungsten-fed-rat liver, human milk, and cow milk (HP, RP, ARP, TRP, RL, TRL, HM and CM, respectively) was assessed using the optimised in-gel assay method. Arrow indicates bands of XO-activity, loading order is described in table. B) Activity gels were scanned and density analysis was performed (Arbitrary Density Units, A.D.U). C) The samples, as described in A, were assayed using the Beckman *et al.*, 1989 method, however only 0.1μg purified XO was used. Assays were duplicated and error bars represent SD.

Equal quantities of total protein were analysed in the in-gel and IXP-based assays. However, to assess the quantity of XOR-protein in each sample in comparison with enzyme activity, Western-blot analysis was performed (see Figure 59). 50ng purified XO and 10μg of each sample were loaded onto a SDS-PAGE gel. Transferred proteins were probed for XO using the Polysciences 1° XO-antibody with relevant

2°. It is interesting to note that even though similar quantities of XO-protein are present in both human and cow's milk (see Figure 59 lanes 10 and 11, respectively), the enzyme activity in these samples is quite different (Figure 58), i.e. far greater activity is present in cow's milk. Also, a band approximately 20kDa is present in plasma samples that is weakly visible or absent from liver and milk samples.

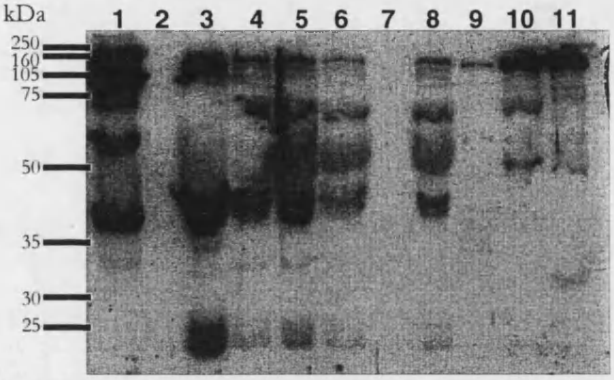

Lane	Sample
1	XO
2	...
3	HP
4	RP
5	ARP
6	TRP
7	...
8	RL
9	TRL
10	HM
11	CM

Figure 59. XOR-Protein Content in In-gel Assay Samples.

The XOR-protein content in the samples used in the in-gel and IXP-based XO-assays was assessed using the Western-Blot technique. Proteins in 10μg of each sample were separated by SDS-PAGE under reducing conditions. Transferred proteins were probed using a 1 in 5000x dilution of Polysciences anti-XO and a 1 in 200x dilution of the relevant secondary antibody. The gel-loading order is given in the table above.

To improve detection of XO-activity in the IXP-based assay, an assay time greater than 1min maybe required. To assess the generation of IXP over time, the activity of purified XO was measured in the presence of 10μM pterin and 10μM methylene blue, with and without 10μM allopurinol at intervals up to 24hrs at 37°C. In this experiment the allopurinol-inhibitable activity of 5ng XO was measured, essentially using the Beckman *et al.*, 1989 assay, however an end-point concentration of IXP generated was calculated for each time point (see Figure 60). The generation of IXP, and therefore XO activity, appears to be linear over a 24hr time period (linear regression analysis of data resulted in $r^2 = 0.95$).

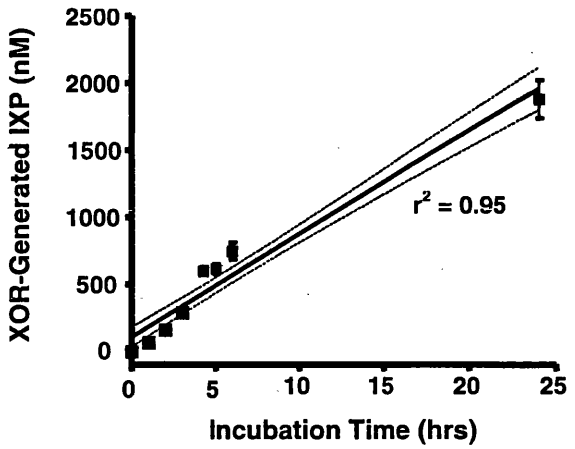

Figure 60. Isoxanthopterin-Based Assay of XO Activity in Long-Term Incubation.

The activity of 5ng purified XO was assayed using IXP-generation method. At desired time points the allopurinol-inhibitable portion of IXP generation was assessed. Each time point was in triplicate and error bars represent SD. Linear regression was performed and 95% confidence intervals are shown.

4.4.4 Uric Acid-Based Xanthine Oxidase Assay

The uric acid generation-based XO-activity assay was also assessed. Using a change in absorbance (at 295nm) over time, this assay detects the generation of uric acid from the substrate xanthine, a reaction catalysed by XOR. The generation of uric acid over 1min was assessed and compared to IXP-generation over the same time period (see Figure 61), examples of raw data collected from both assays is shown in Figure 61A and C and the calculated activity rates in Figure 61B and D. Compared to the IXP-based XO-assay, a greater quantity of purified XO was required in the uric acid-based XO assay to produce a readout where XO activity could easily be calculated.

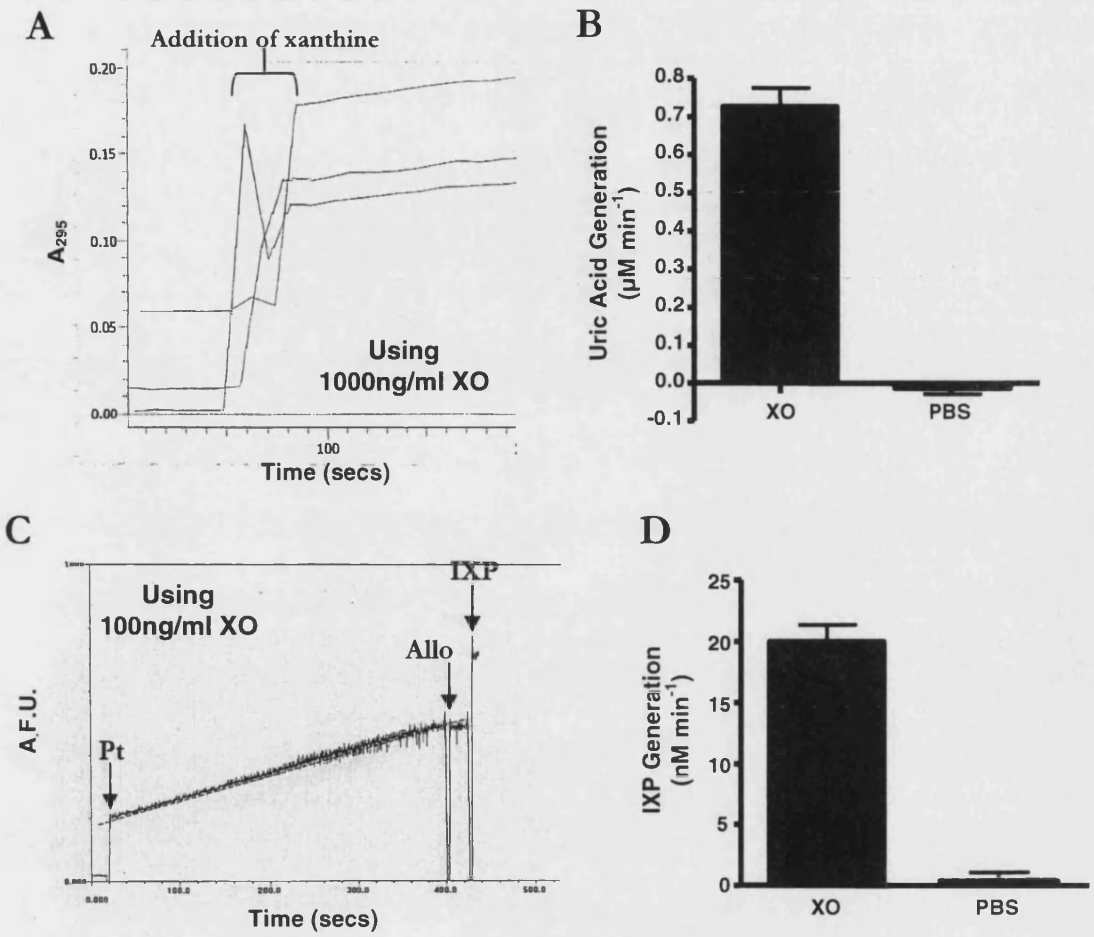

Figure 61. Comparison of the Uric Acid and IXP-Based XO-Assays.

The activity of 1μg purified XO was assessed using the uric-acid assay. The raw data output is shown in A, and activity was calculated from the linear regions of absorbance change (B). As a control the assay was also run in the absence of XO, i.e. with phosphate buffered saline (PBS) and xanthine, see bar labelled PBS (B). For the IXP-assay, only 100ng XO was required to produce easily-measurable activity. The raw data output is shown in C, and activity was calculated from the linear regions of fluorescence generation (arbitrary fluorescence units, A.F.U.) (D). The addition of pterine (Pt), allopurinol (Allo), and isoxanthopterin standard (IXP) are indicated. As a control the assay was also run in the absence of XO, i.e. with phosphate buffered saline (PBS) and pterin, see bar labelled PBS (D). Each assay was repeated in triplicate and error bars represent SD.

4.5 Discussion

4.5.1 The Lucigenin-Based Chemiluminescent XO-Assay

The chemiluminescent XO-assay was sufficiently sensitive to detect XO activity in human milk (Figure 51) and in this respect this assay is comparable to the IXP-assay. It is interesting to note the activity in the series of milk samples tested. Early post-

partum samples contain higher levels of XO activity compared to later samples, this result coincides with findings in other publications where XOR-NO• generation was measured (Stevens *et al.*, 2000).

Although the lucigenin-based chemiluminescent assay is sensitive, the use of this assay for future experiments measuring XO-release from the endothelium was quickly disregarded because the assay is flawed in two ways. Firstly, the assay is not specific to XOR, the activity of any $O_2^{\cdot -}$ generator will be detected. However, a certain amount of specificity can be generated by using XOR-specific substrates. Calculation of XOR-inhibitable portions of activity is not feasible, as no specific inhibitor exists for XOR-NADH oxidase activity. XOR-NADH oxidase activity can be inhibited using diphenyleneiodonium (DPI) (Sanders *et al.*, 1997), however DPI also inhibits other ROS-generating enzymes such as NADPH oxidase and NOS. Secondly, and most importantly, lucigenin can generate $O_2^{\cdot -}$! (Liochev and Fridovich, 1998). As described in section 4.3.2, the mechanism of $O_2^{\cdot -}$-induced luminescence requires the univalent reduction of lucigenin (Luc^{++}), forming $Luc^{+\cdot}$, followed by a secondary reaction with $O_2^{\cdot -}$ that results in the formation of light. However $Luc^{+\cdot}$ has been shown to autoxidise and thus generate $O_2^{\cdot -}$ (Liochev and Fridovich, 1997; Vasquez-Vivar *et al.*, 1997). Furthermore, evidence suggests that $O_2^{\cdot -}$ can not reduce Luc^{++}, and therefore will not induce chemiluminescence alone (Faulkner and Fridovich, 1993), it is believed that some enzymes catalyse the reduction of Luc^{++} to $Luc^{+\cdot}$, however the exact mechanism is not known. Therefore, in the presence of O_2, any system that results in the univalent reduction of Luc^{++} will result in the generation of $O_2^{\cdot -}$ and therefore chemiluminescence, which will result in the false detection of superoxide generation. This process has been shown in systems where $O_2^{\cdot -}$ is not ordinarily produced, as demonstrated using glucose + glucose oxidase in Liochev and Fridovich, 1997. As Luc^{++} may accelerate the formation of $O_2^{\cdot -}$ in $O_2^{\cdot -}$-generating systems and produce false positives for $O_2^{\cdot -}$ generation, this assay should not be used for the detection or quantification of $O_2^{\cdot -}$.

4.5.2 The In-Gel, IXP, and Uric Acid-Based XO Assays

An initial test of the in-gel assay proved that XO activity could be detected in the purified XO control, in rat plasma, rat liver, and in human milk (Figure 53). In this first test the incubation conditions stated in Özer *et al.*, 1998 were followed. One would assume these conditions to be optimal, however further experiments were carried out and it was discovered that by increasing both the NBT concentration and incubation temperature the assay could be improved (Figure 54; Figure 55), i.e. by increasing the intensity and decreasing the formation time of activity-bands. The optimal conditions discovered in this thesis were: incubation at 50°C in an activity-assay solution containing 0.5mM hypoxanthine and 1mM NBT. As a control, both purified XO and rat plasma samples were incubated in an assay medium without hypoxanthine or with allopurinol (Figure 56). Activity was greatly reduced in the presence of allopurinol and absent without hypoxanthine, which suggests that only XO-activity is being measured in this assay. The optimal assay conditions were applied to the original samples tested (Figure 57) and an improvement was seen over the Özer *et al.*, 1998 conditions, i.e. activity-band formation was quicker and XO-activity was detected in all samples tested.

XO-activity measurements from the in-gel assay were compared with another XO-activity assay, the IXP-based assay (Figure 58). The activity measured in each sample was very similar in each assay, suggesting that both assays are measuring XO-activity accurately. However, this experiment highlighted a major flaw in the in-gel assay. Activity readings in the IXP-based assay were easily duplicated as each assay took approximately one minute to perform, whereas the in-gel assay requires several hours preparation before activity can be measured. Also, due to the addition of an IXP standard, XO-activity in the IXP-based assay can be quantified. To quantify the in-gel assay a dilution of purified-XO, of known concentration, would have to be loaded onto each gel, therefore constituting a standard curve from which unknown sample-XO quantities could be calculated. However, this would reduce the number of lanes unknown samples could be loaded onto and make this process more laborious than it

already is. As with the lucigenin-based assay, the problem of specificity also arises in the in-gel assay. NBT will be reduced by any radical-generating system, however using pterin and the addition of allopurinol, the IXP-assay is XO-specific (Beckman *et al.*, 1989). In addition, the IXP-based assay linearly accumulates the IXP reaction product (Figure 60) whereas product formation the in-gel assay appeared to plateau after a few hours incubation. Therefore the IXP-based assay can be used as an end-point reaction where even very low levels of XO-activity could be recorded.

Compared to the IXP-based XO-assay, similar enzyme-specificity should apply to the uric acid assay and theoretically the accumulation of reaction product could be used in the uric acid-based XO-assay. However, this assay was not as sensitive as the IXP-based assay (Figure 61), generation rates of hundreds of nM min^{-1} uric acid were required for detection of activity, whereas tens of nM min^{-1} IXP-generation were easily detected in the IXP-based assay. Therefore the IXP-assay appears to be the most specific, sensitive, and rapid assay tested and will be used to assess the hypothesised secretion of XOR from the vascular endothelium.

4.5.3 Differences in Activity between Samples Assayed

Some interesting results have been generated assaying samples for XO activity with the in-gel and IXP-based protocols. Firstly, comparing the human and cow's milk samples. From the Western blot (Figure 59) it is evident that similar quantities of XO-protein are present in each milk sample and therefore similar quantities of XO-protein will have been measured for activity. However, activity in the cow's milk sample was far greater (Figure 58). Both the IXP-based and in-gel assay require functional MoCo insertion to catalyse the reaction being measured in each assay (see Figure 62) and the reason for discrepancy in activities may lie in the putative differences in the MoCo between the two species, i.e. there maybe a greater proportion of functional MoCo in bovine compared to human milk enzyme (Godber *et al.*, 1997). However, in the experiments in this thesis only one human milk sample

was analysed to form this comparison, and therefore conclusions should not be drawn from these data.

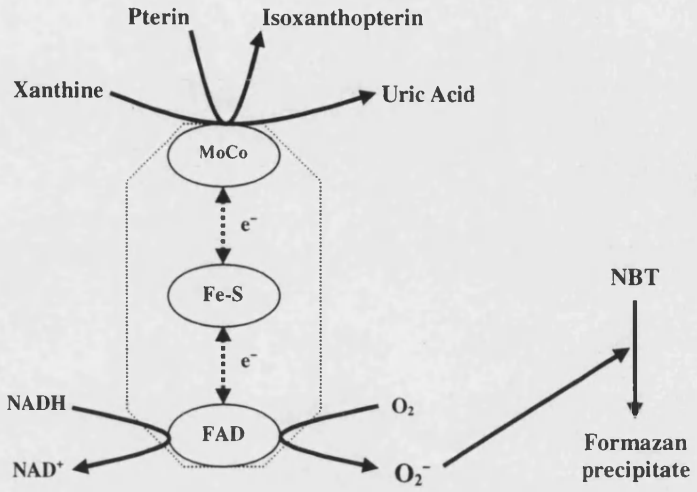

Figure 62. Cofactors Involved in the Xanthine Oxidase Assays.

The in-gel and IXP-based assays require binding of electron-donating substrates (xanthine and pterin, respectively) to the functional MoCo. Pterin is converted to the fluorescent compound IXP, whereas $O_2^{\cdot-}$ generation is required for the formation of the formazan precipitate in the in-gel assay. In comparison the lucigenin-based assay does not require the MoCo, NADH acts an electron donating substrate and binds to the FAD-moiety.

Also of interest was the appearance of a ~20kDa XOR-fragment in plasma which was more pronounced compared to liver and milk samples (in some samples this fragment was absent; Figure 59). A fragment of this size is formed during the irreversible conversion of XDH to XO by proteolytic cleavage (Della-Corte and Stirpe, 1968; Waud and Rajagopalan, 1976; Saksela *et al.*, 1999). It has also been shown that XDH in plasma is rapidly converted to XO (Kooij *et* al., 1994), and in fact the majority of circulating XOR is in the XO form (see results chapter 6). Taken together with the appearance of a ~20kDa XOR-fragment in plasma, these results suggest the existence of a possible plasma protease responsible for XDH-XO conversion.

4.5.4 Summary

Although the lucigenin-based XO-assay appeared to be sensitive, serious flaws exist with this assay, i.e. $Luc^{+\cdot}$ can create $O_2^{\cdot-}$, the XO-generated product the assay should be measuring. Therefore the use of the lucigenin-based assay was disregarded. The in-

gel XO-assay was tested, and although reaction conditions have been optimised beyond those published (Özer *et al.*, 1998), due to its laborious nature the in-gel assay would be inefficient to assay many samples simultaneously, especially as replicates of each sample are required. Therefore a more high-through-put technique was sort after, and based on sensitivity, specificity, and processing speed the IXP-based XO-assay will be used for the assessment of XOR-release from the endothelium.

Chapter 5. The Release of Xanthine Oxidoreductase from the Vascular Endothelium

5 The Release of Xanthine Oxidoreductase from the Vascular Endothelium

5.1 Chapter Aims

The reasons for targeting the vascular endothelium as a potential source of circulating XOR are discussed in the Introductory chapters (especially in the Hypothesis section). The aim of this chapter is to investigate whether the endothelium can release XOR, and experiments will be performed using known endothelial cell protein secretion agonists. The release of vWf will be used as a positive control, and using the sensitive IXP-based XOR assay developed in Chapter 4, the release of XOR from HUVECs will be measured. An initial aim of this Chapter is to develop a lactate dehydrogenase assay to detect whether the concentrations of agonist applied to the HUVECs are cytotoxic.

5.2 Principals, Materials, and Methods

5.2.1 Stimulation of Protein Secretion from HUVECs

5.2.1.1 Materials List

A23187, Colchicine, Histamine, Thrombin (Sigma Aldrich Company Ltd. Dorest, UK).

5.2.1.2 Stimulation Protocol

Note: Cell culture procedures are described in Chapter 3. Confluent P2 HUVECs grown in 12-well plates were used in all HUVEC stimulation studies. Conditioned medium was aspirated from wells and cells were gently washed with 1ml 37°C HBSS to remove any loose extracellular antigen. Cells were exposed to stimulant prepared in 37°C HBSS (always 1ml per well) and were incubated for the desired time at 37°C, 5% CO_2 in air (standard culture conditions). After the desired incubation, medium above the cells was removed and stored on ice before further analysis. 100% secretion of the

protein of interest was achieved by lysing cells with 1ml Triton X-100-based lysis buffer (Park *et al.*, 2001; Anrather *et al.*, 1999; for lysis buffer recipe see Appendix I 8.8) per well, at 4°C for about 5mins or until all cells appeared lysed under the microscope.

5.2.2 XOR Activity Measurements

All measurements of XOR release from HUVEC were performed using the over-night IXP-based XOR assay developed in Chapter 4, the most sensitive assay of those compared. Data generated from this experiment were used to calculate XOR activity expressed as Units XOR, where *one XOR Unit is defined as the quantity of XOR required to cause a reaction to process one micromole of IXP per minute at 37°C.* An example of the calculation, starting from the activity data in the form "IXP generation (nM ml^{-1} 10^6 $cells^{-1}$)", is given below (Figure 63):

XOR-Generated IXP (nMolar) ml conditioned $media^{-1}$ 10^6 viable $cells^{-1}$

↓ Divide by 1000 *

XOR Generated IXP (nmoles) 10^6 viable $cells^{-1}$

↓ Divide by 1260 **

XOR Generated IXP (nmoles) min^{-1} 10^6 viable $cells^{-1}$

↓ Divide by 1000 ***

XOR Units 10^6 viable $cells^{-1}$

(XOR Units may be converted to mUnits or to μUnits by subsequent mulitplications of 1000)

* nMolar = nmoles per litre. As 1ml conditioned media was used in the XOR assay dividing by 1000 gives nmole ml^{-1}.

** The generation of IXP was measured at 37°C for 21hrs (usually), therefore dividing by 1260 converts IXP-generation per minute.

*** Converts the number of nmoles into μmoles and therefore the XOR Enzyme Unit definition.

Figure 63. The Calculation of XOR Units from IXP-based XOR Assay Data

5.2.3 Molybdenum Supplementation of ECGM

5.2.3.1 Materials List

0.22μm syringe filter, Ammonium Molybdate (Fisher Scientific UK Ltd. Leicestershire, UK)

5.2.3.2 Supplementation Protocol

A 50mM ammonium molybdate stock was prepared in PromoCell ECGM and the pH adjusted back to that of fresh ECGM. The stock was filter sterilised using a 0.22μM filter and was diluted to 10, 1, 0.1, 0.01mM working concentrations in ECGM. Confluent HUVECs in 12-well plates were fed 1ml ECGM with and without Mo-supplement per well, for 24hours at 37°C, 5% CO_2 in a humidified incubator. Following the 24hour incubation period HUVECs were washed once in HBSS and lysed in lysis buffer, cell debris was removed by centrifugation at 1600rpm for 5mins. The lysate was analysed for XOR activity using the modified IXP-based XOR assay developed in Chapter 4. Trypan blue-exclusion cell counts were performed to assess whether Mo-supplementation affected viable cell number.

5.2.4 Lactate Dehydrogenase Assay

The cytoplasmic enzyme lactate dehydrogenase (LDH) is released from compromised cells due to a cytotoxic environment. An assay for LDH is commonly used to assess whether treatment of cultured cells has been cytotoxic (Gruenhagen and Yeung, 2004; Kikkawa *et al.*, 2005). In experiments in this thesis, the LDH assay will serve as a control indicating whether proteins (especially vWf and XOR) have been secreted from HUVECs by a controlled mechanism or have been released by compromised cells as the stimulant was cytotoxic.

5.2.4.1 Materials List

Allopurinol, Lactate Dehydrogenase, NAD^+, Sodium Lactate (Sigma Aldrich Company Ltd. Dorest, UK). Diphenyliodonium Chloride (DPI) (ICN Biochemical Inc. OH, USA).

5.2.4.2 Protocol

An established LDH assay protocol (www.worhtington-biochem.com), described below, was optimised for use in experiments in this thesis (see Results section). 2.8ml 0.2M Tris-HCl (pH 7.3), 0.1ml 6.6mM NADH, and 0.1ml 30mM sodium pyruvate were added to a cuvette and incubated in a spectrophotometer at 25°C for 4-5mins to achieve temperature equilibration. Following the addition of 0.1ml enzyme/sample the absorbance at 340nm was recorded over time. The change in NADH concentration was calculated using the extinction coefficient $6.22mM^{-1}\ cm^{-1}$.

5.2.5 Statistical Analysis

Statistical analysis of data collected was performed using GraphPad Prism Version 4.00 (GraphPad Software Inc.). Presented below are the background details to the tests used in the analysis of sample data.

5.2.5.1 The Gaussian (or Normal) Distribution and Normality Testing

Many statistical tests, including ANOVA and t-tests, assume that the population from which you are sampling follows a Gaussian "bell-shaped" distribution. Biological data do not follow the Gaussian distribution, as the Gaussian distribution extends infinitely in both positive and negative directions. However statistical tests, such as the ones mentioned above, work well even if the distribution is only approximately Gaussian. Using a normality test it is possible to determine whether sample data collected are likely to have been selected from a population that follows a Gaussian or normal distribution, an important factor when selecting further statistical analysis. The Prism program uses the Kolmogorov-Smirnov test for deviations from a Gaussian distribution and answers the following question: If you randomly sample

from a Gaussian population, what is the probability of obtaining a sample that deviates from a Gaussian distribution as much (or more so) as this sample does? A high probability would indicate that your sample is likely to be derived from a population with a Gaussian distribution.

5.2.5.2 Standard Deviation

The standard deviation (SD) of a data set quantifies data variability/scatter. Assuming the sample data follow a Gaussian or Normal distribution, then 68% of the values lie within one SD of the mean and 95% of values lie within two SD of the mean. The sample SD is calculated in all instances in this document (rather than the population SD), as data collected are only a sample of the population (i.e. in HUVEC stimulation studies, only a portion of the total HUVEC population is tested, the population SD would only be calculated if all the HUVECs in the world were tested!).

5.2.5.3 Standard Error of the Mean

The standard error of the mean (SEM) is a measure of how far the calculated sample mean is from the true population mean and is derived from the following formula:

$$SEM = SD / \sqrt{N}$$

The SEM will decrease as the sample number increases, as the larger your sample, the closer the sample mean will be to the true population mean. The true population mean does not necessarily lie within the SEM limits. In fact, assuming the sample data follow a Gaussian distribution, there is only a 68% chance that the population mean will fall within this error.

5.2.5.4 Analysis of Variance (ANOVA)

The ANOVA statistical test is commonly used in a laboratory setting for the comparison of a number of different treatments (3 or more unmatched groups) and assumes that sample data are derived from populations with a Gaussian distribution and equal variances (Prism tests variances with Bartlett's test for equal variances). The

ANOVA test partitions variability between treatment means and variability between values within a treatment group (residual or error variation). Residual variability is quantified as the sum of squares (SS) of the differences between each value within a treatment and its treatment mean, whereas variation between groups is quantified as the SS of the differences between treatment means and the grand mean (the mean of all values in all groups). The treatment and residual SS values are used to calculate Mean Square (MS) values (SS divided by degrees of freedom), which are used to calculate the F-ratio (the ratio of Treatment MS / Residual MS). The F-ratio is used to confirm or reject the null hypothesis that the resulting treatment means are equal, i.e. the test will indicate whether different treatments have made any difference to the system being tested.

T-tests should not be used to test between multiple groups (3 or more) of data. Each time a hypothesis test is carried out at the 5% significance level for example, there is a 5% risk of claiming that the means of two treatments differ when they do not. Therefore if multiple tests are performed on the subsets of the same data, the risks of claiming that means differ when they do not, increase.

5.2.5.5 Dunnett's and Bonferroni's Post-Test

The ANOVA test will indicate whether there is a statistical difference between treatment means, but does not indicate where differences may lie. Therefore it is necessary to perform a post test. The Dunnett's and Bonferroni's post-tests are modifications of the t-test which take into account the above mentioned problem of multiple comparisons. The Dunnett's test allows the comparison of one set of data (e.g. a control set) with all other data sets (e.g. treatment groups) and will indicate the level of statistical difference. The Bonferroni's test allows comparisons between selected pairs of data, and will indicate the level of statistical difference between data sets of each pair. Using the Dunnett's and Bonferroni's post-test the following system was used to describe statistical significance: not significant (ns) = $p>0.05$, * = $p<0.05$, ** = $P<0.01$, and *** = $p<0.001$.

5.3 Results

5.3.1 LDH Assay Development

The LDH assay described in the methodology section uses the conversion of NADH to NAD^+ to detect activity. However, in the Introductory chapters, the enzymatic conversion of NADH to NAD^+ was described for XO (i.e. XO NADH-oxidase activity). As the release of XO from HUVECs will be followed (in the same samples where LDH activity will be assayed) it is important to consider this activity and the potential affects on the apparent LDH activity. Therefore it was decided to assay LDH activity measuring the conversion of NAD^+ to NADH, as shown in Figure 64. As XO could potentially utilise any NADH formed, and therefore affect the LDH assay, initial experiments were designed to show the inhibition of XO-NADH oxidase activity using DPI (Figure 65).

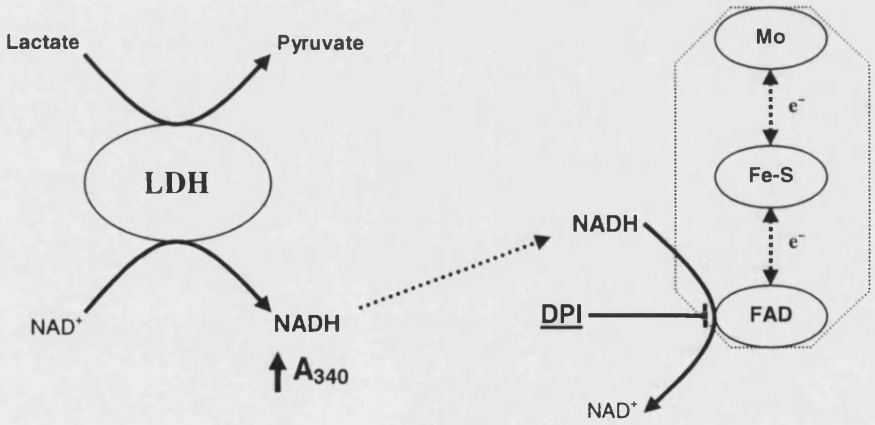

Figure 64. Generation of NADH by LDH and Potential Interference of XO

In the presence of lactate and NAD^+, LDH will generate NADH. The generation of NADH will be followed in the LDH assay by an increase of absorbance at wavelength 340nm. Potentially, XO present in the sample could utilise NADH forming NAD^+, thus interfering with the LDH assay. However, XO NADH-oxidase activity can be inhibited using DPI.

5.3.1.1 DPI inhibits XO NADH Oxidase activity

An initial experiment was designed to show that XO NADH-oxidase activity could be inhibited, and therefore eliminate this activity from interfering with the LDH assay. The inhibitory activity of DPI has been shown in the XO NADH-oxidation process

(Sanders *et al.*, 1997; Zhang *et al.*, 1998), therefore this experiment aimed to show that inhibition occurs in the system used in this thesis. The NADH-oxidase activity of 50μg/ml Biozyme XO was measured using 100μM NADH with or without 1μM DPI. The depletion of NADH was followed at A_{340} for approximately 15mins at 37°C, and NAD^+ generation was calculated from the linear portion of the progress curve using the extinction coefficient of $6.22mM^{-1}\ cm^{-1}$ (Figure 65). In the absence of XO, NADH concentrations do not change, however with XO present NADH is oxidised to NAD^+ and this process is inhibited by DPI. DPI inhibits activity by 91.4%, a similar value as previously described (90.2% inhibition was achieved using the same inhibitor concentration as in this thesis, Sanders *et al.*, 1997).

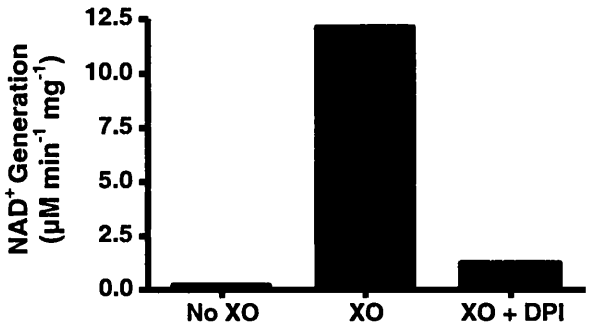

Figure 65. Inhibition of XO NADH-Oxidase Activity using DPI

XO was incubated with NADH with and without DPI and NADH-oxidase activity was measured at wavelength 340nm. In the absence of XO no NADH oxidation occurs, however in the presence of XO NADH is oxidised by a process that is inhibited by DPI. Results are from a single experiment with no replicates.

5.3.1.2 Does DPI Inhibit LDH Activity?

As DPI will be used in the LDH assay to inhibit any XO present in test samples, it was important to control for the effects of DPI on LDH activity. Therefore the activity of 0.05U LDH with 330μM NAD^+ and 1.5mM sodium lactate was measured in the presence of various DPI concentrations. Activity was measured at 37°C at A_{340} and NADH generation was calculated as previously described (Figure 66). The concentrations of DPI tested do not inhibit LDH activity, therefore 1μM DPI may be used in the LDH assay to inhibit XO NADH-oxidase activity without affecting LDH.

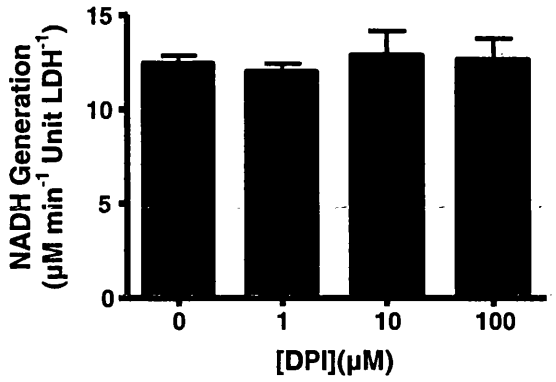

Figure 66. The Affect of DPI on LDH Activity

The activity of 0.05U LDH was measured in the presence of various DPI concentrations. Results are from one experiment performed in triplicate, therefore n=3. Error bar = SD.

5.3.1.3 Optimisation of NAD^+ Concentration in the LDH Assay

The substrate concentration given in the original assay (www.worhtington-biochem.com) referred to NADH. As the LDH assay used in this thesis was run in reverse compared to the original assay, optimisation of the NAD^+ substrate concentration was performed. Here the activity of 0.05U LDH was measured with 1.5mM sodium lactate and a range of NAD^+ concentrations at 37°C at A_{340}. LDH activity was calculated, and maximal activity occured in the presence of 1mM NAD^+ (Figure 67).

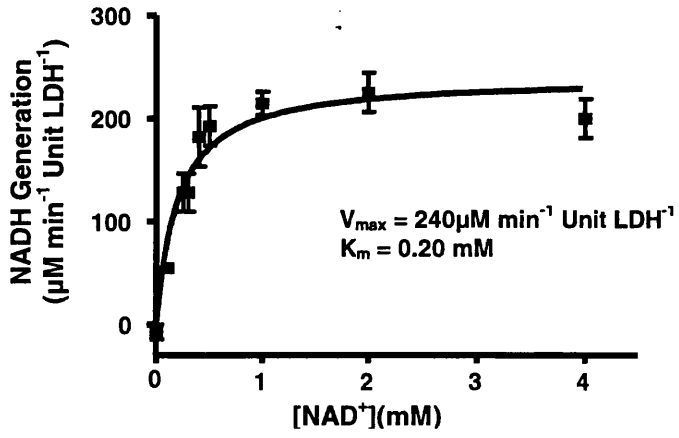

Figure 67. Optimisation of NAD^+ Concentration in the LDH Assay

The activity of 0.05U LDH was measured in the presence of various NAD^+ concentrations. Activity data was fitted with Michaelis-Menton Kinetics. Results are from one experiment performed in triplicate, therefore n=3. Error bar = SD.

5.3.1.4 Optimised LDH Assay Test

The optimised LDH assay (using 1mM NAD^+, 1.5mM sodium lactate, 1μM DPI, and 10μM allopurinol* at 37°C; *allopurinol was added to inhibit XDH that in the presence of substrates hypoxanthine or xanthine could utilise NAD^+ as an electron accepting substrate) was tested on medium samples from compromised cells. MDA-MB-231 cells were grown to confluence (as described in Chapter 3) in T25 flasks, medium was removed and cells were incubated with a range of concentrations of the ROS, H_2O_2 in PBS, for 1.5hours under standard culturing conditions. Under the microscope, compared to the 0mM H_2O_2 treated sample, all cells looked normal except for the 10mM H_2O_2 treated flasks where cells appears stringy and fragmented. Medium above cells was removed for analysis using the LDH assay (Figure 68). A baseline level of LDH activity was measured in cells treated with ≤0.1mM H_2O_2. However in the sample where cells appeared compromised under the microscope (10mM H_2O_2 treated) a greater level of LDH activity was recorded.

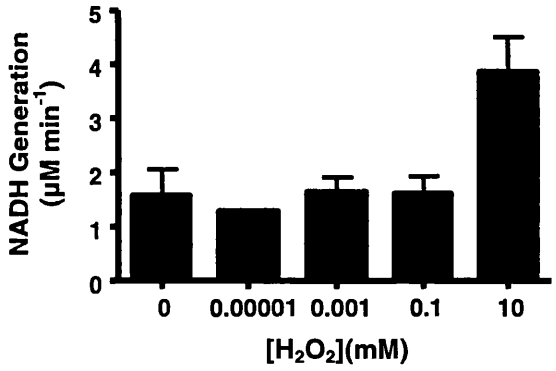

Figure 68. The Optimised LDH Assay Test

MDA-MB-231 cells were exposed to various H_2O_2 concentrations for 1.5hours. The medium above cells was assayed for LDH using the optimised method with XO inhibition. Activity was highest in the sample where cells appeared compromised (10mM H_2O_2). Results are from one experiment performed in triplicate, therefore n=3. Error bar = SD.

5.3.2 Lysate Distribution of HUVEC XOR

As a control to show the IXP-based XOR assay could detect XOR in HUVEC lysates, and to determine whether XO is found in the soluble or insoluble lysate fraction, confluent P2 HUVECs grown in 12-well plates were lysed using 1ml lysis

buffer per well. Following the incubation of cells in lysis buffer for approximately 5mins at 4°C, adherent cell debris was suspended using a cell scraper. The total lysate was removed from each well and cell debris was broken-up by repeated pipetting, lysates were stored on ice until needed. Soluble lysate was prepared by centrifugation of total lysate at 13 000rpm for 5mins, the resulting supernatant constitutes the soluble lysate fraction. XOR activity in both soluble and total lysates was determined using the developed overnight IXP-based XOR assay. XOR activity can be detected in HUVEC lysates, and the majority, if not all activity, is found in the soluble lysate fraction (Figure 69).

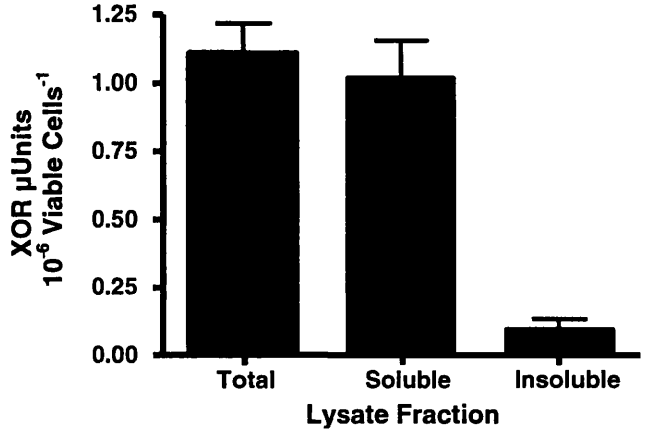

Figure 69. Can XOR Activity be Detected in HUVEC Lysates?

Confluent P2 HUVECs grown in 12-well plates were lysed and soluble and total cell lysate fractions were prepared. XOR activity was determined in each fraction using the IXP-based XOR assay. Results are from one experiment in triplicate, therefore n=3. Error bar =SD.

5.3.3 Supplementation of Endothelial Cell Growth Medium

The aim of the medium supplementation section was to determine whether XOR activity within HUVECs could be increased. From a practical point of view, an increase in HUVEC XOR activity maybe required if the IXP-based assay was not sufficiently sensitive under normal culture conditions, especially in XOR-release studies later in this chapter.

Both molybdenum and FCS supplementation were tested. Firstly, supplementation of cell lines with molybdenum (Mo) has been shown to increase XO activity. For example, L929 fibroblast cell line normally expresses XOR mRNA however does not

contain active XOR, however with Mo supplementation in the millimolar range active XOR was expressed (Falcinani *et al.*, 1994). Mo is an important constituent of the MoCo and supplementation is thought to convert a pool of XOR apoenzyne into its active, holoenzyme, form (Falcinani *et al.*, 1994). Therefore I hypothesis that Mo-supplementation of PromoCell ECGM (which only contains 3nM ammonium molybdate) may assist in the conversion of inactive enzyme to holoenzyme in HUVECs. Secondly, supplementation with FCS will be tested. The PromoCell ECGM contains just 2% FCS, other media routinely contain 10 or 20% FCS (Jaffe *et* al., 1973a; Emeis *et al.*, 1997; Rosnoblet *et al.*, 1999). Therefore a comparison of different FCS concentrations was investigated and the affect on active XOR was measured.

5.3.3.1 Molybdenum Supplementation

HUVECs (P2) grown in 12-well plates were incubated in Mo-supplemented ECGM for 24hrs under normal culture conditions. Following incubation cells were washed in HBSS, lysed using 1ml lysis buffer per well or were dissociated using Accutase for cell viability counts. XOR activity in cell lysates was measured as described in the methodology section to this chapter. Supplementation with 0.01 and 0.1mM ammonium molybdate did not alter cells appearance under the microscope compared to the control (Figure 70B, C). However, with the addition of 1mM ammonium molybdate cells were altered in structure and seemed to contain large vacuoles (Figure70D), and 10mM appeared to be fatal to the HUVECs (Figure 70E). The ammonium molybdate came out of solution at the 50mM concentration (Figure 70F). Cell lysate XOR activity was measured using the IXP-based XOR assay (Figure 71). Data was analysed using one-way ANOVA with Dunnett's post test. Supplementation with 0.1mM ammonium molybdate significantly increases cellular XOR activity compared to the 0mM control. XOR activity in cells grown in medium supplemented with >0.1mM ammonium molybdate should not be compared as cellular appearance was altered in these samples.

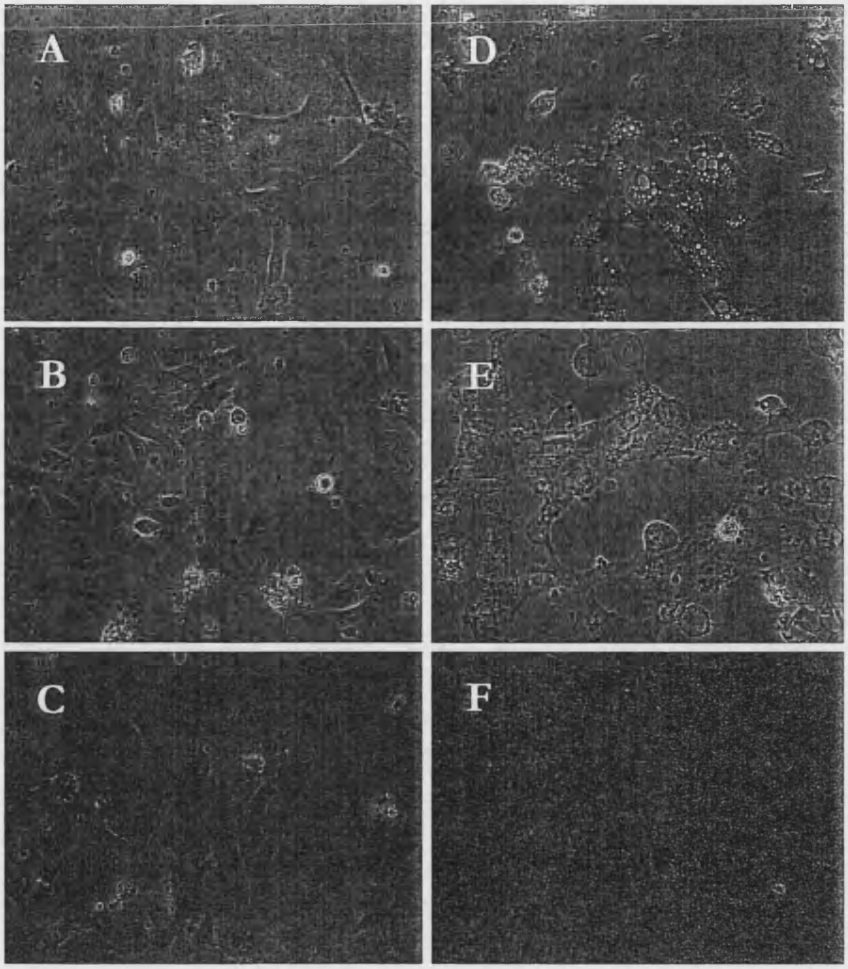

Figure 70. The Effect of Ammonium Molybdate Supplementation of ECGM on HUVEC Appearance

P2 HUVECs were incubated with ECGM supplemented with various concentrations of ammonium molybdate 0mM (A), 0.01mM (B), 0.1mM (C), 1mM (D), 10mM (E), and 50mM (F). Cells were viewed under phase contrast microscopy.

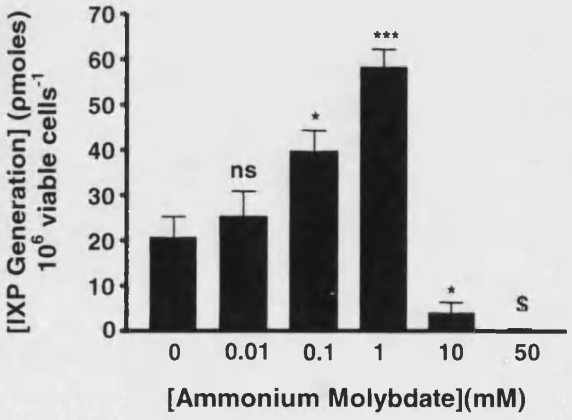

Figure 71. The Effect of Ammonium Molybdate Supplementation of ECGM on HUVEC XOR Activity.

P2 HUVECs were incubated with ECGM supplemented with various concentrations of ammonium molybdate. Cells were lysed and XOR activity was measured using the IXP-based assay. Data was analysed using one-way ANOVA with Dunnett's post test (where ns = not significant ($p>0.05$); * = $p<0.05$, *** = $p<0.001$). Results are from one experiment with five replicates, therefore n=5. Error bar = SD. $ ANOVA analysis requires that all samples have equal variances. The variance of the 50mM sample data was not the same as the other samples (data did not pass Bartlett's test for equal variances with the 50mM data points included) and was therefore not included in statistical analysis.

5.3.3.2 FCS supplementation

HUVECs (P2) grown in 12-well plates were incubated in FCS (GlobePharm. Esher, UK)-supplemented ECGM for 72hrs under normal culture conditions. Cells were washed in HBSS, lysed using 1ml lysis buffer per well or were dissociated using Accutase for cell viability counts. XOR activity was measured as described in the molybdenum-supplementation section. The addition of FCS to ECGM increases cell number in a dose-dependent manner (Figure 72A), however no increase in cellular XOR activity was observed (Figure 72B).

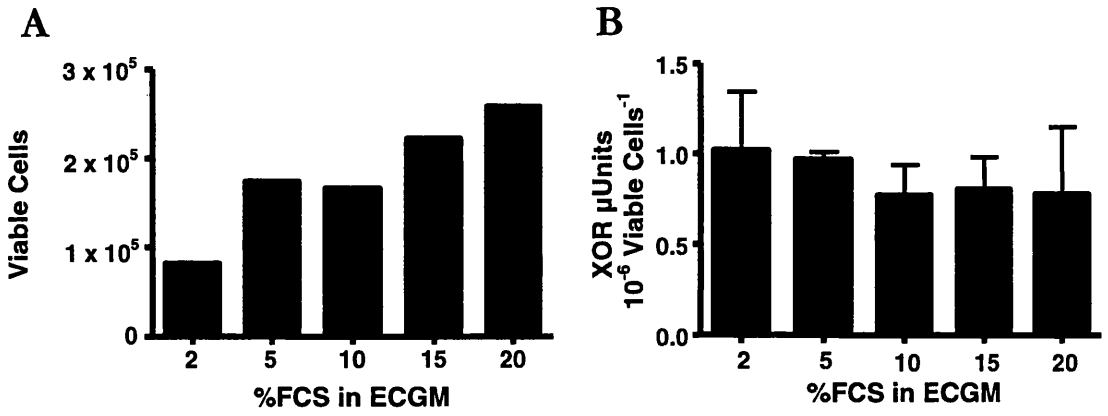

Figure 72. The Effect of FCS-Supplementation of ECGM on HUVEC XOR Activity

P2 HUVECs were incubated with ECGM supplemented with various concentrations of FCS. Cells were lysed and XOR activity was measured using the IXP-based assay. Results are from one experiment with four replicates, therefore n=4. Error bar = SD.

5.3.4 Thrombin Dose-Response

As mentioned in the Introductory chapters to this thesis, thrombin is known to stimulate the release of protein from the vascular endothelium. In particular the

release of vWf has been well characterised and therefore vWf release was used as a positive control for endothelial cell protein release. To begin to investigate whether the vascular endothelium can release XOR, the HUVEC endothelial model was stimulated with known endothelial-protein secretagogues, in this section the effect of thrombin was investigated. Initial experiments measured the effects of various thrombin concentrations on HUVECs. As a guideline, previously published protocols (Hattori *et al.*, 1988; Vischer et al., 1998) were used to judge thrombin concentrations and incubation times that should be used.

5.3.4.1 Thrombin Stimulated vWf Release from HUVECs

Confluent P2 HUVECs, grown in 12-well plates were stimulated with a log dilution of thrombin (1ml total volume per well) for 10mins under normal culture conditions. Following this time, medium above cells was collected for analysis. Also, in each repeat of the thrombin dose-response protocol three wells of HUVECs were lysed in 1ml lysis buffer and the soluble lysate fraction was prepared (as previously described). vWf release into the medium above cells was analysed using the dot-blot technique (as described in Chapter 3). A volume of 10μl of each sample was loaded, and using density analysis the percentage total-cellular release of vWf was calculated from a standard curve generated from a dilution of the HUVEC lysate. An example of a vWf dot-blot is shown in Figure 73A and thrombin stimulated vWf release is shown in Figure 73B. Thrombin stimulates a dose-dependent release of vWf from HUVECs (an exception is seen using 10U/ml where release is not greater than stimulation with 1U/ml thrombin, where the sensitivity of the assay may have reached its upper limits).

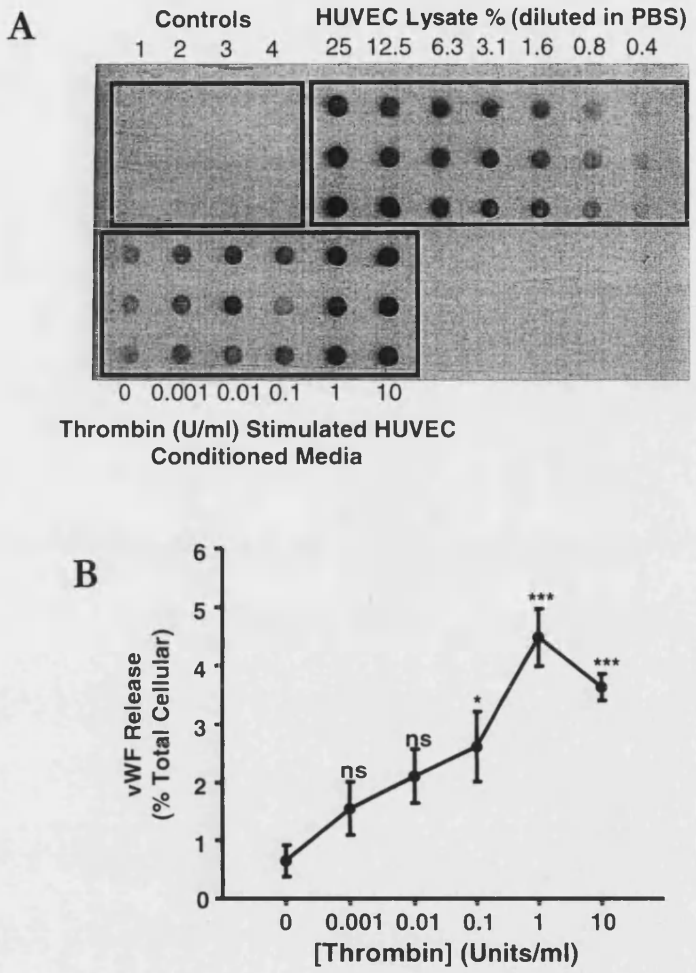

Figure 73. Thrombin Stimulated vWf Release from HUVECs

Confluent P2 HUVECs were stimulated with various concentrations of thrombin. Medium above cells was collected and vWf content was assessed using the dot-blot technique. A) An example of a vWf dot-blot is shown, control samples are 1. HBSS, 2. 10U/ml thrombin in HBSS (unconditioned), 3. 10ng XO in PBS, and 4, lysis buffer. B) vWf release into medium above cells was calculated from a standard curve generated from a dilution of HUVEC lysates. Data were analysed using one-way ANOVA with Dunnett's post test comparing thrombin-stimulated vWf release against the 0U/ml control (ns = not significant ($p>0.05$), * = $P<0.05$, *** = $p<0.001$). Results are from three experiments in triplicate, therefore n=9. Error bar = SEM.

5.3.4.2 Thrombin Stimulated XOR Release from HUVECs

Using the same protocol as described for vWf release, HUVECs were treated with various concentrations of thrombin and medium above cells was collected for analysis. XOR activity in medium above cells was analysed using the over-night IXP-based XOR assay and data collected were converted in Units XOR released using the equation given in the methodology section of this chapter. Controls for the XOR

assay are given in Figure 74. Various negative controls [HBSS, 1000μM histamine in HBSS (unconditioned), 10U/ml thrombin in HBSS (unconditioned) and lysis buffer], and positive controls (5ng XO and cell lysate) were tested. Significant activity was only seen in the positive control samples. These controls also serve the histamine dose-response experiments described later in this chapter.

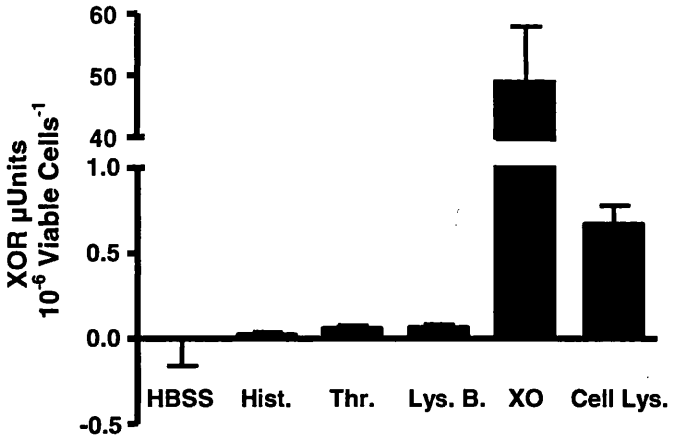

Figure 74. Controls for Thrombin and Histamine Stimulated XOR Release Experiments

Positive and negative controls were run parallel to test samples in the overnight IXP-based XOR assay and the number of XOR units was calculated. Results are from experiments performed in triplicate: HBSS n=24, Hist. n=12, Thr. n=15, Lys. B. n=21, XO n=27, Cell Lys. n=21. Where Hist. = 1000μM histamine (unconditioned), Thr. = 10U/ml thrombin (unconditioned), Lys. B. = Lysis Buffer, XO = 5ng Biozyme XO, and Cell Lys. = Cell Lysate. Error bar = SEM.

XOR activity in medium above thrombin-stimulated HUVECs is shown in Figure 75 XOR activity follows a "bell-shaped" curve, with higher concentrations of agonist reducing the activity measured in the medium above cells after an initial dose-response-like increase in activity. Peak XOR activity is measured in medium above cells that are stimulated with 0.01-1U/ml thrombin. The increase in XOR activity indicates that XOR enzyme has been released from HUVECs in response to thrombin stimulus. The activity curve makes an interesting comparison to the dose-dependent release of the control, vWf.

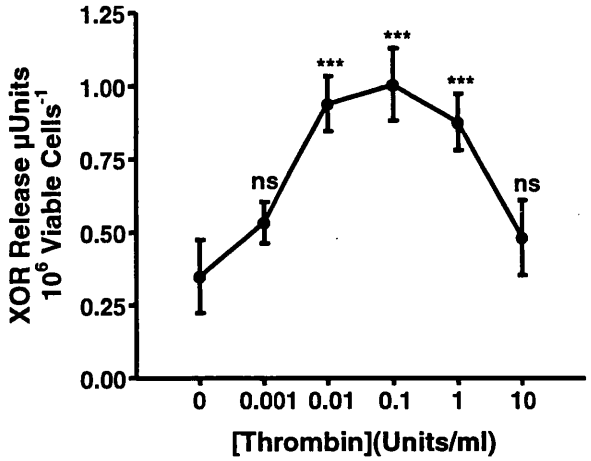

Figure 75. XOR Release from Thrombin Stimulated HUVECs

Confluent P2 HUVECs were stimulated with various concentrations of thrombin. Medium above cells was collected and XOR content was assessed using the overnight IXP-based XOR assay, and XOR activity Units were calculated. Data were analysed using one-way ANOVA with Dunnett's post test comparing thrombin-stimulated XOR release against the 0U/ml control (ns = not significant ($p>0.05$), *** = $p<0.001$). Results are from three experiments in triplicate, therefore n=9. Error bar = SEM.

In an attempt to detect XOR protein released into the medium above cells following thrombin stimulation, the samples used in the XOR activity assay were analysed by dot-blot analysis. 20µl of each sample were loaded onto the dot-blot which was subsequently probed for XOR using the Chemicon Polyclonal XO 1°-antibody. The 10U/ml thrombin negative control is strongly detected in dot-blot process (Figure 76 indicated by an arrow), therefore it is not possible to use this technique to assess XOR protein release with thrombin-stimulation. The apparent release of XO in the conditioned medium samples is likely to be the detection of thrombin only. The experiment was repeated using the Polysciences Polyclonal anti-XO, however this made no difference to the outcome (data not shown).

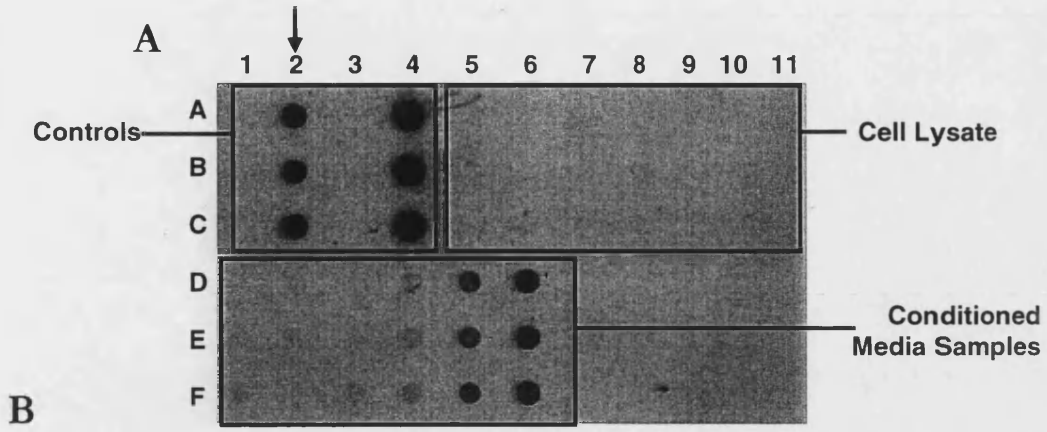

	1	2	3	4	5	6	7	8	9	10	11
A	HBSS	Thr.	Lys. B.	XO	25.0%	12.5%	6.3%	3.1%	1.6%	0.8%	0.4%
B	"	"	"	"	"	"	"	"	"	"	"
C	"	"	"	"	"	"	"	"	"	"	"
D	0U/ml	0.001U/ml	0.01U/ml	0.1U/ml	1U/ml	10U/ml					
E	"	"	"	"	"	"					
F	"	"	"	"	"	"					

Figure 76. Dot-blot Analysis of XOR Released from Thrombin-Stimulated HUVECs

The medium above thrombin-stimulated HUVECs was analysed for XOR protein using the Dot-blot technique. The dot-blot is shown in A and the loading order in B. Where, Thr. = 10U/ml thrombin in HBSS; Lys.B.: Lysis Buffer; XO: 10ng Biozyme XO. Conditioned medium refers to medium above cells stimulated with thrombin, concentrations as indicated.

Two further controls were run to show, i) whether the thrombin concentrations used in the stimulation of HUVECs are toxic and ii), whether thrombin directly effects the activity of XO. To assess whether thrombin treatments were cytotoxic, the medium above cells taken from thrombin dose-response experiments and was analysed for LDH activity using the assay developed at the start of this chapter. In the dose-response experiments described the exposure of HUVECs to thrombin does not cause the release of LDH (Figure 77). Positive (HUVEC lysate) and negative (HBSS) controls for the assay worked as predicated.

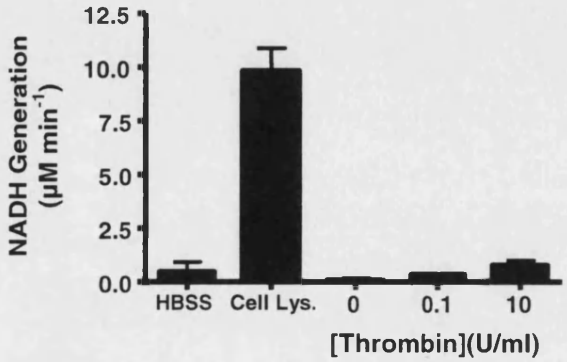

Figure 77. Are the Thrombin Concentrations used in Dose-Response Experiments Cytotoxic?

Confluent P2 HUVECs were stimulated with various concentrations of thrombin. Medium above cells was collected and LDH content was assessed using LDH assay. Results are from one experiment in triplicate, therefore n=3. Error bar = SD.

A further control was run to demonstrate whether XO activity could be directly influenced by thrombin. In these experiments 100ng/ml Biozyme XO was incubated with thrombin (the same concentrations used in the dose-response experiments) for approximately 3mins at room temperature. XO activity was then analysed using the IXP-based assay as described by Beckman *et al.*, 1989. Results show that the presence of thrombin increases XO activity in a dose-dependent manner (Figure 78) that is cell-independent.

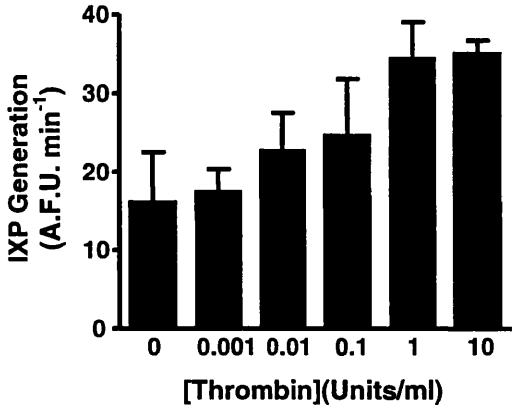

Figure 78. The Effect of Thrombin on XO Activity

Purified XO was incubated at room temperature with thrombin (various concentrations) for ~3mins and XO activity was assessed using the IXP-based XOR assay as described in Beckman *et al.*, 1989. Results are from one experiment perform in triplicate, therefore n=3. Error bar = SD.

5.3.5 Histamine Stimulated XOR Release from HUVECs

5.3.5.1 Histamine Dose-Response Experiments on Isolated HUVECs

The thrombin dose-response experiments were repeated using histamine as an endothelial cell protein secretagogue. As a guideline, previously published protocols (Hattori *et al.*, 1988; Vischer et al., 2000) were used to judge histamine concentrations and incubation times that should be used. Firstly, as a control, the release of vWf from HUVECs stimulated with a log dilution of histamine was investigated. vWf

content in medium above cells was analysed using the protocol described for thrombin-stimulated cells. Similar to thrombin, histamine generated a dose-dependent release of vWf from HUVECs (Figure 79).

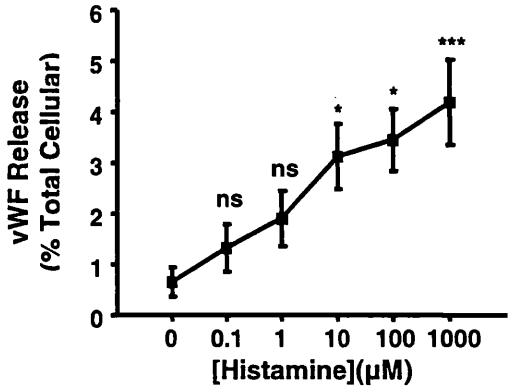

Figure 79. Histamine Stimulated vWf Release from HUVECs

Confluent P2 HUVECs were stimulated with various concentrations of histamine. Medium above cells was collected and vWf content was assessed using the dot-blot technique. The percentage total cellular vWf released into medium above cells was calculated from a standard curve generated from a dilution of HUVEC lysates. Data was analysed using one-way ANOVA with Dunnett's post test comparing histamine-stimulated vWf release against the 0U/ml control (ns = not significant ($p>0.05$), * = $P<0.05$, *** = $p<0.001$). Results are from three experiments in triplicate, therefore n=9. Error bar = SEM.

The medium above histamine stimulated cells was analysed for XOR-activity using the overnight IXP-based XOR assay. Like experiments with thrombin a "bell-shaped" release curve is generated (Figure 80A) in comparison to the dose-dependent release of vWf. Unlike experiments using thrombin however, dot-blot analysis of medium above histamine stimulated HUVECs was possible (i.e. the polyclonal XO antibodies did not bind to the 1000μM histamine unconditioned sample), 20μl of each sample were used in analysis. The release of XOR protein appears to follow the "bell-shaped" curve generated analysing XOR activity (Figure 80B).

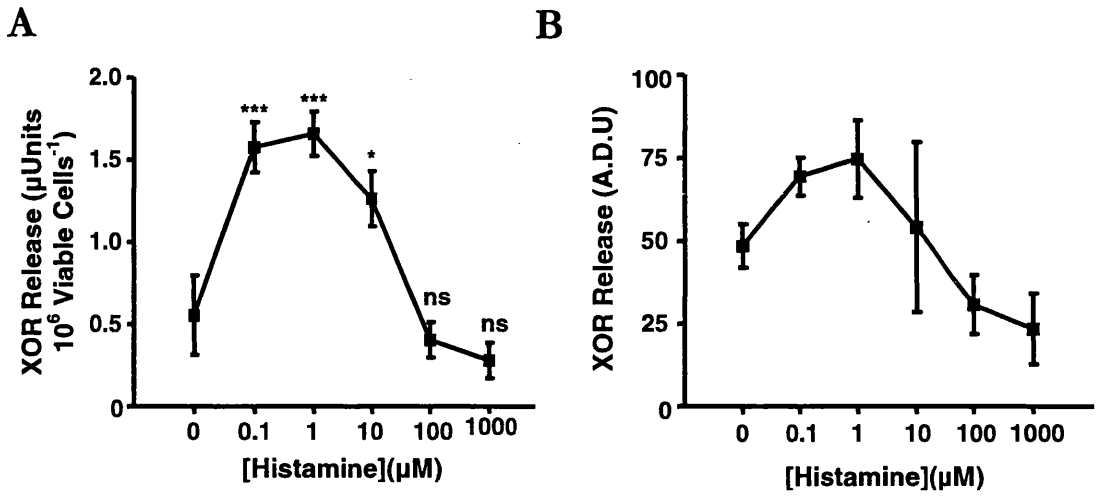

Figure 80. Histamine-Stimulated XOR Release form HUVECs

Confluent P2 HUVECs were stimulated with various concentrations of histamine. Medium above cells was collected and XOR content was assessed using the overnight IXP-based XOR assay, and XOR activity Units were calculated (A). Data were analysed using one-way ANOVA with Dunnett's post test comparing thrombin-stimulated XOR release against the 0U/ml control (ns = not significant ($p>0.05$), *** = $p<0.001$). Results are from three experiments in triplicate, therefore n=9. Error bar = SEM. Medium samples were probed for XOR-protein content using the dot-blot technique (B). Results are from one experiment in triplicate, therefore n=3. Error bar = SD.

The control experiments described in the thrombin dose-response section demonstrating; i) whether the stimulant concentrations used in the stimulation of HUVECs are toxic and ii), whether the stimulant directly affects the activity of XO, were repeated using histamine. Histamine cytotoxicity to HUVECs was assessed using the LDH assay as described in the thrombin dose-response section of this chapter. In the dose-response experiments described, the exposure of HUVECs to histamine does not cause the release of LDH (Figure 81). Positive (HUVEC lysate) and negative (HBSS) controls for the assay worked as predicated.

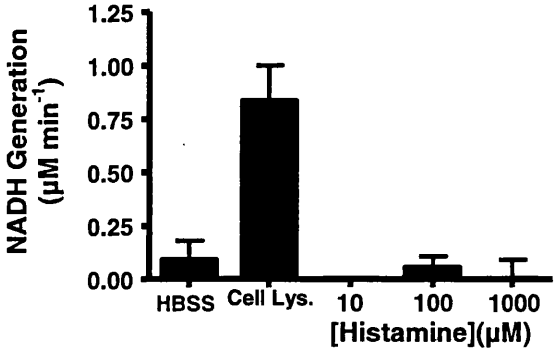

Figure 81. Are the Histamine Concentrations used in Dose-Response Experiments Cytotoixic?

Confluent P2 HUVECs were stimulated with various concentrations of histamine. Medium above cells was collected and LDH content was assessed using LDH assay. Results are from one experiment in triplicate, therefore n=3. Error bar = SD.

A further control was run to demonstrate whether XO activity could be directly influenced by histamine. In these experiments 100ng/ml Biozyme XO was incubated with histamine (the same concentrations used in the dose-response experiments) for approximately 3mins at room temperature. XO activity was then analysed using the IXP-based assay as described by Beckman *et al.*, 1989. In contrast to thrombin, the presence of histamine does not increase the activity of XO (Figure 82).

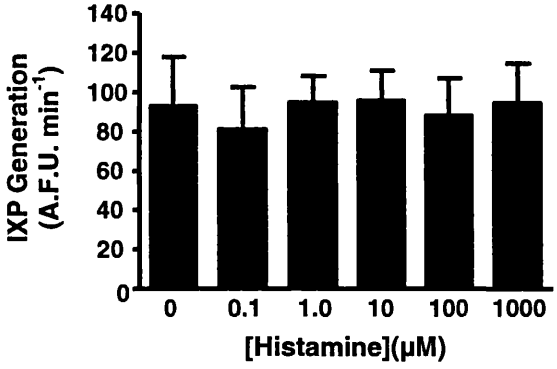

Figure 82. The Effect of Histamine on XO Activity

Purified XO was incubated at room temperature with histamine (various concentrations) for ~3mins and XO activity was assessed using the IXP-based XOR assay as described in Beckman *et al.*, 1989. Results are from one experiment performed in triplicate, therefore n =3. Error bar = SD.

5.3.5.2 Histamine Time Course Experiment on Isolated HUVECs

In dose-response experiments the release of protein from HUVECs was measured following a 10min incubation period with histamine or thrombin. To further characterise the release of XOR from HUVECs stimulated with histamine, a time course experiment was performed. Here, confluent P2 HUVECs grown in 12-well plates were stimulated with 10μM histamine. Cells were incubated under standard culture conditions and at relevant time points medium the above cells was removed and stored on ice before analysis (for each time point three wells of HUVECs were

used). For the time zero sample, 10μM histamine was added to each of three wells and removed instantly. vWf release was analysed using the dot-blot technique and XOR activity was measured using the overnight IXP-based XOR assay as previously described. Release of XOR was rapid with maximal release occurring by the second time point (2.5mins incubation), whereas the release of vWf was a slower process requiring approximately 12.5mins for maximal release to occur (Figure 83).

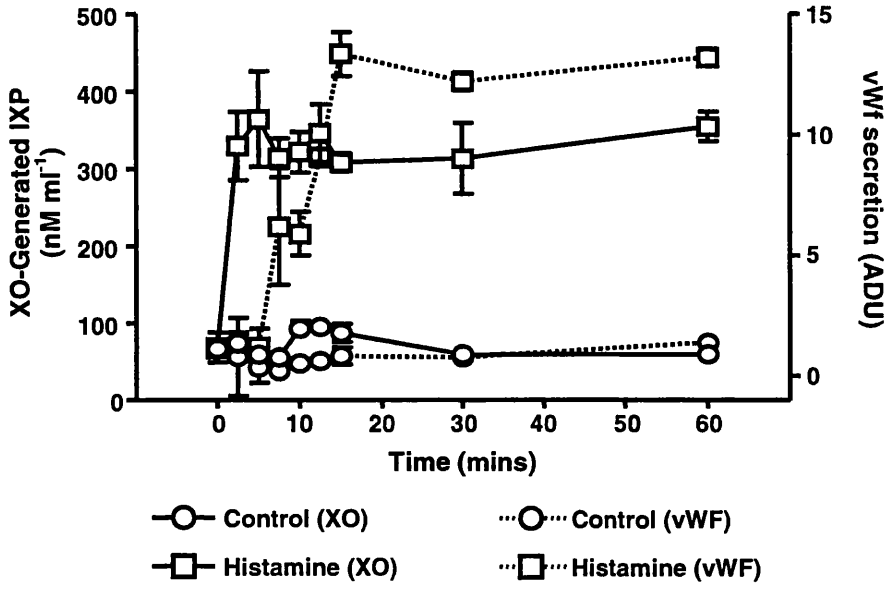

Figure 83. Histamine Stimulation of HUVECs – A Time Course Study

Confluent P2 HUVECs were stimulated with 10μM histamine. At desired time points medium above cells was collected. XOR content was assessed using the overnight IXP-based XOR assay and vWf release was determined using the dot-blot technique. Results are from one experiment in triplicate, therefore n=3. Error bar = SD.

5.3.5.3 Histamine Dose-Response Experiments on Purchased HUVECs

To confirm the results observed using HUVECs isolated in the laboratory, HUVECs were purchased (PromoCell. Heidelberg, Germany) and histamine dose-response experiments were repeated. However, as PromoCell HUVECs arrived as P1 cells, experiments using these HUVECs were performed at P3. The histamine dose-response protocol, medium collection, and analysis for vWf and XOR were performed as described previously. vWf (Figure 84) and XOR (Figure 85B) release

was comparable to that seen with HUVECs isolated within the laboratory. Control experiments demonstrate that active XOR is present in the purchased HUVECs at P3 (Figure 85A).

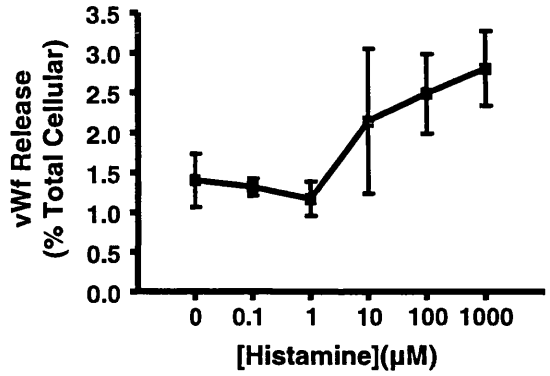

Figure 84. Histamine Stimulated vWf Release from Purchased HUVECs

Confluent P3 HUVECs (PromoCell) were stimulated with various concentrations of histamine, medium above cells was collected, and vWf content was assessed using the dot-blot technique. The percentage total cellular vWf released into medium above cells was calculated from a standard curve generated from a dilution of HUVEC lysates. Results are from one experiments in triplicate, therefore n=3. Error bar = SD.

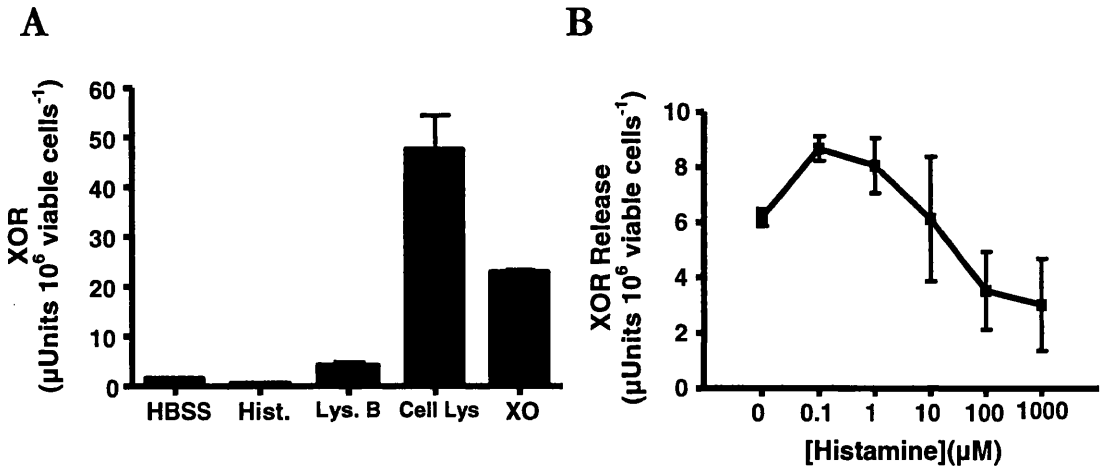

Figure 85. Histamine-Stimulated XOR Release form Purchased HUVECs

Confluent P3 HUVECs (PromoCell) were stimulated with various concentrations of histamine. Medium above cells was collected and XOR content was assessed using the overnight IXP-based XOR assay, and XOR activity Units were calculated (B). Positive and negative controls were run parallel to test samples in the overnight IXP-based XOR assay (A). Results are from one experiment in triplicate, therefore n=3. Error bar = SD.

5.3.6 The Mechanism of XOR Release from Isolated HUVECs

5.3.6.1 A23187 Dose-Response

In the preceding experiments the stimulated release of XOR from HUVECs has been demonstrated. To analyse the mechanism of XOR release in more detail HUVECs were firstly stimulated with the ionophore A23187. The ionophore works by inserting itself into the plasma membrane of a cell forming a pore allowing entry of extracellular cations, such as Ca^{2+}, into the cytoplasm (Alberts *et al.*, 1994). Therefore, by applying the ionophore to HUVECs, the effects of a rise in intracellular calcium can be observed, and may indicate a role of calcium in the signalling processes involved in protein release from HUVECs. The ionophore, A23187, has been shown to stimulate the release of vWf from HUVECs (Hattori *et al.*, 1988). Therefore the release of vWf was used as a positive control to show that stimulation of endothelial cell protein secretion has occurred.

In A23187 dose-response experiments, HUVECs isolated in the laboratory were used. P2 HUVECs were grown in 12-well plates and were stimulated using the same protocol as described for thrombin and histamine dose-response experiments (except A23187 was used in place of the afore-mentioned agonists). Analysis of vWf protein and XOR activity in medium above cells was performed using the previously described protocol. The release of vWf from HUVECs exposed to A23187 was dose-dependent (Figure 86A) and XOR release tended to follow a "bell-shaped" curve (Figure 86B), however the increase in XOR activity was not statistically significant for any A23187 concentration tested. The results described using A23187 are comparable to those seen using thrombin and histamine stimulation.

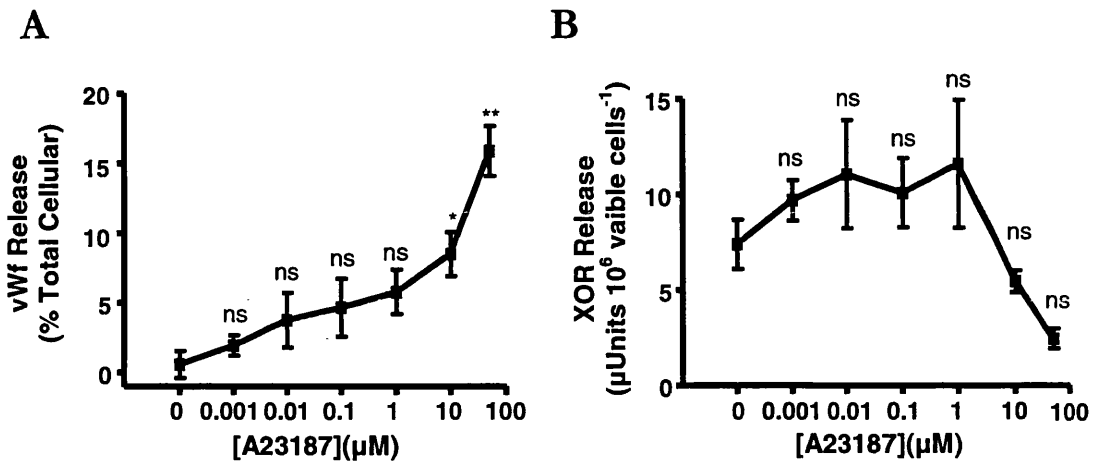

Figure 86. A23187 Stimulated Protein Release from HUVECs

Confluent P2 HUVECs were stimulated with various concentrations of A23187 and medium above cells was collected. vWf content was assessed using the dot-blot technique (A) and XOR content was assessed using the overnight IXP-based XOR assay (B). Data were analysed using one-way ANOVA with Dunnett's post test comparing A23187-stimulated vWf release or XOR activity against the 0µM control (ns = not significant ($p>0.05$), * = $P<0.05$, ** = $p<0.01$). Results are from two experiments in triplicate, therefore n=6. Error bar = SEM.

5.3.6.2 The Effect of Colchicine on Histamine-Stimulated XOR Release from Isolated HUVECs

The observation that HUVEC XOR is found in a "packaged" form was made in Chapter 3. The aim of this section was to discover whether this packaged form could be released, and therefore constitute the source of XOR released into the medium above HUVECs. To achieve this aim, experiments by Vischer *et al.*, 2000 were repeated, however XOR release was assessed. In the experiments by Vischer *et al* (Vischer *et al.*, 2000) the role of microtubules in the release of packaged vWf from HUVECs stimulated by intracellular Ca^{2+} increasing agents (including histamine and thrombin) was established. This was achieved using colchicine-induced microtubule disruption, which inhibited the stimulated release of vWf stores. Similar results were achieved in earlier studies on HUVECs (Sinha and Wagner, 1987).

In experiments in this thesis, P2 HUVECs were grown in 12-well plates using standard culture conditions. Conditioned medium was removed and HUVECs were incubated in fresh ECGM with or without 1µM colchicine for 30mins under standard

culture conditions. The effects of colchicine treatment on microtubule structure are shown in Figure 87. Here HUVECs were fixed using acetone/methanol and stained for β-tubulin and nuclei using the protocol described in Chapter 3. It is apparent that incubation with colchicine breaks down microtubule structure, results are comparable to those seen in other publications (Vischer *et al.*, 2000).

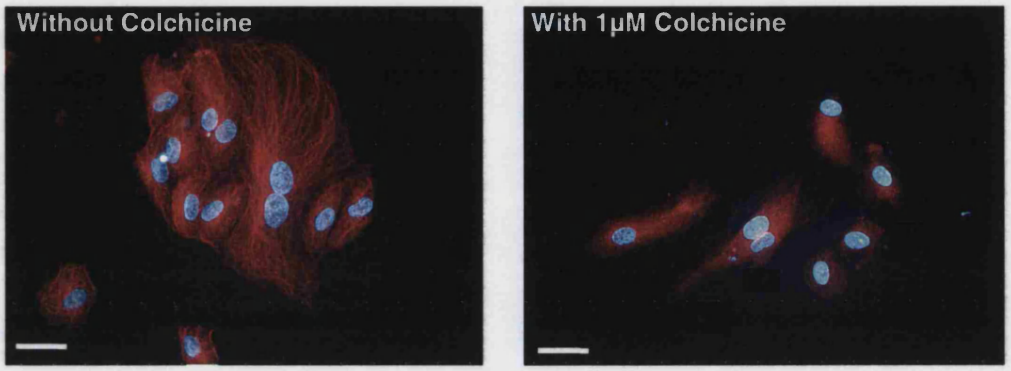

Figure 87. The Effect of Colchicine on HUVEC Microtubule Structure

Laboratory isolated P2 HUVECs were grown on glass cover slips in 12-well plates. HUVECs were incubated with or without colchicine for 30mins and fixed using ice cold acetone/methanol for 5mins at 4°C. Fixed cells were stained for β-tubulin and nuclei as previously described. Bar = 50μm.

Confluent P2 HUVECs grown in 12-well plates treated with or without colchicine, were immediately stimulated with or without 1μM histamine in HBSS for 10mins under standard culture conditions. Following this time period, medium above cells was removed and vWf and XOR content were analysed as previously described. In the absence of colchicine and histamine stimulation vWf is constitutively released, and with histamine stimulation vWf release is increased as expected. The constitutive and histamine-stimulated release of vWf in HUVECs incubated with colchicine is reduced compared to HUVECs without colchicine treatment (Figure 88A). The release of XOR into medium above cells follows the same pattern as described for vWf release (Figure 88B).

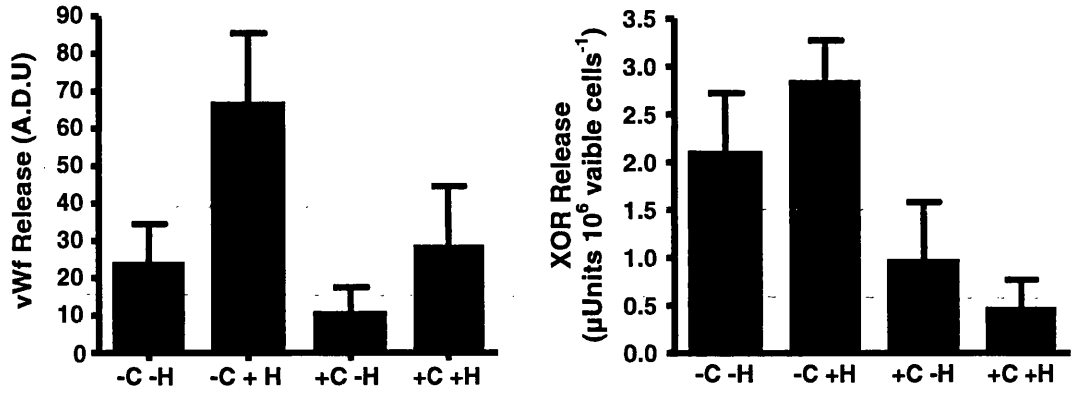

Figure 88. The Effect of Microtubule Disruption on vWf and XOR Release from HUVECs

Confluent P2 HUVECs grown in 12-well plates were incubated with or without colchicine, +C and –C, respectively. Following colchicine treatment HUVECs were immediately stimulated with or without histamine, +H and –H, respectively. The release of vWf and XOR was assayed as previously described. Results are from one experiment with five replicates. Error Bar = SD.

5.4 Discussion

5.4.1 Medium Supplementation

In Chapter 3 it was demonstrated that HUVECs express XOR mRNA and protein. In this chapter, using the overnight IXP-based XOR assay developed in Chapter 4, an initial study proved that HUVEC-expressed XOR was active (Figure 69). Activity was found in the soluble cell-lysate fraction, which was expected as the enzyme was shown to have a diffuse, cytoplasmic, expression (see Chapter 3).

The aim of the medium supplementation experiments were to determine whether the activity of HUVEC XOR could be increased. Potentially, a method to increase HUVEC XOR activity could have been advantageous, especially if XOR activity could not be detected in HUVEC XOR-secretion studies. ECGM contains a level of molybdenum that is sufficient to allow the expression of active XOR in HUVECs. However it appears that the addition of a molybdenum supplement increases the cellular content of active XOR (Figure 71), an effect that was not observed with FCS supplementation (Figure 72). Of the concentrations tested, 100µM ammonium molybdate was optimal for increasing cellular XOR activity. Concentrations greater then this, i.e. ≥1mM, appear to have cytotoxic effects on HUVECs (Figure 70). In

previous studies using fibroblast cell lines, supplementation of medium with up to 50mM ammonium molybdate could be administered before causing cytotoxic effects (Falciani *et al.*, 1994), suggesting that fibroblasts are more resistant to molybdenum or ammonium toxicity compared to HUVECs. If supplementation of ECGM was required or is required in future experiments, it would be interesting to study the effect of riboflavin (Vitamin B_2) and iron-sulphur supplementation on activity, therefore providing substrate for all of the XOR redox centres. Also, as a negative control, supplementation with tungsten could be used.

It is interesting to note that in Falciani *et al.*, 1994 they suggest that under basal conditions or with molybdenum supplementation, HUVECs do not contain active XOR. The data presented in this thesis contradict these findings. The XOR-assay used in Falciana *et al.*, 1994, with a detection limit of 5ρmol of hypoxanthine transformed into xanthine or uric acid, should be senstitive enough. Therefore, to explain this discrepancy, in Falciani *et al.*, 1994 there is no indication of the HUVEC passage number or length of culture prior to experimentation. As a general observation HUVECs tend to lose XOR activity over time, therefore the HUVECs used in Falciani *et al.*, 1994 may have lost XOR activity due to a prolonged culture time.

5.4.2 Thrombin and Histamine Dose-Responses

5.4.2.1 LDH Assays

The LDH assay developed at the start of this chapter proved sensitive enough to detect LDH release from cell cultures that showed morphological signs of cytotoxicity (Figure 68). The respective LDH assay results of medium above HUVECs from the histamine and thrombin dose-response experiments were negative (Figure 77and Figure 81). These results suggest that the concentrations of thrombin and histamine used in each dose-response were not cytotoxic. Therefore the release of vWf and XOR from HUVECs were stimulated by controlled mechanisms and not by compromised cells with fragmented plasma membranes.

5.4.2.2 von Willebrand Factor Release

Synthesised vWf is released by two different secretion pathways, the constitutive or regulated pathways (reviewed in van Mourik *et al.*, 2002). In the dose-response experiments, during the 10min incubation of HUVECs with just HBSS (i.e. 0μM histamine and 0U/ml thrombin) vWf is released into the medium above cells (Figure 73 and Figure 79). This release is probably accounted for by the constitutive release pathway. Using the known vascular endothelial cell protein secretagogues, histamine and thrombin, it was demonstrated that vWf is released in a dose-dependent manner (Figure 73 and Figure 79). vWf release data was analysed using one-way ANOVA with Dunnett's post-test comparing protein release in the presence of an agonist with a control (i.e. no agonist). Statistically significant release of vWf occured at ≥10μM histamine and ≥0.1U/ml thrombin in the dose-response. These results are comparable to previously published data (Hattori *et al.*, 1988; Vischer *et al.*, 1998) and therefore the release of vWf acts as a positive control for stimulation of HUVEC-protein secretion.

5.4.2.3 Xanthine Oxidoreductase Release – Dose-Response

Using the sensitive overnight IXP-based XOR assay and dot-blot techniques the release of XOR from HUVECs into medium above cells was measured (Figure 75, and Figure 80). Although it was possible to measure XOR protein released from histamine stimulated HUVECs this was not possible when using thrombin. It is apparent from dot-blot experiments that the Polysciences and Chemicon polyclonal XO-antibodies were detecting thrombin (Figure 76). This positive detection would suggest that thrombin and XOR share epitope(s), i.e. regions of structural similarity. It is known that both thrombin and XOR can bind to heparin (Adachi *et al.*, 1993; Sheehan *et al.*, 1994), therefore this region could be conserved in both enzymes, and thus be detected by the XOR polyclonal antibodies. A monoclonal XOR-antibody should be assessed for the detection of XOR in the dot-blot technique.

XOR is observed in medium above HUVECs with no agonist simulation, i.e. incubation in just HBSS (Figure 75 and Figure 80), therefore suggesting the constitutive release of XOR from HUVECs. This release mechanism is supported by published work using microvascular endothelial cells (Partridge *et al.*, 1992) and is comparable with the release of vWf as previously described. In addition to a constitutive release pathway, the results in this thesis demonstrate a regulated secretion pathway that is stimulated by histamine or thrombin treatment (Figure 75 and Figure 80). To my knowledge, these experiments are the first demonstration of controlled XOR release by vascular endothelial cells, in fact by any cell type except mammary epithelial cells (Mather and Keenan, 1998). Although XOR may be released by two separate secretion pathways (as with vWf), the dose-response results differ. vWf release is dose-dependent (Figure 73 and Figure 79), whereas XOR release into the medium above cells does not follow the same trend (Figure 75 and Figure 80). Instead a "bell-shaped" release curve is seen for XOR, with lower concentrations of agonist stimulating a significantly higher release of XOR compared to controls, and with higher concentrations of agonist ($\geq$10μM histamine or $\geq$1 U/ml thrombin) XOR release is either reduced or non statistically significant release is seen. As previously described, these results can not be explained by the suggestion that the higher concentrations of agonist are cytotoxic to HUVECs, because, i) vWf release follows a dose-dependent release curve at these higher concentrations, and ii) LDH activity could not be detected in medium above cells following their incubation with histamine or thrombin.

A possible explanation for the apparent reduction in XOR release, when stimulating HUVECs with higher concentrations of agonist, is that XOR is being released but is binding back to the cell surface, to an XOR receptor. To fit this scenario the agonist would have to upregulate the cell-surface expression of an XOR receptor, in a dose-dependent manner, to produce the "bell-shaped" curves seen in (Figure 75 and Figure 80). An XOR receptor has been defined and is believed to be a glycosaminoglycan (GAG) structure (Adachi *et al.*, 1994; Houston *et al.*, 1999), however, there is nothing

in the literature to suggest increased cell-surface expression of GAGs in response to histamine or thrombin stimulation. An obvious group of receptors that are ugregulated in response to histamine and thrombin treatment belong to a group of proteins found integral to the Weibel-Palade body membrane. The Weibel-Palade body is an intracellular storage granule that contains luminal proteins including vWf, and integral proteins including P-selectin, CD63, and fucosyl transferase VI. Following stimulation, these proteins are released when Weibel-Palade bodies fuse with the plasma membrane (reviewed in Michaux and Cutler, 2004). The release of vWf is dose-dependent, therefore the cell-surface expression of Weibel-Palade body membrane integral proteins would follow suit, making them a potential target for an XOR receptor.

To assess whether the cell-surface expression of GAGs is upregulated in response to histamine or thrombin treatment, a cell-based ELISA could be performed. Following stimulation, cells could be fixed with paraformaldehyde, therefore avoiding disruption of the plasma membrane, and be probed for cell-surface expression of GAGs using immunodetection. A similar protocol has been used to assess the cell surface expression of P-selectin in cultured cells (Takano *et al.*, 2002). To demonstrate whether GAGs or any of the Weibel-Palade body-membrane proteins are binding XOR in the dose-response experiments, competitive molecules could be added to see if more XOR remains in the medium above cells. For example, the addition of heparin or a P-selectin antibody to HUVECs with the agonist would compete with XOR for binding to GAGs (Adachi *et al.*, 1993) or P-selectin, respectively. If the concentration of XOR in the medium above cells increases with the addition of a competitive molecule compared to without, it is likely that this receptor is binding XOR following its release from HUVECs. Alternatively, experiments could be run under flow conditions, therefore any XOR released from HUVECs will be given less time to bind to any cell-surface receptors that may be upregulated in response to agonist stimulation.

5.4.2.4 The Influence of Histamine and Thrombin on XO Activity

As a control, the effect of the agonists tested (either histamine or thrombin) on purified XO activity was analysed (Figure 78 and Figure 82). In theory, if the agonist did not alter XO then any changes in XOR activity in medium above cells could be attributed to release of enzyme. Histamine has no effect on XO activity (Figure 78) but thrombin seems to increase XO activity in a dose-dependent manner (Figure 82). Therefore it is not possible to conclude, outright, that thrombin stimulates the release of XOR from HUVECs. It is possible that XOR is constitutively released but the presence of thrombin increases XOR activity. However, in support of thrombin stimulating the release of XOR from HUVECs it must be noted that the "bell-shaped" dose-response curve seen stimulating HUVECs with histamine and A23187 (Figure 86) is also observed with thrombin. Suggesting that release, or lack of, is not an artefact if increased activity from thrombin treatment.The effect of thrombin on XO activity is investigated further (see Chapter 6).

5.4.3 Xanthine Oxidoreductase Release – Time Course

In co-localisation studies of XOR and vWf in Chapter 3 it was demonstrated that vWf and XOR are stored independently of one another. In this chapter an experiment was performed observing the release times of both XOR and vWf (Figure 83). It was shown that XOR release was very rapid compared to vWf. As the release of the two proteins occurred at different rates, this provides more evidence to suggest that XOR and vWf are not associated with one another in the HUVEC.

5.4.4 The Mechanism of XOR Release

Results from this chapter have shown that signalling via thrombin and histamine can stimulate XOR release from HUVECs. However experiments were performed to investigate the release process in more detail. Stimulation of HUVECs with the calcium ionophore A23187 resulted in the dose-dependent release of vWf (Figure 86A). Interestingly, the maximal release of vWf with A23187 treatment was higher

than that seen with thrombin and histamine. This is in agreement with previous findings (Hattori *et al.*, 1988), where release of vWf from HUVECs treated with A23187 is much higher than that from cells exposed to histamine, thrombin, or phorbol 12-myristate 13-acetate. The release of XOR from A23187-stimulated cells (Figure 86B) follows a similar "bell-shaped" curve seen with both thrombin and histamine treatment. Therefore these results suggest that the signalling mechanism for the release of XOR from HUVECs involves a rise in intracellular calcium. This could be confirmed by chelating intracellular calcium stimulated by histamine or thrombin.

To further investigate the mechanism of XOR release, the effect of microtubule disruption was investigated (Figure 88). Incubating HUVECs with colchicine before stimulation with histamine reduced the release of both vWf and XOR. In a similar study observing vWf release it was concluded that intracellular calcium-rising agents (such as histamine, thrombin, and A23187) recruit Weibel-Palade bodies to the plasma membrane for secretion, an effect that is dependent on intact microtubules for granule migration (Sinha and Wagner, 1987; Vischer *et al.*, 2000). Therefore, as XOR release is affected by colchicine in the manner as described for vWf, then similar conclusions can be drawn. That is, XOR release may be dependent on the migration of granules within the cell, which would suggest that the XOR "packages" observed by immunofluorescent and SEM techniques could in fact be storage granules that are the source of secreted XOR.

5.4.5 Other Potential Release Mechanisms

Although the release of XOR by a "traditional" secretion pathway is possible, other mechanisms exist that could potentially suit the release of XOR from the vascular endothelium. As the first alternative release mechanism it is worth discussing the only reported XOR secretion mechanism, the secretion of XOR during the release of milk lipid globules (MLG).

Milk lipid occurs in two forms, as membrane fragments in the skim phase (Kitchen, 1974) and as milk lipid globules (MLGs) that provide essential nutrition to the suckling neonate. MLG precursors are believed to originate from the endoplasmic reticulum of mammary epithelial cells (Deeney et al., 1985) and may fuse with one another during their transit to the apical plasma membrane (APM) to form larger structures (1-5μM in diameter). The release of MLGs from mammary epithelial cells into the mammary alveolar lumen can occur by one of two mechanisms, reviewed in Mather and Keenan, 1998. The most frequently occurring mechanism involves the enveloping of the MLG by the APM which pinches-off, therefore expelling the globule from the cell. The molecular process of globule enveloping, that is the formation of the Milk Lipid Globule Membrane (MLGM), and globule release has been hypothesised by Mather and Keenan, 1998, as a process in which XO is predicted to play a key role (summarised in Figure 89).

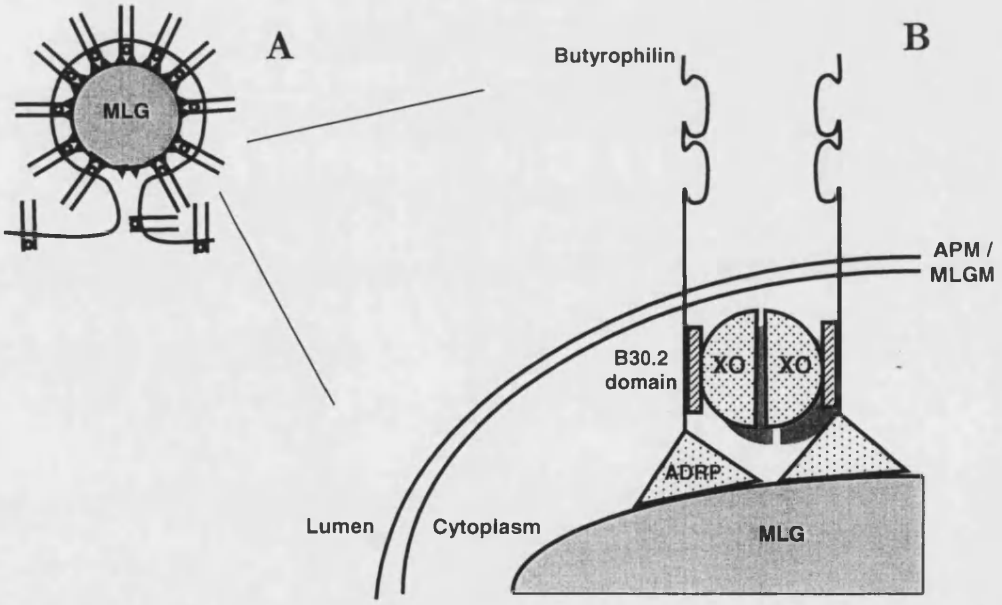

Figure 89. The Release of XO during MLG Secretion from Mammary Epithelial Cells

The release of MLGs from mammary epithelial cells occurs via a mechanism in which the MLG is enveloped in apical plasma membrane (A). The hypothesised protein interactions that are involved in this process are shown (B). The apical transmembrane glycoprotein, butyrophilin, contains a region of about 166 amino acids known as the B30.2 domain (Vernet et al., 1993). Xanthine oxidase has been shown to bind to the cytoplasmic domain of butyrophilin via the B30.2 domain (Ishii et al., 1995), forming the membrane XO-butyrophilin complex which is believed to interact with ADRP on the surface of the MLG (Heid et al., 1996). The formation of the XO-butyrophilin-ADRP has been

proposed to function in the enveloping and eventual "pinching-off" and release of the MLG, therefore resulting in XO secretion from the mammary epithelium.

A limited immunofluorescence microscopic survey of the bovine tissues suggested that butyrophilin was only expressed in mammary epithelial cells during lactation (Franke *et al.*, 1981). Also, the expression of the butyrophilin gene has been examined in many bovine organs including the liver, intestine, and kidney (Jack and Mather, 1990) but yielded negative results. As tissue samples were homogenised for RNA analysis in these experiments, RNA from tissues other than the parenchymal tissue would have been examined, for example the microvascular endothelium. The negative butyrophilin mRNA results would therefore suggest the absence of butyrophilin gene expression in the microvascular endothelium as well. The results from these two experiments would suggest that butyrophilin is only expressed in lactating mammary epithelial tissue and therefore an identical XOR-secretion mechanism in the vascular endothelium is unlikely.

Another potential route for XOR secretion is through the release of membrane microparticles (MPs). MPs are membrane vesicles that are shed from the plasma membrane and contain cytoplasmic components. MPs can be formed by several cells types including platelets, macrophages, and vascular endothelial cells. The release of the cytokine IL-1β, a protein that like XOR does not contain a signal sequence for secretion and is found in the cytoplasm (Wingren *et al.*, 1996), has been shown to occur by MP release in macrophages (MacKenzie *et al.*, 2001). Therefore this process could apply to the release of XOR. However, the stimuli for MP formation in HUVECs only include bacterial lipopolysacchaides, TNFα, IL-1, complement, and A23187, but thrombin did not stimulate MP formation above basal levels (Simak *et al.*, 2002; reviewed in VanWijk *et* al., 2003). As thrombin (1U/ml) did not cause an increase in MP release from HUVECs (Simak *et al.*, 2002) but does stimulate XOR release (results from this thesis), it is unlikely that this mechanism is responsible for XOR release. However, repeating the experiments of Simak *et al.*, 2002, including a histamine stimulus, would be required to confirm this.

5.4.6 Summary

The release of XOR can be stimulated from HUVECs using known endothelial protein secretagogues. XOR release is independent of cell death, and therefore occurs by a controlled process that is independent of vWf. The mechanism of release may require a rise in intracellular calcium and a functioning microtubule network. Packaged XOR is a likely source of the secreted enzyme, however the release of cytoplasmic XOR by microparticle formation remains a possibility.

Chapter 6. The Effect of Thrombin on Xanthine Oxidoreductase Activity

6 The Effect of Thrombin on Xanthine Oxidoreductase Activity

6.1 Introduction: Thrombin in detail

After its formation from prothrombin (reviewed in Mann *et al.*, 2003), thrombin plays paradoxically opposing roles in the blood (Griffin, 1995). As a procoagulant thrombin cleaves the terminal step of the coagulation cascade, the conversion of fibrinogen into insoluble fibrin (as described in Introductory Chapters). In addition, thrombin can proteolytically activate coagulation factor XIII (which is responsible for stabilising the fibrin clot), and factors V, VIII, and XI (Griffin, 1995). However, opposing this role is the function of thrombin as an anticoagulant (reviewed in Esmon, 2000). Thrombin can activate protein C, which in the presence of its cofactor protein S, cleaves and inactivates factors Va and VIIIa (Esmon, 1989), two essential cofactors in the formation of Xa and IXa that are required for thrombin generation. Therefore protein C down-regulates the amplification and progression of the coagulation cascade. Effective thrombin activation of protein C requires thrombin-binding to the endothelial cell-surface receptor, thrombomodulin (Esmon *et al.*, 1982; Esmon, 1989). Binding to thrombomododulin is a key event in the switch from thrombin's procoagulant activity to anticoagulant activity. The interaction with thrombomodulin suppresses the ability of thrombin to cleave fibrinogen and factor V (Esmon *et al.*, 1982) and enhances the specificity (>1000 fold) toward the zymogen protein C (Esmon and Owen, 1981; Owen and Esmon, 1981), the latter reaction being assisted by an endothelial cell receptor for protein C (Taylor *et al.*, 2001).

Additional to the substrates described above thrombin may also cleave other proteins including PARs 1, 3, and 4 (as described in Introductory Chapters), thrombin-activatable fibrinolysis inhibitor (TAFI) (Bajzar *et al.*, 1995), troponin C (Leavis *et al.*, 1978), and growth hormones (Graf *et al.*, 1976). Recognition of substrates is achieved by specific sequences in thrombin's structure. The crystal structure of thrombin has

been investigated in detail (Bode *et al.*, 1992). Thrombin is composed of two polypeptide chains, A and B, which are covalently linked by disulphide bonds. In humans, the A and B-chains consist of 36, and 259 amino-acid residues, respectively (Butkowski *et al.*, 1977). The B-chain has been shown to be homologous to the catalytic domains of other pancreatatic and coagulation trypsin-like proteases, whereas the A-chain, previously thought to have no function (Di Cera, 2003), may have an important role in dictating the conformation and subsequently the activity of the catalytic B-chain (De Cristofaro *et al.*, 2004). The B-chain is shaped like a sponge with deep crevices and protuberances on its water accessible side and contains the active site responsible for cleavage of substrates (Bode *et al.*, 1992). Although thrombin has trypsin-like activity, unlike trypsin thrombin contains regions distant from the active site that are responsible for substrate recognition. The crystal structure of thrombin has revealed two cationic patches on the enzymes surface that are denoted anion binding Exosites I and II (Bode *et al.*, 1992). Through various mutagenesis studies Exosite I has been shown to play an important role in the recognition of the substrates fibrinogen, fibrin, PAR 1, protein C, and thrombomodulin, whereas Exosite II is the locale for interaction with heparin and glycosaminoglycans (reviewed in Leung and Hall, 2000).

Consensus sequences for thrombin recognition and cleavage have been proposed (Rose and Di Cera, 2002). Exosite I-binding sequences have the consensus of ΦPΦ and for active site-binding sequences the L *ins* PRGΦ consensus has been proposed, where substrate cleavage occurs preferentially between the R and G residues (G = glycine , L = Leucine P = proline, R = arginine, and Φ = either phenylalanine, tyrosine, histidine, or proline).

6.2 Chapter Aim

Results in chapter 5 demonstrate that the presence of thrombin increases XO-activity, independent of cell culture, in a dose-dependent manner (Figure 78). Using XOR enzyme from various sources and by inhibiting thrombin's proteolytic activity, the

aim of this chapter is to further characterise the effects of thrombin on XOR activity and attempt to decipher the mechanism by which XOR activity is altered.

6.3 Prinicples, Materials, and Methods

6.3.1 XOR Actvity Measurement

6.3.1.1 Materials

Ascorbic acid, Catalase from bovine liver, Hirudin recombinant from yeast, NADH, SOD from bovine erythrocytes, Thrombin from bovine plasma, Xanthine (Sigma Aldrich Company Ltd. Dorest, UK). Semi-skimmed milk (shop bought)

6.3.1.2 Methods

XOR activity was measured using the IXP- and uric acid-based assays (as described in Chapter 5), and also using the NADH oxidase assay. In the IXP-based assay 100ng/ml Biozyme XO, 73μg/ml rat liver protein, 39μg/ml rat serum protein, and 68μg/ml milk protein were routinely assayed (preparation of rat liver and serum samples are described in Appendix I 8.7). Where appropriate, thrombin, heat-inactivated thrombin (heated to 99°C for 5mins), hirudin, SOD, catalase, or ascorbic acid were added to the assay (as described in results). In the uric acid-based assay 1μg/ml Biozyme XO was used, and thrombin and ascorbic acid were added where indicated in results.

6.3.1.3 XOR-NADH Oxidase Activity Assay

The NADH Oxidase-based XO assay was adapted from Sanders *et al.*, 1997. In this assay, XO was incubated with 100μM NADH at 25°C and the change in absorbance at 340nm (A_{340}) was recorded using a spectrophotometer (Hitachi U-2010 spectrophotometer. Hitachi. Berkshire, UK). The reaction is shown schematically in Figure 90. The change in A_{340} was measured over a period of approximately 5mins and the rate of NADH oxidation was calculated using the extinction coefficient for NADH, $\varepsilon = 6.22 mM^{-1} cm^{-1}$. Following an initial experiment it was discovered that 40μg/ml Biozyme XO was required to generate measurable XO-NADH oxidase activity using this method and was used in subsequent experiments.

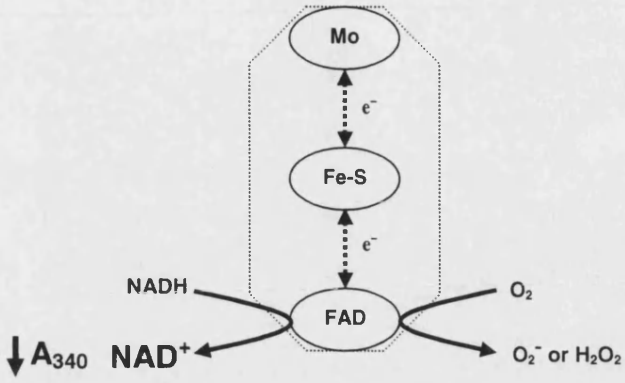

Figure 90. Measurement of XO-NADH Oxidase Activity

NADH oxidation by XO occurs at the FAD-containing moiety. The oxidation of NADH forming NAD^+ can be followed as a decrease in A_{340}. Electrons donated to XO during the oxidation step may be used to reduce molecular oxygen forming O_2^- or H_2O_2.

6.3.2 Escherichia coli Growth and XO Treatment

6.3.2.1 Materials

Agar No. 1 (Oxoid Limited. Hampshire, UK); Allopurinol, Hypoxanthine, Luria Broth, Thrombin, Xanthine (Sigma Aldrich Company Ltd. Dorest, UK). Petri dishes (Fisher Scientific UK Ltd. Leicestershire, UK).

6.3.2.2 Method

6.3.2.2.1 Bacterial Culture

Agar plates were produced by adding 12.5g Luria Broth (LB) and 6g Agar to 500mls distilled water. The LB/Agar mix was sterilised by autoclaving. Sterile, set agar was heated in a microwave until fully dissolved and was poured into Petri dishes to a depth of about 5mm. The Petri dish was covered and the agar was allowed to set at room temperature. The resulting agar plates were stored at 4°C until required. Luria Broth was used for liquid culture of *Escherichia coli*. LB was produced by dissolving 25g LB powder in 1000ml distilled water and was sterilised by autoclaving.

The Long term storage of *Escherichia coli* strain MC4100 (E. coli) was achieved by freezing at -70°C. Using a flamed loop, E. coli from the long-term storage stock were streaked-out onto an agar plate and incubated at 37°C until colonies formed. Once

colonies had formed plates were stored at 4°C. When required single colonies were used to inoculate baffled flasks containing 20mls LB and cultures were incubated overnight at 37°C with continuous agitation.

6.3.2.2.2 Treatment of E. coli with XO

To determine the effect XO activity has on cultures of E. coli (in the presence and absence of thrombin) a 96-well plate method was used (Millar, 1999). In these experiments a 200µl well volume was used and overnight E. coli cultures were diluted in LB to a final optical density 600nm (OD_{600}) of approximately 0.02. E. coli were treated with relevant combinations of 100µM Allopurinol, 100µM hypoxanthine, 10U/ml thrombin, and 50mU/ml Biozyme XO made up in a LB (all values stated are final concentrations). Cultures were incubated at 37°C and OD_{600} was measured every 30mins. An optical reading following the addition of the E. coli culture to the plate constituted time zero. Log optical density values were plotted against time, and generation time was calculated from the linear growth stage of each data set using the equation given in Equation 1.

6.3.3 Amino-acid Sequence Alignments and 3D-Structure Analysis

Relevant amino-acid sequences were retrieved from the National Center for Biotechnology Information Protein database (http://www.ncbi.nlm.nih.gov/entrez/). The following sequences were used in analysis (sequence accession numbers are shown in brackets following the sequence name): Human Coagulation factor II (P00734), V (P12259), VII (P08709), VIII (P00451), XI (P03951), and XIII (CAB99356), Human Fibrinogen Aα (P02671), Human Fibrinogen Bβ (P02675), Human Thrombin Activatable Fibrinolysis Inhibitor (TAFI; g4503005), Human PAR1 (P25116), PAR3 (O00254), and PAR4 (AAC28860), Human Protein C (P04070), Bovine XOR (P80457), Chicken XOR (P47990), Human XOR (P47989), Mouse XOR (Q00519), and Rat XOR (NP 058850). Sequences were aligned using the Clustal W program (Chenna *et al.*, 2003) with default settings. The following symbols

were used to indicate the degree of conservation between the aligned sequences: "*" means amino-acids in that column are identical, ":" means in that column conserved substitutions have occurred according to the table below (Table 3), and "." means in that column semi-conserved substitutions have occurred. 3D protein structures were viewed using the National Center for Biotechnology Information 3D-Structure Database (http://www.ncbi.nlm.nih.gov/entrez/) and Cn3D program version 4.1 (Chen *et al.*, 2003a). Images are displayed using the following settings: rendering setting = tubes, and colouring setting = secondary structure (which distinguishes helix, strand, and coils with different colours). The 3D structure of Bovine XO was deposited by Enroth *et al.*, 2000.

Table 3. Amino-acid Grouping

Amino-Acid	Description
AVFPMILW	Small (small + hydrophobic (including aromatic -Y))
DE	Acidic
RHK	Basic
STYHCNGQ	Hydroxyl + Amine + Basic - Q

The Clustal W program (Chenna *et al.*, 2003) uses the groups of amino-acids described to judge whether conserved substitutions have occurred between amino-acids in aligned sequences.

6.3.4 Fibrin turbidity assay

6.3.4.1 Materials

Fibrinogen Type I-S from bovine plasma; Hirudin recombinant from yeast, Thrombin from bovine plasma (Sigma Aldrich Company Ltd. Dorest, UK).

6.3.4.2 Method

The thrombin-catalysed polymerisation of fibrin was measured using a turbidity-based assay. A previously published procedure (Choi *et al.*, 1998; Chu *et al.*, 2003) was followed, whereby the turbidity of a fibrinogen solution was recorded at absorbance 450nm (A_{450}) on a spectrophotometer (Hitachi U-2010 spectrophotometer. Hitachi. Berkshire, UK). The catalytic activity of thrombin causes the polymerisation of fibrin which increases the turbidity of the assay solution. Briefly, a final concentration of

0.5% (w/v) fibrinogen with hirudin (various concentrations) were made up to 1990µl with buffer (containing 50mM Tris-HCl pH7.4, 5mM $CaCl_2$, and 100mM NaCl) and were allowed to warm to 37°C in the spectrophotometer. With continuous stirring a time course assay at A_{450} was started and a final concentration of 0.5U/ml thrombin was added, constituting time point zero. The assay was run for approximately 3mins and A_{450} was recorded at 10sec intervals.

6.3.5 Cytochrome c – based Superoxide Assay

6.3.5.1 Materials

Cytochrome *c* from equine heart, Hypoxanthine, SOD from bovine erythrocytes (Sigma Aldrich Company Ltd. Dorest, UK).

6.3.5.2 Method

The cytochrome *c* – based method of measuring $O_2^{\cdot -}$ was adapted from the method of McCord and Fridovich (McCord and Fridovich, 1968; McCord and Fridovich, 1969). The generation of $O_2^{\cdot -}$ was calculated as the SOD-inhibitable portion of cytochrome *c* reduction, therefore each assay was repeated in the presence or absence of SOD. In each assay a final concentration of 50µM cytochrome *c* +/- 50U/ml SOD was incubated with 1mU/ml Biozyme XO and 500µM hypoxanthine. Reactions were incubated at 25°C and an absorbance change at 550nm was measured. Linear portions of absorbance change and the extinction coefficient for reduced cytochrome *c* (ε = 21.1mM^{-1} cm^{-1}) were used to calculate the rate of SOD-inhibitable $O_2^{\cdot -}$ generation, as cytochrome *c* is reduced by $O_2^{\cdot -}$ in a molar-to-molar manner then the rate of cytochrome *c* reduction equals the amount of $O_2^{\cdot -}$ generation.

6.4 Results

6.4.1 The Effect of On-Ice-Incubation on XO Activity

For many of the experiments in this chapter a 1ng/µl purified XO stock was prepared and was incubated on ice until required. Potentially the stock could be incubated on ice for several hours before being used in assays. Therefore as a control, the effect of storing the XO stock on ice, over time, was assessed by determining XO-activity at different incubation time points. At selected time points 100µl aliquots of XO stock were measured for activity using the IXP-based XO assay as described in Beckman *et al.*, 1989. Activity was recorded over 1min time periods and was calculated by linear regression from recordings at 20sec intervals (see Figure 91). Over the time period assessed (up to 6hrs) XO activity remained unchanged.

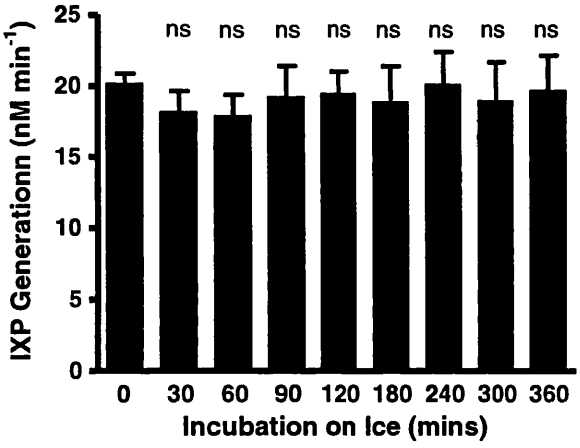

Figure 91. The Effect of Time-on-Ice Incubation on XO-Activity

A 1ng/µl stock solution of pure-XO was incubated on ice. At selected time points enzyme activity was measured. Data was analysed using one-way ANOVA with the Dunnett's post test [results are from two experiments in triplicate, therefore n=6; error bar = SD; ns = not significant (p>0.05)].

6.4.2 Thrombin's Effect on Purified (Biozyme)-XO Activity

6.4.2.1 Dose Response

An initial study was used to confirm the effect of thrombin on XO activity seen in the previous results chapter (Figure 78). Here 100ng/ml pure XO was incubated with various concentrations of thrombin for approximately three minutes at room temperature. The XO/thrombin mixture was assayed for XO activity using the IXP-

based XO assay as described in Beckman *et al.*, 1989 (see Chapter 5), however methylene blue was not used in the reaction process. Using the pterin substrate only, IXP accumulation was measured at 20sec intervals over a one minute period at room temperature, and enzyme-activity was calculated using linear regression of the progress curves (see Figure 92A). As controls, IXP-generation from the pterin substrate was assessed with XO, PBS without XO, and thrombin without XO (see Figure 92B). In accordance with the original study performed in Chapter 5, the presence of thrombin increases XO activity in a dose-dependent manner. Controls indicate that thrombin alone is not responsible for the increase in IXP-generation observed.

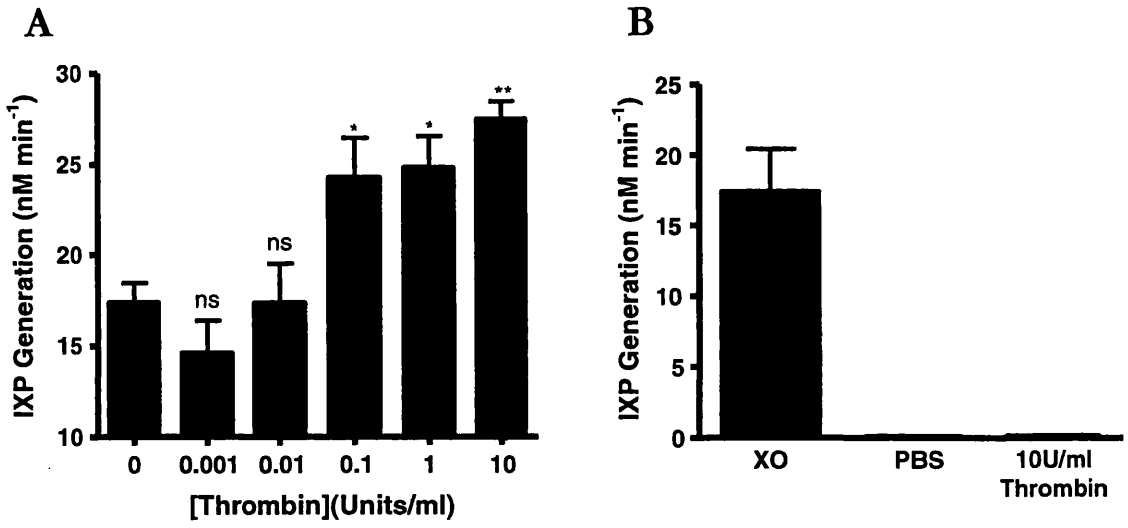

Figure 92. The Effect of Thrombin on the Activity of Pure XO – IXP-Based Assay

A) 100ng/ml Biozyme XO was incubated with various concentrations of thrombin for approximately 3mins at room temperature. Following the incubation step, XO activity was measured using the IXP-based XO assay and XO-activity was calculated. Data was analysed using one-way ANOVA with the Dunnett's post test (results are from three experiments in triplicate, therefore n=9; error bar = SEM; ns = not significant ($p>0.05$), * = $p<0.05$, ** = $p<0.01$). B) Control experiments were performed analysing IXP-generation from the pterin substrate in the presence of 100ng/ml pure XO, without XO with substrate (PBS), and 10U/ml thrombin without XO with substrate (results are from one experiment in triplicate, therefore n=3; error bar = SD)

6.4.2.2 Michaelis-Menton Kinetics

Using the methodology described above, the influence of thrombin on XO activity was compared using different concentrations of ptrein substrate. Enzyme activity was

calculated as previously described and data was fitted to the Michaelis-Menton equation (see Figure 93). In the presence of 1U/ml thrombin XO-V_{max} increases to 26.2 nM min^{-1} from a baseline of 19.5 nM min^{-1} IXP generation.

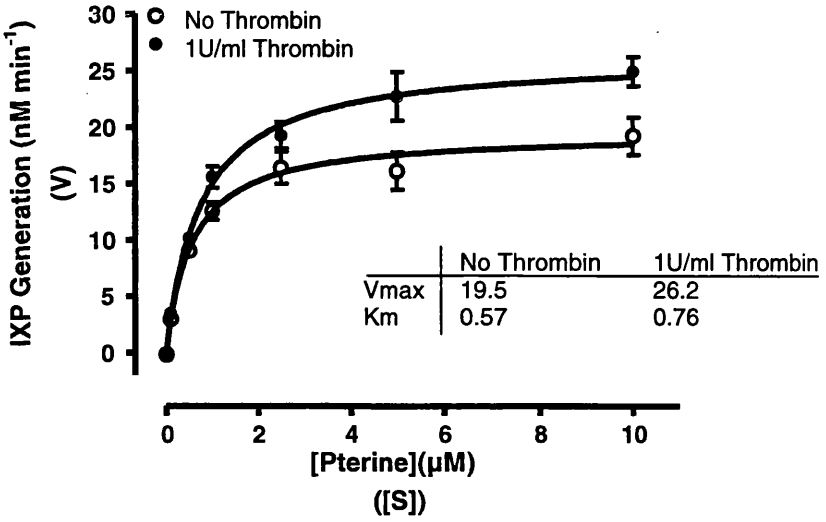

Figure 93. XO-Activity in the Presence and Absence of Thrombin

The effect of thrombin on XO (100ng/ml Biozyme) activity was compared in the presence of various pterin-substrate (S) concentrations. Enzyme activity/velocity (V) was calculated and Michaelis-Menton kinetics were applied (results are from three experiments in triplicate, therefore n=9; error bar = SEM).

6.4.2.3 Is Thrombin's Effect Assay-Dependent?

In chapter 5 it was demonstrated that the pH of the thrombin solutions tested did not deviate from the 0U/ml sample and as the IXP-based assay is pH dependent, this can be ruled out as a possible cause of the change in enzyme activity. However, to support the data derived from the IXP-based assay, the thrombin-dose response assay was repeated, using the uric-acid assay. As with the IXP-based assay, XO and thrombin were incubated together at room temperature for approximately 3mins before XO activity was measured. However, in the uric-acid based assay 1μg/ml XO with thrombin (various concentrations) was assayed using 100μM xanthine, and uric acid generation was measured following an increase in A_{295}, at 25°C, over time. From the linear portion of enzyme activity uric acid generation was calculated using the extinction coefficient ε = 9.6$mM^{-1}cm^{-1}$ (see Figure 94). The influence of thrombin on

XO-activity measured using the uric acid-based assay is comparable to that using the IXP-based assay (see Figure 92).

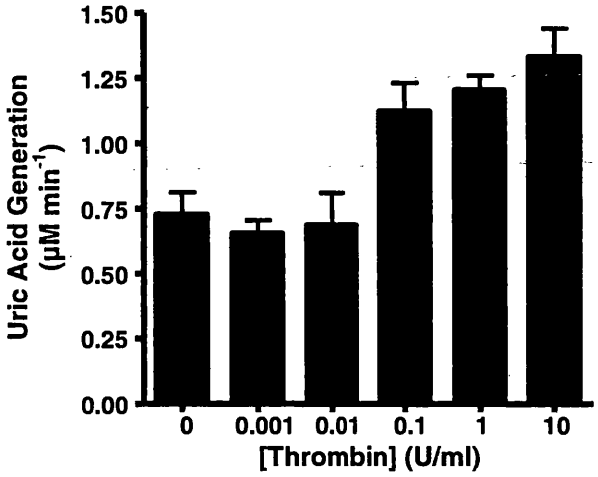

Figure 94. The Effect of Thrombin on the Activity of Pure XO – Uric Acid Based Assay

1μg/ml Biozyme XO was incubated with various concentrations of thrombin for approximately 3mins at room temperature. Following the incubation step, XO activity was measured using the uric acid-based XO assay and XO-activity was calculated (results are from one experiment in triplicate, therefore n=3; error bar = SD).

6.4.2.4 Time Course

In the dose-response experiments described above, XO and thrombin were incubated for approximately 3mins at room temperature prior to enzyme assay. To investigate the effect of incubation time on XO activity, 1U/ml thrombin and 100ng/ml purified XO were incubated for various times before XO activity was assessed using the IXP-based assay (Figure 95). A significant change in XO-activity occurs after 30secs incubation with thrombin with a maximal increase occurring between 60-120secs incubation.

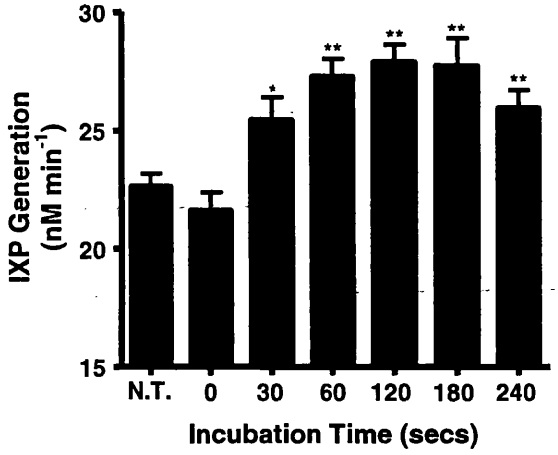

Figure 95. The Effect of Thrombin-XO Incubation Time on XO Activity

1U/ml thrombin was incubated with 100ng/ml Biozyme XO for various time periods at room temperature. After the desired time XO activity was measured and data was analysed using one-way ANOVA with the Dunnett's post test (N.T. = no thrombin; results are from three experiments in triplicate, therefore n=9; error bar = SEM; ns = not significant ($p>0.05$), * = $p<0.05$, ** = $p<0.01$).

6.4.2.5 Superoxide Generation

Thrombin has been shown to increase XO-activity as measured by the formation of uric acid and IXP. As electron donating substrates are being catalysed at a more rapid rate in the presence of thrombin, it would be expected that ROS-products would also be generated at a quicker rate compared to controls. To assess whether the presence of thrombin increases the generation of $O_2^{\cdot -}$ by XO compared to controls, the cytochrome *c* assay was used. In each of the five repeats of the experiment $O_2^{\cdot -}$-generation was greater in the presence of thrombin compared to the no thrombin control. However following data analysis, the increase in $O_2^{\cdot -}$-generation was found not to be statistically significant (Figure 96).

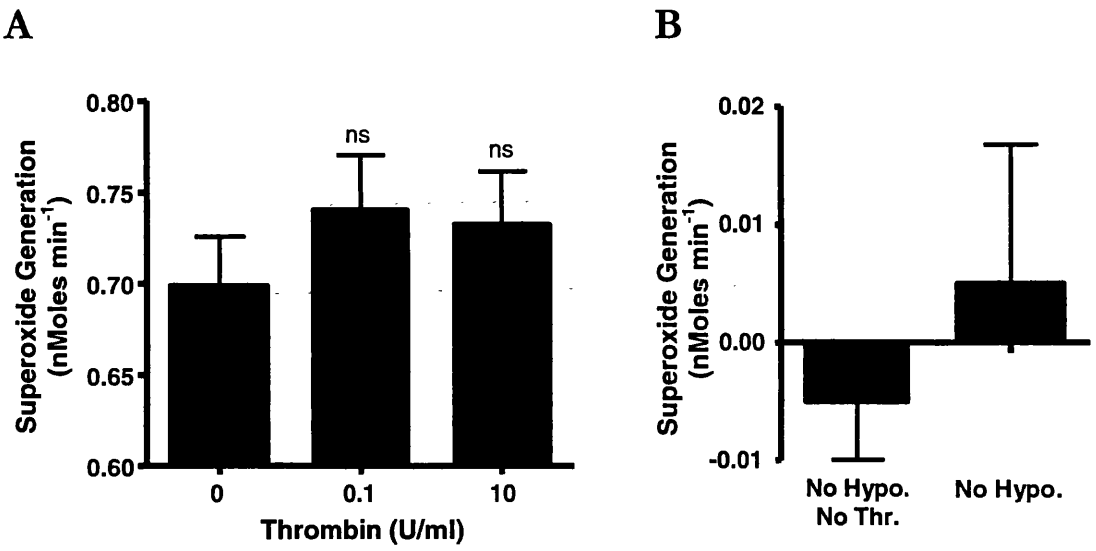

Figure 96. The Effect of Thrombin on XO-$O_2^{\cdot-}$ generation

A) 1mU/ml Biozyme XO was incubated with various concentrations of thrombin for approximately 3mins at room temperature. Following the incubation step, XO-$O_2^{\cdot-}$ generation in the presence of 500μM hypoxanthine was measured using the cytochrome *c* assay. The rate of $O_2^{\cdot-}$ generation was calculated and data was analysed using one-way ANOVA with the Dunnett's post test (results are from five experiments in triplicate, therefore n=15; error bar = SEM; ns = not significant P>0.05). B) Controls showing $O_2^{\cdot-}$ generation with just XO [no hypoxanthine (hypo.), no thrombin (thr.)] and with XO and thrombin without hypoxanthine substrate.

6.4.2.6 XO-NADH Oxidase Activity

In experiments investigating the effect of thrombin on XO activity, the substrates tested (i.e. pterin and xanthine) act at the MoCo redox centre of the enzyme. To gain further insight into how and where thrombin maybe affecting XO, the influence of thrombin on XO-NADH oxidase activity was determined. As mentioned in the Introduction to Chapter 2, the NADH substrate is oxidised at the FAD-containing active site of XO, a reaction that does not require MoCo-binding for catalysis. The influence of thrombin on XO-NADH oxidase activity was assessed using the protocol described in the Methodology section. As a control thrombin was shown to increase XO activity, as measured using the uric acid-based activity assay (Figure 97B), however the presence of thrombin did not alter XO-NADH oxidase activity (Figure 97A).

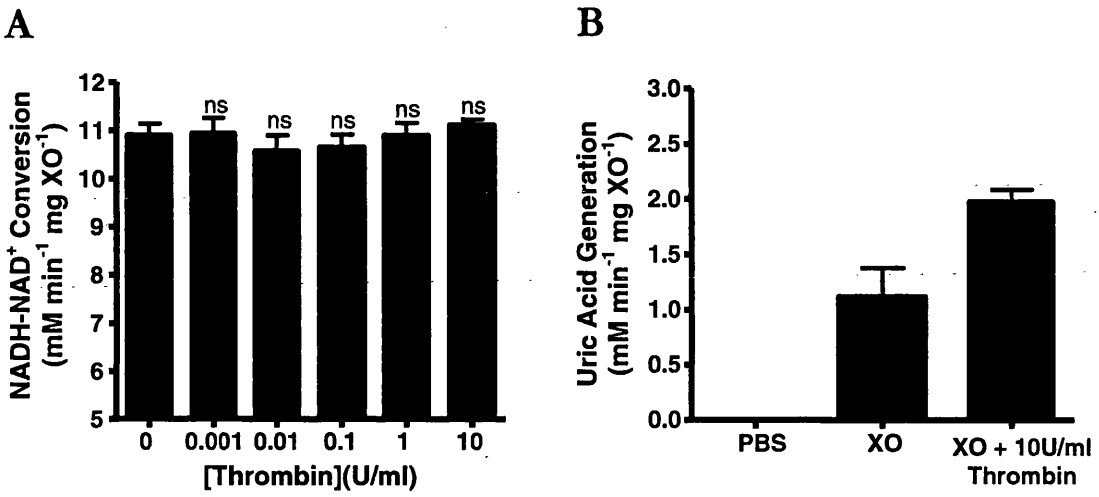

Figure 97. The Effect of Thrombin on XO-NADH Oxidase Activity

A) The influence of thrombin on XO-NADH oxidase activity was assessed following NADH-NAD^+ conversion at A_{340}. The rate of NADH-NAD^+ conversion was calculated and data was analysed using one-way ANOVA with the Dunnett's post test (results are from three experiments in triplicate, therefore n=9; error bar = SEM; ns = not significant P>0.05). B) As a control, i.e. to show that the thrombin stock functions to increase XO-activity as shown in previous experiments, XO-activity was measured using the uric acid-based assay in the presence or absence of thrombin (results are from one experiment in triplicate; error bar = SD).

6.4.3 Thrombin's Effect on Non-Purified-XO Activity

As demonstrated in the experiments described above, thrombin has an effect on purified-XO activity. In this section the influence of thrombin on XOR contained within complex samples was investigated.

6.4.3.1 The Effect of Thrombin on Milk-XO Activity

XO from Biozyme (Biozyme. Blaenavon, UK) is prepared from bovine buttermilk, therefore to determine whether thrombin alters XO from complex samples, bovine milk was initially tested. Dose-response and time course experiments were carried out using the same protocol as described for purified-XO, however, each assay contained 68μg/ml milk protein and in time-course experiments 10U/ml thrombin was incubated with milk for the selected time points. XO-activity was assayed using the IXP-based protocol. In dose-response experiments (Figure 98A), similar to Biozyme-XO, a statistically significant change in XO-activity occurs in the presence of ≥0.1 U/ml thrombin. However in comparison with Biozyme XO a significant change in

activity only occurs after 120secs incubation with thrombin (Figure 98B), even though 10x more thrombin was used in milk-XO studies.

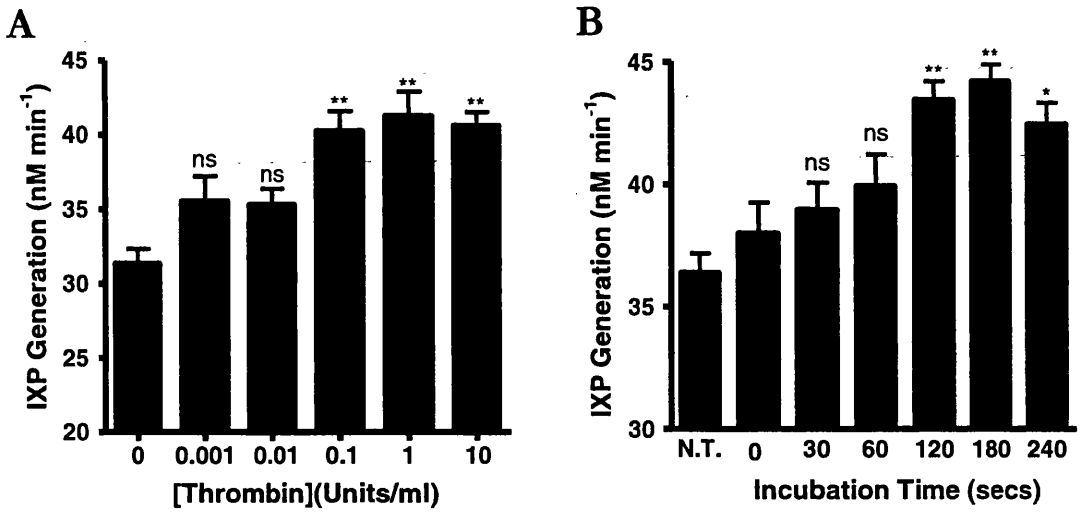

Figure 98. The Effect of Thrombin on XO-Activity in Milk

A) 68μg/ml semi-skimmed milk was incubated with various concentrations of thrombin for approximately 3mins at room temperature. Following the incubation step, XO activity was measured using the IXP-based XO assay and XO-activity was calculated. Data was analysed using one-way ANOVA with the Dunnett's post test (results are from three experiments in triplicate, therefore n=9; error bar = SEM; ns = not significant ($p>0.05$), ** = $p<0.01$). B) 10U/ml thrombin was incubated with 68μg/ml semi-skimmed milk for various time periods at room temperature. After the desired time XO activity was measured and data was analysed using one-way ANOVA with the Dunnett's post test (N.T. = no thrombin; results are from three experiments in triplicate, therefore n=9; error bar = SEM; ns = not significant ($p>0.05$), * = $p<0.05$, ** = $p<0.01$).

6.4.3.2 The Effect of Thrombin on Rat Liver and Serum-XOR Activity

As a continuation into the study into the effect of thrombin on complex XOR-containing samples both rat liver and serum were tested. Previous studies have shown rat liver and serum contains both XDH and XO and activity (Al-Khalidi and Chaglassian, 1965; Stirpe and Della-Corte, 1969; Kooij *et al.*, 1994). Therefore the effect of thrombin on XDH activity could also be determined using these samples. Dose-response and time course experiments were carried out using the same protocol as described for purified-XO, however, each assay contained 73μg/ml and 39μg/ml rat liver supernatant and serum protein, respectively. In time-course experiments 10U/ml thrombin was incubated with rat liver and serum protein for the selected time points. Total XOR and XO-activities were assayed using the IXP-based protocol

in the presence and absence of methylene blue, respectively. In dose-response experiments (Figure 99A), unlike Biozyme-XO and XO contained in milk, a statistically significant change in XO-activity occurs only in the presence of 10U/ml thrombin, and thrombin has no effect on total (XDH/XO) enzyme activity (Figure 99B). However, similar to Biozyme-XO a significant change in XO-activity occurs after just 30secs incubation with thrombin (Figure 99C), but no significant change in total enzyme activity was seen over the incubation time points assessed (Figure 99D).

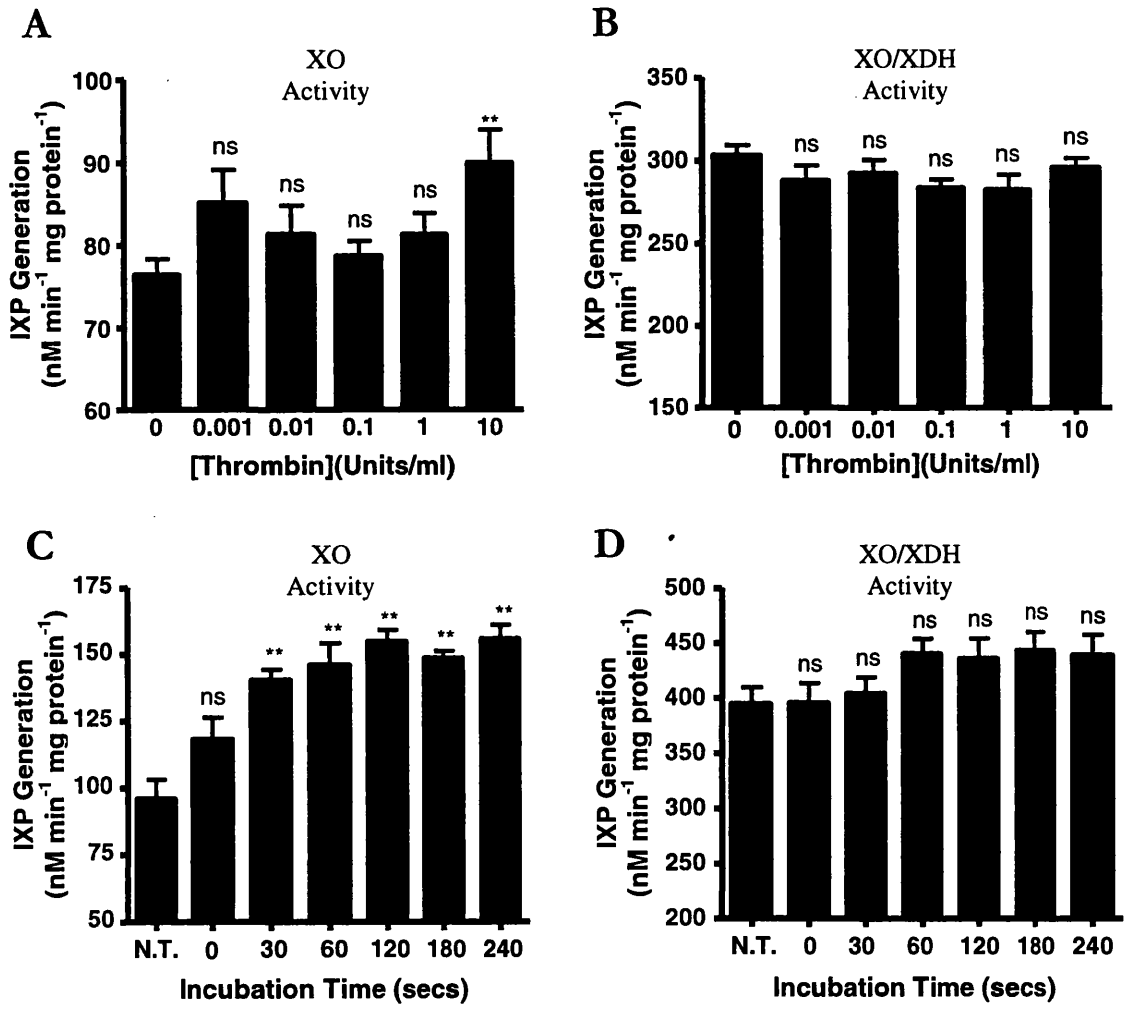

Figure 99. The Effect of Thrombin on XOR-Activity in Rat Liver

73μg/ml rat liver-supernatant was incubated with various concentrations of thrombin for approximately 3mins at room temperature. Following the incubation step, XO (A) and total enzyme activity (B) were measured using the IXP-based XOR assay. Data was analysed using one-way ANOVA with the Dunnett's post test (results are from three experiments in triplicate, therefore n=9; error bar = SEM; ns = not significant ($p>0.05$), ** = $p<0.01$). In incubation time course experiments 10U/ml thrombin was incubated with 73μg/ml rat liver-supernatant for various time periods at room

temperature. After the desired time XO (C) and total enzyme activity (D) activity were measured and data was analysed using one-way ANOVA with the Dunnett's post test (N.T. = no thrombin; results are from three experiments in triplicate, therefore n=9; error bar = SEM; ns = not significant ($p>0.05$), ** = $p<0.01$).

Dose-response experiments were also performed on rat serum samples. Both XO, and XO/XDH-combined activities were measured as described for rat liver-supernatant analysis. However a final concentration of 39μg/ml rat serum protein was assayed (Figure 100A, B). In accordance with dose-response experiments with other XO-containing samples, the XO-activity in rat serum increases in the presence of thrombin. There is no increase in enzyme activity in the presence of methylene blue compared to pterin alone, which suggests that rat serum does not contain measurable XDH activity. This is an interesting comparison with rat liver which contains a greater amount of XDH than XO. Statistical analysis was not performed on this data set due to insufficient replicates.

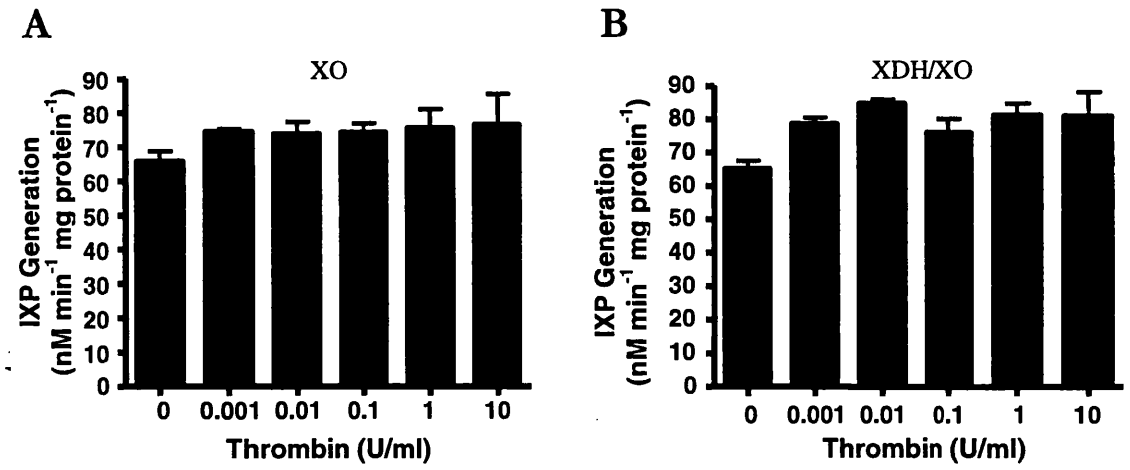

Figure 100. The Effect of Thrombin on XOR-Activity in Rat Serum

39μg/ml rat serum protein was incubated with various concentrations of thrombin for approximately 3mins at room temperature. Following the incubation step, XO (A) and total enzyme activity (B) were measured using the IXP-based XOR assay (results are from one experiment in triplicate, therefore n=3; error bar = SD).

6.4.4 Thrombin and the Antibacterial Properties of XO

ROS generated by XO have been shown to have antibacterial properties, in particular it was shown that H_2O_2 has an antibacterial function (Stevens *et al.*, 2000). The function of XO as an antibacterial agent is discussed in greater detail in Chapter 7

(Main Discussion). In the following set of experiments the effect of thrombin on XO-antibacterial activity was assessed. As thrombin increases XO-activity it is likely that the antibacterial properties of XO will be enhanced in the presence of thrombin. In these experiments overnight cultures of E. coli were diluted and exposed to combinations of hypoxanthine, XO, thrombin, and allopurinol. Bacterial cultures were incubated at 37°C and growth was analysed by measuring a change in absorbance at 600nm (A_{600}). The population generation time was calculated from the exponential growth phase for each condition, an increase in generation time is indicative of an antibacterial or bacteriostatic environment. An example of resulting bacterial growth curves is given in Figure 101A. As a control, each of the substances (hypoxanthine, XO, thrombin, and allopurinol) used in these experiments were added singularly to E. coli cultures, none of the substances had a significant effect on generation time (Figure 101B). Compared to the generation time of control E. coli cultures, the presence of XO and hypoxanthine increase generation time, but this effect is not statistically significant (Figure 101C), more repeats maybe needed to reach statistical significance. However, with the addition of thrombin to XO, the generation time of E. coli cultures is significantly increased ($p<0.01$). The effect of XO and hypoxanthine +/- thrombin on generation time was inhibited back to a level seen in control cultures by allopurinol.

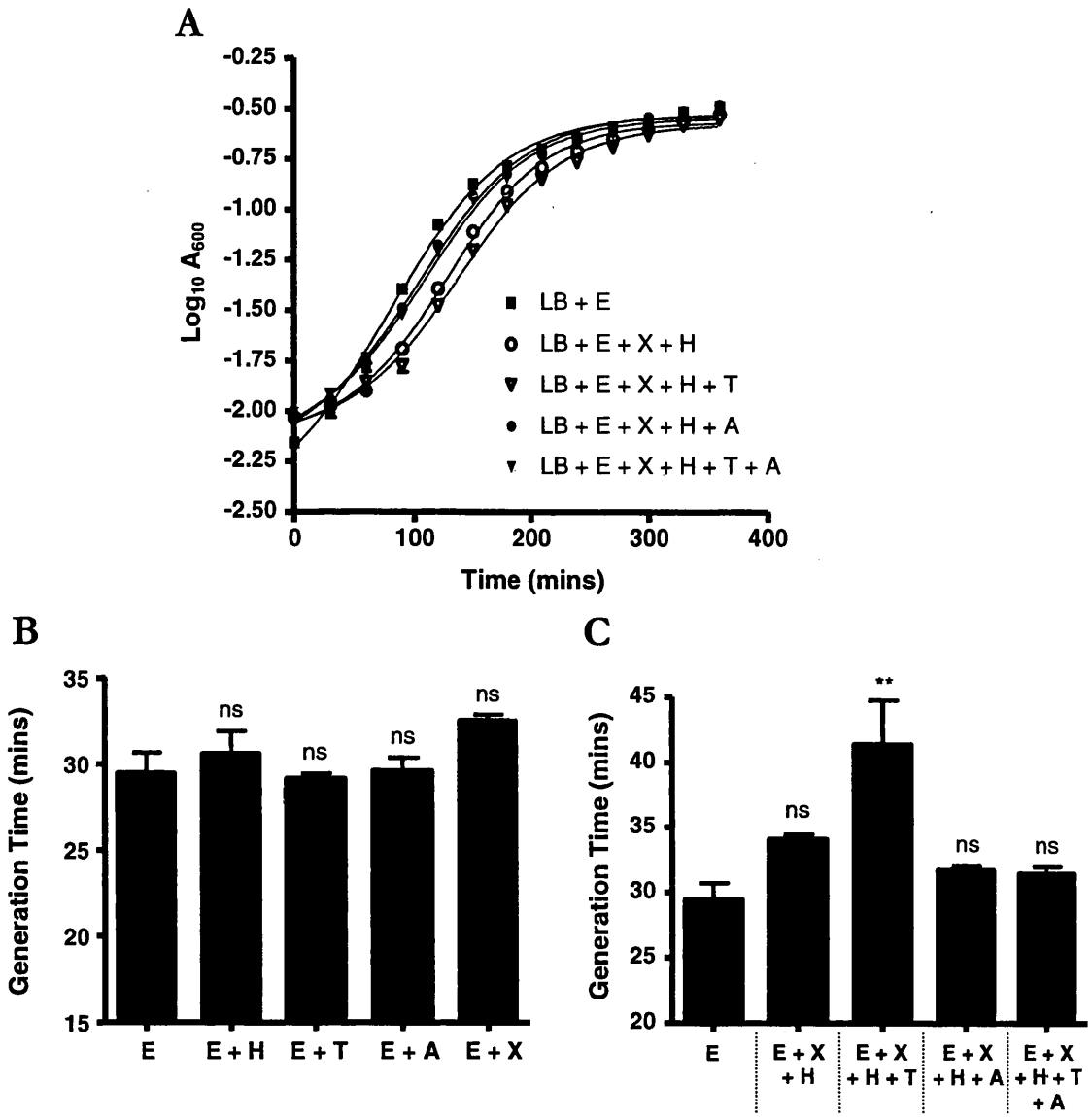

Figure 101. The Effect of Thrombin on XO-Antibacterial Properties

Cultures of E. coli were incubated with combinations of hypoxanthine, XO, thrombin, and allopurinol. Growth curve examples are shown in A, and the effect of substances added on generation time are shown in B and C. Population generation time was calculated from A_{600} readings over time and data was analysed using One-Way ANOVA with Dunnett's post test. Results are from two experiments performed in triplicate, therefore n=6, error bar = SEM (where A = Allopurinol, E = E. coli, H = Hypoxanthine, T = Thrombin, and X = XO).

6.4.5 How Does Thrombin Effect XO Activity?

To begin to decipher the mechanism by which thrombin alters XO activity, this section investigates the possible ways that thrombin effects XO.

6.4.5.1 An Alteration by Enzymatic Cleavage of XO?

As described in the introduction section to this results chapter, thrombin is a protease that cleaves a variety of substrates. It has long been known that proteases affect the activity of the XOR enzyme, particularly in the irreversible conversion of XDH to XO (see Introduction: Chapter 2). In this process, limited proteolytic cleavage of XDH results in structural alteration allowing more efficient oxygen entry to the FAD-containing moiety, and therefore a switch between XDH and XO-activities. The following section investigates the possibility that thrombin could cleave XO resulting in a structural alteration that ultimately allows more efficient substrate turn-over in the enzyme, accounting for the increase in XO-activity seen in the presence of thrombin.

6.4.5.1.1 Do Thrombin-Cleavage and Exosite I Sequences Exist in XO?

To determine whether thrombin could cleave XO, the human XO amino-acid sequence was screened for potential thrombin cleavage and Exosite I recognition sites. The sequences of these sites were derived from Rose and Di Cera, 2002. Using the Clustal-W program the amino-acid sequence of human XO was aligned with the consensus sequence for thrombin cleavage and the actual cleavage sequences from several thrombin substrates (see Table 4). The consensus sequences for thrombin cleavage were not found in the human XO sequence, however the actual sequence for cleavage of human fibrinogen Aα showed good homology to a human XO sequence. The position of the positive alignment lies between human XO amino-acid residues 1222-1225 (see Figure 102). It is interesting to note the leucine residue upstream from the potential thrombin cleavage site in human XO (see Figure 102), as leucine residues up to seven amino-acids from the Argine-Glycine cleavage site of thrombin catalysis forms part of the consensus sequence for thrombin cleavage, and is import for thrombin-substrate contact (Rose and Di Cera, 2002).

Table 4. The Search for Potential Thrombin Cleavage Sites in Human XO

Thrombin Cleavage Sequence	Origin	Homologous Sequence in XO?
PRGF	Consensus	Not Found
PRGY	Consensus	Not Found
PRGH	Consensus	Not Found
PRGP	Consensus	Not Found
PRSE	Coagulation Factor II	Not Found
PRTF	Coagulation Factor II	Not Found
IRSF	Coagulation Factor V	Not Found
PRTF	Coagulation Factor V	Not Found
GRIV	Coagulation Factor VII	Not Found
IRSV	Coagulation Factor VIII	Not Found
PRSF	Coagulation Factor VIII	Not Found
PRIV	Coagulation Factor XI	Not Found
PRGV	Coagulation Factor XIII	Not Found
VRGP	Fibrinogen Aα	TRGP (see below, Figure 102)
ARGH	Fibrinogen Bβ	Not Found
PRSF	PAR1	Not Found
IKTF	PAR3	Not Found
PRGY	PAR4	Not Found
PRLI	Protein C	Not Found
PRAS	TAFI	Not Found

To discover potential sites for thrombin cleavage of human XO, the thrombin-cleavage sequences from known substrates were aligned with the human XO amino-acid sequence.

```
HumXO VQGLGLFTLEELHYSPEGLHTRGPSTYKIPAFGSIPIEFRVSLLRDCPNKKAIYASKAV 1260
FibA  --------------------VRGP-----------------------------------
                           .***
```

Figure 102. The Alignment of Known Thrombin Cleavage Sequences with Human XO

The four amino-acid thrombin-cleavage sequence of human fibrinogen Aα (FibA) shows good homology to the human XO (HumXO) amino-acid sequence position 1222-1225. Note the leucine residue upstream from the potential cleavage site (residue 1220). The number following the sequence indicates the position of the last amino-acid residue shown.

As mentioned in the introduction to this chapter, Exosite I is an important structure within the thrombin protein that is involved in substrate recognition. In the thrombin substrate sequences analysed in the Table above (Table 4), the Exosite I-binding sequence is located not more than 18 amino-acid residues down-stream from the end of the thrombin cleavage consensus sequence. Therefore, using the Clustal-W

program, the region following the potential thrombin-cleavage sequence (1222-TRGP-1225) in XO was analysed for the Exosite I-binding consensus (Rose and Di Cera, 2002) and actual Exosite I-binding sequences found in known thrombin substrates (see Table 5). Exosite I-binding sequences of coagulation factor V and VIII showed homology to the human XO sequence (residues 1240-1242 and 1236-1239, respectively) following the potential thrombin-cleavage site, and lie within 18 amino-acids from the cleavage site (see Figure 103).

Table 5. The Search for Potential Exosite I-Binding Sequences in Human XO

Exosite I-Binding Sequence	Origin	Homologous Sequence in XO Following TRGP?
ΦPΦ	Consensus	Not Found
VPD	Coagulation Factor II	Not Found
RPL	Coagulation Factor II	Not Found
FNL	Coagulation Factor V	FRV (see below, Figure 103)
HSL	Coagulation Factor V	Not Found
CPW	Coagulation Factor VII	Not Found
WDY	Coagulation Factor VIII	Not Found
IPE	Coagulation Factor VIII	IP-E (see below, Figure 103)
WPW	Coagulation Factor XI	Not Found
HLF	Coagulation Factor XIII	Not Found
WPF	Fibrinogen Aα	Not Found
PPP	Fibrinogen Bβ	Not Found
EPF	PAR1	Not Found
FPF	PAR3	Not Found
LDP	PAR4	Not Found
SPW	Protein C	Not Found
YSW	TAFI	Not Found

Using known Exosite I-binding sequences, potential Exosite I-binding sites in the human XO sequence, downstream of the putative thrombin-cleavage site (1222-TRGP-1225), were analysed. Where Φ = amino-acid residues F, H, P, or Y.

```
A          HumXO LHTRGPSTYKIPAFGSIPIEFRVSLLRDCPNKKAIYASKAV 1260
           FacV  --------------------FNL------------------
                                     *.:

B          HumXO     LHTRGPSTYKIPAFGSIPIEFRVSLLRDCPNKKAIYASKAV 1260
           FacVIII   ----------------IP-E---------------------
                                     ** *
```

Figure 103. The Alignment of Known Exosite I Sequences with Human XO

The Exosite I-binding sites of known thrombin substrates were aligned with the human XO amino-acid sequence. The Exosite I-binding sequence of coagulation factor V (FacV) and VIII (FacVIII) show homology to human XO. The number following the sequence indicates the position of the last residue shown.

If the proposed Exosite I and thrombin cleavage sequences in the XO amino-acid sequence are important for enzyme function, i.e. in its interaction with thrombin, then the sequences should be conserved between different species. To investigate this possibility amino-acid sequences (local to the potential thrombin cleavage site), from different species were aligned (see Figure 104). It is interesting to note that the potential thrombin-cleavage sequence (L-TRGP) and the Exosite I sequences (IP-E and FRV) show good homology between species.

```
Rat XOR          LHYSPEGSLHTRGPSTYKIPAFGSIPIEFRV 1241
Mouse XOR        LHYSPEGSLHTRGPSTYKIPAFGSIPIEFRV 1244
Human XOR        LHYSPEGSLHTRGPSTYKIPAFGSIPIEFRV 1242
Bovine XOR       LHYSPEGSLHTRGPSTYKIPAFGSIPTEFRV 1241
Chicken XOR      LRYSPEGNLYTRGPGMYKIPAFGDIPTEFYV 1270
                 *:*****.*:****. *******.** ** *
```

Figure 104. Alignment of Potential Thrombin Cleavage Sequences in XOR from Different Species

Using the Clustal-W program the region of human XOR containing potential thrombin cleavage and Exosite I-binding sites were aligned with XOR from different species. Highlighted (in bold) are the possible thrombin cleavage and Exosite I sites. The number following the sequence indicates the position of the last residue shown.

6.4.5.1.2 Where do the Potential Thrombin-Cleavage and Exosite I Sites Lie in XO?

Using the Clustal-W program, regions homologous to known thrombin Exosite I-binding and cleavage sequences have been discovered in human XO. However, for these sequences to have any functional significance they should be exposed on or near to the surface of the XO-enzyme, where thrombin could interact and cleave. The

crystal structure of monomeric bovine milk XO has been given at 2.5-Å resolution (Enroth *et al.*, 2000) and is deposited on the National Center for Biotechnology Information 3D-Structure Database. Using this sequence viewed with the Cn3D program version 4.1 (Chen *et al.*, 2003) the location of the potential Exosite I-binding and thrombin-cleavage sites were visualised. In Figure 105 the region containing the proposed thrombin cleavage and Exosite I-binding domains (1219-**LHTRGP**STYKIPAFGS**IPIEFRV**-1241) are highlighted in the bovine XO molecule. This 23 amino-acid sequence (see yellow strand) runs through the centre of the XO monomer. The potential thrombin cleavage site (1219-**LHTRGP**-1224) and Exosite I-binding sites (1235-**IPIE**-1238; 1239-**FRV**-1241) regions are shown in Figure 106 (see yellow strands). For clarity the putative thrombin-interacting sequences only, are shown in Figure 106B, demonstrating that potential thrombin-cleavage and Exosite I-binding sequences are found on opposing exposed faces of the XO enzyme.

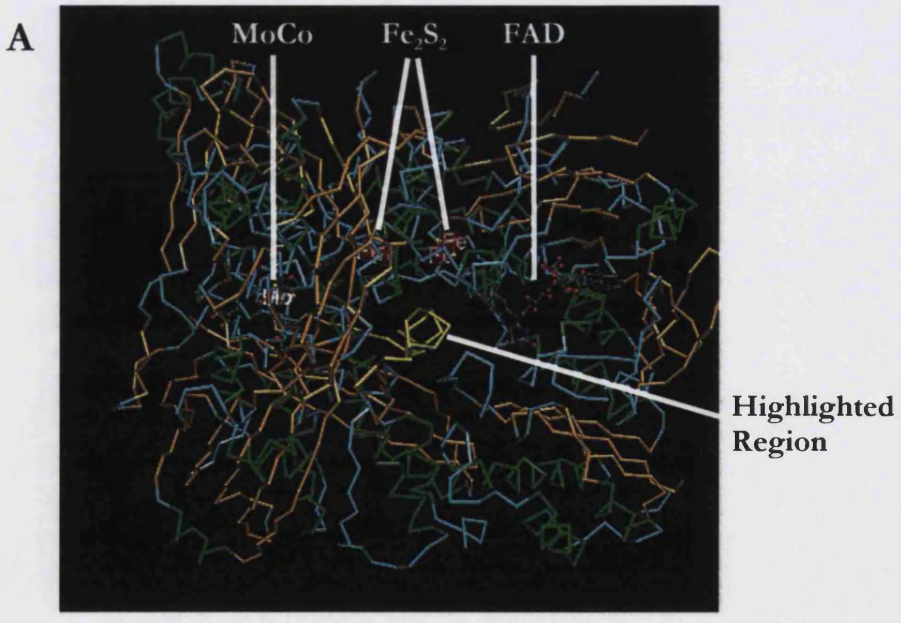

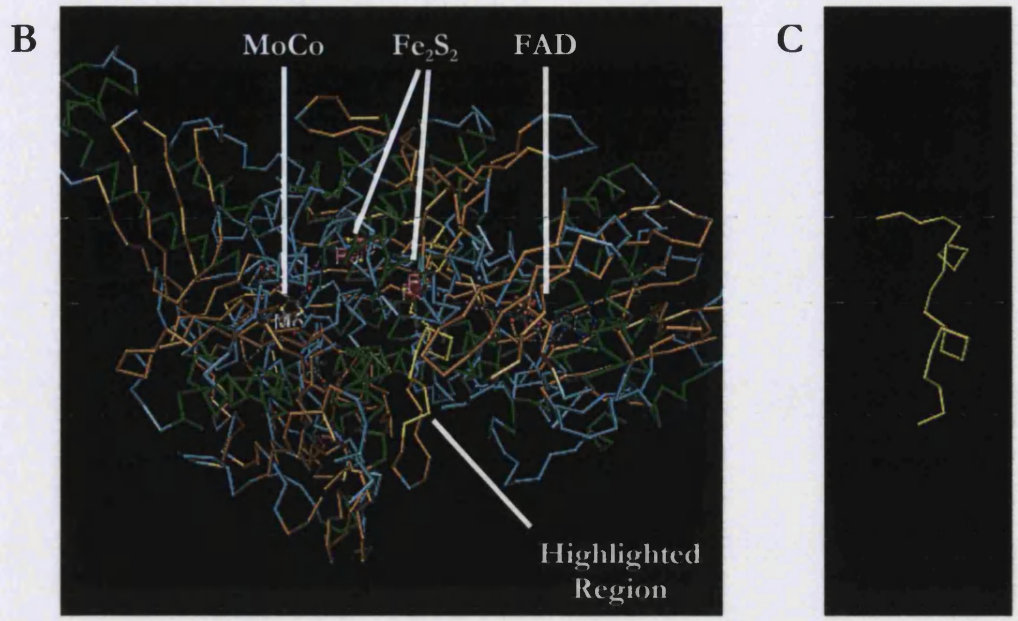

Figure 105. The Region Containing Potential Thrombin-Cleavage and Exosite I-Binding Sequences in the XO Monomer.

The region containing potential thrombin-interaction sequences in XO are highlighted in yellow. The sequence is shown in two XO-orientations (A and B) and for clarity the highlighted region alone is shown in C.

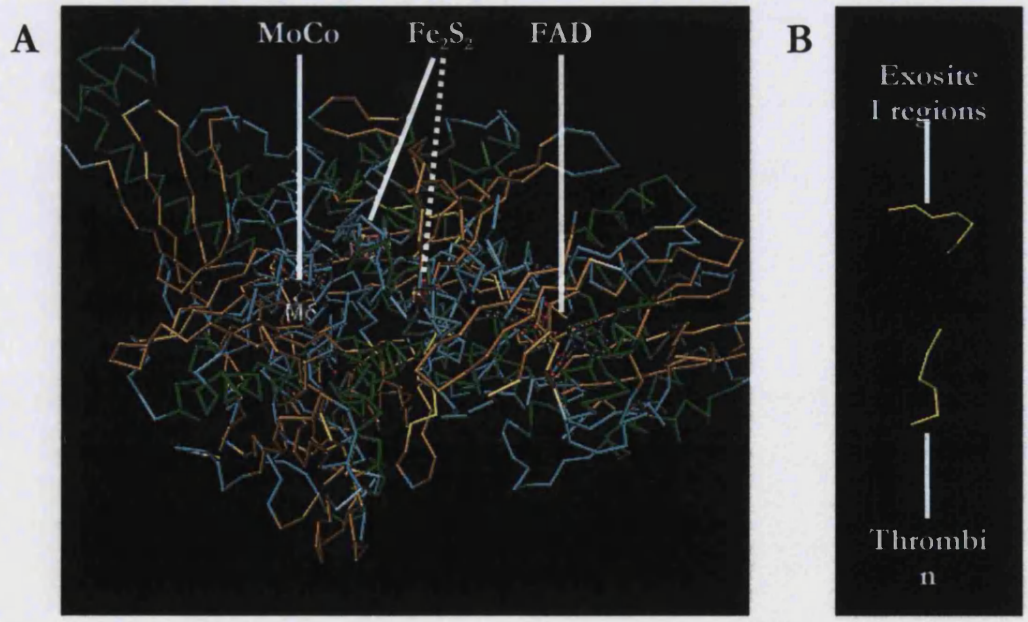

Figure 106. Potential Thrombin-Cleavage and Exosite I-Binding Sequences in the XO Monomer

A) Potential thrombin-interaction sequences in XO are highlighted in yellow and B) for clarity the highlighted sequences are shown alone.

6.4.5.2 Inhibition of Thrombin Activity and the Effect on XO-Activity

Natural inhibitors of thrombin include antithrombin III and heparin, and hirudin (Di Cera, 2003). The inhibitor hirudin is naturally found in leeches, particularly in the salivary secretion of the medicinal leech, *Hirudo medicinalis*. The secretion of hirudin has a distinct advantage to the leech, inhibiting blood coagulation and therefore maintaining blood flow from the site of attachment. Results from crystal structure analysis (Rydel *et al.*, 1990) show that hirudin binds to Exosite I, blocking thrombin-substrate interactions and therefore the coagulation cascade. The genes encoding natural hirudin have been cloned and recombinant variants have been assessed for thrombin inhibition (Lyer and Fareed, 1995). Recombinant hirudins have been developed as anticoagulation drugs, for example Lepirudin (British National Formulary 47, March 2004).

6.4.5.2.1 Hirudin Inhibition and Heat-Inactivation of Thrombin - Controls

To discover whether thrombin-proteolytic activity is required to alter XO activity, in this section the effect of inhibited thrombin (in the presence of hirudin or heat inhibition) will be investigated. Firstly as a control to demonstrate that the addition of hirudin inhibits thrombin activity, and to calculate the quantity of hirudin required to inhibit thrombin, the fibrinogen-turbidity assay was used. The assay described in the Methodology section (Section 6.3.4) was used and the following concentrations of hirudin were tested: 0.05, 0.25, 0.5, and 5U/ml. As a negative control 0.5% fibrinogen was incubated in the absence of thrombin and as a positive control in the presence of 0.5U/ml thrombin with no hirudin (see Figure 107A). The effect of hirudin on thrombin's activity is shown in Figure 107B, in the presence of an equal number of units of thrombin and hirudin, turbidity does not alter and therefore thrombin activity is inhibited.

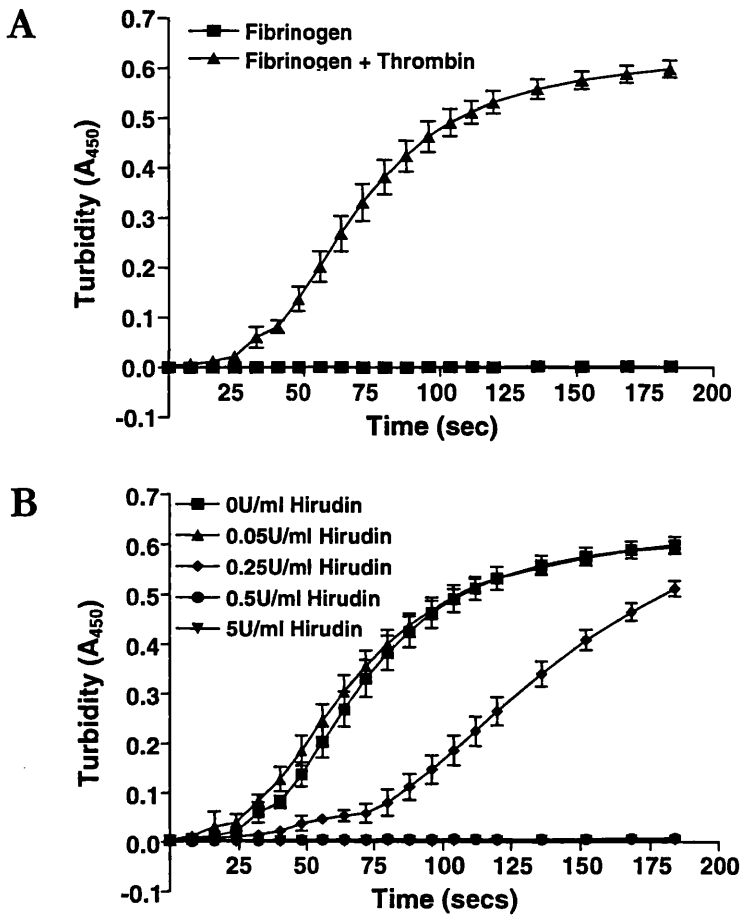

Figure 107. Hirudin Inhibition of Thrombin Activity - Control

The thrombin catalysed formation of fibrin was followed using the turbidity assay. A) Positive and negative controls for the assay were performed in the presence and absence of thrombin. B) A range of hirudin concentrations were analysed for their inhibitory effect on thrombin catalysed fibrin formation. Each condition was repeated in triplicate and error bars represent the SD.

In addition to the thrombin-inhibition method using hirudin, the catalytic activity of thrombin was also inhibited by heat-inactivation. As a control to show heat-inactivation is effective the turbidity assay was used. Unlike the hirudin inhibition experiment, 10U/ml thrombin was used in the incubation. Heat-inactivation was performed on the 1U/µl stock by heating to 99°C for 10mins. As can be seen in Figure 108, the heat-inactivation of thrombin inhibits the increase in A_{450} to a level that was seen in the negative control (in the absence of thrombin).

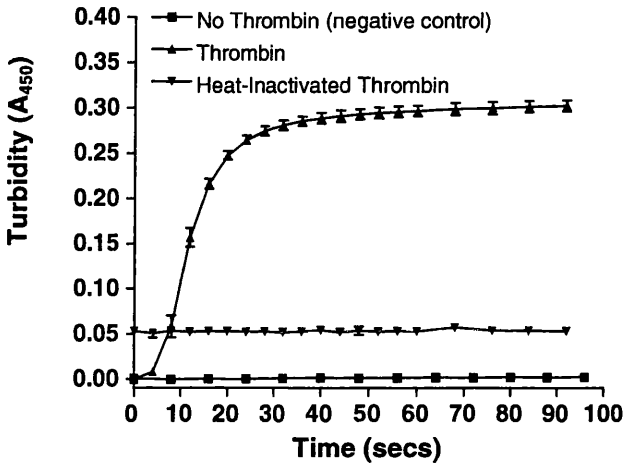

Figure 108. Heat-Inactivation of Thrombin Activity - Control

The thrombin catalysed formation of fibrin was followed using the turbidity assay. As positive and negative controls fibrinogen was incubated with and without thrombin, respectively, and heat-inactivated thrombin was also tested. Each condition was repeated in triplicate and error bars represent the SD.

6.4.5.2.2 The Effect of Inhibited Thrombin on Biozyme XO Activity

To discover whether the catalytic activity of thrombin was required to alter XO activity, thrombin was treated with one of the two established methods of inhibition and was added to XO-containing samples, and compared to controls. Preliminary experiments were carried out on purified XO (Biozyme) using a range of thrombin concentrations in the presence or absence of 5U/ml hirudin. In these experiments thrombin and hirudin were incubated at room temperature for approximately 30secs before being added to 100ng/ml Biozyme XO about 3mins before XO activity was assessed using the method of Beckman *et al.*, 1989. At the higher concentrations of thrombin tested (≥0.1U/ml) the addition of 5U/ml hirudin seems to reduce XO activity compared to thrombin alone (see Figure 109).

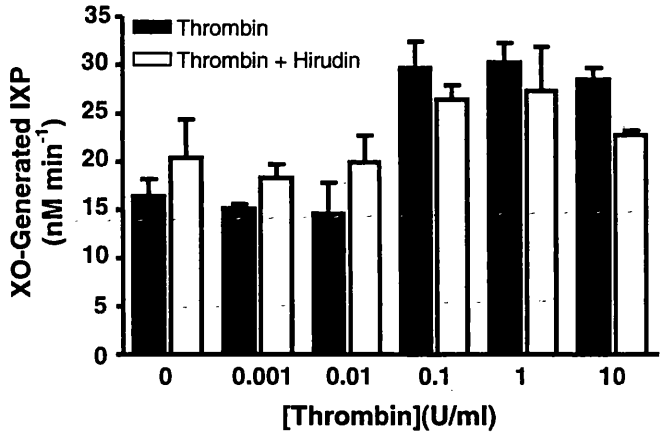

Figure 109. Hirudin-Inhibition of Thrombin and its Effect on XO Activity – A Preliminary Study

A range of concentrations of thrombin with or without 5U/ml hirudin were incubated with 100ng/ml Biozyme XO, and XO activity was measured. Results are from one experiment in triplicate and error bar = SD.

To assess the effect of heat-inactivated thrombin on pure XO compared to native thrombin, a range of thrombin concentrations with or without heat-inactivation were incubated with 100ng/ml Biozyme XO for approximately 3mins at room temperature before XO activity was measured. From these preliminary results (Figure 110) it appears that heat-inactivation of thrombin reduces the change in XO-activity seen with native thrombin concentrations ≥0.01U/ml.

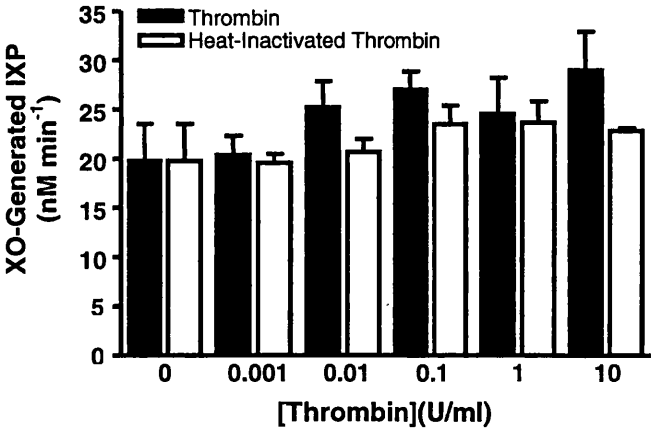

Figure 110. Heat-Inactivation of Thrombin and its Effect on XO Activity – A Preliminary Study

A range of concentrations of thrombin with or without heat-inactivation were incubated with 100ng/ml Biozyme XO, and XO activity was measured. Results are from one experiment in triplicate and error bar = SD.

To further investigate the effect of inhibited-thrombin on XO activity, and in particular compare the XO-activity in the presence of inhibited-thrombin with a non-thrombin treated sample (which was not compared in the preliminary studies), the experiment was repeated using thrombin concentrations where the greatest difference in activities were demonstrated in the preliminary study. Here 100ng/ml XO was incubated with 10U/ml thrombin (native, heat-inactivated at 99°C for 10mins, or incubated at room temperature with 10U/ml hirudin for 30secs) for about 3mins before XO-activity was measured. Data was analysed using one-way ANOVA with Bonferroni's post test (Figure 111). Compared to XO alone, the presence of thrombin increased XO-activity ($p<0.001$) as expected. The presence of inhibited thrombin does not significantly reduce XO activity when compared to the XO + thrombin sample. However, compared to the XO alone control, the increase in XO activity seen in samples with thrombin is statistically less significant when hirudin is included (i.e. XO v's XO + Thrombin: $p<0.001$; XO v's XO + Thrombin + Hirudin: $p<0.01$), which may suggest some inhibition, but this was not apparent when compared to the heat-inactivated thrombin sample (i.e. XO v's XO + Thrombin: $p<0.001$; XO v's XO + Heat-inactivated Thrombin: $p<0.001$).

A

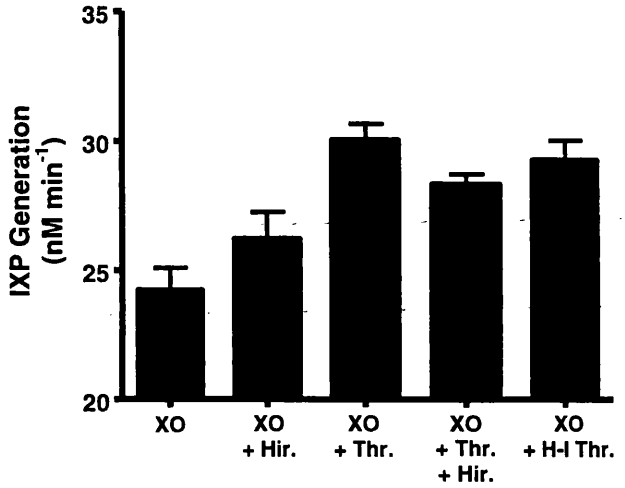

B

Bonferroni's Multiple Comparison Test	P-Value	Star Rating
XO v's XO + Hir.	P>0.05	ns
XO v's XO + Thr.	P<0.001	***
XO v's XO + Thr. + Hir.	P<0.01	**
XO v's XO + H-I Thr.	P<0.001	***
XO + Thr. v's XO + Thr. + Hir.	P>0.05	ns
XO + Thr. v's XO + H-I Thr.	P>0.05	ns

Figure 111. Inhibition of Thrombin and its Effect on XO-Activity

The effect of inhibited thrombin on XO activity was compared to that of native thrombin (A). In all cases thrombin final concentration was 10U/ml. Statistical results of various activity comparisons are shown in B. Results are from three experiments repeated in triplicate, therefore n=9. Error Bar = SEM. Where H-I Thr. = Heat-Inactivated Thrombin, Hir. = Hirudin, Thr. = Thrombin, and ns = not significant.

As results from the latter experiment were not conclusive the procedure was repeated, however a final concentration of 1U/ml thrombin was used in the relevant samples. The concentration of hirudin remained at 10U/ml. Data was analysed using one-way ANOVA with Bonferroni's post test (see Figure 112). Compared to XO alone, the presence of thrombin increased XO-activity ($p<0.001$) as expected. But again, the presence of inhibited thrombin does not significantly reduce XO activity when compared to the XO + thrombin sample. However as before, compared to the XO alone control, the increase in XO activity seen in samples with thrombin is statistically less significant when hirudin is included (i.e. XO v's XO + Thrombin: $p<0.001$; XO v's XO + Thrombin + Hirudin: $p<0.05$), which may suggest some inhibition, and this

was also apparent when compared to the heat-inactivated thrombin sample (i.e. XO v's XO + Thrombin: $p<0.001$; XO v's XO + Heat-inactivated Thrombin: $p<0.01$).

A

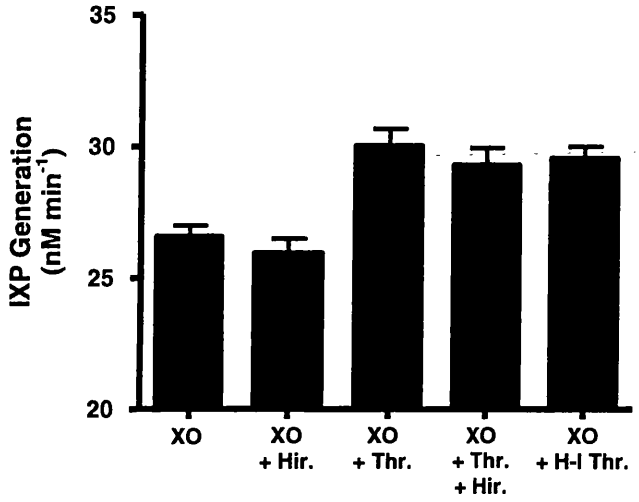

B

Bonferroni's Multiple Comparison Test	P-Value	Star Rating
XO v's XO + Hir.	P>0.05	ns
XO v's XO + Thr.	P<0.001	***
XO v's XO + Thr. + Hir.	P<0.05	*
XO v's XO + H-I Thr.	P<0.01	**
XO + Thr. v's XO + Thr. + Hir.	P>0.05	ns
XO + Thr. v's XO + H-I Thr.	P>0.05	ns

Figure 112. Inhibition of Thrombin and its Effect on XO-Activity - Repeat

The effect of inhibited thrombin on XO activity was compared to that of native thrombin (A). In all cases thrombin final concentration was 1U/ml. Statistical results of various activity comparisons are shown in B. Results are from three experiments repeated in triplicate, therefore n=9. Error Bar = SEM. Where H-I Thr. = Heat-Inactivated Thrombin, Hir. = Hirudin, Thr. = Thrombin, and ns = not significant.

6.4.5.2.3 The Effect of Inhibited Thrombin on XO Activity in Milk

The thrombin-inhibition experiments performed using purified-XO were repeated investigating the effect on milk-XO activity. Here 68μg/ml milk protein was incubated with 10U/ml thrombin (native, heat-inactivated at 99°C for 10mins, or incubated at room temperature with 10U/ml hirudin for 30secs) for about 3mins before XO-activity was measured. Data was analysed using one-way ANOVA with Bonferroni's post test (see Figure 113). Compared to milk alone, the presence of

thrombin increased milk-XO activity ($p<0.05$) as expected. The presence of inhibited thrombin does not significantly reduce milk-XO activity when compared to the milk + native thrombin sample. Unlike the results seen using purified XO, the increase in milk-XO activity in the presence of inhibited-thrombin is not statistically less than the increase seen with native thrombin. (Milk v's Milk + Thrombin: $p<0.05$; Milk v's Milk + Thrombin + Hirudin: $p<0.05$). In fact in the presence of heat-inactivated thrombin, the increase in milk-XO activity compared to that induced by native thrombin is greater (Milk v's Milk + Thrombin: $p<0.05$; Milk v's Milk + Heat-Inactivated Thrombin $p<0.001$).

A

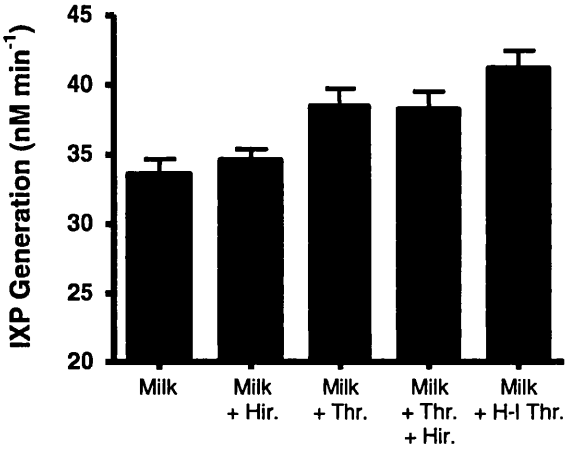

B

Bonferroni's Multiple Comparison Test	P-Value	Star Rating
Milk v's Milk + Hir.	P>0.05	ns
Milk v's Milk + Thr.	P<0.05	*
Milk v's Milk + Thr. + Hir.	P<0.05	*
Milk v's Milk + H-I Thr.	P<0.001	***
Milk + Thr. v's Milk + Thr. + Hir.	P>0.05	ns
Milk + Thr. v's Milk + H-I Thr.	P>0.05	ns

Figure 113. Inhibition of Thrombin and its Effect on Milk XO-Activity

The effect of inhibited thrombin on milk-XO activity was compared to that of native thrombin (A). In all cases thrombin final concentration was 10U/ml. Statistical results of various activity comparisons are shown in B. Results are from three experiments repeated in triplicate, therefore n=9. Error Bar = SEM. Where H-I Thr. = Heat-Inactivated Thrombin, Hir. = Hirudin, ns = not significant, Thr. = Thrombin.

6.4.5.3 Does Thrombin have an Antioxidant Effect and Therefore Increase XO Activity?

An interesting feature of the XO enzyme is that the generation of RONS may regulate enzyme function. A negative feedback process, known as suicide inactivation, was described after it was discovered that RONS derived from XO can inhibit the enzyme. Early studies describe that XO-generated ROS, in particular $O_2^{\cdot-}$ or H_2O_2 reduce enzyme activity (Lynch and Fridovich, 1979; Terada *et al.*, 1988), and that H_2O_2 is likely to affect the MoCo in the inhibitory process (Linder *et al.*, 2003). Also the addition of $ONOO^-$ but not $NO^{\cdot}$ to XO inhibits enzyme activity (Lee *et al.*,2000), however during the generation of $NO^{\cdot}$ from inorganic nitrite it was demonstrated that XO inhibits itself (Godber *et al.*, 2001) likely through the formation of an enzyme-substrate/product complex that inhibits the MoCo by converting it to its desulpho form.

Therefore I hypothesised that if thrombin were to act as an antioxidant and "mop up" the ROS generated by XO, then the XO enzyme could be saved from suicide inhibition. Therefore a greater portion of the enzyme would remain active, which would account for the increase in activity seen in the presence of thrombin and therefore describe a role for thrombin in regulating XO activity. In the XO-activity assay system used in this thesis, ROS but not RNS are generated, therefore antioxidants that are known to act on ROS (see Introductory Chapters) were used in studies to attempt to emulate thrombin's effect on XO (i.e. a dose-dependent increase in XO-activity).

6.4.5.3.1 The Influence of Catalase and SOD on XO Activity

Firstly, the influence of catalase on XO activity was measured. In these experiments the protocol used to investigate the effect of thrombin on XO activity was repeated, i.e. the antioxidant(s) were incubated with 100ng/ml XO for approximately 3mins before activity was measured. Using the Beckman *et al.*, 1989 assay, activity was recorded over a 1min period and rates of IXP generation were calculated as previously described. A dose-response of catalase was tested incorporating effective

concentrations that have been used by other researchers [e.g. 250U/ml catalase, with 10mU/ml XO (~10μg/ml Biozyme XO) and 1mM hypoxanthine, Murrell *et al.*, 1990; and 200U/ml catalase with 10mU/ml XO, Bonini *et al.*, 2004]. The addition of catalase has no effect on XO activity (Figure 114C). As the IXP-based assay was used for activity measurements the pH of working concentration catalase stocks was measured as a control (Figure 114A), also the activity of samples without XO and catalase (PBS) or without XO (Catalase, 500U/ml) were measured as negative controls (see Figure 114B).

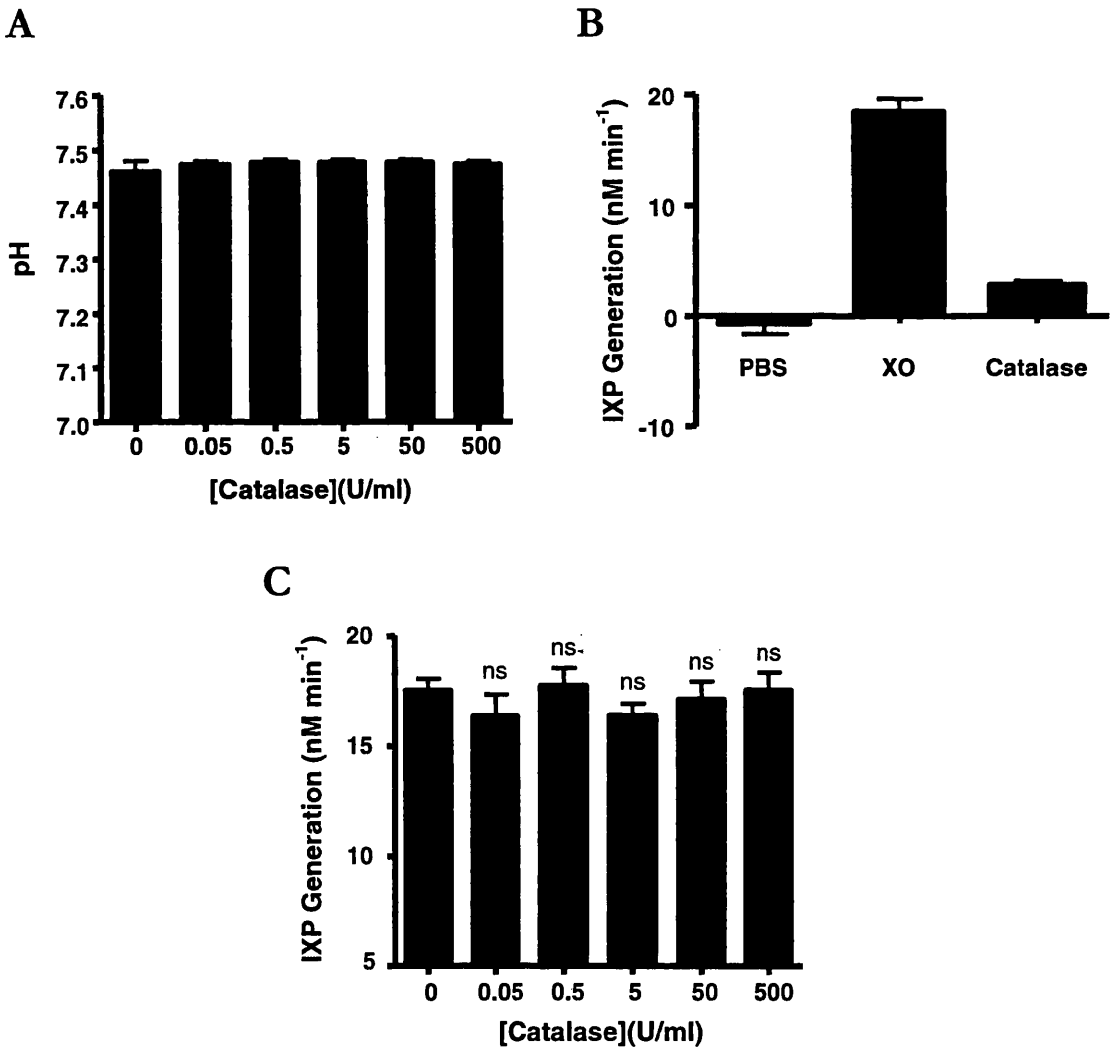

Figure 114. The Effect of Catalase on XO-Activity

A log dilution of catalase was added to pure XO and enzyme activity was measured using the pterin-based assay (C). Results are from three experiments repeated in triplicate, therefore n=9. Error Bar = SEM. Statistical analyses were performed using One-Way ANOVA with Dunnett's post test (ns =

not significant (P>0.05). As controls, the pH of the catalase working concentrations were measured (A) and activity was measured in the absence of XO and catalase (bar labelled PBS) or XO (bar labelled catalase) (B) (in A and B results are from one experiment in triplicate, therefore n=3, and error bar = SD.

The experiments performed using catalase were repeated but in the presence of SOD. Again a log dilution of antioxidant was tested, and the quantity of SOD to include was calculated from the Cytochrome *c*-based $O_2^{\cdot -}$ assay. Cytochrome *c* reduction by $O_2^{\cdot -}$ generated from 1mU/ml XO is completely inhibited using 50U/ml SOD. 1mU/ml XO = ~1μg/ml XO, which is approximately ten times more XO than is used in the pterin-based XO assay. Therefore using ≥50U/ml SOD will easily dismutate $O_2^{\cdot -}$ generated in this assay. The addition of SOD has an inhibitory effect on XO activity (Figure 115C). Once more, as the IXP-based assay was used for activity measurements the pH of working concentration SOD stocks was measured as a control (Figure 115A), also the activity of samples without XO and SOD (PBS) or without XO (SOD, 100U/ml) were measured as negative controls (see Figure 115B).

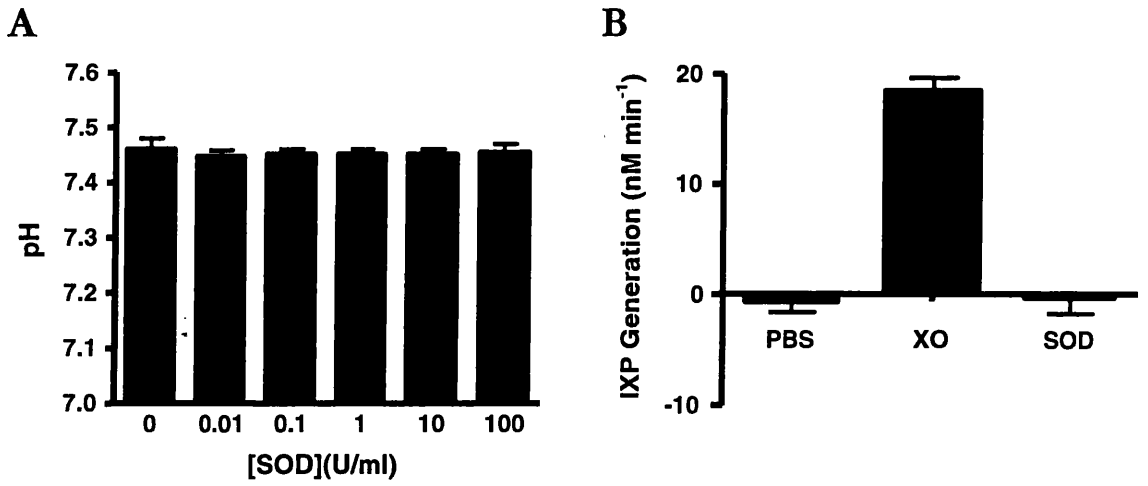

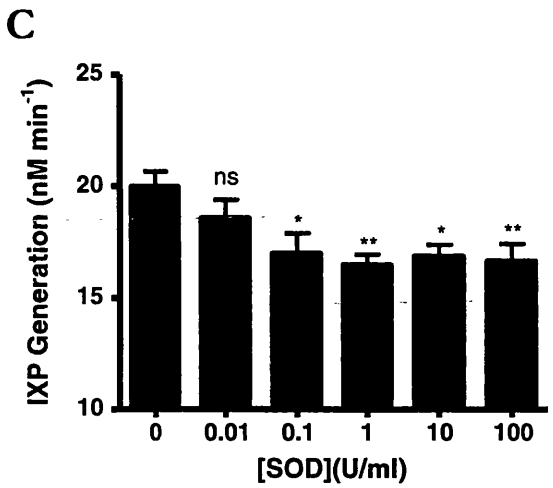

Figure 115. The Effect of SOD on XO-Activity

A log dilution of SOD was added to pure XO and enzyme activity was measured using the IXP-based assay (C). Results are from three experiments repeated in triplicate, therefore n=9. Error Bar = SEM. Statistical analyses were performed using One-Way ANOVA with Dunnett's post test (ns = not significant (P>0.05). As controls, the pH of the SOD working concentrations were measured (A) and activity was measured in the absence of XO and SOD (bar labelled PBS) or XO (bar labelled SOD) (B) (in A and B results are from one experiment in triplicate, therefore n=3, and error bar = SD.

The effect of the combination of catalase and SOD on XO activity was also tested using the same protocol as described. Using a ratio of 5 parts catalase to one part SOD (Figure 116A) it is evident that inhibition of XO occurs, however compared to SOD alone (Figure 115) the inhibition is less. But if a high level of catalase (200U/ml) is present with a range of SOD concentrations then no inhibition or increase in XO activity occurs (Figure 116B).

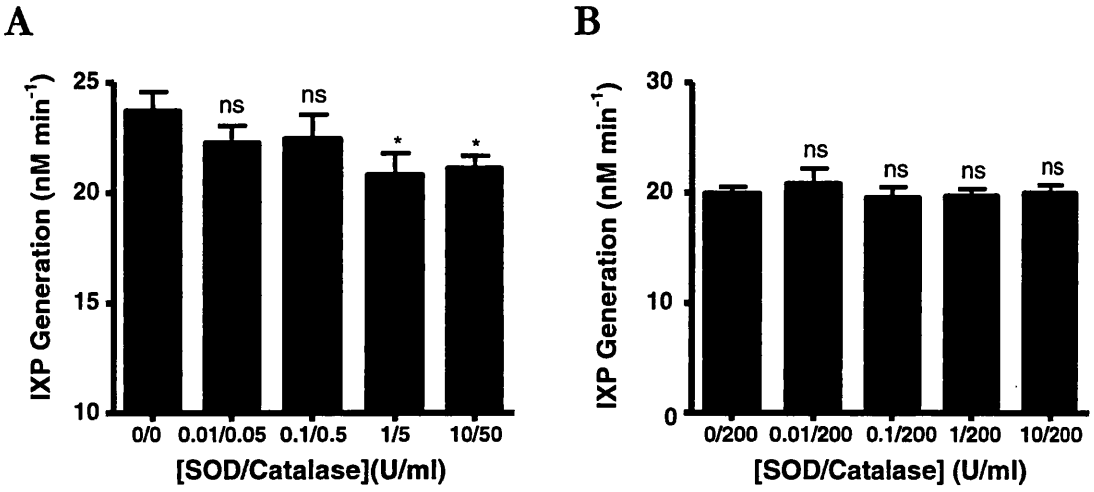

Figure 116. The Effect of SOD and Catalase on XO Activity

A log dilution of SOD in combination with a five times greater concentration of catalase was added to pure XO and enzyme activity was measured using the IXP-based assay (A). This process was repeated with an invariable catalase concentration of 200U/ml (B). Results are from three experiments repeated in triplicate, therefore n=9. Error Bar = SEM. Statistical analyses were performed using One-Way ANOVA with Dunnett's post test (* = $p<0.05$, ns = not significant ($P>0.05$).

6.4.5.3.2 The Influence of Ascorbic Acid on XO Activity

Using the antioxidants SOD and catalase it was not possible to emulate the effect thrombin has on XO activity, therefore another commonly used antioxidant was tested. Using the same protocol described to investigate the effect of thrombin, SOD, and catalase on XO, XO activity was measured in the presence of ascorbic acid. Ascorbic acid was prepared in PBS, however it was important to adjust the pH of stocks to ~7.3 using 1M NaOH, as the acidic solution would likely effect the IXP-based XO assay (Beckman *et al.*, 1989). A log dilution of ascorbic acid was added to XO and activity was calculated over a minute initial reaction period. As a positive control for an increase in activity, 10U/ml thrombin was added to XO (Figure 117 Thr.), and as a negative control activity was measured in the absence of XO (Figure 117 PBS). The addition of ascorbic acid did not increase XO activity as seen with thrombin, instead ascorbic acid inhibited XO activity in a dose-dependent manner (Figure 117).

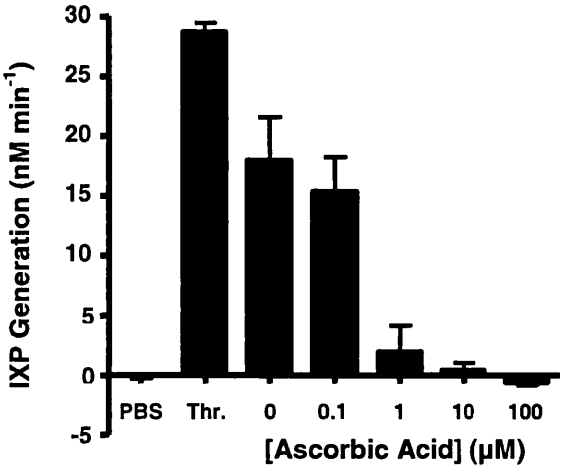

Figure 117. The Effect of Ascorbic Acid on XO Activity in the IXP-Based Assay

A log dilution of ascorbic acid was added to XO and activity was measured using the IXP-based XO assay. As controls XO activity was measured after ~3min incubation with 10U/ml thrombin (Thr.) or in the absence of XO (PBS). Results are from one experiment performed in triplicate, therefore n=3, and error bar = SD.

The effect ascorbic acid has on XO activity was confirmed using the uric acid-based assay (Figure 118), previously described observing the effect of thrombin earlier in this chapter. Comparing the two experiments the inhibitory profile of ascorbic acid was very similar, any differences (especially between the 1μM ascorbic acid samples) can be explained because of differences in XO quantities and substrate concentrations in the two assay protocol.

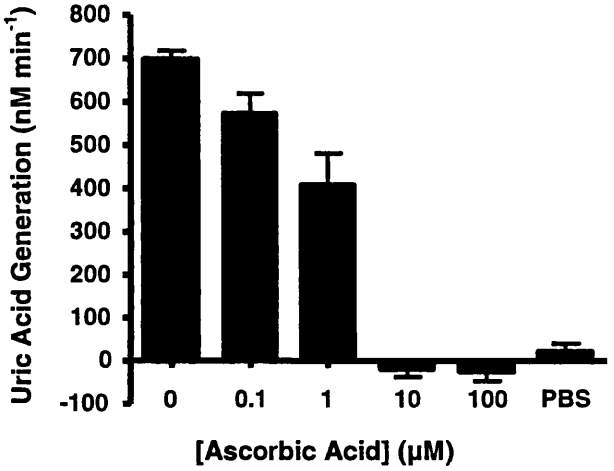

Figure 118. The Effect of Ascorbic Acid on XO Activity in the Uric Acid-Based Assay

A log dilution of ascorbic acid was added to XO and activity was measured using the uric acid-based XO assay. As a control, activity was measured in the absence of XO (PBS). Results are from one experiment performed in triplicate, therefore n=3, and error bar = SD.

To further characterise the effect of ascorbic acid, an effective inhibitory dose of ascorbic acid (10μM) was added during the measurement of XO activity in the IXP-based assay (Figure 119A). It is clear that inhibition occurs following the addition of ascorbic acid and that activity rates significantly drop (Figure 119B). It is interesting to note that addition of the known inhibitor allopurinol at the same concentration (10μM) has similar effect as shown here with ascorbic acid (see Chapter 4: Assessment of Methods for the Measurement of Xanthine Oxidoreductase, Figure 61). Although a control without the addition of ascorbic acid is not shown in Figure

119 the initial XO activity rate is maintained for at least 400secs without the addition of an inhibitor (as shown in see Chapter 4: Assessment of Methods for the Measurement of Xanthine Oxidoreductase, Figure 61).

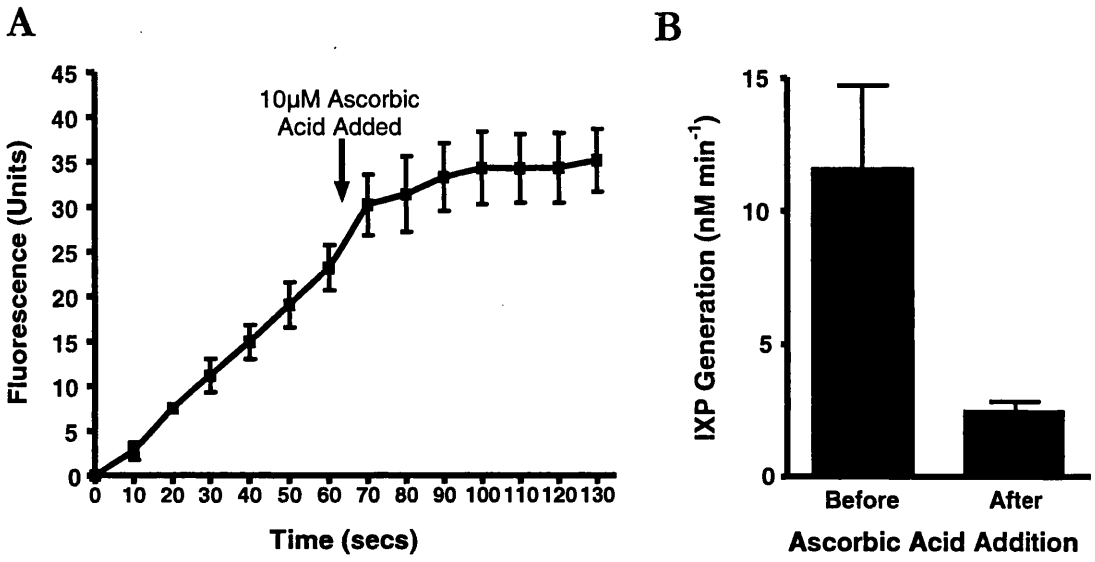

Figure 119. The Effect of Ascorbic Acid on XO Activity During a Time Course Measurement

An effective inhibitory dose of ascorbic acid (10μM) was added to XO during activity measurement in the IXP-based assay. Raw data is given in A and the activities before and after the addition are shown in B. Results are from a single experiment, n = 4, and error bar = SD.

In an attempt to gain an insight into how ascorbic acid may function as an inhibitor of XO the chemical structure of ascorbic acid was compared to that of known substrates and inhibitors (Figure 120). Known substrates (xanthine and pterin) and inhibitors (allopurinol) share a common structure, a six-membered ring containing two nitrogen atoms divided by a single carbon atom, however this structure is not seen in ascorbic acid.

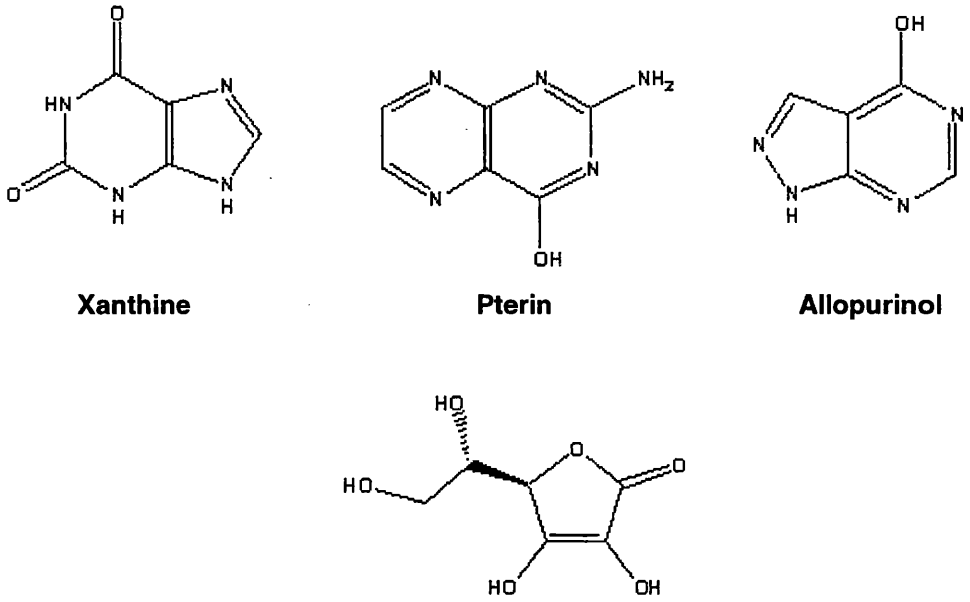

Xanthine **Pterin** **Allopurinol**

Ascorbic Acid

Figure 120. A Comparison of XO Substrate and Inhibitor Chemical Structures with Ascorbic Acid

The chemical structures if xanthine, pterin, allopurinol, and ascorbic acid are given.

6.5 Discussion

6.5.1 The Effect of Thrombin Dose-Response and Incubation Time

In the previous results chapter, the discovery that thrombin alters XO activity in a dose-dependent manner was made. This is a novel finding and warranted further investigation into the processes involved. Initial studies in this chapter replicated the limited study shown in the last chapter and confirmed the finding that thrombin increases purified XO activity in a dose-dependent manner (Figure 92). The presence of thrombin alone does not increase IXP generation (Figure 94B), therefore only changes in XO activity are being measured. To verify the thrombin dose-response finding and remove the possibility that results were method-dependent, the dose-response studies were repeated using the uric acid-based protocol (Figure 94). The same dose-dependent increase in activity was observed. It was interesting to discover that the increased activity seen in the presence of thrombin is not instantaneous. When incubating XO with a fixed amount of thrombin (1U/ml) for different time periods it was discovered that a maximal increase in activity occurs between 60-180secs incubation (Figure 95). Therefore suggesting that an "XO-activation process" takes place in the presence of thrombin.

6.5.2 ROS Generation by XO in the Presence of Thrombin

In enzyme kinetic studies, compared to XO alone, the presence of thrombin increases both the V_{max} and K_m of the enzyme (Figure 93), meaning there was a greater turn-over of substrate and therefore greater XO activity in the presence of thrombin. As electron-donating substrate (pterin or xanthine in these studies) turn-over is increased in the presence of thrombin, one would predict that the generation of ROS by the enzyme would increase equally (i.e. the electrons being donated to the enzyme must be passed to an acceptor substrate for donating substrate to continue being consumed, and as the electron accepting substrate in the system being used is O_2 then ROS generation should increase). However, studies recording the generation of $O_2^{\cdot -}$ by XO in the presence and absence of thrombin were not conclusive. The presence

of 0.1 and 10U/ml thrombin consistently increased the generation of $O_2^{\cdot -}$, however statistical analysis did not demonstrate this increase to be significant (Figure 96). It could be that the assay is not sensitive enough to detect the change in $O_2^{\cdot -}$ generation between treatments, it is worth pointing out that the cytochrome *c* assay requires ten times more XO compared to the IXP-based assay, and therefore the effect of thrombin may not be so pronounced in the assay for $O_2^{\cdot -}$. However, compared to the cytochrome *c* assay a similar concentration of enzyme is used in the uric acid-based assay, where a measurable change in XO activity is seen when thrombin is present (Figure 94). Another explanation lies in the ROS-generation profile of XO. As described in the introductory chapters, fully reduced XO can generate two H_2O_2 and two $O_2^{\cdot -}$ molecules (Porras *et al.*, 1981). Therefore the increase in electron donator (pterin or xanthine) turn-over in the presence of thrombin may result in the increased generation of H_2O_2 which would not be detected by the cytochrome *c* assay. To confirm whether there is an increase in H_2O_2 generation, the experiment would have to be repeated measuring H_2O_2 generation using, for example, a commercially available colourimetric H_2O_2-detection kit.

6.5.3 Antibacterial Properties of XO in the Presence of Thrombin

The antibacterial properties of XO have long been known, and the generation of ROS are known to have this function. Therefore it was interesting to assess whether the increase in XO activity in the presence of thrombin had a functional role, i.e. increase the antibacterial properties of XO. As none of substances added to the E. coli culture alone inhibited growth (Figure 101B), then any alterations in the culture generation time were due XO activity and the generation of ROS. Further more, as thrombin alone did not inhibit the growth of E. coli then differences between samples with and without thrombin were due to altered XO activity. It was discovered that active XO had mild antibacterial properties but in the presence of thrombin the generation time increased significantly (Figure 101C), indicating that the increased XO-activity thrombin induces elevates the antibacterial properties of XO.

The effects of XO, with and without thrombin, were inhibited by allopurinol, supporting the role of active XO as the antibacterial agent. The implications of XO's antibacterial activity are discussed in more detail in the main discussion chapter. It was also interesting to note that by the end of the culture incubation time, all cultures reached approximately the same OD_{600} value (Figure 101A). This could be due to the selection of a resistant bacterial population or more likely, substrate runs out and remaining viable cells continue growing.

As an additional experiment it would be interesting to investigate the effect thrombin has on XO ROS-stimulated expression of P-selectin in the inflammatory process. As an initial step experiments by Takano *et al.*, 2002, investigating P-selectin up-regulation by XO-ROS using a cell-based ELISA, should be repeated with and without thrombin.

6.5.4 The Complex XO-Containing Samples

Comparisons were made between the effect of thrombin on purified-XO and XO contained within complex samples. Firstly, the activity of XO in shop bought bovine milk in thrombin dose-response treatment was similar to that seen with Biozyme XO (Figure 98). This is not unexpected as Biozyme XO is isolated from bovine milk. However, the incubation time required to achieve maximal increase in XO activity was longer in bovine milk compared to purified XO; even though ten times more thrombin was used in the milk studies. This could be due to reduced interactions between XO and thrombin in the more complex milk sample. Compared to both the purified and milk XO samples, the rat liver homogenate shows little increase in XO activity, with a significant increase in activity occurring only in the presence of 10U/ml thrombin (Figure 99). Although, an incubation time of only 30secs with 10U/ml thrombin was sufficient to significantly increase activity, a shorter period compared to the other XO-containing samples. The reason why the dose-response was less effective could be due to the complexity of the liver homogenate or can be accounted for by the presence of a thrombin inhibitor. The thrombin inhibitor

antithrombin III is expressed in the liver (Pallister, 1997) and would therefore be present in the homogenate, interaction with thrombin could decrease activity towards XO and account for the large dose of thrombin required to alter liver XO activity.

The rat serum XOR samples showed a good response to thrombin (an increase in activity in a dose-dependent manner) (Figure 100), with no sign of the inhibition seen with the liver homogenate (statistics were not applied to this data due to low *n* numbers). An interesting finding was made when comparing rat liver results with those from rat serum. In these two samples both XO and total XOR (XDH and XO combined) activities were measured. Rat serum XOR was mainly, if not entirely, in the XO form whereas liver is predominantly in the XDH form [which has previously been described (Della Corte and Stirpe, 1968; Stirpe and Della Corte, 1969)]. This finding reinforces previous data from studies suggesting circulating XOR is mainly in the XO form (Kooij *et al.*, 1994). In Kooij *et al.*, 1994 rat liver XDH incubated with rat plasma was rapidly converted to XO by an unknown factor. The implications of a predominant XO-circulating form are discussed in the main discussion. The results from the complex XO-containing samples reveal that thrombin alters the activity of all XO samples tested and not just the purified sample.

6.5.5 The REDOX Centres Involved in Thrombin Increased XO Activity

As described in the introductory chapters, XO possesses NADH oxidase activity. The process of NADH oxidation and subsequent ROS generation occurs at the FAD-containing moiety, i.e. the other redox centres are not involved in substrate binding for NADH oxidase activity to occur. Using this theory it is possible to discover whether the FAD-moiety is affected by treatments of XO. In this thesis the effect of thrombin on NADH-oxidase activity, and therefore on the FAD-moiety, was investigated. However the idea has been exploited in other published research, for example, Terada *et al.*, 2003 were investigating the inhibitory effect of oxygen and its

metabolites on XO activity. They discovered that increasing oxygen concentrations had no effect on XO NADH-oxidase activity however they abolished the conversion of xanthine to urate. Therefore suggesting the FAD-moiety is unaffected whereas the MoCo is a likely to be involved in the mechanism of inhibition. In this thesis a similar scenario has unfolded, the presence of thrombin increases substrate (xanthine and pterin) turn over at the MoCo, however thrombin has no effect on NADH-oxidase activity (Figure 97). Therefore thrombin is likely to be altering the enzyme in such a way that the environment at the MoCo is altered but the FAD-moiety is unchanged.

6.5.6 Could Thrombin Theoretically Cleave XO?

Thrombin is a serine protease that is known to cleave many proteins. To discover how thrombin is affecting XO activity initial studies investigated the possibility that thrombin could cleave XO. As described in introductory chapters, it is known that limited proteolytic cleavage of XO can result in structural alterations effecting the FAD-moiety and consequently substrate binding at this redox centre of XO (known as irreversible XDH-XO conversion). Potentially a similar process could occur with thrombin which effects substrate binding to the MoCo (results already discussed concluded that the FAD centre is not effected by thrombin).

Initial studies aimed to find consensus sequences within XO for thrombin recognition (the Exosite I sequence) and for cleavage as described in Rose and Di Cera., 2002. A potential thrombin-cleavage sequence was found that showed high homology to that of fibrinogen Aα chain (Table 4). This site contains a leucine residue found two amino-acids upstream from the start of the potential cleavage sequence, which also forms part of the consensus sequence and is found in this position in the thrombin substrates PAR1, 3, and 4, and coagulation factor V (Rose and Di Cera., 2002). Homology searches on the region immediately downstream of the potential cleavage site revealed two potential Exosite I binding sequences, homologous to those found in coagulation factor V and VIII (Table 5). The homologous sequences within the

human XO amino-acid chain are highlighted in the following sequence: 1242-LHYSPEGSLH**TRGP**STYKIPAFGS**IPIEFRV**-1272. The regions highlighted are likely to have an important function within the XO enzyme as they are highly conserved between XO-sequences from several species (Figure 104). The locations of the potential thrombin-interacting sequences were assessed using the published 3D crystal structure of an XO monomer (Figure 105 and Figure 106). Interestingly, the potential cleavage sequence within XO is found on a loop exposed on the enzyme surface, and therefore could theoretically interact with thrombin. This cleavage site forms part of a chain that runs through the centre of the XO monomer close to the redox centres of the enzyme. Therefore cleavage at this site could alter the structure of the enzyme effecting substrate binding to the MoCo. However, the location of the Exosite I-homologous sequence does not suit a role of thrombin recognition and cleavage of XO as it is found on the opposite face of the XO monomer. But this does not eliminate the possibility of an Exosite I-binding site being available to thrombin by virtue of the tertiary structure of the XO protein.

To discover whether XO is cleaved by thrombin, and if so, whether cleavage at the proposed sequence alters the amino-acid structure around the MoCo leading to increased substrate affinity, experiments such as those used in Enroth *et al.*, 2000 would have to be repeated. In these studies the crystal structure of XDH and XO were compared, with particular emphasis on the region surrounding the FAD-moiety. To show whether thrombin influences XO structure, the crystal structure of XO exposed to thrombin would have to be determined and compared to normal XO.

6.5.7 Is Proteolytic Activity of Thrombin Required to Alter XO Activity?

Sequence analysis and structural data presented suggest that thrombin could cleave XO. In an attempt to show this experimentally, the actions of inhibited thrombin were compared to normal thrombin. As controls to show that the thrombin-

inhibition processes were successful, the assay of fibrinogen-fibrin conversion was employed. These experiments demonstrated that thrombin is inhibited using an equal concentration (Units) of hirudin or by heating to 99°C for 5mins (Figure 107 and Figure 108). Initial dose-response experiments, looking at the effect of normal thrombin v's inhibited thrombin on XO activity looked promising. With both inhibition processes, at the higher thrombin concentrations, it appeared that XO activity was reduced in the presence of inhibited thrombin compared to normal thrombin (Figure 109 and Figure 110).

These initial studies were repeated using the higher concentrations of thrombin only (i.e. 1 and 10U/ml) with or without inhibition (10U/ml hirudin or 99°C for 5mins) (Figure 111 and Figure 112). Normal thrombin increased the activity of XO significantly but the presence of inhibited thrombin would not reduce activity levels back to that of XO alone. However, compared to normal thrombin, using inhibited thrombin the increase in XO activity decreased in statistical significance. Therefore indicating that inhibition of thrombin does alter its activity towards XO, however these results are not conclusive.

As further work, it would be interesting to test the effect of other thrombin-inhibitors such as antithrombin III and heparin. However care should be taken and relevant controls put in place as heparin binds to XO (Adachi *et al.*, 1993) and could therefore interfere with activity. To demonstrate whether or not the proposed thrombin-cleavage sequence in XO is cleaved by thrombin, then a mutated form of XO (an amino-acid substitution in the sequence L-TRGP) should be expressed and exposed to thrombin. If the increase in activity is not seen with the mutant then it is probable that this sequence is the target for thrombin cleavage.

6.5.8 Can Thrombin's Effect on XO be Reproduced by Antioxidants?

XO can be inactivated by either self-generated or exogenously derived ROS species (Terada *et al.*, 1988; Linder *et* al., 2003). Therefore the presence of antioxidants, such as catalase, SOD, and ascorbic acid are likely to be beneficial to enzyme function. I hypothesised that if the presence of antioxidants increased XO activity in comparison to their absence (similarly to the effect of adding thrombin), then maybe thrombin could function in this manner (as an antioxidant) and therefore explain the actions of thrombin on XO activity. However, analysing XO activity in the presence of log dilutions of antioxidants did not fit my hypothesis. The addition of catalase had no effect on XO activity (Figure 114), but in the presence of SOD XO activity was inhibited (Figure 115). With the combination of both SOD and catalase the inhibition of XO activity observed with SOD alone was abolished (Figure 116), but no increase in XO activity was seen. As described in the introductory chapters SOD functions to dismutate $O_2^{\cdot -}$ generating H_2O_2, and catalase functions in the degradation of H_2O_2 forming H_2O and O_2. Therefore the results from the experiments described above suggest that SOD and XO-generated H_2O_2 inhibits the enzyme. This finding agrees in part with results from Terada *et al.*, 1988, whereby the combination of SOD and catalase protect XO from ROS-mediated inhibition. However, their protocol differed from the one used in this thesis. In Terada *et al.*, 1988 XO was incubated with hypoxanthine for 30mins before assessment of activity, and the protective effects of antioxidants were assessed by their addition during the 30min incubation. They discovered that SOD or catalase alone do not fully protect enzyme activity but do improve activity compared to their absence, suggesting that $O_2^{\cdot -}$ inhibits the enzyme. As the assessment of activity was only over a one minute period (in this thesis) the effects of $O_2^{\cdot -}$ may not have been detected, however it is possible that H_2O_2 is inhibiting the enzyme in the system used in this thesis. To check this, exogenous H_2O_2 could be added to XO and changes in activity could be measured.

The antioxidant ascorbic acid was also tested against XO and inhibited the enzyme in a dose-dependant manner (Figure 117). The addition of 10μM ascorbic acid during the XO-assay has a very similar effect compared to allopurinol at the same concentration and shows good inhibition of the enzyme (Figure 119). How ascorbic acid effects XO is not known, but other enzymes are inhibited by ascorbic acid, for example tyrosine hydroxylase (Roskoski *et al.*, 1993). A comparison between the chemical structures of ascorbic acid, allopurinol, and the XO-substrates xanthine and pterin (Figure 120) revealed that ascorbic acid has no homologous structures and therefore is unlikely to inhibit XO by the same process as allopurinol, or bind in a manner similar to pterin and xanthine. To discover the mechanism of ascorbic acid inhibition of XO, kinetic studies should be performed to determine whether ascorbic acid is a competitive or non-competitive inhibitor, also the effect of ascorbic acid on the XO-NADH oxidase assay should be assessed and would give a clue as to which redox centre of XO is being inhibited.

The discovery that ascorbic acid inhibits XO is not novel. In 1952 Feigelson (Fiegelson, 1952) found that ascorbic acid inhibits XO activity in an assay based on the conversion of xanthine to uric acid. Results in the published paper agree with those in this thesis, however in the publication no attempt was made to look at the effect of the addition of ascorbic acid to active enzyme as shown in this thesis.

The inhibitory action of ascorbic acid on XO is an important point that is not acknowledged in the present literature. Although there are numerous examples of where authors have not recognised XO-inhibition by ascorbic acid only two papers will be given here as examples. Firstly, the potential of ascorbic acid to prevent the toxic effects of ROS on the rat lens was investigated using the xanthine oxidase/xanthine system (Varma *et al.*, 1986). Lenses were incubated in a medium containing XO and xanthine with or without ascorbic acid. Authors discovered that in the absence of ascorbic acid lenses were damaged, however in its presence lenses

escaped damage. Authors concluded that one of the functions of high levels of ascorbic acid in the aqueous humour is to protect the lens and surrounding tissue from ROS damage. However, their experiment is seriously flawed as the XO/xanthine system may not have been generating ROS in the presence of ascorbic acid as XO activity was probably inhibited. In a study of the failing heart in an animal model, Saavedra *et al.*, 2002 were assessing the effects of reducing ROS generation. The authors discovered that "ascorbate (1000mg) mimicked the beneficial energetic effects of allopurinol, increasing both contractility and efficiency, suggesting an antioxidant mechanism. Allopurinol had no additive effect beyond that of ascorbate" (Saavedra *et al.*, 2002). To claim that ascorbic acid was working by an antioxidant mechanism may be false, as the inhibition of ROS generation by XO may have occurred. This possibility is reinforced by their statement that allopurinol was no more effective than ascorbic acid, probably as both substances have the same function, i.e. inhibiting XO.

In conclusion the process by which thrombin increases XO activity is unlikely to be by an antioxidant-based mechanism, as the addition of known antioxidants do not reproduce the effects of thrombin (also there is no mention in the literature of thrombin acting as an antioxidant). It is possible that thrombin effects XO by a proteolytic process, however the failure to inhibit thrombin activity with hirudin may rule this out. The binding of thrombin to XO may occur and cause an allostric effect on enzyme activity rather than a direct cleavage of the protein.

Chapter 7. General Discussion – The Endothelial XOR Release Model and its Implications in Vascular Physiology and Pathology

7 General Discussion - The Endothelial XOR-Release Model and its Implications in Vascular Physiology and Pathology.

7.1 Results Chapter Summary

In order to investigate the hypothesis that the vascular endothelium can release XOR, HUVECs were chosen as an endothelial model. In Chapter 3 the cells isolated from the human umbilical cord vein by collagenase digestion were characterised. Using morphological and immunofluorescent techniques the cell type isolated was shown to be of endothelial origin and therefore was indeed the HUVEC. Also in this chapter the expression of the *xor* gene and protein in the endothelial model were shown using RT-PCR, Western blot, and immunofluorescent techniques. In HUVECs XOR is found diffusely within the cytoplasm and also in punctate structures that indicate a packaged form of the enzyme. The XOR enzyme is not found in Weibel-Palade bodies as co-localisation with vWf was not observed. In order to measure the hypothesised release of XOR from the vascular endothelial model a sensitive assay was required. In Chapter 4 a range of XOR-assay techniques were optimised for sensitivity and compared. Compared to the two assays based on $O_2^{\cdot -}$ generation (the in-gel assay and lucigenin-luminescence assay) and the uric acid assay, the fluorescence-based assay detecting the formation of IXP proved the most sensitive. In the extended time course, the generation of IXP was linear and therefore reaction-product could accumulate before fluorescence measurements were taken, thus making the assay more sensitive.

In Chapter 5, known endothelial cell protein secretion agonists were applied to HUVECs and the release of vWf was used as a positive control for endothelial activation. In the presence of both histamine and thrombin vWf was released in a dose-dependent manner, independent of cell death. It was shown that HUVECs could release XOR. Release of XOR was constitutive but could also be stimulated,

and in dose-response experiments "bell-shaped" release curves were observed. The release rate of XOR and vWf in histamine stimulated HUVECs differed, providing more evidence to suggest that these two proteins are not associated within the endothelium. XOR release from HUVECs can be stimulated by a rise in intracellular calcium and is reliant on microtubule function, as demonstrated in A23187 dose-response and colchicine-treatment experiments, respectively. As a control the direct effect of histamine and thrombin on purified XO was assessed. Histamine, in the concentrations used in the HUVEC dose-response experiments, did not affect XO activity, however thrombin caused a dose-dependent increase in enzyme activity.

In chapter 6 the unexpected discovery that thrombin alters XO activity was explored in more detail. Firstly, dose-response experiments were repeated on purified XO and confirmed findings from the preceding chapter. The dose-dependent effect of thrombin was also seen with milk and rat serum XO, but not with rat liver, and was confirmed using two different XO assays. The change in XO activity was not immediate, instead a short incubation time (minutes) was required for thrombin's effect on XO to be measured. Although thrombin increased XO electron-donating substrate turnover a statistically significant increase in the generation of $O_2^{\cdot -}$ by XO was not observed, however the presence of thrombin enhanced XO's antibacterial properties which could be due to increase H_2O_2 generation. The effect of thrombin on XO could be slightly reduced using known thrombin inhibitors, however results were not conclusive. Analysis of the XO amino-acid sequence and crystal structure revealed an accessible thrombin cleavage sequence homologous to that found in the fibrinogen Aα chain. Thus suggesting that thrombin could cleave XO, a process that could potentially alter enzyme confirmation and therefore activity.

7.2 The Consequences of XOR Release from the Vascular Endothelium – The Results in Context

7.2.1 A Pathological Role

Data presented in this thesis demonstrate that XOR is released by the vascular endothelium; within this section the potential roles for the circulating enzyme will be discussed. As mentioned in the introductory chapters, XOR has several pathogenic roles within the vasculature. In these disease states a rise in circulating enzyme has often been attributed to the pathogenic effects of XOR, for example in pancreatitis-dependent acute respiratory distress syndrome. As previously described (see Introduction chapters) a rise in circulating XO in patients with pancreatitis has been shown to instigate a secondary inflammatory event at the lung that can lead to ARDS. Until now the source of circulating XO responsible for this life threatening disease could not be explained. However data from this thesis suggests that inflammatory mediators in the pancreas could stimulate the release of XO from the local vascular endothelium, thus accounting for the increase in plasma enzyme levels.

Similarly patients with burns often suffer secondary complications such as ARDS (Bhatia and Moochhala, 2004). In animal models, plasma XO levels are shown to increase following thermal injury (Friedl *et al.*, 1989), and as in pancreatitis-dependent ARDS circulating XO could link burns with secondary inflammatory complications. Interestingly, in animal studies, the levels of circulating XO correlate with levels of histamine. Approximately 15mins following thermal injury, plasma histamine levels peak at about 1.4μM which corresponds to a peak in plasma XO (Friedl *et al.*, 1989). Data from this thesis fit this observation perfectly, firstly dose-response experiments have demonstrated that histamine stimulates the release of XOR from endothelial cells, and a concentration of 1μM histamine was shown to cause maximal release. Therefore raising the possibility that following thermal injury an increase in plasma histamine levels could stimulate the release of XOR from the endothelium, thus accounting for the increase in circulating enzyme in this pathology.

In the pathologies that lead to secondary inflammation in the lung (for example pancreatitis and thermal injury) that may be linked by circulating XO, it is important to raise the question, why are the lungs affected and not other organs? As described in the introduction, the presence of O_2 is important for inflammation in the lung to occur (Granell *et al.*, 2004), and it was hypothesised that compared with other organs, only free-oxygen concentrations in the lung are able to support sufficient ROS-generation by XO to initiate an inflammatory event (Granell *et al.*, 2004). However, theoretically this is not the case. In the presence of xanthine, XO has half maximal $O_2^{\cdot-}$-generating activity at ~26μM O_2 (Millar, 2004). Physiological dissolved plasma oxygen concentrations range from 120-135μM on the arterial side to 55-70μM on the venous side. At these concentrations of oxygen, $O_2^{\cdot-}$-generating activity will be close to maximal in the venous side and maximal activity would be achieved on the arterial side (Millar, 2004). Therefore any potential increase in $[O_2]$ at the lung would not increase XO $O_2^{\cdot-}$-generating activity compared to other organs. Alternatively, one could speculate that as the lungs constitute the first vascular bed encountered by XO following its release, from the pancreas in pancreatitis for example, XO is more likely to concentrate at the lungs before reaching any other organ and thus causes inflammation at this site. The retention of XO at the vascular endothelium is possibly mediated by the endothelial cell-surface XO-receptor, the GAG (Adachi *et al.*, 1993), therefore through endothelial association the circulating XO form may concentrate at the lungs (as discussed in the example above) and therefore cause oxidative damage at sites distant from release.

It should be noted that the contribution of XO to other vascular pathologies (for example chronic heart failure and coronary heart disease) were discussed in the introductory chapters. It is conceivable that an increase in circulating XO could contribute to the aetiology of these disease states.

7.2.2 Beneficial Roles of Circulating XO?

As with many inflammatory mediators their primary function does not lie in pathological processes. Their role within the body is to exert a protective function, hence their retention through evolution. This also appears to be true for XOR. The expression of XOR is up-regulated by inflammatory mediators, suggesting a role within inflammation, and XOR generated RONS contribute to the inflammatory process (reviewed in the introductory chapters). Although the inflammatory roles of XOR are highlighted in pathological processes a protective antimicrobial function (due to XOR-RONS generating properties) for the enzyme is becoming clear. It has long been known that XOR has bactericidal properties in the presence of the substrate hypoxanthine (Green and Pauli, 1943). More recently the defensive properties of XOR were demonstrated in mice infected with *Salmonella typhimurium* (Umezawa *et al.*, 1997) where the generation of not just $O_2^{\cdot -}$ but also $ONOO^-$ were proposed to be antibacterial. Also, XO-derived ROS are important for phagocytic killing in macrophages (Takao *et al.*, 1996; Potoka *et al.*, 1998).

In the presence of nitrite, the ability of XOR to generate $ONOO^-$ (reviewed in the introductory chapters), a powerful bactericidal agent (Brunelli *et al.*, 1995), have lead researchers to speculate that the high quantities of XOR in milk may act to sterilise the gut. Indeed the generation of $NO^{\bullet}$ by human milk XOR is greatest in the first 5 weeks postpartum, where protection of the neonatal gut would be most beneficial (Stevens *et al.*, 2000). Although nitrite concentrations in the gut are not particularly high, the source of substrate for $ONOO^-$ generation by XOR may actually be derived from bacterial pathogens themselves (DeMoss and Hsu, 1991). XOR may attach to bacterial pathogens via GAG-like structures on the bacterial surface (Roberts, 1996) and therefore catalyse the generation of RONS in the bacterial microenvironment where nitrite is secreted and concentrations are adequate. Therefore the bacteria may initiate their own destruction.

There is a great deal of evidence to suggest an antimicrobial role for XOR and the enzyme potentially forms an important part of the innate immune system. Using data from this thesis a model for a protective function of XOR in the wound environment has been proposed (see Figure 121).

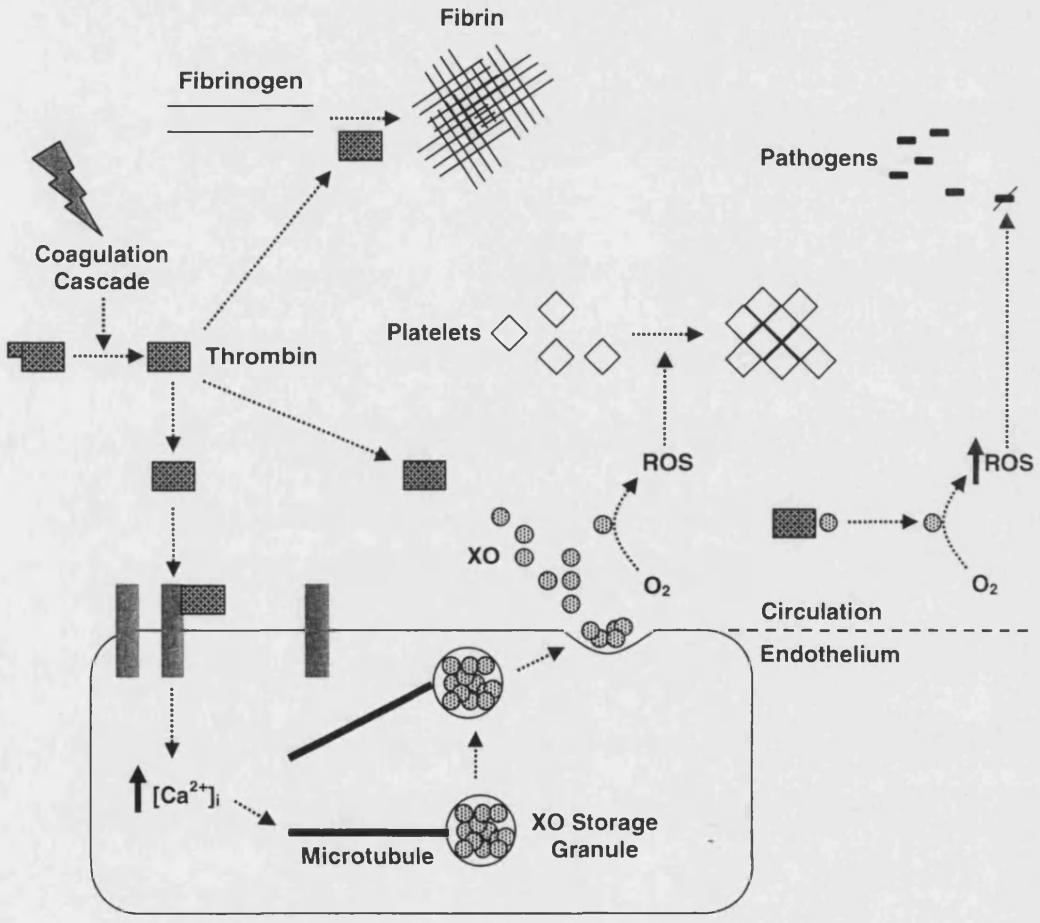

Figure 121. The Proposed Model of XO-Release from the Vascular Endothelium in a Wound

Rupture of blood vessels in a wound disrupts the endothelium and allows entry of pathogens. The exposure of sub-endothelial structures initiates the coagulation cascade resulting in the formation of active thrombin. In the vascular endothelial cell XO may be stored in granules (see Chapter 3). Thrombin stimulates the release of XO from the endothelium in a process that is likely to involve a rise in intracellular calcium and granule migration by functional microtubules (see Chapter 5). XO-generated ROS can contribute to platelet adhesion and therefore the formation of the primary haemostatic plug, which is reinforced by fibrin generated from fibrinogen in a process catalysed by thrombin. Interaction of thrombin with XO increases XO activity that may enhance the platelet adhesion process and augments XO's antibacterial properties (see Chapter 6), therefore providing protection to the wound. The generation of ROS by XO may up-regulate the expression of inflammatory cell-adhesion molecules on the endothelial surface and therefore initiate the inflammatory process (not shown in diagram).

7.2.3 Substrates and Inhibition of Circulating XO

For circulating XO to have a pathological or protective function electron donating substrates (such as hypoxanthine or xanthine) would have to be available to the enzyme for ROS-generation to occur. To reinforce the role of XO in ARDS, it has been demonstrated that plasma levels of hypoxanthine in ARDS patients increase to ~37.5μM in non-survivors and ~15.2μM in survivors, compared to control levels of 1.4μM (Quinlan *et al.*, 1997), therefore substrate is available. As already mentioned, XO can bind to the vascular cell surface via GAGs. Following binding it has been demonstrated that XO may be endocytosed and remain active (Houston *et al.*, 1999). Therefore XO could also have access to an intracellular pool of substrate, however it has not been demonstrated whether endocytosed XO remains active in the endosome or is released into the cytoplasm.

Inhibition of XO may become a standard treatment for certain disease states, XO-inhibition in pancreatitis-dependent ARDS, for example, is likely to be beneficial. As shown in animal models of pancreatitis, the administration of the specific XO-inhibitor oxypurinol is effective at reducing ARDS (Folch *et al.*, 1998; Folch *et al.*, 1999). Also, the use of allopurinol is likely to be beneficial in the treatment of other vascular pathologies, such as chronic heart failure and coronary heart disease (as described in the Introductory Chapters). Allopurinol is currently used as a treatment for gout (Rott and Agudelo, 2003) and therefore its administration for other pathologies is feasible. It was interesting to re-discover the inhibitory function of ascorbic acid over XO-activity in this thesis, and potentially ascorbic acid could be used as a XO-inhibitor in the pathologies mentioned. Evidence in support of this statement comes from a publication demonstrating that ascorbic acid supplementation reduces serum uric acid (the reaction product of XOR) concentrations (Huang *et al.*, 2005).

7.2.4 Indications from Xanthinuria

The potential roles of XOR within the body should be highlighted in xanthinuria, a hereditary disease that presents with inactive XOR enzyme. Two forms exist; Type I xanthinuria is caused by a mutation in the *xor* gene that can result in a truncated dysfunctional enzyme (Ichida *et al.*, 1997), while in Type II a mutation in the molybdenum cofactor sulphurase gene results in MoCo-deficiency and inactive XOR enzyme (Ichida *et al.*, 2001). One could hypothesis that if XOR-antibacterial function, for example, was vital in host defence then patients suffering xanthinuria would have recurrent infection. However, there are no reports of patients with xanthinuria suffering from abnormal bacterial or fungal infections. Either a suitable study has not been performed or there are other processes in the body that can compensate for lack of XOR activity. For example, the generation of $O_2^{\cdot -}$ by NADPH oxidase may suit this role. To reinforce this possibility, in the absence of functional NADPH oxidase, in chronic granulomatous disease (reviewed in Fang, 2004), recurrent bacterial and fungal infections occur. Therefore suggesting that NADPH oxidase is an important source of $O_2^{\cdot -}$ in host defence, which may compensate for the loss of XOR activity in xanthinuria. However the studies mentioned in the Beneficial Roles of Circulating XO section suggest XO does function as an antimicrobial agent and does function in various pathologies. Therefore, detailed studies in xanthinuria patients or animal models would be of great interest to investigate the antimicrobial and inflammatory roles of the XOR enzyme.

7.3 In Summary

In this thesis it was demonstrated that the vascular endothelium is a potential source of circulating XOR and therefore the hypothesis was achieved. XOR maybe be released from the vascular endothelium by stimulation with pro-inflammatory and pro-thrombotic mediators by a process independent of cell death. The mechanism can be stimulated by a rise in intracellular calcium and may require functional microtubules. XO activity increases in the presence of thrombin, possibly due to

proteolytic cleavage of XO. A protective role for XO was described using the wound environment as an example. The release process should be investigated in more detail, the effects of thrombin on XO studied in mutation experiments, and the role of XOR within the body explored in xanthinuria patients.

Appendix

8 Appendix I - Methology

8.1 Haematoxylin and Eosin Stain Protocol

Tissues sections mounted on slides were treated by submersion in the following solvents for the times indicated:

- Ice cold acetone : 1-5mins (Tissue Fixation)
- Tap water : 5mins (Rehydrate tissue)
- Harris Haematoxylin (prepared 1 part Haematoxylin : 3 parts water) : 5mins
- Tap water : 5mins
- Acid alcohol (1% HCl in IMS) : 1min with gentle agitation
- Tap water : 5mins
- Eosin : 0.5min
- Tap water : 5mins
- IMS : 1min
- IMS : 1min
- Xylene : 1min
- Xylene : 1min
- A coverslip was mounted onto the treated tissue sample with excess DePeX mounting medium.

8.2 SDS-PAGE, Western and Dot Blot Recipes

SDS-PAGE Resolving Gel (8%)

- 10.66mls dH_20
- 4.0mls 40% Acrylamide (Anachem. Bedfordshire, UK)
- 5.02mls 1.5M Tris/Base pH8.8 (Promega UK Ltd. Southampton, UK)
- 100µl 20% SDS (Sigma Aldrich Company Ltd. Dorset, UK)
- 200µl 10% Ammonium Persulphate (Sigma Aldrich Company Ltd. Dorset, UK)
- 15µl N, N, N′, N′-Tetra-methyl-ethylenediamine (TEMED) (Sigma Aldrich Company Ltd. Dorest, UK)

SDS-PAGE Stacking Gel (4%)

- 4.98mls dH_20
- 660µl 40% Acrylamide
- 840µl 1.0M Tris/Base pH6.8
- 33.4µl 20% SDS
- 66µl 10% Ammonium Persulphate
- 8µl TEMED

SDS-PAGE Running Buffer

- 14.4g Glycine (VWR International Ltd. Dorset, UK)
- 3.06g Tris/Base

- 1.0g SDS
- 1000mls dH_20 pH8.3

SDS-PAGE Sample Buffer

- 6.75mls dH_20
- 0.75mls 1M Tris/Base pH6.8
- 2.0g Sucrose (VWR International Ltd. Dorset, UK)
- 1mg Bromophenol Blue (Promega UK Ltd. Southampton, UK)
- 0.5mls 2-mercaptoethanol (Sigma Aldrich Company Ltd. Dorset, UK)

Western and Dot Blot Transfer Buffer

- see SDS-PAGE Running Buffer but made with 20% Methanol (VWR International Ltd. Dorset, UK)

Western and Dot Blot Washing Buffer

- 0.5% Tween 20 (Sigma Aldrich Company Ltd. Dorset, UK) in PBS

Western and Dot Blot Blocking Buffer

- 5% Marvel non-fat dried milk powder in Washing Buffer

8.3 Antibodies

8.3.1 Primary Antibodies

- Mouse Monoclonal Anti-Huamn β-tubulin Cy3-Conjugated (1mg/ml stock) (Sigma Aldrich Company Ltd. Dorest, UK).
- Mouse Monoclonal Anti-Human vWF (240µg/ml) (DAKO. Chambridgeshire, UK).
- Mouse Monoclonal Anti-Human Xanthine Oxidase/Aldehyde Oxidase (200µg/1ml) (NeoMarkers. CA, USA).
- Rabbit Polyclonal Anti-Human vWF (5.7mg/ml stock) (DAKO. Chambridgeshire, UK).
- Rabbit Polyclonal Anti-Bovine XO (10mg/ml stock) (Chemicon Europe Ltd. Hampsire, UK).
- Rabbit Polyclonal Anti-Bovine XO Peroxidase-Conjugated (10mg/ml stock) (Biodesign. ME, USA).
- Rabbit Polyclonal Anti-Bovine XO (10mg/ml stock) (Polysciences Inc. PA, USA).

8.3.2 Secondary Antibodies

- Donkey Anti-Rabbit IgG-fluorescein isothiocyanate (FITC) conjugated (400µg/ml stock) (Santa Cruz Biotechnology. CA, USA)
- Donkey Anti-Rabbit IgG-Rhodamone conjugated (400µg/ml stock) (Santa Cruz Biotechnology. CA, USA).
- Goat Anti-Rabbit Whole Antibody-Ultra Small Gold Conjugate (Aurion. Wageningen, The Netherlands).

- Goat Anti-Rabbit F(ab)^2-Ultra Small Gold Conjugate (Aurion. Wageningen, The Netherlands).
- Horse Anti-Mouse IgG-FITC conjugated (1mg/ml) (Vector Laboratories. CA. USA)
- Swine Anti-Rabbit IgG-Horse Radish Peroxidase (HRP) conjugated (1.3mg/ml stock) (DAKO. Chambridgeshire, UK).

8.4 Preparation of HUVECs for Electron Microscopy

Cell Seeding

- Dissociate P1 HUVECs using Cell Dissociation Solution.
- Seed ~1000 viable cells/capsule (15µl of 66000cell/ml ECGM).
- Fill reservoirs of multi-well plate with 200µl dH_2O.
- Incubate o/n at 37°C / 5% CO_2.

Note: In the following protocol the application of solutions are in 15µl volumes/capsule.

Fixation

- Wash 4 times in PBS.
- Fix with 4% Paraformaldehyde solution in PBS for 15mins at RT.
- Wash 4 x 10mins in 1% BSA/PBS pH8.2.

Quench Aldehyde Groups

- Residual aldehyde groups present after aldehyde fixation must be quenched using 50mM Glycine in PBS, incubate with cells for 5mins at RT.
- Wash 3 x 10mins in 1% BSA/PBS.

Permeablisation

- Incubate cells with 0.2% Triton X-100 in PBS for 10mins at RT.
- or with Saponin in PBS 0.1% for 10mins at RT.
- Wash 3 x 10mins in 1% BSA/PBS.

Note: For saponin treated cells add saponin to all solutions following the permeablisation step)

Blocking

- Incubate cells for 30mins at RT in 5% goat serum in 1% BSA/PBS +/- 0.1% Saponin (serum of species secondary antibody was raised).

Primary Antibody Application

- DAKO Rabbit Anti-Human vWf 150x dilution in blocking buffer, incubate for 1hr at RT.
- or Polysciences Rabbit Anti-Bovine XO 150x dilution in blocking buffer, incubate for 1hr at RT.

Wash Step

- Wash 4 x 10mins at R/T in 1%BSA/PBS +/- 0.1% Saponin.

Secondary Antibody Application

- Aurion Goat Anti-Rabbit Ultra Small Gold Conjugate (whole antibody used in Triton X-100 permabilised cells and $F(ab)^2$ for saponin permeabilised cells). 100x dilution in blocking buffer, incubate for 1.5-2hr R/T.

Wash Step

- Wash 4 x 10mins at R/T in 1%BSA/PBS +/- 0.1% Saponin.

Silver Enhancement

- Wash cells 10 x 5 mins in dH_2O (Cells must be rinsed thoroughly with dH_2O before the addition of silver enhancement reagents, see manufacturers instructions).
- Mix equal volumes of enhancer and initiator and apply to cells for 30mins at RT.

Note: After a certain time silver may precipitate spontaneously producing a background signal. This time is temperature dependent, at 24°C the solution will be stable for at ~35mins. If enhancement is needed beyond this time period remove old solution and apply a fresh solution to cells.

- Wash 5 x 5mins in dH_2O.

Uranyl Acetate Stain

- Apply a 0.1% solution of UA in distilled water to the cells for 5mins.
- Wash 2 x 5mins in dH_20.

Note: staining for this period will result in a light stain of cellular components that shouldn't interfere with the immuno-gold staining.

Imaging Buffer

- Aspirate and fill with QX-102 imaging buffer.
- Close the capsule for imaging using back scattered electron detection in a scanning electron microscope.

8.5 PCR

8.5.1 Primer sequences

GAPDH:
GAPDH-Forward 5' AAA GGG TCA TCA TCT CTG GC 3'
GAPDH-Reverse 5' TGA CAA AGT GGT CGT TGA GG 3'
Stock concentration = 7.5ρmoles/μl
Expected Product Size = 576 base pairs

Rat XOR:
XOR-Forward 5' CTG TCC ATC GAG ATC CCC TA 3'
XOR-Reverse 5' TCT CAG CCC TCA AGA CCA CT 3'
Stock concentration = 100ρmoles/ml
Expected Product Size = 288 base pairs

8.5.2 PCR Programmes

GAPDH:
Initial Denaturation: 5mins, 94°C

Denaturation:	45secs, 94°C	} 30 cycles
Annealing:	45secs, 55°C	
Extension:	45secs, 72°C	

Final Extension: 10mins, 72°C
Final Hold: 4°C

Rat XOR:
Initial Denaturation: 5mins, 94°C

Denaturation:	45secs, 94 °C	} 30 cycles
Annealing:	45secs, 58°C	
Extension:	60secs, 72°C	

Final Extension: 10mins, 72°C
Final Hold: 4°C

8.5.3 Agarose Gel Recipe

Tris-Borate (TBE) Buffer (5x):
54g Tris-Base
27.5g Boric Acid
2.92g EDTA

1000mls Milli-Q water
pH8

- Add 0.3g Agarose per 25mls 1x TBE buffer (heated until agarose dissolved).
- Cool under running cold water.
- Add 2µl 1mg/ml ethidium bromide per 25mls TBE buffer used.
- Pour gel into casting tank in fume hood and leave at room temperature until set.

8.6 In-Gel Assay XOR-Activity Detection Solution

Concentrations used in Özer *et al.*, 1998 are listed below. The concentrations of these solutions were optimised in experiments decribed in Section 4.4.2.

- 50mM Tris-HCl, pH7.6
- 500µM Xxanthine
- 250µM Nitroblue Tetrazolium

8.7 Preparation of Rat Liver and Plasma Samples

Female Lewis rats (Harlan-Olac. Lincolnshire, UK), weighing approximately 200g each, were fed with either:

i) 50mg/kg/d allopurinol suspended in 1% caroxymethylcellulose (Sigma Aldrich Company Ltd. Dorest, UK.) or,
ii) rat chow (ICN Biochemicals. Ohio, USA) supplemented with 0.7g sodium tungstate/kg.

After a period of three weeks animals were humanely killed by CO_2 exposure. From each animal 1ml of blood was collected in an eppendorf containing 100µl of 80mg/ml trisodium citrate, inverted twice, and centrifuged at 7152rpm for 3mins. Plasma was pipetted into a fresh eppendorf and was stored at -70°C before analysis. Livers were also isolated and were snap-frozen in liquid-N_2. Samples of rat liver were ground in liquid-N_2 and the resulting powder was suspended in 50mM potassium phosphate buffer (pH7.4), containing 0.1mM EDTA, 0.1mM PMSF, and 1µg/ml

pepstatin, leupeptin, antipain, and aprotinin (Sigma Aldrich Company Ltd. Dorest, UK). Suspensions were centrifuged at 13'000rpm for 10mins. The supernatant was collected in a fresh eppendorf and stored at -70°C before analysis.

8.8 Lysis Buffer

0.2% Triton X-100 in HBSS

+ 1μg/ml Antipain (Sigma Aldrich Company Ltd. Dorest, UK)

+ 1μg/ml Aprotinin (Sigma Aldrich Company Ltd. Dorest, UK)

+ 1μg/ml Leupeptin (Sigma Aldrich Company Ltd. Dorest, UK)

+ 1μg/ml Phenylmethylsulphonyl Floride (PMSF; Sigma Aldrich Company Ltd. Dorest, UK)

Chilled to 4°C before use.

References

9 References

Adachi, T., Fukushima, T., Usami, Y., & Hirano, K. (1993). Binding of human xanthine oxidase to sulphated glycosaminoglycans on the endothelial-cell surface. *The Biochemical Journal.* **289**, 523-527.

Alberts, B., Bray, D., Lewis, J., Raff, M., Roberts, K., & Watson, J.D. (1994). The cytoskeleton. In *Molecular Biology of the Cell* (Eds.Robertson, M., Adams, R., Cobert, S.M., & Goertzen, D). pp 787-861. Garland Publishing Inc. London, UK.

Al-Khalidi, U.A.S., & Chaglassian, T.H. (1965). The species distribution of xanthine oxidase. *Biochemical Journal.* **97**, 318-320.

Amaya, Y., Yamazaki, K-I., Sato, M., Noda, K., Nishino, T., & Nishino, T. (1990). Proteolytic conversion of xanthine dehydrogenase from the NAD-dependent type to the O_2-dependent type. **265**, 14170-14175.

Angermuller, S., Bruder, G., Volkl, A., Wesch, H., & Fahimi, H.D. (1987). Localisation of xanthine oxidase in crystalline cores of peroxisomes. A cytochemical and biochemical study. *European Journal of Cell Biology.* **45**, 137-144.

Anrather, J., Csizmadia, V., Soares, M.P., & Winkler, H. Regulation of NF-κB RelA phosphorylation and transcriptional activity by $p21^{ras}$ and protein kinase Cζ in primary endothelial cells. *The Journal of Biological Chemistry.* **274**, 13594-13603.

Archer, S.L., Huang, J.M.C., Hampl, V., Nelson, D.P., Shultz, P.J., & Weir, E.K. (1994). Nitric oxide and cGMP cause vasoreleaxation by activation of a charybdoxin-sensitive K channel by cGMP-dependent protein kinase. *PNAS.* **91**, 7583-7587.

Avis, P.G., Bergel, F. and Bray, R.C. (1956) Cellular constituents. The chemistry of xanthine oxidase. Part III. Estimates of co-factors and the catalytic activities of enzyme fractions from cow's milk. *Journal of Chemical Society.* 1219–1226.

Bacallao, R., Kiai, K., & Jesaitis, L. (1995). Guiding principles of specimen preservation. In *Handbook of Biological Confocal Microscopy.* (Ed. Pawley, J.B.) pp. 311-325. Plenum Press, New York, USA.

Bajzar, L., Manuel, R., & Nesheim, M.E. (1995). Purification and characterisation of TAFI, a thrombin-activatable fibrinolysis inhibitor. *The Journal of Biological Chemistry.* **270**, 14477-14484.

Battelli, M.G., Abbondanza, A., Musiani, S., Buonamici, L., Strocchi, P., Tazzari, P.L., Gramantieri, L., & Stirpe, F. (1999). Determination of xanthine oxidase in human

serum by a competitive enzyme-linked immunosorbent assay (ELISA). *Clinica Chimica Acta.* **281**, 147-158.

Battelli, M.G., Musiani, S., Valgimigli, M., Gramantieri, L., Tomassoni, F., Bolondi, L., & Stripe, F. (2001). Serum xanthine oxidase in human liver disease. *The American Journal of Gastroenterology.* **96**, 1194-1199.

Bayele, H.K., Murdock, P.J., Perry, D.J., & Pasi, K.J. (2002). Simple shifts in redox/thiol balance that perturb blood coagulation. *FEBS Letters.* **510**, 67-70.

Bayraktutan, U., Blayney, L., & Shah, A.M. (2000) Molecular characterisation and localisation of the NAD(P)H oxidase components gp91-*phox* and p22-*phox* in endothelial cells. *Arteriosclerosis, Thrombosis, and Vascular Biology.* **20**, 1903-1911.

Beckman, J. S., Parks, D.A., Pearson, J.D., Marshall, P.A., & Freeman, B.A. (1989). A sensitive fluorometric assay for measuring xanthine dehydrogenase and oxidase in tissues. *Free Radical Biology and Medicine.* **6**, 607-615.

Bellorini, M., Lee, D.K., Dontonel, J.C., Zemzourumi, K., Roeder, R.G., Tora, L., & Mantovani, R. (1997). CCAAT binding NF-Y – TBP interactions: NF-YB and NF-YC require short domains adjacent to their histone fold motifs for association with TBP basic residues. *Nucleic Acids Research.* **25**, 2174-2181.

Berg, J.M., Tymoczko, J.L., & Stryer, L. (2001). Nucleotide Biosynthesis. In: *Biochemistry.* (Eds. Moran, S., Santee, M., DiVittorio, S., Hadler, G.L., Zimmerman, P., & Wong, V). pp. 693-714. W. H. Freeman and Company, New York, USA.

Berglund, L., Rasmussen, J.T., Andersen, M.D., Rasmussen, M.S., & Petersen, T.E. (1995). Purification of the bovine xanthine oxidoreductase from milk fat globule membranes and cloning of complementary deoxyribonucleic acid. *Journal of Dairy Science.* **79**, 196-204.

Bevilacqua, M.P., Pober, J.S., Mendrick, D.L., Cotran, R.S., & Gimbrone, M.A. (1987). Identification of an inducible endothelial-leukocyte adhesion molecule. *PNAS.* **84**, 9238-9242.

Bhatia, M., & Moochhala, S. (2004). Role of inflammatory mediators in the pathophysiology of acute respiratory distress syndrome. *The Journal of Pathology.* **202**, 145-156.

Birch, K.A., Ewenstein, B.M., Golan, D.E., & Pober, J.S. (1994). Prolonged peak elevations in cytoplasmic free calcium ions, derived from intracellular stores, correlate with the extent of thrombin-stimulated exocytosis in single human umbilical vein endothelial cells. *Journal of Cellular Physiology.* **160**, 545-554.

Bode, W., Turk, D., & Karshikov, A. (1992). The refined 1.9-Å X-ray crystal structure of D-Phe-Pro-Arg chloromethylketone-inhibited human α-thrombin: structure analysis, overall structure, electrostatic properties, detailed active-site geometry, and structure-function relationships. *Protein Science.* **1**, 426-471.

Bonini, M.G., Miyamoto, S., Di Mascio, P., & Augusto. (2004). Production of the carbonate radical anion during xanthine oxidase turnover in the presence of biocarbonate. *The Journal of Biological Chemistry.* **279**, 51836-51843.

Bounassisi, V., & Venter, J.C. (1976). Hormone and neurotransmitter receptors in an established vascular endothelial cell line. *PNAS.* **73**, 1612-1616.

Bradford, M.M. (1976). A rapid and sensitive method for the quantitation of microgram quantities of protein utilizing the principle of protein-dye binding. *Analytical Biochemistry.* **72**, 248-254.

Bradley, J.R., Johnson, D.R., & Pober, J.S. (1993). Endothelial activation by hydrogen peroxide. Selective increases of intracellular adhesion molecule-1 and major histocompatibility complex class I. *The American Journal of Pathology.* **142**, 1598-1609.

Brizio, C., Barile, M., & Brandsch, R. (2002). Flavinylation of the precursor of mitochondrial dimethylglycine dehydrogenase by intact and solubilised mitochondria. *FEBS Letters.* **522**, 141-146.

Brunelli, L., Crow, J.P., Beckman, J.S. (1995). The comparative toxicity of nitric oxide and peroxynitrite to *Escherichia coli. Archives in Biochemistry and Biophysics.* **316**, 327-334.

Butkowski, R.J., Elion, J., Downing, M.R., & Mann, K.G. (1977). Primary structure of human prothrombin 2 and α-thrombin. *The Journal of Biological Chemistry.* **252**, 4942-4957.

Cazzaniga, G., Terao, M., Schiavo, P.L., Galbiti, F., Segalla, F., Seldin, M.F., & Garattini, E. (1994). Chromosomal mapping, isolation, and characterisation of the mouse xanthine dehydrogenase gene. *Genomics.* **23**, 390-402.

Chance, B., Sies, H., & Boveris, A. (1979). Hydroperoxide metabolism in mammalian organs. *Physiological Reviews.* **59**, 527-605.

Chen, X-L., Zhang, Q., Zhao, R., Ding, X., Tummala, P.E., & Medford, R.M. (2003). Rac1 and superoxide are required for the expression of cell adhesion molecules induced by tumor necrosis factor-α in endothelial cells. *The Journal of Pharmacology and Experimental Therapeutics.* **305**, 573-580.

Chen, J., Anderson, J.B., DeWeese-Scott, C., Fedorova, N.D., Geer, L.Y., He, S., Hurwitz, D.I., Jackson, J.D., Jacobs, A.R., Lanczycki, C.J., Liebert, C.A., Liu, C., Madej, T., Marchler-Bauer, A., Marchler, G.H., Mazumder, R., Nikolskaya, A.N., Rao, B.S., Panchenko, A.R., Shoemaker, B.A., Simonyan, V., Song, J.S., Thiessen, P.A., Vasudevan, S., Wang, Y., Yamashita, R.A., Yin, J.J., & Bryant, S.H. (2003a). MMDB: Entrez's 3D-structure database. *Nucleic Acids Research.* **31,** 474-477.

Chenna, R., Sugawara, H., Koike, T., Lopez, R., Gibson, T.J., Higgins, D.G., & Thompson, J.D. (2003). Multiple sequence alignment with the Clustal series of programs. *Nucleic Acids Research.* **31**, 3497-3500.

Choi, K-S., Ghuman, J., Kassam, G., Kang, H-M., Fitzpatrick, S.L., & Waisman, D.M. (1998). Annexin II tetramer inhibits plasmin-dependent fibrinolysis. *Biochemistry.* **37**, 648-655.

Chu, A.J., Beydoun, S., Mathews, S.T., & Hoang, J. (2003). Noval anticoagulant polyethylenimine: inhibitors of thrombin-catalyzed fibrin formation. *Archives of Biochemistry and Biophysics.* **415**, 101-108.

Clutton, P., Miermount, A., & Freedman, J.E. (2004). Regulation of endogenous reactive oxygen species in platelets can reverse aggregation. *Arteriosclerosis, Thrombosis, and Vascular Biology.* **24**, 187-192.

Cooper, D., Stokes, K.Y., Tailor, A., & Granger, D.N. (2002). Oxidative stress promotes blood cell-endothelial cell interactions in the microcirculation. *Cardiovascular Toxicology.* **02**, 165-180.

Corbisier, P., Houbion, A., & Remacle, J. (1987). A new technique for highly sensitive detection of superoxide dismutase activity by chemiluminescence. *Analytical Biochemistry.* **164**, 240-247.

Czerniecki, B., Gad, S.C., Reilly, C., Smith, A.C., & Witz, G. Phorbol diacetate inhibits superoxide anion radical production and tumor promotion by mezerein. *Carcinogenesis.* **7**, 1637-1641.

Davie, E.W., & Ratnoff, O.D. (1964). Waterfall sequence for intrinsic blood clotting. *Science.* **145**, 1310-1312.

Deeney, J.T., Valivullah, H.M., Dapper, C.H., Dylewski, D.P., & Keenan, T.W. (1985). Microlipid droplets in milk secreting mammary epithelial cells: evidence that they originate from endoplasmic reticulum and are precursors of milk lipid globules. *European Journal of Cell Biology.* **38**, 16-26.

De Cristofaro, R., Akhavan, S., Altomare, C., Carotti, A., Peyvandi, F., & Mannucci, P.M. (2004). A natural prothrombin mutant reveals an unexpected influence of A-chain structure on the activity of human α-thrombin. *The Journal of Biological Chemistry.* **279**, 13035-13043.

Della Corte, E., & Stirpe, E. (1968). Regulation of xanthine oxidase in rat liver: modifications of enzyme activity of rat liver supernatant on storage at 20 degrees. *The Biochemical Journal.* **108**, 349-351.

Della Corte, E., & Stirpe, E. (1972). The regulation of rat liver xanthine oxidase. *The Biochemical Journal.* **126**, 739-745.

DeMoss, J.A., & Hsu, P.Y. (1991). NarK enhances nitrate uptake and nitrite excretion in *Escherichia coli. Journal of Bacteriology.* **173**, 3303-3310.

Di Cera, E. (2003). Thrombin interactions. *CHEST.* **124**, 11S-17S.

Dickinson, D.A., & Forman, H.J. (2002). Cellular glutathione and thiols metabolism. *Biochemical Pharmacology.* **64**, 1019-1026.

DiGregorio, K.A., Cilento, E.V., & Lantz, R.C. (1987). Measurement of superoxide release from single pulmonary alveolar macrophages. *American Journal of Physiology.* **252**, C677-C683.

Dikov, A., Alexandrov, I., Russinova, A., & Boyadjieva-Michailova, A. (1988). Ultracytochemical demonstration of enzymes by reduction of potassium hexacyanoferrate (III). A method for demonstration of xanthine oxidase. *Acta Histochemica.* **83**, 107-115.

Doehner, W., Schoene, N., Rauchhaus, M., Leyva-Leon, F., Pavitt, D.V., Reaveley, D.A., Schuler, G., Coats, A.J.S., Anker, S.D., & Hambrecht, R. (2002). Effects of xanthine oxidase inhibition with allopurinol on endothelial function and peripheral blood flow in hyperuricemic patients with chronic heart failure. *Circulation.* **105**, 2619-2624).

Doel, J.J., Godber, B.L., Eisenthal, R., & Harrison, R. (2001) Reduction of organic nitrates catalysed by xanthine oxidoreductase under anaerobic conditions. *Biochimica et Biophysica Acta.* **1527,** 81-87.

Edmondson, D.E., & Newton-Vinson, P. (2001). The covalent FAD of monoamine oxidase: structural and functional role and mechanism of the flavinylation reaction. *Antioxidants and Redox Signalling.* **3**, 789-806.

Ehrhardt, C., Kneuer, C., & Bakowsky, U. (2004). Selectins-an emerging target for drug delivery. *Advanced Drug Delivery Reviews.* **56**, 527-549.

Emeis, J.J., van den Eijnden-Schrauwen, Y, van den Hoogen, C.M., de Priester, W., Westmuckett, A., & Lupu, F. (1997). An endothelial storage granule for tissue-type plasminogen activator. *The Journal of Cell Biology.* **139**, 245-256.

Enroth, C., Eger, B.T., Okamoto, K., Nishino, T., Nishino, T., & Pai, E.F. (2000). Crystal structures of bovine milk xanthine dehydrogenase and xanthine oxidase: structure-based mechanism of conversion. *PNAS.* **97**, 10723-10728.

Esmon, C.T., & Owen, W.G. (1981). Identification of an endothelial cell cofactor for thrombin-catalyzed activation of protein C. *PNAS.* **78**, 2249-2252.

Esmon, C.T., Esmon, N.L., & Harris, K.W. (1982). Complex formation between thrombin and thrombomodulin inhibits both thrombin-cataylzed fibrin formation and factor V activation. *The Journal of Biological Chemistry.* **257**, 7944-7947.

Esmon, N.L., Owen, W.G., & Esmon, C.T. (1982). Isolation of a membrane-bound cofactor for thrombin-catalyzed activation of protein C. *The Journal of Biological Chemistry.* **257**, 859-864.

Esmon, C.T. (1989). The roles of protein C and thrombomodulin in the regulation of blood coagulation. *The Journal of Biological Chemistry.* **264**, 4743-4746.

Esmon, C.T. (2000). Regulation of blood coagulation. *Biochimica et Biophysica Acta.* **1477**, 349-360.

Falciani, F., Terao, M., Goldwurm, S., Ronchi, A., Gatti, A., Minoia, C., Calzi, M.L., Salmona, M., Cazzaniga, G., & Garattini, E. (1994). Molybdenum (VI) salts convert the xanthine oxidoreductase apoprotein into the active enzyme in mouse L929 fibroblastic cells. *Biochemical Journal.* **298**, 69-77.

Farquharson, C.A.J., Butler, R., Hill, A., Belch, J.J.F., & Struthers, A.D. (2002). Allopurinol improves endothelial dysfunction in chronic heart failure. *Circulation.* **106**, 221-226.

Faulkner, K., & Fridovich, I. (1993). Luminol and lucigenin as detectors for O2.-. *Free Radical Biology and Medicine.* **15**, 447-451.

Feigelson, P. (1952). The inhibition of xanthine oxidase in vitro by trace amounts of *l*-ascorbic acid. *The Journal of Biological Chemistry.* **197**, 843-850.

Fleming, I. (2001). Cytochrome P450 enzymes in vascular homeostasis. *Circulation Research.* **89**, 753-762.

Folch, E., Gelpi, E., Rosello-Catafau, J., & Closa, D. (1998). Free radicals generated by xanthine oxidase mediate pancreatitis-associated organ failure. *Digestive Diseases and Science.* **43**, 2405-2410.

Folch, E., Salas, A., Panes, J., Gelpi, E., Rosello-Catafau, J., Anderson, D.C., Navarro, S., Pique, J.M., Fernandez-Cruz, L., & Closa, D. (1999). Role of P-selectin and ICAM-1 in pancreatitis-induced lung inflammation in rats: significance of oxidative stress. *Annals of Surgery.* **230**, 792-798.

Folch, E., Salas, A., Prats, N., Panes, J., Pique, J.M., Gelpi, E, Rosello-Catafau, J., & Closa, D. (2000). H_2O_2 and PARS mediate lung P-selectin upregulation in acute pancreatitis. *Free Radical Biology and Medicine.* **28**, 1287-1294.

Forman, H.J., & Azzi, A. (1997). On the virtual existence of superoxide anions in mitochondria: thoughts regarding its role in physiology. *FASEB Journal.* **11**, 374-375.

Furchgott, R.F., & Zawadzki, J.V. (1980). The obligatory role of endothelial cells in the relaxation of arterial smooth muscle by acetylcholine. *Nature.* **288**, 373-376.

Fraaije, M.W., van Den Heuvel, R.H., van Berkel, W.J., & Mattevi A. (2000). Structural analysis of flavinylation in vanillyl-alcohol oxidase. *Journal of Biological Chemistry.* **275**, 38654-38658.

Franke, W.W., Heid, H.W., Grund, C., Winter, S., Freudenstein, C., Schmid, E., Jarasch, E-D., & Keenan, T.W. (1981). Antibodies to the major insoluble milk fat globule membrane-associated protein: specific location in apical regions of lactating epithelial cells. *The Journal of Cell Biology.* **89**, 485-494.

Frazzon, J., Fick, J.R., & Dean, D.R. (2002). Biosynthesis of iron-sulphur clusters is a complex and highly conserved process. *Biochemical Society Transactions.* **30**, 680-685.

Frederiks, W.M., & Vreeling-Sindelarova, H. (2002). Ultrastructural localisation of xanthine oxidoreductase activity in isolated rat liver cells. *Acta Histochemica.* **104**, 29-37.

Freedman, J.E., Loscalzo, J., Barnard, M.R., Alpert, C., Keaney, J.F., & Michelson, A.D. (1997). Nitric oxide is release from activated platelets inhibits platelet recruitment. *Journal of Clinical Investigation.* **100**, 350-356.

Frenette, P.S., Denis, C.V., Weiss, L., Jurk, K., Subbarao, S., Kehrel, B., Hartwig, J.H., Vestweber, D., & Wagner, D.D. (2000). P-selectin glycoprotein ligand 1 (PSGL-1) is

expressed on platelets and can mediate platelet-endothelial interactions in vivo. *The Journal of Experimental Medicine.* **191**, 1413-1422.

Fridovich, I. (1978). The biology of oxygen radicals. *Science.* **201**, 875-880.

Fridovich, I. (1997). Superoxide anion radical, superoxide dimutases, and related matters. *The Journal of Biological Chemistry.* **272**, 18515-18517.

Friedl, H.P., Till, G.O., Ryan, U.S., & Ward, P.A. (1989). Mediator-induced activation of xanthine oxidase in endothelial cells. *FASEB Journal.* **3**, 2512-2518.

Friedl, H.P., Till, G.O., Trentz, O., & Ward, P.A. (1989). Roles of histamine, complement and xanthine oxidase in thermal injury of skin. *American Journal of Pathology.* **135**, 203-217

Furie, B., & Furie, B.C. (1992). Molecular and cellular biology of blood coagulation. *The New England Journal of Medicine.* **326**, 800-806.

Gaboury, J., Woodman, R.C., Granger, D.N., Reinhardt, P., & Kubes, P. (1993). Nitric oxide prevents leukocyte adherence: role of superoxide. *American Journal of Physiology.* **265**, H862-867.

Gaboury, J.P., Anderson, D.C., Kubes, P. (1994). Molecular mechanisms involved in superoxide-induced leukocyte-endothelial cell interactions in vivo. *American Journal of Physiology. Heart and Circulatory Physiology.* **266**, H637-H642.

Garattini, E., Mendel, R., Romao, M.J., Wright, R., & Terao, M. (2003). Mammalian molbdo-flavoenzymes, an expanding family of proteins: structure, genetics, regulation, function and pathophysiology. *Biochemical Journal.* **372**, 15-32.

Geng, J.G., Bevilacqua, M.P., Moore, K.L., McIntyre, T.M., Prescott, S.M., Kim, J.M., Bliss, G.A., Zimmerman, G.A., & McEver, R.P. (1990). Rapid neutrophil adhesion to activated endothelium mediated by GMP-140. *Nature.* **343**, 757-560.

Ghio, A.J., Kennedy, T.P., Stonehuerner, J., Carter, J.D., Skinner, K.A., Parks, D.A., & Hoidal, J.R. (2002). Iron regulates xanthine oxidase activity in the lung. *American Journal of Physiology. Lung Cellular and Molecular Physiology.* **283**, L563-L572.

Godber, B., Sanders, S., Harrison, R., Eisenthal, R., and Bray, R.C. (1997). > or = 95% of xanthine oxidase in human milk is present as the demolybdo form, lacking molybdopterin. *Biochemical Society Transactions.* **25**, 519S.

Godber BL, Doel JJ, Durgan J, Eisenthal R, Harrison R (2000). A new route to peroxynitrite: a role for xanthine oxidoreductase. *FEBS Letters.* **475**, 93-96.

Godber, B.L.J., Doel, J.J., Goult, T.A., Eisenthal, R., & Harrison, R. (2001). Suicide inactivation of xanthine oxidoreductase during reduction of inorganic nitrite to nitric oxide. *The Biochemical Journal.* **358**, 325-333.

Görlach, A., Brandes, R.P., Nguyen, K., Amidi, M., Dehghani, F., & Busse, R. (2000). A gp91phox containing NADPH oxidase selectively expressed in endothelial cells is a major source of oxygen radical generation in the arterial wall. *Circulation Research.* **87**, 26-32.

Grabovsky, V., Feigelson, S., Chen, C., Bleijs, D.A., Peled, A., Cinamon, G., Baleux, F., Arenzana-Seisdedos, F., Lapidot, T., van Kooyk, Y., Lobb, R.R., & Alon, R. Subsecond induction of α4 integrin clustering by immobilized chemokines stimulates leukocyte tethering and rolling on endothelial vascular cell adhesion molecule 1 under flow conditions. *The Journal of Experimental Medicine.* **192**, 495-505.

Graf, L., Barat, E., Borvenbeg, J., Hermann, I., & Patthy, A. (1976). Action of thrombin on ovine, bovine and human pituitary growth hormones. *European Journal of Biochemistry.* **64**, 333-340.

Granell, S., Serrano-Mollar, A., Folch-Puy, E., Navajas, D., Farre, R., Bulbena, O., & Closa, D. (2004). Oxygen in the alveolar space mediates lung inflammation in acute pancreatitis. *Free Radical Biology & Medicine.* **37**, 1640-1647.

Graven, K.K., Troxler, R.F., Kornfeld, H., Panchenko, M.V., & Farber, H.W. (1994). Regulation of endothelial cell glyeraldehyde-3-phosphate dehydrogenase expression by hypoxia. *The Journal of Biological Chemistry.* **269**, 24446-24453.

Green, D.E., & Pauli, R. (1943). The antibacterial action of the xanthine oxidase system. *Proceedings of the Society for Experimental Biology and Medicine.* **54**, 148-150.

Griffin, J.H. (1995). The thrombin paradox. *Nature.* **378**, 337-338.

Gruenhagen, J.A., & Yeung, E.S. (2004). Investigation of G protein-initiated, Ca^{2+}-depedent release of ATP from endothelial cells. *Biochimica et Biophysica Acta.* **1693**, 135-146.

Gryglewski, R.J., Palmer, R.M.J., & Moncada, S. (1986). Superoxide anion is involved in the breakdown of endothelium-derived vascular relaxation factor. *Nature.* **320**, 454-456.

Guice, K.S., Oldham, K.T., Caty, M.G., Johnson, K.J., & Ward, P.A. (1989). Neutrophil-dependent, oxygen-radical mediated lung injury associated with acute pancreatitis. *Annals of Surgery.* **210**, 740-747.

Guthikonda, S., Sinkey, C., Barenz, T., & Haynes, W.G. (2003). Xanthine oxidase inhibition reverses endothelial dysfunction in heavy smokers. *Circulation.* **107**, 416-421.

Gyllenhammer, H. (1987). Lucigenin chemiluminescence in the assessment of neutrophil superoxide production. *Journal of Immunological Methods.* **97**, 209-213.

Haining, J.L., & Legan, J.S. (1967). Fluorometric assay for xanthine oxidase. *Analytical Biochemistry.* 21, 337-343.

Hancock, J.T. (1999). Nitric oxide, hydrogen peroxide, and carbon monoxide. In *Cell Signalling.* pp 167-184. Addison Wesley Longman Limited, England, UK.

Hancock, J.T., Salisbury, V., Ovejero-Boglione, M.C., Cherry, R., Hoare, C., Eistenthal, R., & Harrison, R. (2002). Antimicrobial properties of milk: dependence on presence of xanthine oxidase and nitrite. *Antimicrobial Agents and Chemotherapy.* **46**, 3308-3310.

Harris, C.M., & Massey, V. (1997). The reaction of reduced xanthine dehydrogenase with molecular oxygen. *The Journal of Biological Chemistry.* **272**, 8370-8379.

Harrison, R. (2002). Structure and function of xanthine oxidoreductase: where are we now? *Free Radical Biology and Medicine.* **33**, 774-797.

Hattori, R., Hamilton, K.K., Fugate, R.D., McEver, R.P., & Sims, P.J. (1988). Stimulated secretion of endothelial von Willebrand Factor is accompanied by rapid redistribution to the cell surface of the intracellular granule membrane protein GMP-140. *The Journal of Biological Chemistry.* **264**, 7768-7771.

Haugland 2002a. Accessories and resources. In *Handbook of Fluorescent Probes and Research Products.* (Eds. Gregory, J., and Spence, M.T.Z.). pp 877-908. Molecular Probes. USA.

Hayashi, Y., Sawa, Y., Nishimura, M., Fukuyama, N., Ichikawa, H., Ohtake, S., Nakazawa, H., & Matsuda, H. (2004). Peroxynitrite, a product between nitric oxide and superoxide anion, plays a cytotoxic role in the development of post-bypass systemic inflammatory response. *European Journal of Cardio-thoracic Surgery.* **26**, 276-280.

Heid, H.W., Schnolzer, M., & Keenan, T.W (1996). Adipocyte differentiation-related protein is secreted as a constituent of milk lipid globule membrane. *Biochemical Journal.* **320**, 1025-1030.

Hirano, K., & Kanaide, H. (2003). Role of protease-activated receptors in the vascular system. *Journal of Atherosclerosis and Thrombosis.* **10**, 211-225.

Homer, K.A., and Beighton, D. (1990). Fluormoteric determination of bacterial protease activity using fluorescein isothiocyanate labeled proteins as substrates. *Analytical Biochemistry.* **191**, 133-137.

Hornig, B., Arakawa, N., Kohler, C., & Drexler, H. (1998). Vitamin C improves endothelial function of conduit arteries in patients with chronic heart failure. *Circulation.* **97**, 363-368.

Hough, L.B. (2001). Genomics meets histamine receptors: new subtypes, new receptors. *Molecular Pharmacology.* **59**, 415-419.

Houston, M., Estevez, A., Chumley, P., Aslan, M., Marklund, S., Parks, D.A., & Freeman, B.A. (1999). Binding of xanthine oxidase to the vascular endothelium. *The Journal of Biological Chemistry.* **274**, 4985-4994.

Hoyer, L.W., de los Santos, R.P., & Hoyer, J.R. (1973). Localization in endothelial cells by immunofluorescent microscopy. *The Journal of Clinical Investigation.* **52**, 2737-2744.

Hsu-Lin, S-C., Berman, C.L., Furie, B.C., August, D., & Furie, B. (1984). A platelet membrane protein expressed during platelet activation and secretion studies using a monoclonal antibody specific for thrombin-activated platelets. *The Journal of Biological Chemistry.* **259**, 9121-9126.

Huang, Y-C, T., Ghio, A.J., Nozik-Grayck, E., & Piantadosi, C.A. (2001). Vascular release of nonheme iron in perfused rabbit lungs. *American Journal of Physiology. Lung Cellular and Molecular Physiology* **280**, L474-L481.

Huang, H.Y., Appel, L.J., Choi, M.J., Gelber, A.C., Charleston, J., Norkus, E.P., & Miller, E.R. (2005). The effects of vitamin C supplementation on serum concentrations of uric acid: results from a randomised controlled trial. *Arthritis and Rheumatism.* **52**, 1843-1847.

Huie, R.E., & Padmaja, S. (1993). The reaction of NO with superoxide. *Free Radical Research Communications.* **18**, 195-199.

Hunt, J., & Massey, V. (1994). Studies of the reductive half-reaction of milk xanthine dehydrogenase. *The Journal of Biological Chemistry.* **269**, 18904-18914.

Huo, Y., & Ley, K. (2001). Adhesion molecules and atherogenesis. *Acta Physiologica Scandinavica.* **173**, 35-43.

Hynes, R.O. (1992). Integrins; versatility, modulation, and siganling in cell adhesion. *Cell.* **69**, 11-25.

Ichida, K., Amaya, Y., Noda, K., Minoshima, S., Hosoya, T., Sakai, O., Shim, N., & Nishino, T. (1993). Cloning of the cDNA encoding human xanthine dehydrogenase (oxidase): structural analysis of the protein and chromosomal location of the gene. *Gene.* **133**, 279-284.

Ichida, K., Amaya, Y., Kamayani, N., Nishino, T., Hosoya, T., & Sakai, O. (1997). Indentification of two mutations in human xanthine dehydrogenase gene responsible for classical type I xanthinuria. *The Journal of Clinical Investigation.* **99**, 2391-2397.

Ichida, K., Matsumura, T., Sakuma, R., Hosoya, T., & Nishino, T. (2001). Mutation of human molybdenum cofactor sulfurase gene is responsible for classical xanthinuria type II. *Biochemical and Biophysical Research Communications.* **282**, 1194-1200.

Ichikawa, M., Nishino, T., Nishino, T., & Ichikawa, A. (1992). Subcellular localisation of xanthine oxidase in rat hepatocytes: high-resolution immunoelectron microscopic study combined with biochemical analysis. *The Journal of Histochemistry and Cytochemistry.* **40**, 1097-1103.

Ichikawa, H., Wolf, R.E., Aw, T.Y., Ohno, N., Coe, L., Granger, D.N., Yoshikawa, T., & Alexander, J.S. (1997). Exogenous xanthine promotes neutrophil adherence to cultured endothelial cells. *American journal of Physiology.* **273**, G342-G347.

Ignarro, L.J., & Kadowitz, P.J. (1985). The pharmacological and physiological role of cyclic GMP in vascular smooth muscle relaxation. *Annual Reviews: Pharmacology and Toxicology.* **25**, 171-191.

Ignarro, L.J., Buga, G.M., Wood, K.S., Byrns, R.E., & Chaudhuri, G. (1987). Endothelium-derived relaxing factor produced and released from artery and vein is nitric oxide. *PNAS.* **84**, 9265-6269.

Ingenito, E.F., Craig, J.M., Labesse, J., Gautier, M., & Rutstein, D.D. (1958). Cells of human heart and aorta grown in tissue culture. *A.M.A. Archives of Pathology.* **65**, 355-359.

Inoue, S., Nakao, A., Kishimoto, W., Murakami, H., Itoh, K., Itoh, T., Harada, A., Nonami, T., & Takagi, H. (1995). Anti-neutrophil antibody attenuates the severity of acute lung injury in rats with experimental acute pancreatitis. *Archives of Surgery.* **130**, 93-98.

Ishhi, T., Aoki, N., Noda, A., Adachi, T., Nakamura, R., & Matsuda, T. (1995). Carboxy-terminal cytoplasmic domain of mouse butyrophilin specifically associates

with a 150-kDa protein of mammary epithelial cells and milk fat globule membrane. *Biochimica et Biophysica Acta.* **1245**, 285-292.

Jack, L.J.W., & Mather, I.H. (1990). Cloning and analysis of cDNA encoding bovine butyrophilin, an apical glycoprotein expressed in mammary tissue and secreted in association with the milk-fat globule membrane during lactation. *The Journal of Biological Chemistry.* **265**, 14481-14486.

Jaffe, E.A., Nachman, R.L., Becker, C.G., & Minick, C.R. (1973). Culture of human endothelial cells derived from umbilical veins. *The Journal of Clinical Investigation.* **52**, 2745-2756.

Jaffe, E.A., Hoyer, L.W., & Nachman, R.L. (1973a). Synthesis of antihemophilic factor antigen by cultured human endothelial cells. *The Journal of Clinical Investigation.* **52**, 2757-2674.

Jahn, B., & Hansch, G.M. (1990). Oxygen radical generation in human platelets: dependence on 12-lipoxygenase activity and on glutathione cycle. *International Archives of Allergy and Applied Immunology.* **93**, 73-79.

Jarasch, E-D., Grund, C., Bruder, G., Heid, H.W., Keenan, T.W., & Franke, W.W. (1981). Localisation of xanthine oxidase in mammary-gland epithelium and capillary endothelium. *Cell.* **25**, 67-82.

Jarasch, E-D., Bruder, G., & Heid, H.W. (1986). Significance of xanthine oxidase in capillary endothelial cells. *Acta Physiologica Scandinavica: Supplementum.* **548**, 39-46.

Johnson, K.J., Fantone, J.C., Kaplan, J., & Ward, P.A. (1981). In vivo damage of rat lungs by oxygen metabolites. *The Journal of Clinical Investigation.* **67**, 983-993.

Jones, D.A., Abbasi, O., McIntire, L.V., McEver, R.P., & Smith, C.W. (1993). P-selectin mediates neutrophil rolling on histamine stimulated endothelial cells. *Biophysical Journal.* **65**, 1560-1569.

Joneson, T., & Bar-Sagi, D. A rac1 effector site controlling mitogensis through superoxide production. *The Journal of Biological Chemistry.* **273**, 17991-17994.

Kagawa, H., & Fujimot, S. (1987). Electron-microscopic and immunohistochemical analyses of Weibel-Palade bodies in the human umbilical vein during pregnancy. *Cell and Tissue Research.* **249**, 557.563.

Kahn, M.L., Nakanishi-Matsui, M., Shapiro, M.J., Ishihara, H., & Coughlin, S.R. (1999). Prwotease-activated receptors 1 and 4 mediate activation of human platelets by thrombin. *The Journal of Clinical Investigation.* **103**, 879-887.

Keith, T.P., Riley, M.A., Kreitman, M., Lewontin, R.C., Curtis, D., & Chambers, G. (1987). Sequence for the structure gene xanthine dehydrogenase (rosy locus) in Drosophila melangaster. *Genetics.* **116**, 67-73.

Kelm, M. (1999). Nitric oxide metabolism and breakdown. *Biochimica et Biophysica Acta.* **1411**, 273-289.

Kikkawa, R., Yamamoto, T., Fukushima, T., Yamada, H., & Horii, I. (2005). Investigation of a hepatotoxicity screening system in primary cell cultures. *The Journal of Toxicological Sciences.* **30**, 61-72.

Kisker, C., Schindelin, H., & Rees, D.C. (1997). Molybdenum-cofactor-containing enzymes: structure and mechanism. *Annual Review of Biochemistry.* **66**, 233-267.

Kitchen, B.J. (1974). A comparison of the properties of membranes isolated from bovine skim milk and cream. *Biochimica et Biophysica Acta.* **356**, 257-269.

Knop, M., & Gerke, V. (2002). Ca^{2+}-regulated secretion of tissue-type plasminogen activator and von willebrand factor in human endothelial cells. *Biochimica et Biophysica Acta.* **1600**, 162-167.

Koike, K., Moore, F.A., Moore, E.E., Read, R.A., Carl, V.S., & Banerjee, A. (1993). Gut ischemia mediates lung injury by a xanthine oxidase-dependent neutrophil mechanism. *Journal of Surgical Research.* **54**, 469-473.

Kooij, A., Schiller, H.J., Schijns, M., Van Noorden, C.J.F., & Frederiks, W.M. (1994). Conversion of xanthine dehydrogenase into xanthine oxidase in rat liver and plasma at the onset of reperfusion after ischemia. *Hepatology.* **19**, 1488-1495.

Kristensen, S.R. (1994). Mechanisms of cell damage and enzyme release. *Danish Medical Bulletin.* **41**, 423-433.

Kubes, P., Suzuki, M., & Granger, D.N. (1991). Nitric oxide: an endogenous modulator of leukocyte adhesion. *PNAS.* **88**, 4651-4655.

Kuhlmann, C.R.W., Most, A.K., Li, F., Munz, B.M., Schaefer, C.A., Walther, S., Raedle-Hurst, T., Walddecker, B., Piper, H.M., Tillmanns, H., & Wiecha, J. (2005). Endothelin-I-induced proliferation of human endothelial cells depends on activation of K^+ channels and Ca^{2+} influx. *Acta Physiologica Scandinavica.* **183**, 161-169.

Kunst. F., Ogasawara, N., Moszer, I., et al. (1997). The complete genome sequence of the gram-positive bacterium Bacillus subtilis. *Nature.* **390**, 249-256.

Kuppusamy, P., & Zweier, J.L. (1989). Characterization of free radical generation by xanthine oxidase. Evidence for hydroxyl radical generation. *Journal of Biological Chemistry.* **264**, 9880-9884.

Kuwabara, Y., Nishino, T., Okamoto, K., Matsumura, T., Eger, B.T., Pai, E.F., & Nishino, T. (2003). Unique amino acids cluster for switching from the dehydrogenase to oxidase form of xanthineoxidoreductase. *PNAS.* **100**, 8170-8175.

Landmesser, U., & Drexler, H. (2002). Allopurinol and endothelial function in heart failure. Future or fantasy? *Circulation.* **106**, 173-175.

Landmesser, U., Speikermann, S., Dikalov, S., Tatge, H., Wilke, R., Kohler, C., Harrison, D.G., Hornig, B., & Drexler, H. (2002). Vascular oxidative stress and endothelial dysfunction in patients with chronic heart failure: Role for xanthine-oxidase and extracellular superoxide dismutase. *Circulation.* **106**, 3073-3078.

Landmesser, U., Dikalov, S., Price, S.R., McCann, L., Fukai, T., Holland, S.M., Mitch, W.E., & Harrison, D.G. (2003). Oxidation of the tetrahydrobiopterin leads to uncoupling of endothelial cell nitric oxide synthase in hypertension. *The Journal of Clinical Investigation.* **111**, 1201-1209.

Laposata, M., Dovnarsky, D.K., & Shin, H.S. (1983). Thrombin-induced gap formation in confluent endothelial cell monolayers in vitro. *Blood.* **62**, 549-556.

Larsen, E., Celi, A., Gilbert, G.E., Furie, B.C., Erban, J.K., Bonfanti, R., Wagner, D.D., Furie, B. PADGEM protein: a receptor that mediates the interaction of activated platelets with neutrophils and monocytes. *Cell.* **59**, 305-312.

Leavis, P.C., Rosenfeld, S., & Lu, R.C. (1978). Cleavage of a specific bind in troponin C by thrombin. *Biochimica et Biophysica Acta.* **535**, 281-286.

Lee, C-I., Liu, X., & Zweier, J.L. (2000). Regulation of xanthine oxidase by nitric oxide and peroxynitrite. *The Journal of Biological Chemistry.* **275**, 9369-9376.

Leung, L.L.K., & Hall, S.W. (2000). Dissociation of thrombin's substrate interactions using site-directed mutagenesis. *Trends in Cardiovascular Medicine.* **10**, 89-92.

Li, J-M., & Shah, A.M. (2002). Intracellular localisation and preassembly of the NADPH oxidase complex in cultured endothelial cells. *The Journal of Biological Chemistry.* **277**, 19952-19960.

Li, J-M., & Shah, A.M. (2004). Endothelial cell superoxide generation: regulation and relevance for cardiovascular pathophysiology. *American Journal of Physiology. Regulatory, Integrative, and Comparative Physiology.* **287**, R1014-R1030.

Linder, N., Rapola, J., & Raivio, K.O. (1999). Cellular expression of xanthine oxidoreductase protein in normal human tissue. *Laboratory Investigation.* **79**, 967-973.

Linder, N., Martelin, E., Lapatto, R., & Raivio, K.O. (2003). Posttranslational inactiviation of human xanthine oxidoreductase by oxygen under standard cell culture conditions. *The American Journal of Physiology: Cell Physiology.* **285**, C48-C55.

Linke, A., Recchia, F., Zhang, X., & Hintze, T.H. (2003). Acute and chronic endothelial dysfunction: implications in development of heart failure. *Heart Failure Reviews.* **8**, 87-97.

Liovich, S.I., & Fridovich, I. (1997). Lucigenin (Bis-*N*-methylacridinium) as a mediator of superoxide anion production. *Archives of Biochemistry and Biophysics.* **337**, 115-120.

Liovich, S.I., & Fridovich, I. (1998). Lucigenin as mediator of superoxide production: revisited. *Free Radical Biology and Medicine.* **25**, 926-928.

Liu, Y., Fiskum, G., & Schubert, D. (2002). Generation of reactive oxygen species by the mitochondrial electron transport chain. *Journal of Neurochemistry.* **80**, 780-787.

Lo, W.W., & Fan, T.P. (1987). Histamine stimulates inositol phosphate accumulation via the H1-receptor in cultured human endothelial cells. *Biochemical and Biophysical Research Communications.* **148**, 47-53.

Lo, S.K., Janakidevi, K., Lai, L., & Malik, A.B. (1993). Hydrogen peroxide-induced increase in endothelial adhesiveness is dependent on ICAM-1 expression. *American Journal of Physiology. Lung Cellular and Molecular Physiology.* **264**, L406-412.

Loscalzo, J. (2001). Nitric oxide insufficiency, platelet activation, and arterial thrombosis. *Circulation Research.* **88**, 756-762.

Loschen, G., Flohe, L., & Chance, B. (1971). Respiratory chain linked H_2O_2 production in pigeon heart mitochondria. *FEBS Letters.* **18**, 261-264.

Loschen, G., Azzi, A., Richter, C., & Folhe, L. (1974). Superoixde radicals as precursors of mitochondrial hydrogen peroxide. *FEBS Letters.* **42**, 68-72.

Lowry, O.H., Bessey, O.A., & Crawford, E.J. (1949). Pterine Oxidase. *Journal of Biological Chemistry.* 180, 399-410.

Lum, H., & Roebuck, K.A. (2001). Oxidant stress and endothelial cell dysfunction. *American Journal of Physiology: Cell Physiology.* **280**, C719-C741.

Lyer, L., & Fareed, J. (1995). Determination of the specific activity of recombinant hirudin using a thrombin titration method. *Thrombosis Research.* **78**, 259-263.

Lynch, R.E., & Fridovich, I. (1979). Autoinactivation of xanthine oxidase: the role of superoxide radical and hydrogen peroxide. *Biochimica et Biophysica Acta.* **571**, 195-200.

MacFarlane, R.G. (1964). An enzyme cascade in the blood clotting mechanism, and its function as a biochemical amplifier. *Nature.* **202**, 498-499.

Maciag, T., Kadish, J., Wilkins, L., Stemerman, M.B., & Weinstein, R. (1982). Organizational behaviour of human umbilical vein endothelial cells. *The Journal of Cell Biology.* **94**, 511-520.

MacKenzie, A., Wilson, H.L., Kiss-Toth, E., Dower, S.K., Morth, R.A., & Surprenant, A. (2001). Rapid secretion of interleukin-1β by microvesicle shedding. *Immunity.* **8**, 825-835.

Madej, T., Marchler-Bauer, A., Marchler, G.H., Mazumder, R., Nikolskaya, A.N., Rao, B.S., Panchenko, A.R., Shoemaker, B.A., Simonyan, V., Song, J.S., Thiessen, P.A., Vasudevan, S., Wang, Y., Yamashita, R.A., Yin, J.J., & Bryant, S.H. (2003). MMDB: Entrez's 3D-structure database. *Nucleic Acids Research.* **31**, 474-477.

Mann, K.G., Butenas, S., & Brummel, K. (2003). The dynamics of thrombin formation. *Arteriosclerosis, Thrombosis, and Vascular Biology.* **23**, 17-25.

Mantovani, R. (1998). A survey of 178 NF-Y binding CCAAT boxes. *Nucleic Acid Research.* **26**, 1135-1143.

Mantovani, R. (1999). The molecular biology of the CCAAT-binding factor NF-Y. *Gene.* **239**, 15-27.

Markley, H.G., Faillace, L.A., & Mezey, E. (1973). Xanthine oxidase activity in rat brain. *Biochimica et Biophysica Acta.* 309, 23-31.

Martelin, E., Palvimo, J.J., Lapatto, R., & Raivio, K.O. (2000). Nuclear factor Y activates the human xanthine oxidoreductase gene promoter. *FEBS Letters.* **480**, 84-88.

Martelin, E., Lapatto, R., & Raivio, K.O. (2002). Regulation of xanthine oxidoreductase by intracellular iron. *America Journal of Physiology. Cell Physiology.* **283**, C1722-C1728.

Maruyama, Y. (1963). The human endothelial cell in tissue culture. *Zeitschriff fur Zellforschung und Mikroscopische Anatomie.* **60**, 60-69.

Massey, V., Brumby, P.E., & Komai, H. (1969). Studies on milk xanthine oxidase. Some spectral and kinetic properties. *Journal of Biological Chemistry.* **244**, 1682-1691.

Massey, V., Komai, H., Palmer, G., & Elion, G.B. (1970). On the mechanism of inactivation of xanthine oxidase by allopurinol and other pyrazolo[3,4-d]pyrimidines. *The Journal of Biological Chemistry.* **245**, 2837-2844.

Mather, I.H., & Keenan, T.W. (1998). Origin and secretion of milk lipids. *Journal of Mammary Gland Biology and Neoplasia.* **3**, 259-273.

McCord, J.M., & Fridovich, I. (1968). The reduction of cytochrome c by milk xanthine oxidase. *The Journal of Biological Chemistry.* **243**, 5753-5760.

McCord, J.M., & Fridovich, I. (1969). Superoxide dismutase an enzymic function for erythrocuprein (hemocuprein). *The Journal of Biological Chemistry.* **244**, 6049-6055.

McCord, J.M. (1985) Oxygen-derived radicals in postischemic tissue injury. *The New England Journal of Medicine.* **312**, 159-163.

McEver, R.P., Beckstead, J.H., Moore, K.L., Marshall-Carlson, L., & Bainton, D.F. (1989). GMP-140, a platelet α-granule membrane protein, is also synthesized by vascular endothelial cells and is localized in Weibel-Palade bodies. *The Journal of Clinical Investigation.* **84**, 92-99.

McManaman, J.L., Hanson, L., Neville, M.C., & Wright, R.M. (2000). Lactogenic hormones regulate xanthine oxidoreductase and beta-casein levels in mammary epithelial cells by distinct mechanisms. *Archives of Biochemistry and Biophysics.* **373**, 318-327.

McManaman, J.L., & Bain, D.L. (2002). Structural and conformational analysis of the oxidase to dehydrogenase conversion of xanthine oxidoreductase. *Journal of Biological Chemistry.* **277**, 21261-21268.

McPerson, D.B., Kilker, R.P., & Foley, T.D. (2002). Superoxide activates constitutive nitric oxide synthase in a brain particulate fraction. *Biochemical and Biophysical Research Communications.* **296**, 413-418.

Michaux, G., & Cutler, D.F. (2004). How to roll an endothelial cigar: the biogenesis of Weibel-Palade bodies. *Traffic.* **5**, 69-78.

Millar TM, Stevens CR, Benjamin N, Eisenthal R, Harrison R, & Blake DR (1998). Xanthine oxidoreductase catalyses the reduction of nitrates and nitrite to nitric oxide under hypoxic conditions. *FEBS Letters.* **427**, 225-228.

Millar, T.M. (1999). Novel aspects of the function and activity of xanthine oxidase. *Doctoral Dissertation.* University of Bath, UK.

Millar, T.M., Kanczler, J.M., Bodamyali, T., Blake, D.R., & Stevens, C.R. (2002). Xanthine oxidase is a peroxynitrite synthase: newly identified roles for a very old enzyme. *Redox Report.* **7**, 65-70.

Millar, T.M. (2004). Peroxynitrite formation from the simultaneous reduction of nitrite and oxygen by xanthine oxidase. *FEBS Letters.* **562**, 129-133.

Miura, H., Bosnjak, J.J., Ning, G., Saito, T., Miura, M., & Gutterman, D.D. (2003). Role for hydrogen peroxide in flow-induced dilation of human coronary arterioles. *Circulation Research.* **92**, e31-e40.

Münzel, T., & Harrison, D.G. (1999). Increased superoxide in heart failure: a biochemical baroreflex gone awry. *Circulation.* **100**, 216-218.

Münzel, T., Feil, R., Mülsch, A., Lohmann, S.M., Hofmann, F., & Walter, U. (2003). Physiology and pathophysiology of vascular signalling controlled by cyclic guanosine 3', 5'-cyclic monophosphate-dependent protein kinase. *Circulation.* **108**, 2172-2183.

Murrell, G.A.C., Francis, M.J.O., & Bromley, L. (1990). Modulation of fibroblast proliferation by oxygen free radicals. *The Biochemical Journal.* **265**, 659-665.

Nachman, R.L., & Jaffe, E.A. (2004). Endothelial cell culture: beginnings of modern vascaulr biology. *The Journal of Clinical Investigation.* **114**, 1037-1040.

Nishino, T., & Okamoto, K. (2000). The role of the [2Fe-2S] cluster centers in xanthine oxidoreductase. *Journal of Inorganic Biochemistry.* **82**, 43-49.

O'Byrne, S., Shirodaria, C., Millar, T., Stevens, C., Blake, D., & Benjamin, N. (2000). Inhibition of platelet aggregation with glyceryl trinitrate and xanthine oxidoreductase. *The Journal of Pharamcology and Experimental Therapeutics.* **292**, 326-330.

Ossovkaya, V.S., & Bunnett, N.W. (2003). Protease-activated receptors: contribution to physiology and disease. *Physiological Reviews.* **84**, 579-621.

Oury, T.D., & Day, B.J., & Crapo, J.D. (1996). Extracellular superoxide dismutase in vessels and airways of humans and baboons. *Free Radical Biology and Medicine.* **20**, 957-965.

Owen, W.G., & Esmon, C.T. (1981). Functional properties of an endothelial cell cofactor for thrombin-catalyzed activation of protein C. *The Journal of Biological Chemistry.* **256**, 5532-5535.

Özer, N., Muftuoglu, M., & Hamdi, O.I. (1998). A simple and sensitive method for the activity staining of xanthine oxidase. *Journal of Biochemical and Biophysical Methods.* **36**, 95-100.

Pagano, P.J., Tornheim, K., & Cohen, R.A. (1993). Superoxide anion production by rabbit thoracic aorta: effect of endothelium-derived nitric oxide. *American Journal of Physiology.* **265**, H707-H712.

Page, S., Powell, D., Benboubetra, M., Stevens, C.R., Blake, D.R., Selase, F., Wolstenholme, A.J., & Harrison, R. (1998). Xanthine oxidoreductase in human mammary epithelial cells: activation in response to inflammatory cytokines. *Biochimica et Biophysica Acta.* **1381**, 191-202.

Pallister, C. (1994). Haemostasis: an overview. In *Blood Physiology and Pathophysiology.* pp. 447-480. (Eds. Not Published). Butterworth-Heinemann, Oxford, UK.

Palmer, R.M., Ferrige, A.G., & Moncada, S. (1987). Nitric oxide release accounts for the biological activity of endothelial-derived relaxing factor. *Nature.* **327**, 524-526.

Park, I-W, Ullrich, C.K., Schoenberger, E., Ganju, R.K., & Groopman, J.E. (2001). HIV-1 tat induces microvascular endothelial apoptosis through caspase activation. *The Journal of Immunology.* **167**, 2766-2771.

Partridge, C.A., Blumenstock, F.A., & Malik, A.B. (1992). Pulmonary microvascular endothelial cells constitutively release xanthine oxidase. *Archives of Biochemistry and Biophysics.* **294**, 184-187.

Patel, K.D., Zimmerman, G.A., Precott, S.M., McEver, R.P., & McIntyre, T.M. (1991). Oxygen radicals induce human endothelial cells to express GMP-140 and neutrophils. *The Journal of Cell Biology.* **112**, 749-759.

Perrella, M.A., & Yet, S.F. (2003). Role of heme oxygenase-1 in cardiovascular function. *Current Pharmaceutical Design.* **9**, 2479-2487.

Pfeffer, K.D., Hueckstead, T.P., & Hoidal, J.R. (1994). Xanthine dehydrogenase and xanthine oxidase and gene expression in renal epithelial cells. Cytokine and steroid regulation. *The Journal of Immunology.* **153**, 1789-1797.

Pocock, G., & Richards, C.D. (1999). The heart and circulation. In *Human Physiology the Basis of Medicine.* Oxford University Press. Oxford, UK.

Porasuphatana, S., Tsai, P., & Rosen, G.M. (2003). The generation of free radicals by nitric oxide synthase. *Comparative Biochemistry and Physiology.* **134**, 281-289.

Porras AG, Olson JS, Palmer G. (1981). The reaction of reduced xanthine oxidase with oxygen. Kinetics of peroxide and superoxide formation. *Journal of Biological Chemistry.* **256**, 9096-9103.

Potoka, D.A., Takao, S., Owaki, T., Bulkley, G.B., & Klein, A.S. (1998). Endothelial cells potentate oxygen-mediated Kuppfer cell phagocytic killing. *Free Radical Biology and Medicine.* 24, 1217-1227.

Prescott, L.M., Harley, J.P., & Klein, D.A. (1996). Microbial growth. In *Microbiology.* (Eds. Sievers, E.M., Stanton, T., Wilde, J.L., Banowetz, J.K., & Hancock, L). pp114-151. Wm. C. Brown Publishers, London, UK.

Quinlan, G.J., Lamb, N.J., Tilley, R., Evans, T.W., & Gutteridge, J.M. (1997). Plasma hypoxanthine levels in ARDS: implications for oxidative stress, morbidity, and mortality. *American Journal of Respiratory and Critical Care Medicine.* **155**, 479-484.

Rang, H.P., Dale, M.M., Ritter, J.M., & Moore, P.K. (2003). The vascular system. In *Pharamcology.* pp 285-313. (Eds. Hunter, L). Churchill Livingstone, London, UK.

Radomski, M.W., Palmer, R.M., & Moncada, S. (1987) The anti-aggregating proerties of vascular endothelium: interactions between prostacyclin and nitric oxide. *British Journal of Pharmacology.* **92**, 639-646.

Rajagopalan, K.V. (1997). Biosynthesis and processing of the molybdenum cofactors. *Biochemical Society Transactions.* **25**, 757-761.

Reiss, J., & Johnson, J.L. (2003). Mutations in the molybdenum cofactor biosynthetic genes MOCS1, MOCS2, and GEPH. *Human Mutation.* **21**, 569-576.

Roberts, I.S. The biochemistry and genetics of capsular polysaccharide production in bacteria. *Annual Reviews in Microbiology.* **50**, 285-315.

Rose, T., & Di Cera, E. (2002). Three-dimensional modelling of thrombin-fibrinogen interaction. *The Journal of Biochemicstry.* **277**, 18875-18880.

Roskoski, R., Gahn, L.G., & Roskoski, L.M. (1993). Inactivation of phosphorylated rat tyrosine hydroxylase by ascorbate in vitro. *Euorpean Journal of Biochemistry.* **218**, 363-370.

Rosnoblet, C., Vischer, U.M., Gerard, R.D., Irminger, J-C., Halban, P.A., & Kruithof, E.K.O. (1999). Storage of tissue-type plasminogen activator in Weibel-Palade bodies of human endothelial cells. *Arteriosclerosis, Thrombosis, and Vascular Biology.* **19**, 1796-1803.

Rotrosen, D., & Gallin, J.I. (1986). Histamine type I receptor occupancy incrwases endothelial cytosolic calcium, reduces F-actin, and promotes albumin diffusion across cultured endothelial monolayers. *The Journal of Biological Chemistry.* **103**, 2379-2387.

Rott, K.T., & Agudelo, C.A. (2003). Gout. *JAMA.* **21**, 2857-2860.

Rouquette, M., Page, S., Bryant, R., Benoubetra, M., Stevens, C.R., Blake, D.R., Whish, W.D., Harrison, R., & Tosh, D. (1998). Xanthine oxidoreductase is asymmetrically localised on the outer surface of human endothelial and epithelial cells in culture. *FEBS Letters.* **426**, 397-401.

Rydel, T.J., Ravichandran, K.G., Tulinsky, A., Bode, W., Huber, R., Roitsch, C., & Fenton, J.W. (1990). The structure of a complex of recombinant hirudin and human alpha-thrombin. *Science.* **249**, 277-280.

Saavedra, W.F., Paolocci, N., St John, M.E., Skaf, M.W., Stewart, G.C., Xie, J-S., Harrison, R.W., Zeichner, J., Mudrick, D., Marban, E., Kass, D.A., & Hare, J.M. (2002). Imbalance between xanthine oxidase and nitric oxide synthase signalling pathways underlies mechanoenergetic uncoupling in the failing heart. *Circulation Research.* **90**, 297-304.

Sadler, J.E. (1998). Biochemistry and genetics of von Willebrand factor. *Annual Review in Biochemistry.* **67**, 395-424.

Saksela, M., Lapatto, R., & Raivio, K.O. (1999). Irreversible conversion of xanthine dehydrogenase into xanthine oxidase by a mitochondrial protease. *FEBS Letters.* **443**, 117-120.

Salvemini, D., de Nucci, G., Sneddon, J.M., & Vane, J.R. (1989). Superoxide anions enhance platelet adhesion and aggregation. *British Journal of Pharmacology.* **97**, 1145-1150.

Sanders, S.A., Eisenthal, R., & Harrison, R. (1997). NADH oxidase activity of human xanthine oxidoreductase. *European Journal of Biochemistry.* **245**, 541-548.

Sasaki, S., Osanai, T., Tomita, H., Matsunaga, T., Magota, K., & Okumura, K. (2004). Tumor necrosis factor alpha as an endogenous stimulator for circulating coupling factor 6. *Cardiovascular Research.* **62**, 578-586.

Sase, K., & Michel, T. (1995). Expression of constitutive endothelial nitric oxide synthase in human blood platelets. *Life Sciences.* **57**, 2049-2055.

Schardinger, F. (1902). Über das Verhalten der Kuhmilch gegen Methylenblau und seine Verwendung zur Unterscheidung von ungekochter und gekochter Milch. *Untersuch Nahrungs Genussmittel.* **5**, 1113-1121.

Schultz, A.C., Nygaard, P., & Saxild, H.H. (2001). Functional analysis of 14 genes that constitute the purine catabolic pathway in Bacillus subtilis and evidence for a novel regulon controlled by the PucR transcription activator. *Journal of Bacteriology.* **183**, 3293-3302.

Schultz, E., Anter, E., & Keaney, J.F. (2004). Oxidative stress, antioxidants, and endothelial function. *Current Medicinal Chemistry.* **11**, 1093-1104.

Sheehan, J.P., & Sadler, J.E. (1994). Molecular mapping of the heparin-binding exosite of thrombin. *PNAS.* **91**, 5518-5522.

Simak, J., Holada, K., & Vostal, J.G. (2002). Release of annexin V-binding membrane microparticles from cultured human umbilical vein endothelial cells after treatment with camptothecin. *BMC Cell Biology.* **3**:11.

Sinha, S., & Wagner, D.D. (1987). Intact microtubules are necessary for complete processing, storage and regulated secretion of von Willebrand factor by endothelial cells. *European Journal of Cell Biology.* **43**, 377-383.

Skrypina, N.A., Timofeeva, A.V., Khaspekovm G.L., Savochkina, L.P., &Beabealashvilli, R.S. (2003). Total RNA suitable for molecular biology analysis. *Journal of Biotechnology.* **105**, 1-9.

Smith, C.J., Sun, D., Hoegler, C., Roth, B.S., Zhang, X., Zhao, G., Xu, X.B., Kobari, Y., Pritchard, K., Sessa, W.C., & Huntze, T.H. (1996). Reduced gene expression of vascular rneothelial NO synthase and cyclooxygenase-1 in heart failure. *Circulation Research.* **78**, 58-64.

Speden, D.J. (2003). Xanthine oxidase in inflammatory arthritis. Doctoral dissertation. University of Bath, Bath, UK.

Spiekermann, S., Landmesser, U., Dikalov, S., Bredt, M., Gamez, G., Tatge, H., Reepdchläger, N., Hornig, B., Drexler, H., & Harrison, D.G. (2003). Electron spin resonance characterisation of vascaulr xanthine and NAD(P)H oxidase activity in patients with coronary artery disease. *Circulation.* **107**, 1383-1389.

Springer, T.A. (1994). Traffic signals for lymphocyte recirculation and leukocyte emigration; the multistep paradigm. *Cell.* **76**, 301-314.

Staniek, K., & Nohl, H. (2000). Are mitochondria a permanent source of reactive oxygen species? *Biochimica et Biophysica Acta.* **1460**, 268-275.

Stamler, J.S., Singel, D.J., Loscalzo, J. (1992). Biochemistry of nitric oxide and its redox-active forms. *Science.* **258**, 1898-1902.

Stevens, C.R., Millar, T.M., Clinch, J.G., Kanczler, J.M., Bodamyali, T., & Blake, D.R. (2000). Antibacterial properties of xanthine oxidase in human milk. *The Lancet.* **356**, 829-830.

Stirpe, F., & Della Corte, E. (1969). The regulation of rat liver xanthine oxidase. *Journal of Biological Chemistry.* **244**, 3855-3863.

Storch, J., & Ferber, E. (1988). Detergent-amplified chemiluminescence of lucigenin for determination of superoxide anion production by NADPH-oxidase and xanthine oxidase. *Analytical Biochemistry.* **169**, 262-267.

St-Pierre, J., Buckingham, J.A., Roebuck, S.J., & Brand, M.D. (2002). Topology of superoxide production from different sites in the mitochondrial electron transport chain. *The Journal of Biological Chemistry.* **277**, 44784-44790.

Stralin, P., Karlsson, K., Johansson, B.O., & Marklund, S.L. (1995). The interstitium of the human arterial wall contains very large amounts of extracellular superoxide dismutase. *Arteriosclerosis, Thrombosis, and Vascular Biology.* **15**, 2032-2036.

Sugama, Y., Tiruppathi, C., Janakidevi, K., Anderson, T.T., Fenton, J.W., & Malik, A.B. (1992). Thrombin-induced expression of endothelial P-selectin and intracellular adhesion molecule-1: a mechanism of stabilising neutrophil adhesion. *The Journal of Cell Biology.* **119**, 935-944.

Suzuki, M., Inauen, W., Kvietys, P.R., Grisham, M.B., Meininger, C., Schelling, M.E., Granger, H.J., & Granger, D.N. (1989). Superoxide mediates reperfusion-induced leukocyte-endothelial cell interactions. *American Journal of Physiology.* **257**, H1740-H1745.

Tabengwa, E.M., Benza, R.L., Grenett, H.E., & Booyse, F.M. (2000). Hypertriglyceridemic VLDL downregulates tissue plasminogen activator gene transcription through cis-repressive region(s) in the tissue plasminogen activator promoter in cultured human endothelial cells. *Arteriosclerosis, Thrombosis, and Vascular Biology.* **20**, 1675-1681.

Takano, M., Meneshian, A., Sheikh, E., Yamakawa, Y., Wilkins, K.B., Hopkins, E.A., & Bulkley, G.B. (2002). Rapid upregulation of endothelial P-selectin expression via reactive oxygen species generation. *American Journal of Physiology.* **283**, H2054-H2061.

Takao, S., Smith, E.H., Wang, D., Chan, C.K., Bulkley, G.B., & Klein, A.S. (1996). Role of reactive oxygen intermediates in murine peritoneal macrophage phagocytosis and phagocytic killing. *American Journal of Physiology. Cell Physiology.* **271**, C1278-C1284.

Tan, S., Yokoyama, Y., Dickens, E., Cash, T.G., Freeman, B.A., & Parks, D.A. Xanthine oxidase activity in the circulation of rats following hemorrhagic shock. *Free Radical Biology & Medicine.* **15**, 407-415.

Taylor, F.B., Peer, G.T., Lockhart, M.S., Ferrell, G., & Esmon, C.T. (2001). Endothelial cell protein C receptor plays an important role in protein C activation in vivo. *Blood.* **97**, 1685-1688.

Terada, L.S., Beehler, C.J., Banerjee, A., Brown, J.M., Grosso, M.A., Harken, A.H., McCord, J.M., & Repine, J.E. (1988). Hyperoxia and self- or neutrophil-generated O_2 metabolites inactivate xanthine oxidase. *Journal of Applied Physiology.* **65**, 2349-2353.

Terada, L.S., Dormish, J.J., Shanley, P.F., Leff, J.A., Anderson, B.O., & Repine, J.E. (1992). Circualting xanthine oxidase mediates lung neutrophil sequestration after intestinal ischemia-reperfusion. *American Journal of Physiology.* **263**, L394-L401.

Terada, L.S., Hybertson, B.M., Connelly, K.G., Weill, D., Piermattei, D., & Repine, J.E. (1997). XO increases neutrophil adherence to endothelial cells by a dual ICAM-1 and P-selectin-mediated mechanism. *Journal of Applied Physiology.* **82**, 866-873.

Terao, M., Cazzaniga, C., Ghezzi, P., Bianchi, M., Falciani, F., Perani, P., & Garattini, E. (1992). Molecular cloning of cDNA coding for mouse liver xanthine dehydrogenase. Regulation of its transcript by interferons in vivo. *The Biochemical Journal.* **283**, 863-870.

Tilly, B.C., Tertoolen, L.G., Lambreachts, A.C., Remorie, R., de Laat, S.W., & Moolenaar, W.H. (1990). Histamine-H1-receptor-mediated phosphoinositide hydrolysis, Ca2+ signalling and membrane-potential oscillations in human HeLa carcinoma cells. *The Biochemical Journal.* **266**, 235-243.

Turrens, J.F., & Boveris, A. (1980). Generation of superoxide anion by the NADH dehydrogenase of bovine heart mitochondria. *The Biochemical Journal.* **191**, 421-427.

Turrens, J.F., Alexandre, A., & Lehninger, A.L. (1985). Ubisemiquinone is the electron donor for superoxide formation by complex III of heart mitochondria. *Archives of Biochemistry and Biophysics.* **237**, 408-414.

Umezawa, K., Akaike, T., Fujii, T., Suga, M., Setoguchi, K., Ozawa, A., & Maeda, H. (1997). Induction of nitric oxide synthesis and xanthine oxidase and their roles in the antimicrobial mechanism against Salmonella typhimurium infection in mice. *Infection and Immunity.* **65**, 2932-2940.

van Mourik, J.A., de Wir, T.R., & Voorberg, J. (2002). Biogenesis and exocytosis of Weibel-Palade bodies. *Histochemistry and Cell Biology.* **117**, 113-122.

VanWijk, M.J., VanBavel, E., Sturk, A., & Nieuwland, R. (2003). Microparticles in cardiovascular diseases. *Cardiovascualr Research.* **59**, 277-278.

Varma, S.D., Morris, S.M., Bauer, S.A., & Koppenol, W.H. (1986). In vitro damage to rat lens by xanthine-xanthine oxidase: protection by ascorbate. *Experimental Eye Research.* **43**, 1067-1076.

Vasquez-Vivar, J., Hogg, N., Pritchard, K.A., Martasek, P., & Kalyanaraman, B. (1997). Superoxide anion formation from lucigenin: an electron spin resonance spin-trapping study. *FEBS Letters.* **403**, 127-130.

Vasquez-Vivar, J., Kalyanaraman, B., Martasek, P., Hogg, N., Masters, B.S.S., Karoui, H., Tordo, P., & Pritchard, K.A. (1998). Superoxide generation by endothelial nitric oxide synthase: the influence of cofactors. *PNAS.* **95**, 9220-9225.

Vasquez-Vivar, J., Kalyanaraman, B., & Martasek, P. (2003). The role of tetrahydrbiopterin in superoxide generation from eNOS: enzymology and physiological implications. *Free Radical Research.* **37**, 121-127.

Vernet, C., Boretto, J., Mattei, M-G., Takahashi, M., Jack, L.J.W., Mather, I.H., Rouquier, S., & Pontarotti, P. (1993). Evolutionary study of multigeneic families mapping close to the human MHC class I region. *Journal of Molecular Evolution.* **37**, 600-612.

Vischer, U.M., & Wollheim, C.B. (1997). Epinepherine induces von Willebrand factor release from cultured endothelial cells: involvement of cyclic AMP-dependent signalling in exocytosis. *Thrombosis and Haemostasis.* **77**, 1182-1188.

Vischer, U.M., Lang, U., & Wollheim, C.B. (1998). Autocrine regulation of endothelial exocytosis: von willebrand factor release is induced by prostacyclin in cultured endothelial cells. *FEBS Letters.* **424**, 211-215.

Visher, U.M., Barth, H., & Wollhein, C.B. (2000). Regulated von Willebrand factor secretion is associated with agonist-specific patterns of cytoskeletal remodelling in cultured endothelial cells. *Arteriosclerosis, Thrombosis, and Vascular Biology.* **20**, 883-891.

Vergnolle, N., Hollenburg, M.D., & Wallace, J.L. (1999). Pro- and anti-inflammatory actions of thrombin: a distinct role proteinase-activated receptor-1 (PAR-1). *British Journal of Pharmacology.* **126**, 1262-1268.

Vergnolle, N., Derian, C.K., Andrea, M.R.D., Steinhoff, M., & Andrade-Gordon, P. (2002). Characterization of thrombin-induced leukocyte rolling and adherence: a potential proinflammatory role for proteinase-activated receptor-4. *The Journal of Immunology.* **169**, 1467-1473.

Von Andrian, U.H., Hansell, P., Chambers, D., Berger, E.M., Filho, I.T., Butcher, E.C., & Arfors, K.E. (1992). L-selectin function is requires for β_2-integrin-mediated neutrophil adhesion at physiological shear stress rates in vivo. *The American Journal of Physiology.* **263**, H1034-H1044.

Wang, J., Van Praagh, A., Hamilton, E., Wang, Q., Zou, B., Muranjan, M., Murphy, N.B., & Black, S.J. (2002). Serum xanthine oxidase: origin, regulation, and contribution to control of trypanosome parasitemia. *Antioxidants and Redox Signaling.* **4**, 161-178.

Watson, P., Jones, A.T., & Stephens, D.J. (2005). Intracellular trafiicking pathways and drug delivery: fluorescence imaging of living and fixed cells. *Advanced Drug Delivery Reviews.* **57**, 43-61.

Waud, W.R., & Rajagopalan, K.V. (1976). The mechanism of conversion of rat liver xanthine dehydrogenase from an NAD^+-dependent form (type D) to an O_2-dependent form (type O). *Archives of Biochemistry and Biophysics.* **172**, 365-379.

Weber, K.S., von Hundelshausen, P., Clark-Lewis, I., weber, P.C., & Weber, C. (1999).Differential immobilization and hierarchical involvement of chemokines in monocyte arrest and transmigration on inflamed endothelium in shear flow. *European Journal of Immunology.* **29**, 700-712.

Weibel, E.R., & Palade, G.E. (1964). New cytoplasmic components in arterial endothelia. *The Journal of Cell Biology.* **23**, 101-112.

Wentzel, P., Ejdesjo, A., & Eriksson, U.J. (2003). Maternal diabetes in vivo and high glucose in vitro diminish GAPDH activity in rat embryos. *Diabetes.* **52**, 1222-1228.

White, C.R., Darley-Usmer, V., Berrington, W.R., McAdams, M., Gore, J.Z., Thompson, J.A., Parks, D.A., Tarpey, M.M., &Freeman, B.A. (1996). Circulating plasma xanthine oxidase contributes to vascular dysfunction in hypercholesterolemic rabbits. *PNAS.* **93**, 8745-8749.

Wingren, A.G., Bjorkdahl, O., Labuda, T., Bjork, L., Andersson, U., Gullberg, U., Hedlund, G., Sjogren, H.O., Kalland, T., Widegren, B., & Dohlsten, M. (1996). Fusion of a signal sequence to the interleukin-1 beta gene directs the protein from cytoplasmic accumulation to extracellular release. *Cellular Immunology.* **169**, 226-237.

Woltmann, G., McNulty, C.A., Dewson, G., Symon, F.A., & Wardlaw, Andrew. (2000). Interleukine-13 induces PSGL-1/P-selectin-dependent adhesion of eosinophils, but not neutrophils, to human umbilical vein endothelial cells under flow. *Blood.* **95**, 3146-3152.

Wright, R.M., Vaitaitis, G.M., Wilson, C.M., Repine, T.B., Terada, L.S., & Repine, J.E. (1993). cDNA cloning, charaterization, and tissue-specific expression of human xanthine dehydrogenase/xanthine oxidase. *PNAS.* **90**, 10690-10694.

Xu, P., Huecksteadt, T.P., & Hoidal, J.R. (1996). Molcular cloning and charaterization of the human xanthine dehydrogenase gene (XDH). *Genomics.* **34**, 173-180.

Xu, P., Zhu, X.L., Huecksteadt, T.P., Brothman, A.R., & Hoidal, J.R. (1994). Assignment of human xanthine dehydrogenase gene to chromosome 2p22. *Genomics.* **23**, 289-291.

Xu, P., LaVallee, P., & Hoidal, J.R. (2000). Repressed expression of the human xanthine oxidoreductase gene. E-box and TATA-like elements restrict ground state transcriptional activity. *Journal of Biological Chemistry.* **275**, 5918-5926.

Yamawaki, H., Haendeler, J., &Berk, B.C. (2003). Thioedoxin a key regulator of cardiovascular function. *Circulation Research.* **93**, 1029-1033.

Yao, L., Pan, J., Setiadi, H., Patel, K.D., & McEver, R.P. (1996). Interleukin 4 or oncostatin M induces a prolonged increase in P-selectin mRNA and protein in human endothelial cells. *The Journal of Experimental Medicine.* **184**, 81-92.

Zhang, Z., Blake, D.r., Stevens, C.R., Kanczler, J.M., Winyard, P.G., Symons, M.C., Benboubetra, M., & Harrison, R. (1998). A reappraisal of xanthine dehydrogenase and oxidase in hypoxia-reperfusion injury: the role of NADH as an electron donor. *Free Radical Research.* **28**, 151-164.

Zhou, Q., Hellermann, G.R,. & Solomonson, L.P. (1995). Nitric oxide release from resting human platelets. *Thrombosis Research.* **77**, 87-96.

Zimmerman, G.A., McIntyre, T.M., Mehra, M., & Prescott, S.M. (1990). Endotheial cell-associated platelet-activating factor: a novel mechanism for signalling intercellular adhesion. *The Journal of Cell Biology.* **110**, 529-540.

Zouki, C., Zhang, S-L, Chan, J.S.D., & Filep, J.G. (2001). Peroxynitrite induces integrin-dependent adhesion of human neutrophils to endothelial cells via activation of the Raf-1/MEK/Erk pathway. *FASEB Journal.* **15**, 25-27.

Zupancic, G., Ogden, D., Magnus, C.J., Wheeler-Jones, C., & Carter, T.D. (2002). Differential exocytosis from human endothelial cells evoked by high intracellular Ca_2^+ concentration. *Journal of Physiology.* **544.3**, 741-755.